Stony Brook University

Ontogeny of Locomotion in *Saimiri boliviensis* and *Callithrix jacchus*: Implications for Primate Locomotor Ecology and Evolution

A Dissertation Presented

by

Jesse Wyatt Young

to

The Graduate School

in Partial Fulfillment of the

Requirements

for the Degree of

Doctor of Philosophy

in

Anthropology

(Physical Anthropology)

Stony Brook University

May 2008

STONY BROOK UNIVERSITY

The Graduate School

Jesse Wyatt Young

We, the dissertation committee for the above candidate for the
Doctor of Philosophy degree, hereby recommend
acceptance of this dissertation.

Brigitte Demes, Ph. D., Professor
Dissertation Advisor
Department of Anatomical Sciences

Susan Larson, Ph. D., Professor
Chairperson of the Defense
Department of Anatomical Sciences

William Jungers, Ph. D., Professor
Department of Anatomical Sciences

Audrone Biknevicius, Ph. D., Associate Professor
Outside Member
Department of Biomedical Sciences
Ohio University College of Osteopathic Medicine

This dissertation is accepted by the Graduate School.

Lawrence Martin

Dean of the Graduate School

Abstract of the Dissertation

Ontogeny of Locomotion in *Saimiri boliviensis* and *Callithrix jacchus*: Implications for Primate Locomotor Ecology and Evolution

by

Jesse Wyatt Young

Doctor of Philosophy

in

Anthropology

(Physical Anthropology)

Stony Brook University

2008

Most studies of primate locomotion in an evolutionary context have concentrated on the morphology and behavior of adults. In this dissertation, I present three "case studies" exploring the functional implications of ontogenetic changes in locomotion. The studies accessed a comprehensive mixed longitudinal dataset on squirrel monkey and common marmoset growth and development, in which high-speed videography, force platform analysis, and morphometrics were used to study many aspects of primate locomotion that are often examined in isolation.

In the first study I examined how ontogenetic changes in limb kinematics and kinetics can help growing squirrel monkeys overcome developmental limits on locomotor performance. I found that young squirrel monkeys were able to limit forelimb and hind limb joint loading *via* a combination of changes in limb posture and limb force distribution, thus compensating for limited muscle mass at younger ages. These results complement morphometric studies showing that anatomical measures of limb muscle mechanical advantage decline with age and suggest that immature mammals may utilize a combination of behavioral and anatomical mechanisms to mitigate ontogenetic limits on locomotor performance.

In the second study, I investigated the influence of substrate and body size on asymmetrical gait dynamics in growing marmosets and squirrel monkeys. I found that both species displayed a variety of kinematic adjustments when using asymmetrical gaits on a simulated arboreal substrate (i.e., an elevated pole). Together, these adaptations permitted the monkeys to reduce peak vertical forces, thus ensuring arboreal stability. Marmosets generally showed greater adjustments to pole locomotion than did squirrel monkeys, perhaps as a result of their reduced grasping abilities. Interestingly,

ontogenetic changes in body size had little independent influence on asymmetrical gait dynamics during pole locomotion, despite biomechanical theory suggesting that potential for arboreal instability is exacerbated as body size increases relative to substrate diameter.

In the last study, I employed morphological, kinematic and kinetic variation in the growing squirrel monkeys as a model system to evaluate the biomechanical bases of "hind limb dominance" in limb force distribution among primates. Over the course of development, squirrel monkeys transitioned from "forelimb dominant" infants to "hind limb dominant" juveniles. Changes in limb force distribution were accompanied by a net caudal translation in the position of the whole-body COM, a trend that explained 57% of the variation in forelimb-hind limb force distribution during growth. Growing monkeys also tended to place their feet closer to the midline of the body, further increasing hind limb forces. Overall, I was able to show that relatively simple parameters, such as whole-body COM position and hand and foot placement, were able to explain the majority of variation in limb force distribution in growing squirrel monkeys, suggesting that the biomechanical bases of limb force distribution across primates may warrant reassessment.

In sum, the studies presented here demonstrate how ontogenetic studies of somatic growth and locomotor development can serve as "natural experiments" testing hypothetical form-function relationships. As such, developmental studies of primate locomotion represent a generally untapped resource with the potential to broadly inform our understanding of primate locomotor ecology and evolution.

This work is dedicated to my wife Angela and my son Ethan, who have supported me throughout and taught me all I need to know about growth and development.

Table of Contents

List of Figures

List of Tables

Acknowledgments

This work would not have been possible without the generous support and encouragement of many individuals. From the moment I arrived on the Stony Brook University campus, Brigitte Demes has been a perfect advisor. She is as generous as she is insightful. Without her patient help, I would have never learned anatomy, biomechanics, soldering, or any of the countless other skills that have been required of me over the last six years. Bill Jungers, as ever, provided indispensable statistical advice throughout the design and analysis of this research, frequently steering me back on course whenever I went wondering off into statistical left field. He also has an uncanny ability to explain complex anatomical and biomechanical relationships with clarity and levity. Susan Larson's work on primate quadrupedal locomotion not only motivated many of the ideas tested here, but also fostered my early interests in primate locomotion and helped pull me away from developmental psychology to pursue anthropology at Stony Brook. Her critical mind and broad knowledge of primate and mammalian locomotor mechanics has greatly improved my work throughout my graduate career. Finally, although Audrone Biknevicius was a late addition to my dissertation committee, she proved to be invaluable, helping ground this research in a broader biological and biomechanical context.

Almost this entire dissertation was written during the first eight months of my "postdoctoral" research appointment with Liza Shapiro in the Department of Anthropology at the University of Texas at Austin. During that time, Liza was extremely accommodating, allowing ample me time to finish up and ensuring that I only had to pull one or two all-nighters. She also provided a smart, critical ear to bounce ideas off of and her comments on early versions of my dissertation talks and parts of this document greatly improved the presentation of my research. I look forward to the next 16 months of working with her.

The research reported here was performed at two NIH-funded National Primate Research Centers. The marmoset research was done at the Southwest National Primate Research Center in San Antonio, TX from May to August 2006. I am indebted to Dr. Suzette Tardif for facilitating my visit to the SNPRC and ensuring that I had all the resources I needed. Donna Layne was indispensable, assisting me during every one of my experiments and sharing some her vast accumulated knowledge about marmoset biology. The squirrel monkey portion of this research was carried out at the Center for Neotropical Primate Research and Resources in Mobile, AL from August 2006 to March 2007. Dr. Larry Williams facilitated my visit to the CNPRR and was always available and helpful during all logistical problems that plague the beginning of a research project. A number of veterinary technicians assisted me during the months of infant monkey measuring and wrangling, including Bethany Brock, Heather Hyer, Virginia Parks and particularly Leigh Ann Long.

Before this dissertation, I was completely mechanically inept. I'm now a little less so afterwards, but only because several people helped me get over the many technological hurdles. Dan Riskin gave me crash course in force plate construction prior to my foray into engineering, provided helpful advice along the way, and cheered me up when I felt all was doomed to fail. Brigitte Demes taught me how to solder and spent many hours discussing Wheatstone bridge configuration and other fun topics. Dan Talley helped me design and construct the runway used in all the locomotor experiments. His

ideas and craftsmanship were amazing - he's truly an artist. Anne Su gave me the first push I needed to get into MATLAB and provided some crucial advice during my first baby steps into software coding. Denné Reed got me started on path analyses and has corrected many of my statistical misconceptions during the analysis phase of the project.

Funding for this project came from many sources. My primary source of funding was a generous grant from the L.S.B. Leakey Foundation (Grant 38648). Additionally, this research was supported by the Stony Brook University Interdepartmental Doctoral Program in Anthropological Sciences, the Stony Brook University Graduate School and a National Science Foundation Graduate Research Fellowship.

I am grateful to all of the Stony Brook graduate students and faculty (past and present) who have supported me, encouraged me and cheered me up over the past six years, including: Summer Arrigo-Nelson, Andrea Baden, Matthew Banks, Carola Borries, Doug Boyer, Kris Carlson, Marc Coleman, Anja Deppe, Abigail Derby, Wendy Erb, Andy Farke, David Fernández, John Fleagle, Theresa Franz, Chris Gilbert, Justin Georgi, Ari Grossman, Meg Hall, Chris Heesy, Mitch Irwin, Jason Kamilar, Nate Kley, Andreas Koenig, Eileen Larney, Jessica Lodwick, Amy Lu, Chris Noto, Pat O'Connor, Kerry Ossi, Lisa Paciulli, Biren Patel, Callum Ross, Danielle Royer, Karen Samonds, Liz St. Clair, Clara Scarry, Matthew Sisk, Tanya Smith, Jack Stern, Nancy Stevens, Randy Susman, Brandon Wheeler and Sireen El Zaatari.

Finally, I'd like to thank my parents, Jacqueline Fague and Sloan Young, who've supported me throughout my long education and my family, Angela and Ethan, who remind me daily that there is much more to life than books and papers.

Chapter 1: Introduction

Most studies of locomotion in an evolutionary context have concentrated on the morphology and behavior of adults. Recently, however, an increasing number of studies have focused on the functional implications of ontogenetic changes in locomotion (Hurov, 1991; Carrier, 1996; Herrel and Gibb, 2006). Despite reduced body size and an immature musculoskeletal system, juvenile animals must often compete with adults for common resources, keep pace during group travel and evade common predators. Because, by definition, juvenile animals have yet to reproduce, growth trajectories should be under strong selection to produce compensatory mechanisms that permit adult-like levels of locomotor performance, at least for short durations (Carrier, 1996; Trillmich et al., 2003; Main and Biewener, 2004; Herrel and Gibb, 2006; Lawler, 2006). Additionally, locomotor development occurs within the context of increasing body mass and, frequently, allometric changes in body shape (Jungers and Fleagle, 1980; Carrier, 1983; Gomez, 1992; Hartwig-Scherer and Martin, 1992; Jungers and Cole, 1992; Ravosa et al., 1993; Heinrich et al., 1999; Liu et al., 1999; Lammers and German, 2002; Ruff, 2003b; Main and Biewener, 2004; Raichlen, 2005b; Schilling and Petrovitch, 2006). Therefore, simultaneous study of locomotor development and somatic growth offers a model system in which to test hypothetical form-function relationships (German and Meyers, 1989; Hurov, 1991; Main and Biewener, 2004; Raichlen, 2005a; Lawler, 2006; Raichlen, 2006; Dial et al., 2008).

1.1. Functional aspects of locomotor development in primates and other mammals

In many ways, the study of primate locomotor development is still in its infancy. Most studies of primate locomotor development have focused on cataloging the timing of skill acquisition without association to somatic growth or biomechanics (e.g., Schusterman and Sjoberg, 1968; Castell and Sackett, 1972; Ehrlich, 1974; Elias, 1977; Eaglen and Boskoff, 1978; Mack, 1979; Chalmers, 1980; Altmann, 1980/2001; Dolhinow and Murphy, 1982; Negayama et al., 1983; Escobar-Paramo, 1989; Morland, 1990; Dunbar and Badam, 1998; Radhakrishna and Singh, 2004; Workman and Covert, 2005). Additional studies have provided detailed kinematic and kinetic descriptions of primate locomotor development, but have failed to place the findings in a broader evolutionary context (e.g., Vilensky and Gankiewicz, 1986; Kimura, 1987; Vilensky and Gankiewicz, 1989; Vilensky et al., 1989; Kimura, 2000). The potential for ontogenetic studies of locomotion to inform the broader understanding of primate locomotor ecology and evolution was first overtly discussed by Hurov (1991). He outlined three broad questions intended to motivate future research. Hurov's (1991) questions can serve as a useful framework for reviewing previous research on somatic growth and locomotor development in primates and other mammals.

As animals grow, do they use different parts of their total available environment for locomotor behavior? Studies of sympatric adult monkeys of varying size have shown consistent links between body mass, locomotor repertoire and substrate selection (Fleagle and Mittermeier, 1980; McGraw, 1996; Fleagle, 1999). In general, larger primates tend use suspensory postures more often and select larger substrates for locomotion, whereas smaller primates leap more often and use a wider array of small and large substrates. Similar associations often characterize ontogenetic increases in body size. For instance, Doran (1992; 1997) found that much of the variation in chimpanzee

(*Pan troglodytes*), bonobo (*Pan paniscus*) and gorilla (*Gorilla gorilla*) locomotion is attributable to body size variation, such that juvenile individuals of the larger taxa tend to utilize the same locomotor behaviors and substrates as mature individuals of the smaller taxa. Similarly, Crompton (1983) found that juvenile Senegal bushbabies (*Galago senegalensis*) tended to utilize higher levels of the canopy and narrower supports than adults. However, Crompton (1983) also noted that body size was not necessarily the primary determinant of ontogenetic variation in galagid positional behavior – maturational differences in muscle strength and agility were equally important. For example, juvenile thick-tailed bushbabies (*Otolemur crassicaudatus*), the other species in Crompton's (1983) study, tended to use *lower* levels of the canopy and *larger* supports than adults and both species engaged in more quadrupedalism and less leaping at younger ages. Nevertheless, widespread reports that juvenile primates tend to be more acrobatic than adults generally support the notion that ontogenetic and interspecific variation in body size exert similar influences on positional behavior and substrate use (Sugardjito and van Hooff, 1986; Doran, 1992, 1997; Dunbar and Badam, 1998; Wright, 2003; Workman and Covert, 2005).

Previous studies have documented similar trends among non-primate animals. For example, several studies have found that juvenile anole lizards (*Anolis* species) tend to use narrower substrates and jump more frequently than adults (Schoener and Schoener, 1971b, 1971a; Moermond, 1979; Irschick et al., 1998). Laboratory-based studies have also shown that infant gray short-tailed opossums (*Monodelphis domestica*) can efficiently travel on narrow supports (i.e., 6.25 mm in diameter), whereas adults traveling on the same supports frequently lose balance (Shapiro et al., 2008). Additional studies of the interaction between growth and substrate utilization in sugar gliders (*Petaurus breviceps*) and mouse lemurs (*Microcebus murinus*) are currently underway (Shapiro and Young, unpublished data).

In what manner does ontogenetic change in body size and limb proportions influence motor behavior? Recent work by Shapiro and Raichlen (e.g., Raichlen, 2005a; Shapiro and Raichlen, 2005; Raichlen, 2006; Shapiro and Raichlen, 2006; Raichlen et al., 2007; Shapiro and Raichlen, 2007a; Shapiro and Raichlen, 2007b) provides the clearest illustration to date of how studies of locomotor development and somatic growth can serve as "model systems" to answer broader questions about primate biomechanics and locomotor evolution. Primate quadrupedal locomotion is known to be kinematically distinct from the locomotion of other mammalian quadrupeds in a number of ways (Larson, 1998; Schmitt and Lemelin, 2002; Schmitt, 2003b). For instance, primates typically take longer strides at lower frequencies than other similarly-sized mammals (Alexander and Maloiy, 1984; Reynolds, 1987). Additionally, most adult primates predominantly use diagonal sequence (DS) gaits when walking and running, during which hind limb touchdowns are followed by contralateral forelimb touchdowns. By contrast, most non-primate mammals use lateral sequence (LS) gaits, during which hind limb touchdowns are followed by ipsilateral forelimb touchdowns (Muybridge, 1887; Hildebrand, 1967; Prost, 1969; Rose, 1973; Rollinson and Martin, 1981; Vilensky and Larson, 1989; Meldrum, 1991; Cartmill et al., 2002; Schmitt and Lemelin, 2002).

In a series of papers, Shapiro and Raichlen used longitudinal data on baboon (*Papio cynocephalus*) growth and locomotor development to investigate the biomechanical bases for these unique features of primate gait. Raichlen (2005a) found

that ontogenetic variation in relative stride length tracked limb mass distribution, such that baboons took relatively longer strides early in life, when the hands and feet were comparatively large and limb mass was distally distributed. Essentially, the limbs behaved as suspended pendula: distributing mass distally increased the effective length of the limb pendulum, increased swing phase duration and displacement, and ultimately increased total stride length. Raichlen et al. (2007) recently applied this ontogenetic insight to studying interspecific differences in stride length, finding that differences in limb mass distribution and effective pendulum length explained stride length variation across a sample of goats, dogs, baboons, chimpanzees and humans. According to this argument, primates' use of relatively long strides may be a byproduct of an overall distal distribution of forelimb and hind limb mass resulting from selection for grasping hands and feet (Preuschoft et al., 1992; Preuschoft et al., 1996).

In a similar vein, Shapiro and Raichlen (2005; 2007b; 2007a) used the ontogenetic baboon dataset to effectively challenge some previous notions of the adaptive value of DS gaits in primates. Whereas most adult primates predominantly use DS gaits, infants and juveniles are much more variable in gait selection, often transitioning between LS and DS gaits before reaching a stable pattern of expression (Hildebrand, 1967; Rose, 1977; Rollinson and Martin, 1981; Hurov, 1982; Kimura, 1987; Vilensky and Gankiewicz, 1989; Nakano, 1996; Shapiro and Raichlen, 2006). Shapiro and Raichlen utilized the ontogenetic variability in baboon gait selection to show that 1) DS gaits do not uniquely confer stability by placing a protracted hind limb under the whole-body center of mass prior to forelimb touchdown (contra Cartmill et al., 2002, 2007a, 2007b) and that 2) the placement of the center of gravity vector relative to the hands and feet (i.e., static stability: Alexander, 2002) likely has very little influence on gait selection in primates or other mammals (contra Tomita, 1967; Rollinson and Martin, 1981; also see Vilensky and Larson, 1989; Wallace and Demes, 2007; Young et al., 2007). In sum, research by Shapiro and Raichlen amply illustrates the potential for combined studies of locomotor development and somatic growth to provide insight into primate locomotor biomechanics and evolution.

In an analogous fashion, Dial and colleagues have recently proposed that ontogenetic studies of bird growth and locomotor development could serve as a model system to investigate the transitional stages leading to evolution of avian flight (Bundle and Dial, 2003; Dial, 2003; Dial et al., 2008). Many ground birds are not born with functional wings, but instead possess short "proto-wings" with underdeveloped plumage. Although hatchlings are incapable of flapping flight, when climbing steep slopes they are able to use their proto-wings to generate aerodynamic forces normal to the slope surface, thus increasing traction and permitting ascent on substrates that would otherwise be insurmountable. Similarly, immature birds descending from perches can use the proto-wings to generate small amounts of lift, slowing descent to the ground and reducing impact speed. Dial and colleagues propose that the proto-wings of young ground birds are analogous to the incipient wings of theropod dinosaurs and that "wing-assisted incline running" may represent the adaptive niche into which wings first arose on the path towards flapping flight.

Other studies have demonstrated how allometric patterns of limb growth can facilitate locomotor performance in both immature animals and adults. Across mammals, infants and juveniles typically have relatively larger hands and feet than adults (i.e., hand

and foot lengths scale with negative allometry during growth), permitting young animals to navigate relatively wide substrates and maintain a larger base of support (Jungers and Fleagle, 1980; Carrier, 1983; Ravosa et al., 1993; Turner et al., 1997; Lammers and German, 2002; Lawler, 2006; Schilling and Petrovitch, 2006; Shapiro and Raichlen, 2006). Allometric growth can also "prepare" growing animals for the demands of mature locomotion. In a comparison of two closely related capuchin monkey species (*Cebus albifrons* and *Cebus apella*), Jungers and Fleagle (1980) found that the more "cursorial" species, *Cebus albifrons*, also showed significantly stronger positive allomety of limb growth, resulting in a more gracile and lanky body frame in adults. Similarly, Eilam and colleagues (Blumberg-Feldman and Eilam, 1995; Eilam, 1997) found that the developmental onset of specialized asymmetrical gaits among rodents (i.e., gerbils, jirds, dormice and jerboas) was coincident with the acquisition of adult locomotor morphology (i.e., exaggerated hind limb length and strongly kyphotic spines). Prior to this, the rodents used less-specialized primitive gaits, such as LS walking and trotting.

How do growth-related changes in structural design determine motor behavior? Immature animals tend to have less mineralized limb bones than adults, decreasing the elastic modulus (Torzilli et al., 1981; Carrier, 1983; Currey, 1984; Brear et al., 1990; Heinrich et al., 1999; Currey, 2001; Main and Biewener, 2004, 2007). Provided limb loading and bone geometry scale isometrically during growth, lower elastic moduli should lead to proportionally greater bone deformation in younger animals. Nevertheless, recent experimental and morphometric findings belie this prediction. Immature goats (*Capra hircus*) and emus (*Dromaius novaehollandiae*) experience *lower* peak bone strains than adults (Main and Biewener, 2004, 2007). Similarly, morphometric proxies suggest that limb bone safety factors decrease with age in growing muskoxen (Heinrich et al., 1999). Rather, it appears that young animals are able to maintain similar bone strains across development via pervasive negative allometry of limb bone diameters and second moments of area (Carrier, 1983; Heinrich et al., 1999; Lammers and German, 2002; Ruff, 2003a; Main and Biewener, 2004, 2007), increasing the bones' resistance to axial compression and bending. In other words, younger animals are comparatively "overbuilt" (Biewener, 2005).

Few studies have examined the ontogenetic scaling of limb bone cross-sectional geometry in non-human primates. Nevertheless, available data suggest that primates follow the general trends observed in other animals. Hartwig-Scherer (1995) found that humeral and femoral diameters scaled with negative allometry in an ontogenetic sample of chimpanzees, gorillas and orangutans, suggesting that, like other animals, immature great apes are also "overbuilt". Similarly, Ruff (2003b) found that humeral and femoral polar section modulus, a measure of average bending strength, tended to decline among growing baboons. Finally, Young and colleagues (2006; in preparation) used a longitudinal radiographic series of growing capuchin monkeys (Fleagle and Samonds, 1975; Thurm et al., 1975) to estimate allometric changes in humeral and femoral cross-sectional geometry throughout development. As previously documented for other animals, estimated cortical area (a measure of resistance to axial compression) and polar moment of area (a measure of resistance to bending and torsion) scaled to body mass with negative allometry in both species. Although no previous study of primate locomotion has explicitly focused on the interaction between ontogenetic changes in limb

bone geometry and material properties, the morphometric results reviewed here indicate that this may be a fruitful topic for future inquiry.

1.2. Overview of the dissertation

In the chapters that follow, I present three "case studies" illustrating how detailed examination of locomotor development and somatic growth can elucidate the ecological and biomechanical pressures shaping primate/mammalian developmental trajectories and, on a broader level, inform our understanding of the proximate determinants of primate locomotor mechanics. All three studies access the same longitudinal data set on Bolivian squirrel monkey (*Saimiri boliviensis*) development. Analyses of substrate effects on asymmetrical gait dynamics (Chapter 3) were supplemented by a smaller data set on common marmoset (*Callitrhix jacchus*) locomotor development. The squirrel monkey sample included six infants (age range: 76-302 days; body mass range: 218-535 grams). The marmoset sample included three infants (age range: 85-320 days; body mass range: 143-339 grams) and two adults (ages: 2.4 and 12.2 years; mean body mass: 328 grams). I performed a total of 145 locomotor experiments, including 108 squirrel monkey experiments and 37 marmoset experiments. In all, I collected data on 1,881 trials of squirrel monkey locomotion and 182 trials of marmoset locomotion, for a grand total of 2,063 trials. My experimental set-up included high-speed videography for measuring locomotor kinematics and two custom-built force platforms for measuring single-limb forces and whole-body center of mass (COM) mechanics. By combining these techniques, I was able to study simultaneously many aspects of primate locomotion that are often examined in isolation, such as footfall patterns (i.e., gait), joint and limb angular kinematics, single-limb kinetics, joint moments, and COM movements. In order to assess the influence of substrate type on locomotor behavior across development, monkeys were tested on the flat ground and on a raised horizontal pole. Additionally, body mass, static whole-body COM position and limb lengths were measured at regular intervals in all study animals, permitting me to probe associations between ontogenetic changes in locomotor behavior and somatic growth. To my knowledge, this dataset is the most extensive ever collected on primate locomotor development in a controlled laboratory setting.

In Chapter 2, "Ontogeny of Limb Joint Mechanics in Squirrel Monkeys (*Saimiri boliviensis*): Implications for Mammalian Limb Growth and Locomotor Development", I use the squirrel monkey data set to examine how changes in limb kinematics and kinetics during growth can mitigate or exacerbate ontogenetic limits on locomotor performance. In Chapter 3, "Substrate Determines Asymmetrical Gait Dynamics in Marmosets (*Callithrix jacchus*) and Squirrel Monkeys (*Saimiri boliviensis*)", I use the marmoset and squirrel monkey data sets to investigate the influence of substrate and body size on asymmetrical gait mechanics. Finally, in Chapter 4, "Ontogeny of Limb Force Distribution in Squirrel Monkeys (*Saimiri boliviensis*): Implications for Understanding Primate Locomotor Kinetics", I use the squirrel monkey data set as a model system to investigate the biomechanical bases of "hind limb dominance" of limb force distribution in primates. Each chapter is presented as a self-contained study, with all tables and figures collated at the end of the chapter. In Chapter 5, I present an overall summary of the dissertation and explore directions for future research.

Chapter 2: Ontogeny of Limb Joint Mechanics in Squirrel Monkeys (*Saimiri boliviensis*): Functional Implications for Mammalian Limb Growth

2.1. Introduction

Juvenile animals must often compete against adults for common resources, keep pace during group travel, and evade common predators in spite of reduced body size and an immature musculoskeletal system. Because, by definition, juveniles have yet to reproduce, growth trajectories should be under strong selection to produce compensatory mechanisms that enhance locomotor performance despite ontogenetic limitations (Pennycuick, 1975; Carrier, 1983; Carrier, 1996; Trillmich et al., 2003; Main and Biewener, 2004; Young, 2005; Herrel and Gibb, 2006; Lawler, 2006). This study focuses on how allometric changes in joint mechanics might allow growing squirrel monkeys to compensate for ontogenetic limits on locomotor performance.

At a given limb joint, the total muscular force necessary to counteract gravity is inversely proportional to the average distance of all muscle force vectors from the center of the joint (i.e., average of all muscle moment arms) and directly proportional to the product of the substrate reaction force (SRF) magnitude and its perpendicular distance from the joint (i.e., SRF moment arms). This relationship can be represented as:

$$F_m r = F_s R$$

where F_m is total muscle force, r is average muscle moment arm length (weighted by individual muscle force), F_s is the magnitude of the SRF, and R is the SRF moment arm (i.e., distance of the SRF vector from the center of the joint: Gray, 1968; Biewener, 1983). Relative to whole body mass, newborn mammals typically have half as much muscle mass as adults (Grand, 1977; Goldspink, 1980; Grand, 1983; Atzeva et al., 2007; Bolter and Zihlman, 2007). Among squirrel monkeys, forelimb muscle mass increases by 50% from neonates to adults and hind limb muscle mass more than doubles (Johnson, 1998). Young mammals therefore have relatively less available muscle force than adults, potentially compromising their ability to maintain joint postures during periods of intense limb loading and thus reducing performance capacity.

In a seminal study, Carrier (1983) documented growth trajectories in black-tailed jackrabbits (*Lepus californicus*) and domestic cats (*Felis domesticus*) which should theoretically permit these species to overcome ontogenetic limits on locomotor performance. In these animals, the length of the olecranon process at the elbow and the calcaneal tuberosity at the ankle, proportional to the average moment arms of *m. triceps brachii* and *m. triceps surae*, respectively, scaled with negative allometry to the length of the anatomical segments distal to these joints (i.e., these muscles acted on a longer lever arm in younger animals). In a separate study of limb growth and locomotor development in domestic cats, Peters (1983) confirmed Carrier's (1983) findings. Assuming that SRF load arms are proportional to limb length and SRF magnitudes are proportional to body weight, negative allometry of anatomical lever arms relative to limb length suggests that muscle mechanical advantage (i.e., r/R) should be greater in young animals, perhaps compensating for reduced muscle mass and smaller body size. In a follow-up study, Carrier (1995) found that young jackrabbits were indeed able to achieve adult-like jumping velocities at only 30% of adult body size, thus confirming the link between allometric growth trajectories and locomotor performance. Carrier (1983) suggested that because identical scaling trends were found in distantly related jackrabbits and cats,

negative allometry of muscle mechanical advantage might represent a generalized mammalian solution to ontogenetic limits on locomotor performance. In support of Carrier's (1983) hypothesis, Young (2005) recently documented a similar pattern of negative ontogenetic scaling for *m. triceps brachii* mechanical advantage in arboreal capuchin monkeys (*Cebus apella* and *Cebus albifrons*).

Carrier's (1983) and Young's (2005) analyses assumed that joint postures did not change during development and that SRF magnitudes remained a constant multiple of body weight. In other words, in order for the negative allometry of bony muscle lever arms to have the assumed effects, joint moments[1] should scale isometrically to body size. If, however, developmental changes in joint postures and SRF magnitudes cause joint moments to scale allometrically, muscle lever growth trajectories may be more difficult to interpret. If joint moments are relatively greater among young animals, relatively longer bony muscle lever arms may not be sufficient to achieve adult-like levels of locomotor performance. Conversely, if relative joint moments are smaller at early ages and increase over development, young mammals may not require relatively longer bony levers to increase performance.

This study focused on locomotor development in Bolivian (i.e., black-capped) squirrel monkeys (Platyrrhini: *Saimiri boliviensis*, Geoffroy and Blainville 1834). *S. boliviensis* natively inhabits the upper Amazon basin of Peru, southwest Brazil and Bolivia (Boinski, 1999; Jack, 2007). As a result of their small body size (mean adult body mass = 811 g: Smith and Jungers, 1997), most squirrel monkey populations are under intense predation pressure (Fedigan et al., 1996). Predation risk has profoundly affected many aspects of squirrel monkey biology, including growth and development (Boinski, 1987, 1999; Boinski et al., 2003). In a detailed study of red squirrel monkey (*Saimiri oerstedi*) behavioral ecology in Costa Rica, Boinski (1987) found that infants experienced higher rates of predation than any other age class, with more than 50% of infants dying within the first 6 months of life. Similar rates of predation have been reported for *S. boliviensis* in Peru (Boinski et al., 2002). The greatest number of deaths resulted from raptor predation while infants were clinging to their mothers' back, perhaps intensifying selection for rapid locomotor development. As a means of coping with predation risk, squirrel monkey behavioral development is markedly precocial relative to that of other primates. Following an extended gestation period, squirrel monkeys are born with a brain that is already 60% of adult size and essentially ceases to grow after two months of life (Elias, 1977; Hartwig, 1995). Infants engage in independent locomotion within the first month, begin foraging independently after seven weeks, are weaned by four months of age, and are completely independent from their mothers by eight months of age (Elias, 1977; Kaack et al., 1979; Boinski and Fragaszy, 1989; Fragaszy et al., 1991). In the wild, the foraging activity and locomotor repertoires of juvenile red squirrel monkeys are generally indistinguishable from adults by six months of age, when they are only 40-50% of adult size (Boinski, 1989; Boinski and Fragaszy, 1989). Moreover, once juvenile squirrel monkeys have become independent, they must

[1] For simplicity, external (i.e., SRF) joint moments and joint moment arms will be referred to simply as joint moments and joint moment arms in the remainder of this manuscript. When referring to internal moments, the terms muscle moment and muscle lever arm will be used.

travel an average of 2-4 km per day and maintain home ranges of 2.5 km^2 in order to remain with the group and gain access to distributed foraging resources (i.e., fruit and invertebrate prey: Terborgh, 1983; Mitchell, 1990; Boinski, 1999).

In sum, squirrel monkeys are an excellent group in which to investigate how developmental differences in limb mechanics might impact locomotor performance in young mammals. As a means of coping with intense predation risk, infant and juvenile squirrel monkeys are distinctly precocial in their locomotor behavior. As a consequence of early independence, young squirrel monkeys must often compete against adults for common resources and keep pace during extended periods of group travel, despite small body size and musculoskeletal immaturity. In this study, I used standard kinematic and kinetic techniques to investigate the ontogenetic scaling of joint postures, SRF magnitudes and SRF joint moments in growing Bolivian squirrel monkeys. To document the monkeys' locomotor repertoires as fully as possible, both symmetrical gaits (i.e., walking and running) and asymmetrical gaits (i.e., galloping and bounding) were sampled on terrestrial and simulated arboreal substrates. Additionally, because previous studies of morphological development have assumed that limb length and body weight are the primary determinants of SRF joint moments, I measured limb segments at regular intervals to test for growth allometry and used least-squares regression, hierarchical partitioning (Chevan and Sutherland, 1991; Quinn and Keough, 2002) and path analysis (Sokal and Rohlf, 1995; Shipley, 2000) to dissect the independent influence of limb length, posture and body mass on developmental changes in SRF moments. Following Carrier (1983) and Young (2005), I tested three primary hypotheses. First, when growing squirrel monkeys are traveling at the same absolute speed, joint kinematics, SRF magnitudes, joint moment arms and joint moments will scale isometrically to body size. Second, limb growth is the primary determinant of ontogenetic variation in joint moment arm lengths. Third, joint moment magnitudes vary in direct proportion to the product of body weight and limb length.

2.2. Methods

2.2.1. Animal subjects

A total of 106 experiments were conducted at the Center for Neotropical Primate Research and Resources (CNPRR: Mobile, AL) from August 2006 to March 2007. The CNPRR supports a long-established squirrel monkey breeding colony and staff members have ample experience facilitating external research projects. Veterinary technicians assisted with animal care, management and motivation during experiments. Institutional Animal Care and Use Committees (IACUC) at Stony Brook University and the CNPRR approved all procedures prior to the beginning of this research.

Five female squirrel monkeys comprised the sample for these experiments. Collectively, the monkeys ranged in age from 74-302 days and body mass from 218-535 grams (29-71% of adult size). An additional individual (Animal 4433) participated in two experiments but had to be withdrawn from the study due to an unrelated tail injury. My sample included monkeys belonging to each of the three main developmental stages described in the literature: infants less than four months of age, dependent juveniles between four and eight months of age, and independent juveniles older than eight months of age. Because body mass was linearly related to age in all individuals (Fig. 2.1), body mass, rather than chronological age or developmental stage, was used as the primary

independent variable in all analyses. Moreover, as a result of the precocial nature of squirrel monkey behavioral development (see above), size should have a stronger effect on locomotor mechanics than age *per se* (Schilling, 2005). Finally, body mass is generally accepted as the size variable of choice for studies of allometric scaling (Schmidt-Nielsen, 1975; Jungers, 1984, 1985).

FIGURE 2.1 HERE

All of the infants in this study were chosen from a cohort that had been initially hand-reared by veterinary staff, following perinatal rejection by their birth mothers. The use of hand-reared infants minimized any undue stress on that might have been placed upon early mother-infant relationships. Additionally, all nursery infants and juveniles were well habituated to veterinary staff, thus facilitating locomotor training. Previous research at the CNPRR has suggested that during the first 45 days of life, nursery-reared infants have reduced strength and balance when compared to dam-reared peers. Such developmental delays are likely the result of restricted environmental interaction while in the nursery (Williams, 2004). Nevertheless, because all of the infants in this study were nursery-reared under similar conditions, developmental delays relative to dam-reared infants should not be a confounding factor. After weaning at 1-2 months of age, hand-raised infants were integrated into social groups of 15-30 individuals and fostered onto surrogate mothers. Social groups were housed in large 1.5m x 2.1m x 4.5m enclosures with 35-40 linear meters of perches and substrates for free-ranging locomotor activity.

Information on individual monkeys is provided in Tables 2.1 and 2.2, including age-specific body masses and sample sizes. Summaries of ground strides are provided in Table 2.1 and summaries of pole strides are provided in Table 2.2.

TABLE 2.1 HERE

TABLE 2.2 HERE

2.2.2. Data collection

I used a Motionmeter 1000 high-speed digital video camera (Redlake MASD Incorporated, San Diego, CA) to film monkeys as they traversed a 2.75m x 0.3m x 0.53m runway (Fig. 2.2). The camera was placed perpendicular to the center of the runway at a distance of at least 2.5 meters and focused on a one-meter wide region surrounding two force platforms. This region was lit with three halogen lights placed perpendicular to the runway and one halogen light placed directly above the force platforms. The camera was electronically shuttered at a rate of 1/2500s and operated at 250Hz. This filming speed was sufficient to prevent aliasing of cyclic locomotor data (e.g., stride lengths and durations: Polk et al., 2005). Composite video output from the camera was converted to digital video using a Canopus ADVC-55 Analog-Digital converter (Canopus Corporation, San Jose, CA). Digital video from each experiment was stored on an Apple Macintosh Powerbook computer (Apple Incorporated, Cupertino, CA) for later processing.

FIGURE 2.2 HERE

Between trials, monkeys could be placed in two 60 cm x 30 cm x 53 cm enclosures located at the two ends of the runway. Sliding doors on either side of the enclosures permitted veterinary staff access to the monkey and allowed the monkey to enter the runway. The floor of the runway was constructed from vinyl-coated plywood (Omega Signboard, Laminators Incorporated, Hatfield, PA). The top and front wall of

the runway were formed from a single piece of angled Plexiglass, allowing the subject to be easily lighted and filmed. A 32 cm x 61 cm section was cut out from the center of the runway to mount two force platforms flush with the runway surface. Depending on experimental condition (e.g., ground vs. pole), monkeys traversed either the flat runway floor or a 2.5 cm diameter PVC pipe elevated 10.7 cm above the surface of the runway. Both substrates were coated with a mixture of polyurethane and non-skid paint additive (Behr Process Corporation, Santa Ana, CA) in order to increase traction.

2.2.2.1. Kinematic data collection

Prior to the beginning of each experiment, individuals were weighed and the skin over the approximate center of rotation of the shoulder, elbow, wrist, hip, knee and ankle joints was shaved and marked with retro-reflective tape (3M Corporation, St. Paul, MN). Anatomical landmarks used to identify joint centers of rotation are listed in Table 2.3. Because the monkeys traveled in one direction throughout the experiment, joints were marked on only one side of the body. I also recorded arm, forearm, thigh and leg lengths at this time. Segment lengths were measured with sliding digital calipers as the distance between the centers of the relevant landmarks. Total forelimb and hind limb lengths were computed as the sum of adjacent limb segments. None of the above procedures required the use of anesthesia.

TABLE 2.3 HERE

During data collection, squirrel monkeys were placed in one of the enclosed boxes at the end of the runway. A veterinary technician stood at the opposite end of the runway and verbally coaxed the monkey across. This approach usually induced monkeys to travel at high speeds using asymmetrical gaits. In order to elicit slower speeds and symmetrical gaits, the technician would slowly lead the monkey across the runway using a food reward (e.g., yogurt). After crossing the runway, monkeys were given 60 seconds of rest before the beginning of the next trial. Experiments consisted of 12-30 such trials and lasted for no more than 30 minutes. Once the experiment was over, reflective markers were removed and the monkey was returned to its social group.

2.2.2.2. Kinetic data collection

Two force platforms, placed in series, were used to measure single-limb forces during locomotion. The platforms were located in the center of the runway, allowing monkeys to reach steady speeds of locomotion prior to contact. Small gaps separated the force platforms from the runway and from each other, thus insuring each platform was mechanically isolated. The force platforms were custom-built for this study, following the spring-blade design described by Heglund (1981), Biewener and Full (1992), and Riskin et al. (2005). The surface of each platform consisted of a 30.5cm x 30.5cm x 12.7cm honeycomb fiberfoam panel (Teklam Corporation, Corona, CA) epoxied to two transverse 43.2cm x 1.9cm x 1.9cm aluminum box beams using Trubond Clear 2-ton Epoxy (Devcon, Danvers, MD). Each transverse beam was supported at the ends by two vertically oriented 10.2cm x 1.9cm x 1.9cm beams that were affixed to a heavy aluminum base. Aluminum-aluminum joints were secured with J-B Weld Epoxy (J-B Weld, Sulphur Springs, TX). At the four corners of each platform, the transverse and vertical box beams were milled to produce three sets of double cantilevers, each set oriented orthogonal to either the vertical, fore-aft or mediolateral axis. Single element strain

gauges (CEA-13-062UW-120, Vishay Micro-measurements Corporation, Raleigh, NC) were bonded to the cantilevers (ME A10 Adhesive, Vishay Micro-measurements Corporation, Raleigh, NC), allowing deflection of the double cantilevers to be measured in each direction. During the simulated arboreal trials, PVC segments (30.5 cm long and 2.5 cm in diameter) were attached to each force platform via bolts secured directly to the transverse beams.

Stain gauges were wired into four 10V Wheatstone bridge circuits. The system measured vertical deflection in the front and rear box beams via two independent circuits. Fore-aft and mediolateral deflections were monitored via one circuit each. The input and output from each circuit was routed to a separate channel in a multi-channel signal conditioning system (SC-2345 chassis containing four SCC-SG24 bridge amplifiers: National Instruments, Austin, TX). Analog output from the each channel was digitized using a National Instruments DAQCard-6036E analog-digital converter and stored as a text file using a custom-written National Instruments LabVIEW program running on a notebook PC (Dell Inspiron 1150, Dell Computers, Austin, TX).

The force platforms were calibrated each day an experiment took place, following the procedures described by Biewener and Full (1992). Briefly, the platforms were loaded in each direction with a series of ten weights spanning the expected range of forces to be measured. Linear least-squares regressions were then used to compute load-voltage calibration factors. Prior to computing vertical force calibration factors, the two vertical outputs from each plate were normalized to control for differences in sensitivity and summed. Coefficients of determination (i.e., R^2) from calibration regressions were always greater than 0.999, indicating a linear relationship between applied force and voltage output.

Cross-talk between the force channels on each platform was calculated by measuring the output of one channel while loading one of the other two channels. Cross-talk was generally low, ranging between 0.3% and 3.5% without the pole segment and 0.3% and 10.5% when the pole segment was attached. Details on the amount of cross-talk between specific channels is provided in Table 2.4 for each substrate.

TABLE 2.4 HERE

Kinetic and kinematic data were synchronized via a 3.3V square-wave pulse, generated by the master-slave port of the Redlake camera, that was routed separately to a bank of LEDs positioned on the back wall of the runway and to the notebook computer via a National Instruments SCC-AI04 analog input module connected to the SC-2345 chassis. This circuit was normally interrupted by means of a handheld switch. During each trial, the switch was briefly closed, simultaneously illuminating the LEDs in the video frame and changing the shape of the square wave in the data file. Using this procedure, it was possible to synchronize video and kinetic data to a resolution of 4 ms.

2.2.3. Data processing

2.2.3.1. Kinematic data processing

Digital video files from each experiment were converted to AVI files using Apple iMovie software (Apple Incorporated, Cupertino, CA). AVI files were then imported into the MATLAB DLT Dataviewer 2 digitizing platform (Hedrick, 2007) for coding on a trial-by-trial basis. Using this software, the X (horizontal) and Y (vertical) coordinates of all landmarks were recorded at three events during a single forelimb and hind limb

step within each stride: touchdown (the first frame that a limb made contact with the substrate), mid-stance (frame in which the shoulder/hip marker was most directly above the wrist/ankle marker) and lift-off (the final frame before the limb left the substrate). This convention for identifying lift-off events will tend to underestimate actual stance phase durations. However, at a filming speed of 250Hz, error magnitudes could never exceed 4 ms, or approximately 3% of average forelimb and hind limb stance phase durations.

For trials including kinetic data, limb landmarks and the position of the fifth metapodial head were digitized at peak vertical force. Due to the small size of the young monkeys, reflective markers could not be attached to the skin overlying the metacarpal and metatarsal heads. Therefore, the position of these landmarks was estimated to be at the base of the fifth manual/pedal ray. The coordinates of the hip and the shoulder marker were also recorded across the entire video clip in order to calculate average speed. The force platforms were used as calibration objects (combined length of force platforms: 0.6096m) to transform raw pixel coordinates into real-world units.

2.2.3.2. Kinetic data processing

Force data from each trial were imported into a custom-written MATLAB program (Mathworks, Natick, MA) where the raw voltages were calibrated and corrected for cross-talk. Force traces from each channel were smoothed using a zero-lag fourth-order Butterworth low pass filter with a cut-off frequency of 25 Hz. Baseline drift during and between trials was corrected by sampling the average values of unloaded periods immediately prior to and following platform contact and subtracting these values from the force traces.

The DLTdataviewer2 software was used to identify and record valid single-limb contacts for the calculation of SRF magnitudes and joint moments. Single-limb contacts began when a forelimb or hind limb contacted the force platform in isolation and ended when the limb either left the platform or another limb touched down. Forelimb contacts were usually the first contact on the force platform, whereas hind limb contacts were usually the last contact. Because the squirrel monkeys frequently placed limbs in close proximity when walking and running or used short lead times when galloping and bounding, obtaining isolated single-limb contacts was often difficult. Trials with overlapping limb contacts on a single force platform were retained only when peak vertical force was clearly identifiable and the vertical force trace had returned to 50% of the peak value prior to rising again with subsequent limb contacts in the case of forelimb contacts, or began its rise at no more than 50% of the former vertical force peak in the case of hind limb contacts.

2.2.4. Dependent variables

Scaled X- and Y-coordinates, combined with force platform data, were used to calculate a total of 24 kinematic and kinetic variables (Table 2.5). Segment angles (e.g., forelimb protraction) were measured at touchdown, peak vertical and lift-off. Variables related to the calculation of joints moments were only measured at peak vertical force. Joint angles (e.g., elbow angle) were measured at all of the four step events. Finally, a subset of variables was calculated across entire steps (e.g., joint yields and segmental

angular excursions). All computations were performed using custom-written MATLAB software.

TABLE 2.5 HERE

2.2.4.1. Speed

I calculated average locomotor speed from the displacement of either the hip or the shoulder, depending on which marker was represented in the greatest number of video frames. Polk el al. (2005) have recently shown that the use of a moving marker, such as the hip or shoulder, allows for more accurate calculations of speed than using a "stationary" marker, such as the wrist or ankle. I used a zero-lag fourth-order low pass Butterworth filter operating at 10 Hz to correct marker trajectories for digitizing noise. This cutoff frequency was selected as optimal using a residual analysis procedure described by Winter (1990). I used the piecewise cubic interpolation function of MATLAB to interpolate over gaps of missing data ≤ 10 frames (i.e., 40ms). Linear least-squares regressions of corrected displacement data on time were used to estimate overall horizontal and vertical velocities across each stride. Total speed was calculated as the resultant magnitude of horizontal and vertical velocity. However, because vertical velocity was essentially zero when averaged across an entire stride, resultant velocity is tantamount to horizontal velocity. In order to ensure that only steady-speed locomotion was examined, trials in which the coefficient of determination (i.e., R^2) of reference marker position against time was less than 0.99 were discarded.

The primary focus of this study was to compare joint mechanics among growing monkeys traveling at the same absolute speed, as this is the most ecologically relevant parameter for a young monkey fleeing from a predator or attempting to keep pace during group travel. However, comparisons among animals traveling at physiologically equivalent speeds may be more informative when testing for allometric change (Alexander and Jayes, 1983; Perry et al., 1988). Therefore, to control for differences in body mass across the sample, Froude number (Alexander, 1984; Hof, 1996; Polk, 2002; Bullimore and Donelan, 2008) was calculated as:

$$\frac{u}{\sqrt{gh}}$$

where u is velocity, g is gravitational acceleration ($9.81 ms^{-2}$) and h is effective hind limb length at midstance (i.e., the Euclidean distance from the hip to the shoulder). Note that this quantity is actually the square root of the "original" Froude number (i.e., $u^2(gh)^{-1}$) introduced by Alexander and Jayes (1983). However, both forms of the Froude number are dimensionless ratios and correct for body size effects on locomotor speed.

2.2.4.2. Gait

To distinguish between symmetrical and asymmetrical strides, stride symmetry was calculated as the absolute duration between the touchdowns of the right and left hind limbs expressed as a percentage of total stride duration (Hildebrand, 1966, 1977). Strides in which symmetry was between 43.75% and 56.25% were designated symmetrical. All other strides were designated asymmetrical.

2.2.4.3. Joint kinematics

Segment angles (e.g., forelimb angle and arm angle) were calculated as the two-dimensional vector angle between the relevant limb segment and a vertical line through the proximal pivot (i.e., hip/shoulder). Forelimb and hind limb segments at touchdown (protraction) and lift-off (retraction) were defined by lines joining the shoulder/hip to the wrist/ankle, respectively. Segments measured at peak vertical force were defined by a line joining the proximal pivot to the metapodial head. Positive segment angles indicate protraction; negative segment angles indicate retraction. Segmental angular excursions were calculated as the sum of the absolute value of protraction and retraction angles.

Joint angles (e.g., elbow or knee angle) were calculated as the two-dimensional vector angle between the relevant limbs segments (e.g., arm and forearm or thigh and leg). Following Larney and Larson (2004), elbow and knee joint yields were calculated as the difference between joint angles at touchdown and at mid-stance. Positive values indicate the joint became more flexed between the two events; negative values indicate the joint became more extended. To correct for out-of-plane distortions (i.e., having the segments abducted or adducted relative to the sagittal plane: Plagenhoef, 1979), three-dimensional elbow and knee angles were calculated using the methods of Stevens et al. (2006). This method uses the ratio of apparent segment length to actual segment length to estimate segment adduction/abduction angles and reconstruct Z-coordinates for the three landmarks defining the angle (e.g., shoulder, elbow and wrist for elbow angles). These coordinates are then used to compute three-dimensional vector angles at the joint in question. However, because most apparent segment lengths (as measured from the video) were longer than actual segment lengths, corrected joint angles were only available for a small subset of strides (see Section 2.2.5.1 below).

2.2.4.4. Kinetic variables

I measured joint moments and moment arms at peak vertical force for all steps in which simultaneous kinematic and kinetic data were available. Because raw kinematic data were two-dimensional, most calculations of joint moments and moment arms were restricted to the sagittal plane. The angle of the SRF with respect to the vertical (y) axis was calculated as:

$$\tan^{-1}\left(\frac{F_{x(Vpk)}}{F_{y(Vpk)}}\right)$$

where $F_{x(Vpk)}$ and $F_{y(Vpk)}$ are, respectively, the magnitudes of the fore-aft and vertical components of the SRF at peak vertical force. A SRF angle of 0° indicates that the SRF vector pointed directly vertically, at 90° to the substrate surface. Negative values indicate SRF angles were caudally inclined, whereas positive angles indicate SRF angles were cranially inclined. The resultant magnitude of the sagittal component of the SRF was calculated as:

$$\sqrt{F_{x(Vpk)}^{\ 2} + F_{y(Vpk)}^{\ 2}}$$

Following previous studies of mammalian joint mechanics, (e.g., Biewener, 1983, 1989, 1991; Schmitt, 1995; Polk, 2001, 2002; Witte et al., 2002), the SRF was assumed to pass through the metacarpal head for forelimb joints and the metatarsal head for hind limb joints. Joint moments were calculated as the cross (i.e., vector) product of the SRF and a two-dimensional position vector connecting the metacarpal/metatarsal head to the

joint in question (Ozkaya and Nordin, 1999). Moment arm lengths were computed by dividing joint moments by the scalar magnitude of the sagittal component of the SRF (Polk, 2001). Positive values signify flexing moments and moment arms (dorsiflexing at the wrist and ankle), whereas negative values signify extending moments and moment arms (palmar- and plantarflexing at the wrist and ankle).

Additionally, resultant three-dimensional elbow and knee joint moments and moment arms were calculated for the subset of trials where joint angles could be corrected using the Stevens et al. (2006) method. In these cases, joint moments about the X-, Y-, and Z-axes were calculated as the cross product of the three-dimensional resultant SRF and a three-dimensional position vector connecting the metacarpal/metatarsal head to the elbow/knee joint. The magnitude of the resultant moment was then calculated as:

$$\sqrt{M_x^{\,2} + M_y^{\,2} + M_z^{\,2}}$$

where M_x, M_y and M_z denote moments about the X, Y and Z axes. The resultant three-dimensional joint moment arm was calculated by dividing the magnitude of the resultant moment by the total magnitude of the resultant SRF (Polk, 2001).

It should be noted that the method used here to calculate joint moments is only an approximation, as it does not include the inertial effects of segments distal to the joint being analyzed. Proper accounting of inertial forces has been shown to be critical for accurately measuring proximal joint moments in large animals (e.g., hip joint moments in walking humans: Wells, 1981; Winter, 2005). However, in the small-bodied quadrupeds examined here, inertial forces are likely to be minor relative to SRF. Indeed, Witte et al. (2002) have recently shown that inertial forces account for no more than 10% of total limb joint moments among small quadrupedal mammals (i.e., 150-400g in body mass).

A variety of procedures were used to adjust kinetic variables for differences in body size. Relative SRF magnitudes were calculated as the quotient of absolute magnitudes (in Newtons) and body weight. Relative joint moment arms were calculated in two ways, following Polk (2001). First, to adjust for generalized differences in body size, moment arms were divided by the cube root of body mass. Additionally, in order to adjust for allometric differences in limb length and posture with respect to body mass, moment arms were scaled to effective forelimb/hind limb length at peak vertical force (i.e., Euclidean distance from the shoulder/hip to the metapodial head).

The proper method of adjusting joint moments to body size differences is controversial (Hof, 1996; Polk, 2001; Moisio et al., 2003). If the goal of scaling is to estimate the magnitude of substrate reaction moments relative to the magnitude of available muscle moments, body mass should be used as the scaling factor. This argument follows from the isometric expectation that muscle lever arm lengths, as linear dimensions, scale to the cube root of body mass (i.e., $\propto M_b^{0.33}$), whereas muscle force, proportional to physiological cross-sectional area, scales to the two-thirds power of body mass (i.e., $\propto M_b^{0.67}$). Therefore muscle moments, equal to the product of force and length, should scale directly to body mass (i.e., $M_b^{0.33} \times M_b^{0.67}$). However, if the goal of scaling is to produce a dimensionless ratio, joint moments should be scaled to the product of body weight and limb length. Although Hof (1996) advocates the latter method, Polk (2001) suggests that it may in fact overcorrect for differences in body mass. Additionally, this method assumes that across body sizes, SRF magnitudes remain a constant proportion of body weight and SRF moment arm lengths remain a constant proportion of limb length (i.e., posture does not change with body size). As shown in the

results below, such assumptions are not necessarily tenable. Nevertheless, in a recent study of the effects of body size on hind limb joint moments in humans, Moisio et al. (2003) showed that the methods of scaling moments produce statistically similar results at most joints. To explore the consequences of the scaling methods among the small quadrupedal monkeys examined here, joint moments were scaled to both body mass and body weight times effective limb length below the joint (i.e., the Euclidean distance between the joint and the metacarpal/metatarsal head).

2.2.5. Accuracy and precision of kinematic data

2.2.5.1. Accuracy of kinematic data

Accuracy refers to the discrepancy between a measured value and the actual value (Sokal and Rohlf, 1995). Within a single video image (i.e., frame), the accuracy of kinematic data is primarily limited by the accuracy obtained in measuring the three-dimensional position of each landmark. As such, the accuracy of the kinematic data presented here is possibly affected by two sources of error. First, because reflective markers were applied to the skin overlying the relevant joints, skin movement and changes in luminance may have caused digitized marker position to deviate from actual (i.e., skeletal) joint position. Recent attempts to mitigate movement artifacts have included the use of cineradiography (e.g., Whitehead and Larson, 1994; Schmidt and Fischer, 2000; Fischer et al., 2002; Witte et al., 2002; Schilling, 2005; Schmidt, 2005; Schilling and Hackert, 2006) and bone screws (Ross and Reed, 2007) to directly track skeletal displacement. However, these technologies were not available for the current study. Moreover, skin markers have been used in the vast majority of research on tetrapod locomotor kinematics.

A second possible source of error in the current dataset arises from parallax distortion – the apparent change in the size of an object due to its distance from the observer (Plagenhoef, 1979). In the context of two-dimensional videography (e.g., photogrammetry: Koff, 1995), parallax distortion results from the subject moving either the limbs or the entire body away from the calibrated plane of the image. Because the apparent length of the front and back of the force platforms never varied by more than 10%, parallax distortion arising from whole-body movement away from the calibration plane (i.e., transverse center of the force platforms) could account for no more than 5% error in measuring segment lengths (Plagenhoef, 1979).

To investigate possible sources of error in measuring limb marker positions, I calculated percentage differences between measured segment lengths and digitized segment lengths at touchdown, mid-stance and liftoff for all available forelimb and hind limb steps. Mean measurement errors, grouped by substrate, segment and step event, are shown in Table 2.6. Differences in the frequency and magnitude of measurement errors were tested using chi-squared tests and multivariate analyses of variance, respectively. Pairwise differences in error magnitude between substrates, segments and step events were compared using Dunn-Sidak adjusted t-tests (Sokal and Rohlf, 1995).

TABLE 2.6 HERE

Overestimation errors ranged in average magnitude from 2.5-9.5% of segment length and were found in 11.9-82.5% of all strides, depending on substrate, segment and step event. Underestimation errors ranged in average magnitude from 2.3-7.9% of segment length and were found in 14.6%-81.8% of strides. Overestimation errors tended

to be more frequent on the ground (χ^2=5.5, p<0.05) but of greater magnitude on the pole (t=-0.29, p<0.05). Underestimation errors were both more frequent (χ^2=19.5, p<0.001) and larger on the pole (t=-0.74, p<0.001).

For the forelimb, overestimation errors were of greater magnitude for the arm than the forearm across substrates (t≥2.2, p<0.001) and, for pole locomotion, more frequent for the arm as well (χ^2=13.8, p<0.001). Underestimation errors for forelimb segments did not differ in magnitude on either substrate, but were more frequent (χ^2=13.3, p<0.001) for the arm than the forearm during pole locomotion. For the hind limb, overestimation errors tended to be greater in the thigh than the leg across substrates (t≥1.2, p<0.001). Hind limb overestimation errors did not differ in frequency on the ground and were more frequent for the leg segment when monkeys were on the pole (χ^2=51.1, p<0.001). The magnitude of hind limb underestimation errors did not significantly differ between segments on either substrate. The frequency of hind limb underestimation errors did not differ in ground locomotion but was greater for the leg segment when monkeys were travelling on the pole (χ^2=55.9, p<0.001). Although the comparisons were not always statistically significant, overestimation errors tended to be lower and less frequent at mid-stance than at touchdown and liftoff across substrates for all segments except the thigh. In contrast, underestimation errors for all segments but the thigh tended to be greater and more frequent at mid-stance, particularly during pole locomotion.

In summary, although the distribution of measurement errors varied considerably among substrates, segments and step events, several trends are discernible. *Overestimation* errors tended to be greater and more frequent in proximal segments and at touchdown and lift-off. *Underestimation* errors tended to be greater and more frequent on the pole and at mid-stance. Together, these patterns suggest that measurement errors arose primarily from movement artifacts at the beginning and end of steps, when the joints are more extended, and from limb abduction/adduction at mid-stance, when the joints are more flexed, particularly during pole locomotion. As noted above, the method outlined by Stevens et al. (2006) was used to correct joint angles for out-of-plane movement where possible. However, it should be noted that measurement errors were generally small. The largest average measurement error, 9.5% of arm length, equated to 4.3 mm in absolute units. Errors of similar relative magnitude have been obtained in studies utilizing more precise three-dimensional kinematic methods with much larger monkeys (Polk, 2001). For all but a few comparisons, corrected joint angles showed the same allometric trends as observed in the two-dimensional data set (see Results section below). Overall, these data suggest that 1) in the set-up outlined above it was possible to measure segmental lengths and joint kinematics within tolerable limits and 2) only a minimal amount of bias was introduced by assuming that limb movements were restricted to the sagittal plane.

2.2.5.2. Precision of kinematic data

Precision refers to the discrepancies within a series of repeated measurements of the same quantity (Sokal and Rohlf, 1995). To estimate precision in the current dataset, 20 randomly selected trials were coded three times on different days. As a metric of precision, coefficients of variation (i.e., mean value/standard deviation*100%) were calculated for each raw kinematic variable and compared to the average amount of "intra-

experimental" variation within the experiments from which the randomly selected trials were drawn. Table 2.7 presents mean values, standard deviations and coefficients of variation for each kinematic and kinetic parameter. Coefficients of variation ranged from 0.02% to 26.9%, with an overall mean value of 5.7% and a median value of 2.2%. Variables with high coefficients of variation either relied on estimated metapodial positions (e.g., joint moments and moment arms) or had low mean values (e.g., hind limb angle at touchdown and knee joint moments and moment arms), resulting in high CVs despite biologically insignificant levels of error variation (e.g., 1.3% for hind limb angle at touchdown). Increased coefficients of variation for joint moments may also be a function of their higher dimensionality relative to the other variables (Lande, 1977). When these sources of increased variation are excluded, all remaining variables have coefficients of variation under 5%. Moreover, variation due to measurement error was consistently less than variation within sampled experiments. Overall, these results indicate that the precision of the experimental procedures used here remains within tolerable limits.

TABLE 2.7 HERE

2.2.6. Statistical analyses

In order to increase statistical power, data from individual monkeys were combined to create mixed longitudinal samples for all morphometric, kinematic and kinetic analyses (Cock, 1966). Limb growth data were tested for allometry by fitting log-transformed segment lengths and body masses to the standard allometric power function (Huxley, 1932) using Model II Reduced Major Axis (RMA) regression. Model I Least Squares (LS) regressions were deemed unjustified because both the independent variable (body mass) and dependent variables (limb lengths) were measured with error terms (Ricker, 1984). Nevertheless, for the sake of completeness, LS regressions were also computed. Confidence intervals on RMA slopes were calculated following Pitman (1939). Allometry was recognized if the 95% confidence intervals for the calculated slopes did not include 0.333. RMA regressions were calculated using the (S)MATR software package (Falster et al., 2003). LS regressions were calculated using SPSS 11.0 for Macintosh (SPSS Inc, Chicago, IL, USA).

I used the Generalized Linear Model (GLM) module of SPSS 11 to compare the magnitude of absolute joint moments within limbs and characterize intra-limb variability in joint loading across the ontogenetic sample. Analyses were performed separately for each of the four gait-by-substrate groupings (i.e., symmetrical and asymmetrical gaits on the ground and on the pole). Joint moments measured within each limb were specified as within-subjects factors for a repeated measures analysis of variance (ANOVA). Where limb joint moments varied as a linear function of body mass and/or speed, repeated measures analyses of covariance (ANCOVA) were used in lieu of ANOVA, specifying mass and/or speed as the covariate(s). Paired T-tests between group means (least squares adjusted means with ANCOVA) were used to test for significant differences between joints. The α-levels for all post-hoc tests were adjusted using the Dunn-Sidak method to mitigate experiment-wise error (Sokal and Rohlf, 1995).

I used correlation analyses to test for significant size-related changes in all size-adjusted kinematic and kinetic parameters. Pearson product-moment correlations were used to test for bivariate associations between each dependent variable and absolute

speed, Froude number, and body mass. Partial correlations were used to investigate the influence of body mass on each variable while controlling for absolute or relative speed. In each case, the null hypothesis was that body mass had no association with the dependent variable in question. Because all variables were either dimensionless (i.e., angles) or were adjusted for body size differences prior to analysis, any significant correlation indicated allometry (Mosimann and James, 1979). These analyses were performed separately by gait type and substrate using SPSS 11.

Hierarchical partitioning (Chevan and Sutherland, 1991; MacNally, 2002; Quinn and Keough, 2002) and path analysis (Li, 1975; Sokal and Rohlf, 1995; Shipley, 2000; Grace, 2006) were used to dissect the independent influence of limb length, joint posture, limb placement (i.e., forelimb/hind limb segment angles) and SRF angle on observed variation in absolute joint moment arm lengths. Both hierarchical partitioning and path analysis can be thought of as extensions of multiple regression analysis. Given a linear model with one dependent variable (Y) and *k* independent variables (X_1, X_2, X_3…X_k), hierarchical partitioning quantifies the independent contribution of each X variable to the total coefficient of determination for Y. For example, given three independent variables, the independent contribution of a variable X_1 is quantified as the average change in R^2 produced by adding X_1 to a hierarchical series of increasingly complex models (i.e., X_1 alone, X_1+X_2, X_1+X_3, $X_1+X_2+X_3$). This procedure is carried out sequentially for all *k* independent variables. The significance of each variable's independent contribution to the total coefficient of determination can be tested using a randomization procedure introduced by MacNally (2002). Hierarchical partitioning was performed using the hier.part package (MacNally and Walsh, 2004) of the R statistical platform (http://www.R-project.org). Because my goal was to test the assumption that joint moment arms were directly proportional to anatomical limb length distal to the joint in question, I only analyzed those joints for which the relevant limb lengths were available (i.e., shoulder, elbow, hip and knee joints). Analyses were performed separately by gait type and substrate.

I used path analyses to clarify the independent and associative influence of limb lengths on moment arm lengths. Path analysis allows one to investigate patterns of direct and indirect correlation within a set of independent (i.e., predictor) and dependent (i.e., criterion) variables by specifying an directed causal network linking the variables together (Li, 1975; Sokal and Rohlf, 1995; Shipley, 2000). In a path analysis, each hypothesized causal link (i.e., direct association) between variables is represented diagrammatically by a single-headed arrow and is associated with a unique path coefficient – equivalent to a standardized partial regression coefficient in a multiple least squares regression. Path coefficients describe the direction of the relationship between variables (i.e., positive or negative correlation) and are proportional to the amount of criterion variance explained by each predictor after controlling for all other predictors. Additionally, predictor variables can be joined via undirected double-headed arrows (equivalent to a standard bivariate correlation), signifying that the variables are related to one another without specifying a necessary causal structure.

Once a path diagram has been constructed, and all associated path and correlation coefficients have been specified, the "indirect" association between any predictor and a criterion variable can be quantified as the summation of all the products of coefficients corresponding to chain of paths connecting the two variables. For

example, in a fully-specified path model with two predictor variables, X_1 and X_2, and one criterion variable, Y, the direct association between X_1 and Y would be equal to the path coefficient of X1 (p_1). The indirect association between X_1 and Y would be equal to the product of the correlation between X_1 and X2 (r_{12}) and the path coefficient of X_2 (p_2) - or $r_{12}*p_2$.

Path diagrams specifying the hypothesized influence of limb lengths, joint postures, limb placements and SRF angles on joint moment arm lengths were constructed and evaluated separately for each joint, gait and substrate combination. The general organization of the path diagrams and specific predictions for each relationship are presented in Figure 2.3. Directed causal paths were predicted between each of the four predictor variables and moment arm lengths. Undirected correlations were predicted between limb lengths and joint angles, joint angles and limb angles, joint angles and SRF angles, and limb angles and SRF angles. For all joints, limb length was predicted to have a positive effect on moment arm length. Because joint extension is a well-established means of shortening joint moment arms (Gray, 1968; Biewener, 1989, 1990, 1991; Polk, 2002; Biewener, 2005), larger (i.e., more extended) joint angles were predicted to exert a negative effect on joint moment arm length. The influence of limb angles was predicted to vary according to limb and joint. Across quadrupeds, forelimbs typically perform a net braking function, leading to negative (i.e., caudal) SRF angles at peak force, whereas hind limbs typically perform a net propulsive function, leading to positive (i.e., cranial) SRF angles at peak force (Heglund et al., 1982; Demes et al., 1994). Therefore, increasing forelimb *protraction* and hind limb *retraction* should bring the limb axis more in line with the SRF vector, thereby shortening shoulder/hip moment arms, but increasing the distance between the middle joint and the SRF vector, thereby lengthening elbow and knee moment arms. In sum, forelimb angles should be negatively associated with shoulder moment arm lengths but positively associated with elbow moment arm lengths. By contrast, hind limb angles should be positively associated hip moment arm lengths but negatively associated with knee moment arm lengths. Similarly, increasing forelimb SRF angles should have a negative effect of shoulder moment arm lengths but a positive effect on elbow moment arm lengths, whereas increasing hind limb SRF angles should have a positive effect on hip moment arm lengths and a negative effect of knee moment lengths. Limb lengths and joint angles were predicted to be positively correlated, following previous research showing that, all else being equal, longer-limbed individuals typically adopt more extended joint postures (Polk, 2002; Gruss, 2007). Assuming the limbs functions at least partly as struts, SRF vectors should be equal in magnitude and opposite in direction to the force exerted along the limb's axis (e.g., Gray, 1944; Pontzer, 2005; Carrier et al., 2007). Therefore, limb angles and SRF angles should be negatively correlated. No predictions were made regarding the correlation between joint angles and limb angles or joint angles and SRF vectors.

FIGURE 2.3 HERE

The overall fit of each path diagram was evaluated by calculating chi-squared tests, goodness-of-fit indices (GFI) and root mean squared errors of approximation (RMSEA). Each of these tests measures the absolute difference (e.g., chi-squared test) or relative difference (e.g., GFI and RMSEA) between the empirically observed correlation matrix and the correlation matrix implied by the path model. Non-significant chi-squared tests, GFI of 0.95 or greater, and RMSEA not significantly different from 0.05 indicate a

good fit between the model and the data (see Schermelleh-Engel et al., 2003 for details). All path analyses and associated tests of fit were performed using the AMOS 7 software package (AMOS Development Corporation, Spring House, PA).

Finally, I used LS regressions to test the hypothesis that joint moment magnitudes varied in direct proportion to the product of body weight and anatomical limb length distal to the joint in question. Again, only those joints for which the relevant morphological data were available were included (i.e., shoulder, elbow, hip and knee joints). The null hypothesis for these analyses was that actual joint moments would scale in direct proportion to predicted joint moments (i.e., with a slope of 1 and an R^2 of 1.00). All regressions were performed in SPSS 11.0.

2.3. Results

A total of 1168 strides were analyzed, including 152 symmetrical strides and 462 asymmetrical strides on the ground and 230 symmetrical strides and 324 asymmetrical strides on the pole. A subset of 706 single-limb contacts was available for kinetic analyses, including 172 forelimb steps and 86 hind limb steps on the ground and 265 forelimb steps and 183 hind limb steps on the pole.

2.3.1. Ontogenetic allometry of limb segment lengths

Estimated RMA and LS slopes for growth data, Y-axis intercepts from RMA regressions, and confidence intervals on these values are shown in Table 2.8. Scatter plots of growth data and estimated RMA slopes are presented in Figure 2.4.

TABLE 2.8 HERE

FIGURE 2.4 HERE

Irrespective of line-fitting method, all segment lengths scaled to body mass with strong positive allometry, indicating that smaller and younger monkeys were relatively short-limbed. Forelimb segments tended to scale with greater positive allometry than hind limb segments, although only the forearm scaled significantly faster than hind limb segments ($p \leq 0.01$ for all comparisons). Scaling exponents describing overall forelimb and hind limb growth (bottom rows in Table 2.8) indicated strong positive allometry for both limbs. Forelimbs scaled with significantly greater positive allometry than hind limbs ($p=0.034$). Because hind limb segments were absolutely longer than forelimb segments at all ages (note the y-axis intercepts in Table 2.8 and Fig. 2.4), the intermembral index – forelimb length as a percentage of hind limb length – was always less than 100. Across development, the greater positive allometry of forelimb segments resulted in a small, but significant, positive correlation between body mass and intermembral index ($r=0.25$, $p=0.014$; Fig. 2.5). Among monkeys older than eight months of age, the age at which juveniles in the wild become fully independent, the mean intermembral index was 79.9. This value closely matches values previously reported for adult squirrel monkeys (79.1: Jungers, 1985; 79: Napier and Napier, 1985; 80: Fleagle, 1999).

FIGURE 2.5 HERE

2.3.2. Ontogenetic allometry of joint mechanics

Across the ontogenetic sample, most forelimb and hind limb joints primarily experienced flexing (i.e., positive) joint moments at peak vertical force (Fig. 2.6),

regardless of gait type or substrate. The only exception was the knee joint, which experienced a combination of weak flexing and extending moments. Elbow joints consistently experienced the largest moments of all the forelimb joints, regardless of substrate or gait (paired t-tests: all $t \geq 9.4$, all $p \leq 0.01$). Shoulder and wrist moments were similar across all conditions except for asymmetrical gaits on the ground, where wrist moments were significantly greater ($t=12.7$, $p<0.001$). Within the hind limb, knee joints consistently experienced the lowest moments (all $t \geq 2.6$, all $p \leq 0.011$). Regardless of substrate, hip moments were significantly greater than ankle moments during symmetrical gaits (all $t \geq 6.5$, all $p<0.001$) but were statistically similar to ankle moments during asymmetrical gaits.

FIGURE 2.6 HERE

2.3.2.1. Symmetrical strides on the ground

Pearson product-moment (i.e., zero-order) correlations and first-order partial correlations relating speed, Froude number, body mass and all dependent kinematic and kinetic variables for symmetrical strides on the ground are shown in Table 2.9. Body mass was not significantly associated with either absolute or relative speed when monkeys were using symmetrical gaits on the ground ($r \leq 0.06$, $p \geq 0.05$). Only slight developmental differences in forelimb kinematics were evident. With increasing body mass, monkeys placed their forelimbs in a slightly more protracted position at touchdown and peak vertical force. Younger monkeys had their forelimbs closer to a neutral position at peak vertical force, with the shoulder positioned directly over the hand. Arm protraction at touchdown and peak vertical force, as well as total angular excursion, also increased as monkeys grew. Almost no changes in two-dimensional or three-dimensional elbow angles were evident, aside from slightly greater flexion at liftoff. There were no size-related changes in wrist joint angles at peak vertical force.

TABLE 2.9 HERE

Compared with the forelimb data, developmental changes in hind limb kinematics were much more pronounced. Hind limb protraction and angular excursion significantly increased with body mass, as did thigh protraction and angular excursion. Larger monkeys also significantly increased knee flexion at mid-stance and tended to use more flexed knee postures at peak vertical force, leading to greater knee yield over a hind limb step. Although corrected knee angles did not show these same trends, the discrepancy is most likely due the very small sample size of the three-dimensional data set. There were no size-related changes in ankle joint angles at peak vertical force.

Relative to body size, forelimb SRF magnitudes significantly decreased over development. Sagittal forelimb SRF angles decreased (i.e., pointed more caudally). Reorientation of the SRF vector likely coincided with increases in forelimb protraction at peak vertical force. In contrast to forelimb SRF magnitudes, relative hind limb SRF magnitudes significantly increased as monkeys grew. Thus, smaller monkeys experienced relatively greater forelimb forces and relatively lower hind limb forces than older and larger monkeys, even when traveling at similar absolute and relative speeds. The relative length of joint moment arms did not change at any forelimb or hind limb joint. Nevertheless, allometric increases in hind limb SRF magnitudes resulted in positive allometry of hip and ankle joint moments, regardless of scaling method. Relative forelimb joint moments did not change when scaled to body mass. When scaled

to the product of body weight and effective limb length, however, elbow and wrist moments displayed significant negative allometry.

2.3.2.2. Asymmetrical strides on the ground

Pearson product-moment correlations and partial correlations for asymmetrical strides on the ground are shown in Table 2.10. Body mass was significantly positively correlated with both absolute speed ($r=0.33$, $p<0.001$) and relative speed ($r=0.12$, $p<0.05$) when monkeys were using asymmetrical gaits on the flat runway, indicating monkeys tended to travel more quickly as body size increased. Again, few developmental differences in forelimb segment angles were observed. When controlling for relative, but not absolute, speed, larger monkeys used slightly more retracted forelimb postures at lift-off, thus significantly increasing forelimb angular excursion. Larger monkeys also used slightly more protracted arm postures at touchdown and less retracted arm postures at liftoff, although the latter trend was not significant when controlling for absolute speed. Size-related differences in two-dimensional elbow angles were more pronounced. Elbow flexion at mid-stance and elbow yield were slightly greater in larger individuals when monkeys were traveling at similar relative, but not absolute, speeds. Elbow flexion at peak vertical force and elbow extension at liftoff significantly increased with size. Changes in three-dimensional elbow angles paralleled the patterns observed in the two-dimensional data set, although the trends did not always reach significance. Wrist postures at peak vertical force did not change with size.

TABLE 2.10 HERE

Aside from slight, but significant, decreases in angular excursion with increasing size, there were no significant size-related changes in hind limb kinematics. Changes in thigh kinematics were more pronounced, most likely as a result of developmental differences in knee postures (see below). Due to relatively strong decreases in protraction angles at touchdown and only slight increases in retraction angles at liftoff, thigh angular excursion significantly decreased with size. Knee postures at touchdown, mid-stance and lift-off became significantly more extended during growth, although only touchdown and mid-stance comparisons remained significant when controlling for absolute speed. Corrected knee angles paralleled the trends seen in the two-dimensional data set, although the trends were not always significant. Ankle postures at peak vertical force did not change during development.

Relative forelimb SRF magnitudes significantly decreased during growth, and forelimb SRF angles became more caudally directed. Relative hind limb SRF magnitudes significantly increased with size, although this trend was only significant when controlling for relative speed. Few size-related trends in relative joint moment arms were evident for either the forelimb or hind limb. Regardless of scaling method, relative shoulder moment arm lengths tended to slightly increase with body size when controlling for absolute, but not relative, speed. Hip joint moment arms significantly increased when scaled to the cube root of body mass, but not when scaled to effective limb length. When scaled to body mass, shoulder joint moments increased with size only when monkeys were traveling at the same absolute speed, whereas elbow joint moments increased only when monkeys were traveling at the same relative speeds. When scaled to the product of body weight and effective limb length, wrist joint moments significantly declined with body size; all other forelimb joint moments remained isometric. In the

hind limb, hip and ankle moments significantly increased with size when scaled to body mass. When scaled to the product of body weight and effective limb length, however, only the increase in hip joint moments remained significant.

2.3.2.3. Symmetrical strides on the pole

Pearson product-moment correlations and partial correlations for symmetrical strides on the pole are shown in Table 2.11. Body size was significantly negatively correlated with absolute speed ($r=-0.20$, $p<0.01$) and relative speed ($r=-0.27$, $p<0.001$), indicating that larger monkeys traveled more slowly when using symmetrical gaits on the pole. Forelimb and hind limb kinematics displayed several significant size-related trends. Forelimb and arm protraction and retraction increased with body size, leading to significant increases in angular excursion. In both the two- and three-dimensional datasets, elbow postures became more flexed at mid-stance and peak vertical force as body size increased, leading to greater elbow yield over a step. Elbow postures at liftoff appeared to become slightly more extended at liftoff in the two-dimensional dataset. However, correction for out-of-plane movement indicated that liftoff postures actually became more flexed as monkeys aged. Wrist postures at peak vertical force did not change with size.

TABLE 2.11 HERE

Comparable developmental trends were evident for hind limb segmental and joint kinematics. Larger and older individuals used significantly more protracted hind limb and thigh postures at touchdown and more retracted postures at lift-off, leading to an increase in overall hind limb and thigh angular excursion. Two-dimensional knee angles became slightly more extended at touchdown and more flexed at mid-stance and at peak vertical force, leading to size-related increases in knee yield. Correction for out-of-plane movement suggested that knee postures in fact became more flexed at touchdown and that there were no significant size-related trends in knee yield. However, this last result should be viewed with caution given the relatively small sample size for corrected knee yield ($n=13$). As a result of the changes in knee posture, thigh angles at peak vertical force became significantly more protracted. Ankle postures at peak vertical became more flexed as size increased, although this trend was not significant after controlling for absolute speed.

Whereas relative forelimb SRF magnitudes significantly decreased with size, relative hind limb SRF magnitudes significantly increased. No significant developmental changes in SRF angles were observed. Relative two- and three-dimensional elbow joint moment arms significantly increased during growth, regardless of scaling method. After controlling for speed, no other size-related trends in relative fore- or hind limb joint moment arm lengths were observed. Two- and three-dimensional elbow moments significantly increased with size, but only when scaled to body mass. When scaled to the product of body weight and effective limb length, shoulder and wrist joint moments displayed significant declines with increasing body size. Hip joint moments increased with body size, but only when adjusted to body mass. Finally, ankle joint moments significantly increased with both size, irrespective of scaling method.

2.3.2.4. Asymmetrical strides on the pole

Pearson product-moment correlations and partial correlations for asymmetrical strides on the pole are shown in Table 2.12. Body size was significantly positively correlated with absolute ($r=0.40$, $p<0.001$) and relative speed ($r=0.29$, $p<0.001$), indicating that larger monkeys traveled at significantly slower speeds when using asymmetrical strides on the pole. Several significant size-related trends were apparent for both forelimb and hind limb kinematics. Forelimb protraction and retraction increased with size, leading to positive allometry of total angular excursion during development. Elbow postures at touchdown, mid-stance and peak vertical force became more flexed as size increased. Because increases in flexion was more pronounced at mid-stance than at touchdown, elbow yield was also greater among larger monkeys. Due to these size-related increases in elbow flexion, larger monkeys tended to use more retracted arm postures at all points during the step cycle. Wrist postures at peak vertical force became significantly more extended as monkeys grew.

TABLE 2.12 HERE

Hind limb protraction, retraction and angular excursion significantly increased with body size. Thigh retraction and angular excursion were also significantly greater among larger monkeys. Additionally, hind limb and thigh postures also became more protracted at peak vertical force, relative to a more neutral position in smaller individuals. Uncorrected (i.e., two-dimensional) knee postures became more extended at touchdown and more flexed at mid-stance and peak vertical force. As a result, knee yield increased with body mass. Due to small available sample sizes, no significant trends in three-dimensional knee angles were observed. Ankle postures at peak vertical force did not significantly change with size.

Forelimb SRF magnitudes significantly decreased with body size. In contrast to all other substrate-gait conditions, hind limb SRF magnitudes remained isometric. Most likely as a result of changes in hind limb positioning at peak vertical force, hind limb SRF angles were significantly negatively correlated with body mass, indicating that the SRF vector was more vertically oriented in larger monkeys. However, this trend was not significant after controlling for absolute speed. Regardless of scaling method, relative elbow joint moment arms lengthened with body mass. In contrast, relative wrist joint moment arms became shorter, most likely as a consequence of size-related increases in wrist extension. No other significant changes in forelimb or hind limb moment arm length were observed. When scaled to body mass, elbow, hip and ankle joint moments increased with size. When scaled to the product of body weight and effective limb length, however, none of these trends remained significant and wrist joint moments displayed significant negative allometry.

2.3.3. Joint moment arm length: covariation with limb length and posture

The results of hierarchical partitioning and path analyses of the effects of limb length and posture on shoulder, elbow, hip and knee moment arm lengths are presented graphically in Figures 2.7-2.10. The direct, indirect and total effects of limb lengths on moment arm lengths, as implied by the path models, are shown in Table 2.13. The relatively simple path model described above was generally able to predict correlations among limb lengths, joint postures, limb postures, SRF orientations and moment arm lengths very well, irrespective of joint, gait or substrate. In almost all cases, chi-squared

values were not significant, GFI were greater than 0.95 and RMSEA did not significantly deviate from 0.05. The only exception was the knee joint during asymmetrical strides on the ground, where the chi-squared value just reached significance (p=0.05) and the GFI equaled 0.947. However, according to the criteria listed in Schermelleh-Engel et al. (2003:52), a model with these parameters still represents a "good fit".

TABLE 2.13 HERE

2.3.3.1. Shoulder joint moment arms

Forelimb length, arm angle, forelimb angle and forelimb SRF angle were collectively able to explain 97.5-98.8% of the variance in shoulder moment arm lengths across the ontogenetic sample (Fig. 2.7). Forelimb angle and SRF direction were consistently the best predictors of shoulder moment arm length, irrespective of gait or substrate. Together, these two variables were able to explain 80.6-94.0% of moment arm variance. As predicted, forelimb and SRF angles were negatively correlated. Increases in forelimb angles and concomitant decreases in SRF angles resulted in smaller shoulder joint moment arms. This result supports the notion that a more protracted forelimb places the shoulder joint more in line with the SRF vector, thus mitigating moment arms and moments.

FIGURE 2.7 HERE

Forelimb length was able to explain just 2.2-7.1% of the variance in shoulder moment arm length. Contrary to my predictions, longer forelimbs were positively associated with arm flexion at peak vertical force. Additionally, although the use of more extended joint postures was predicted to shorten joint moment arms across joints, increases in arm extension were weakly associated with an unexpected increase in shoulder moment arm lengths. Across conditions, most of the total correlation between forelimb length and shoulder moment arm length was due to the direct effects of forelimb length (Table 2.13). A negative correlation between forelimb length and arm angle, combined with the positive effect of arm angle on moment arm lengths, resulted in a negative indirect effect for forelimb length (i.e., effects of limb length due to association with arm angle), thus mitigating the total correlation between forelimb length and shoulder moment arm lengths. In sum, longer forelimbs were weakly associated with increases in shoulder joint moment arms lengths, and this relationship is made even weaker when the effects of limb length on arm posture are included in the model.

2.3.3.2. Elbow joint moment arms

Forearm length, elbow angle, forelimb angle and forelimb SRF angle were able to explain 84.9-87.1% of the variance in elbow moment arm lengths (Fig. 2.8). Across most gait and substrate conditions, elbow joint angle explained most of the variance in elbow moment arm length. The only exception was during symmetrical strides on the ground, where forelimb posture was able to explain a higher percentage of the variance (37.7% for forelimb angle versus 26.8% for elbow angle). In each condition, forearm length followed elbow posture as the next best predictor of elbow moment arm length, explaining between 11.8% and 27.8% of the variance. Together, forearm length and elbow angle were able to explain more than half of the variance in elbow moment arm length in all conditions except for symmetrical strides on the ground.

FIGURE 2.8 HERE

As predicted, increases in forearm length, elbow flexion, forelimb protraction and forelimb SRF inclination all led to longer elbow moment arms. Contrary to my predictions, forearm length and elbow angle were negatively correlated, irrespective of gait or substrate. Therefore, forearm length exerted a relatively strong positive direct effect on elbow moment length as well as a strong positive indirect effect due to the tendency of longer-limbed monkeys to use more flexed elbow postures. Due to the strong direct and indirect effects of forearm length, the total association between limb length and moment arm length at the elbow was greater than at any other joint (Table 2.13).

2.3.3.3. Hip joint moment arms

Together, hind limb length, thigh angle, hind limb angle and hind limb SRF angle were able to explain 97.9-98.9% of the variation in hip moment arm lengths across the ontogenetic sample (Fig. 2.9). Hind limb and SRF angles were consistently the best predictors, together explaining between 67.7% and 81.1% of the variance in hip moment arm length. As predicted, increases in total hind limb length were associated with longer hip joint moment arms. However, the explanatory power of hind limb length was generally very weak. In almost all gait and substrate conditions, hind limb length was unable to explain a significant portion of moment arm variance. The one exception was asymmetrical strides on the ground, where 13.2% of the variation in hip moment arm length was attributable to changes in hind limb length. The greater explanatory power of hind limb length in this case may simply be due to the relatively minimal variance in hind limb kinematics (see Table 2.10).

FIGURE 2.9 HERE

As predicted, longer hip moment arms were associated with greater hind limb protraction at peak vertical force and a more cranial inclination of the hind limb SRF. Additionally, the predicted relationship between thigh angles and hip moment arms was upheld, with more extended thigh positions exerting a weak, but significant, negative effect on hip moment arm length. Because longer-limbed individuals tended to use more extended thigh postures, shortening hip joint moment arms, the slight positive direct effect of hind limb length was mitigated, leading to lower total correlations between hind limb length and hip moment arm length (Table 2.13).

2.3.3.4. Knee joint moment arms

Leg length, knee angle, hind limb angle and hind limb SRF angle were able to explain 92.5-97.6% of the variance in knee joint moment arm lengths (Fig. 2.10). Most of the variation in moment arm lengths was again attributable to the combination of hind limb posture and SRF angle, which together explained between 56.5% and 70.4% of moment arm variance. As predicted, decreases in knee moment arm lengths were associated with greater hind limb protraction and a more cranial orientation of the hind limb SRF. Knee joint posture was the second best predictor, explaining 19.9-34.7% of the variance in moment arm length across the sample. As predicted, increasing knee extension shortened knee moment arm lengths.

FIGURE 2.10 HERE

Leg length was consistently a poor predictor of moment arm length, explaining just 1.4-7.2% of the variance. Contrary to my predictions, longer-legged individuals

tended to use more flexed knee postures, thus increasing knee joint moment arms. Because the direct effect of knee posture on moment arm length was much stronger than the direct effect of leg length, most of the total correlation between leg length and knee moment arm length could be attributed to indirect effects operating *via* knee joint posture (Table 2.13).

2.3.4. Joint moments: covariation with body weight and limb length

Calculated slopes, 95% confidence intervals on these slopes and coefficients of determination from regressions of shoulder, elbow, hip and knee moments on the product of body weight and limb length below each joint are presented in Table 2.14. Limb length and body weight were consistently poor predictors of joint moment magnitudes. Regardless of joint, gait type, or substrate, predicted joint moments always overestimated actual joint moments (i.e., slopes were significantly less than 1.0). Predicted and actual joint moments were most congruent at the elbow joint. This was particularly true when monkeys were using asymmetrical gaits, where actual moments scaled to predicted moments with a slope of 0.666 for ground strides and 0.794 for pole strides. At all other joints, predicted joint moments overestimated actual moments by a factor of at 2.5 or more. Moreover low R^2 values for most regressions indicate that the relationship between predicted and actual joint moments was quite variable. Predicted joint moments never explained more than 64.2% of the variance in actual joint moments. If elbow data are excluded, no more than 50.4% of the variance in joint moments was attributable to differences in body weight and limb length.

TABLE 2.14 HERE

2.4. Discussion

2.4.1. Ontogenetic allometry of joint postures and moment arms in S. boliviensis

Growing squirrel monkeys displayed several size-related changes in joint kinematics. When traveling on the pole, larger monkeys significantly increased forelimb protraction at touchdown and retraction at liftoff, leading to greater forelimb angular excursions. In all gait and substrate conditions except for symmetrical strides on the ground, larger monkeys also used more flexed elbow postures at mid-stance and peak vertical force, thus increasing elbow yield from touchdown to mid-stance. Similar changes were evident in hind limb kinematics. In all conditions except for asymmetrical gaits on the ground, larger monkeys significantly increased hind limb protraction and retraction, leading to larger total angular excursions as size increased. Knee flexion at mid-stance and peak vertical force increased with size when monkeys were using symmetrical gaits on the ground and during all locomotion on the pole. Wrist and ankle postures at peak vertical force changed relatively little. When traveling on the pole, larger monkeys used more extended wrist postures during asymmetrical gaits and more flexed ankle postures during symmetrical gaits. However, the latter correlation was not significant after controlling for absolute speed. Collectively, these data indicate that smaller, younger monkeys tended to use more extended joints with reduced limb excursions, compared to the more "compliant" gait of older and larger monkeys (McMahon, 1985; Farley et al., 1993; Schmitt, 1994, 1999). Increased joint flexion may have permitted older and heavier monkeys to lower their center of gravity relative to the

substrate, thus increasing stability when walking on arboreal supports (Napier, 1967; Schmitt, 1994, 1999, 2003c; Stevens, 2003). Relatively crouched postures also permit squirrel monkeys and other small mammals (i.e., less than 1 kg in body mass) to use the limbs as "shock absorbers" when navigating variable terrain or make quick adjustments to speed and direction (Jenkins, 1971, 1974; Biewener, 1983; Fischer, 1994; Fischer et al., 2002; Reilly et al., 2007).

Ontogenetic changes in joint postures were sufficient to impact the relative length of joint moment arms. Moment arm lengths at several joints, particularly in the forelimb, were relative shorter in younger monkeys. Relative shoulder and hip joint moment arms increased with body size when monkeys were using asymmetrical gaits on the ground. When monkeys were traveling on the pole, relative elbow joint moment arms increased with size regardless of gait type, whereas relative wrist joint moment arms decreased with size during asymmetrical gaits. With the exception of the size-related increases in hip joint moment arms during asymmetrical strides on the ground (which were only significant when scaled to the cube root of body mass), all allometric changes in moment arm lengths were significant regardless of scaling method (i.e., cube root of body mass or effective limb length).

Previous studies of postural development have indicated marked variability between taxa. Among vervet monkeys, cats, tree shrews, chickens and humans, early locomotor efforts are characterized by increased joint flexion (Peters, 1983; Vilensky and Gankiewicz, 1989; Howland et al., 1995; Muir et al., 1996; Schilling, 2005; Hallemans et al., 2006a; Hallemans et al., 2006b). Increased flexion during early locomotion has also been qualitatively noted for tufted capuchin monkeys (*Cebus apella*: Fragaszy, 1990), rhesus macaques (*Macaca mulatta*: Hildebrand, 1967), Japanese macaques (*Macaca fuscata*: Nakano, 1996), and chimpanzees (*Pan troglodytes*: Kimura, 1987). Among other animals, such as rats and desert iguanas, young individuals use more extended limb postures than older individuals and adults (Westerga and Gramsbergen, 1990; Irschick and Jayne, 2000). Finally, some animals, such as cuis and baboons, show a combination of patterns, increasing flexion at some joints and extension at others (Schilling, 2005; Zeininger, 2007). Excessive joint flexion during early locomotor efforts has usually been attributed to underdeveloped postural muscles and a poorly organized motor control system (Tomanek, 1975; Vilensky and Gankiewicz, 1989; Howland et al., 1995; Jouffroy and Medina, 1996; Muir et al., 1996; von Mering and Fischer, 1999; Bewick et al., 2004; Jouffroy and Medina, 2004; Schilling, 2005). On this account, weak and poorly coordinated extensor muscles cause the limb joints to collapse into flexion during stance phase. However, with the exception of Hallemans and colleagues' (2005, 2006) recent studies on the ontogeny of human walking, previous studies have not explicitly considered the implications of postural development on moment arms and joint loading during ontogeny. Translating postural changes into requisite muscle force necessitates the explicit consideration of SRF magnitude and direction. Only the current study and recent work by Hallemans and colleagues (2005, 2006) have considered these factors, and the current study is the first to do so in quadrupeds. Nevertheless, the data presented in this study show that postural changes in joint angles and limb placement relative to the vertical axis explained 50-75% of the variation in moment arm length among growing squirrel monkeys, irrespective of limb length or SRF direction. Therefore, it is likely that flexed joint postures during early locomotion are sufficient to significantly lengthen joint

moments arms in the species discussed above. Provided SRF magnitudes scale isometrically during growth, as is the case in at least of few animals (see below), joint moments are likely to be greater as well. These observations support Carrier's (1983) and Young's (2005) assumption that compensatory growth patterns, such as negative ontogenetic allometry of body lever arm lengths leading to greater anatomical mechanical advantage at early ages, would be required for young mammals to overcome ontogenetic limits on performance. Without morphological compensation, locomotor ability would be compromised, and young animals would likely be dependent on adults during rapid or extended transport.

Why, then, do young squirrel monkeys differ from most other animals in habitually using more extended joint postures relative to older and larger individuals? It should be noted that the youngest monkeys in my sample were already 10 weeks old. Perhaps a different pattern would have emerged had I included even younger ages. However, the goal of this research was to examine size-related changes in joint mechanics once monkeys began traveling independently. Although infant squirrel monkeys are precocial relative to other primates, they still do not attempt independent locomotion for the first four weeks after birth and do not begin foraging until seven weeks of age (Elias, 1977; Kaack et al., 1979; Boinski and Fragaszy, 1989; Fragaszy et al., 1991). Therefore, including younger monkeys in my sample would not have been ecologically relevant. Rather, it seems likely that the observed kinematic trajectories represent behavioral compensation for ontogenetic limits on locomotor performance. Among the taxa reviewed above, most animals showing increased joint extension and reduced limb excursions early in life are also relatively precocial in their locomotor development. Cuis and desert iguanas must locomote independently soon after birth (Irschick and Jayne, 2000; Schilling, 2005). Although rats and tree shrews are born in an altricial state, rats show mature gait patterns only 20 days after birth and tree shrews are weaned and independent by 39 days after birth (Westerga and Gramsbergen, 1990; Schilling 2005). Path analyses and hierarchical partitioning (see Figs. 2.7-2.10) of the current dataset emphatically demonstrated that walking with erect, strut-like limbs – where the SRF vector is aligned with the limb's axis – was the most effective way of shortening SRF moment arms among developing squirrel monkeys (also see Carrier et al., 2007). Postural adjustments of SRF moment arms have also been cited as the primary means of mitigating limb muscle force requirements between gaits within individuals (Biewener, 2004), between differently sized individuals within the same species (Polk, 2001, 2002, 2004; Gruss, 2007), and between differently sized species (Biewener, 1983, 1989, 1990, 1991; Polk, 2002; but see Day and Jayne, 2007). In sum, extended joints and reduced limb excursions may constitute an effective behavioral means for fast-developing animals to shorten joint moment arms, reduce joint loading, and limit the muscle force required to maintain joint postures. To address the generality of this hypothesis, future studies should include animals encompassing a diverse array of life history strategies, sample a wider range of age stages (i.e., not just young infants and adults) and incorporate both kinematic and kinetic measures of locomotor development.

2.4.2. Ontogenetic allometry of SRF vectors in S. boliviensis

Relative forelimb SRF magnitudes (adjusted to body weight) consistently declined as body size increased, regardless of gait type or substrate. In contrast, in all

gait and substrate conditions except for asymmetrical gaits on the pole, relative hind limb SRF magnitudes tended to increase with body size, although this trend was only significant during symmetrical gaits. The net effect of these changes was that whereas younger squirrel monkeys were "forelimb dominant" in limb force distribution, older monkeys were "hind limb dominant". Hind limb dominance of limb force distribution (i.e., greater hind limb than forelimb peak vertical forces) is often cited as one of the chief characteristics distinguishing primate quadrupedal locomotion from that of other mammals (e.g., Kimura et al., 1979; Demes et al., 1994; Larson, 1998; Schmitt and Lemelin, 2002; Schmitt, 2003a; Li et al., 2004; Schmitt and Hanna, 2004; Schmitt and Lemelin, 2004). Kimura (1987; 2000) examined the ontogeny of vertical peak force distribution in chimpanzees and Japanese macaques. The typical primate pattern of hind limb dominance in body weight support was evident in chimpanzees throughout development and in macaques from three months of age onwards. Prior to this age, infant macaques distributed vertical peak forces equally between the forelimbs and hind limbs. A generalized biomechanical explanation for primates' unique mode of limb force distribution remains elusive (but see Gray, 1944; Reynolds, 1985a, 1985b; Schmitt, 1994, 1999; Schmitt and Hanna, 2004; Raichlen et al., 2007). The factors underlying the ontogenetic changes in limb force distribution in the current sample is more fully explored in Chapter 4.

Kimura (1987, 2000) also found that relative forelimb and hind limb vertical forces (scaled to body weight) were significantly greater among younger chimpanzees and macaques. However, Kimura's (1987, 2000) analyses did not control for the effects of speed. If younger individuals were traveling at faster relative speeds than older individuals and adults, this may account for the apparent differences in relative force magnitudes. Nevertheless, studies of human locomotor development have documented similar patterns of relatively decreasing vertical SRF magnitudes with increasing age, even after controlling for the effects of speed (Beck et al., 1981; Diop et al., 2005). Additionally, using an approximation of SRF based on average limb contact time, Pennycuick (1975) estimated that free-ranging infant gnus (*Connochaetes taurinus*) experience significantly greater peak forces than adults traveling at identical speeds

In contrast, other studies of a small, but diverse, group of animals have documented isometric variation in SRF magnitudes during ontogeny. Main and Biewener (2004; 2007), found that SRF magnitudes scaled in direct proportion to body weight in growing goats (*Capra hircus*) and emus (*Dromaius novaehollandiae*). Hallemans et al. (2006a) found that size-adjusted peak vertical and propulsive forces were similar among newly walking infants and adults, although size-adjusted peak mediolateral forces were significantly greater among infants. As indicated by the level of variation between different species and between different studies of the same species (i.e., humans), greater research on the patterns and causes of ontogenetic variation in SRF magnitudes is clearly needed.

When monkeys were traveling on the ground, SRF angles significantly decreased (i.e., became more caudally oriented) as body size increased, indicating that SRF vectors pointed more vertically in smaller, younger individuals. During asymmetrical strides on the pole, hind limb SRF angles tended to become less cranially oriented, (i.e., more vertical) as body size increased, although this trend was not significant after controlling for differences in absolute speed. Decreasing forelimb SRF angles indicate that the ratio

of braking force to vertical force (at the moment of peak vertical force) tended to increase with size. Therefore, size-related decreases in relative forelimb vertical peak forces, if not matched by decreases in relative braking forces, could cause a significant reorientation of the force vector. Alternatively, because SRF orientation was generally highly correlated with limb positioning (see Figs. 2.7-2.10), changes in forelimb position could account for the observed decrease in SRF angles. However, whereas larger monkeys used significantly more protracted limbs at peak vertical force during symmetrical gaits on the ground, forelimb position at peak vertical force did not change during asymmetrical gaits on the ground. In any case, ontogenetic changes in SRF orientations were minimal relative to changes in SRF magnitudes. Main and Biewener (2007) also found that SRF orientations changed minimally during emu ontogeny.

2.4.3. Ontogenetic allometry of joint moments in S. boliviensis

Ontogenetic variation in joint postures, moment arm lengths and SRF magnitudes significantly impacted relative joint moments in several of the gait and substrate conditions tested here. When scaled to body mass, moments at several forelimb and hind limb joints increased with size, including shoulder moments during asymmetrical gaits on the ground, elbow moments during all locomotion on the pole, and hip and ankle moments across all gait and substrate conditions. Size-related increases were documented in eleven of the twenty-four joint by gait by substrate comparisons (i.e., six joints × two gait types × two substrates). In the remaining thirteen comparisons, joint moments scaled isometrically to body mass. Because relative forelimb SRF magnitudes significantly declined with body size in all conditions, increases in relative shoulder and elbow moments were entirely due to postural influences on moment arm lengths. Hip and ankle moment arm lengths changed minimally during development. Therefore, size-related increases in joint moments likely resulted from relatively greater hind limb SRF magnitudes.

Assuming that muscle force and muscle moment arm lengths scale isometrically to body mass, increases in mass-scaled joint moments suggest that younger (i.e., smaller) monkeys would require proportionally less muscle force to maintain joint postures. Although previous studies have found that muscle mass typically doubles during mammalian growth (Goldspink, 1980; Atzeva et al., 2007), biomechanical theory suggests that young squirrel monkeys would still require relatively less muscle force to maintain posture. A doubling of whole body muscle mass would cause muscle force to scale to body mass with an exponent closer to 1.3 than 1.0 (i.e., $\propto M_b^{1.3}$). Therefore, available muscle force should scale $\propto M_b^{0.87}$ (i.e., $M_b^{1.3} \times M_b^{0.67}$), and muscle moments should scale $\propto M_b^{1.2}$ (i.e., $M_b^{0.87} \times M_b^{0.33}$), still less than the isometric expectation for SRF moments of $\propto M_b^{1.33}$. Moreover, provided muscle fiber length tracks limb length during growth, pervasive positive allometry of limb growth (see below) suggests that at least part of the observed ontogenetic increases in muscle mass may be due to allometric increases in fiber length. Therefore, strong positive allometry of muscle mass may not necessarily translate into strong positive allometry of muscle cross-sectional area and, consequently, muscle force. In sum, given the available data, positive allometry of mass-scaled joint moments suggests that young squirrel monkeys were able to use a combination of postural changes and shifts in body weight distribution to mitigate joint loading, thereby overcoming ontogenetic limits on locomotor performance. Interestingly,

the joints showing the most pervasive patterns of positive allometry – the elbow, hip and ankle joints – also experienced the absolutely greatest moments, even after controlling for body mass and speed influences (Fig. 2.6). Reducing the required muscle force to maintain posture at these joints would be particularly advantageous.

Allometric patterns were more difficult to interpret when joint moments were scaled to the product of body weight and effective limb length. Size-related increases were only found in four of the twenty-four comparisons: relative hip moments during symmetrical and asymmetrical strides on the ground and relative ankle moments during symmetrical strides on the ground and the pole. Size-related decreases were found in six of the twenty-four comparisons, including shoulder moments during symmetrical strides on the pole, elbow moments during symmetrical strides on the ground, and wrist moments in all four gait and substrate conditions. Relative joint moments scaled isometrically in the remaining fourteen comparisons. If the goal of scaling is to gauge the efficacy of available muscle moments as body size increases, dividing SRF moments by the product of body weight and limb length will over-adjust for size (Polk, 2001). Therefore, ontogenetic increases in relative hip and ankle moments indicate that older and larger monkeys would require substantially more muscle force to maintain hind limb posture. Negative allometry of forelimb joint moments was most likely due to ontogenetic decreases in forelimb SRF magnitudes. However, given the tendency of this scaling method to overcompensate for size differences, these patterns do not necessarily indicate that young monkeys require relatively more forelimb muscle force to maintain posture.

2.4.4. Limb growth and joint mechanics in developing mammals

Squirrel monkey limb growth during the first 10 months of life was characterized by extremely strong positive allometry, indicating that young monkeys have relatively short limbs for their size (Table 2.8). Because correlation coefficients were not extremely high, LS slopes were consistently lower than RMA values (Jungers, 1985). Nevertheless, strong positive allometry of limb growth obtained regardless of line-fitting method. Stronger positive allometry of forelimb segment lengths resulted in significant increases in the intermembral index during growth. This pattern distinguishes squirrel monkeys from most other primates, who typically show ontogenetic decreases in the intermembral index (Schultz, 1956; Aiello and Dean, 1990; Falsetti and Cole, 1992; Schaefer and Nash, 2007). By contrast, across primate species, increasing body size is typically associated with increasing intermembral indices (Jungers, 1985).

In order to place squirrel monkey limb growth data in a broader context, data on ontogenetic allometry of limb growth in other primates and mammals were collated from the literature and are presented in Tables 15 and 16. A comparison of my results to previous studies shows that RMA scaling exponents describing squirrel monkey arm and forearm growth are the greatest yet documented for any mammal. Although measuring bone length from directly radiographs might have provided a better test of growth allometry, external measurements tend to underestimate actual bone lengths (Gruss, 2007), suggesting that my data may in fact be conservative. Only capuchin monkeys (*Cebus albifrons* and *Cebus apella*), platyrrhine monkeys belonging to the same family as squirrel monkeys (Cebidae), show limb growth exponents of similar magnitude. These data, though sparse, suggest that strong positive allometry of limb growth may be unique

to platyrrhines or even just to cebids (also see Levitch, 1987). More longitudinal studies of growth allometry in cebids and other platyrrhine primates are needed to test this hypothesis.

TABLE 2.15 HERE

TABLE 2.16 HERE

Although the magnitude of squirrel monkey limb growth allometry is unique, positive allometry of limb growth is typical of most mammals. Among primates, the proximal and middle limb segments (i.e., stylopodia and zeugopodia) grow with positive allometry in almost every species studied. Species showing isometry or negative allometry are either adapted for vertical clinging and leaping (i.e., sifakas: *Propithecus spp.*), a very peculiar form of arboreal locomotion, or are more terrestrial than most other primates (i.e., baboons: *Papio cynocephalus*). With the exception of tree shrews (*Tupaia glis*), all non-primate mammalian species that display consistent isometry or negative allometry of long bone growth are behaviorally precocial, requiring them to stand and locomote with adults soon after birth (i.e., chinchillas: *Chinchilla lanigera*, cuis: *Galea musteloides*, and pigs: *Sus domesticus*). In these species, relatively longer limbs would allow perinatal animals to keep pace with older and larger conspecifics during extended periods of terrestrial travel and evade predation (Howell, 1944; Pennycuick, 1975).

Pervasive positive allometry of proximal and middle limb segment growth may, in itself, constitute an independent solution to ontogenetic limits on locomotor performance. Provided joint postures and relative SRF magnitudes do not appreciably change with size, relatively shorter limbs would shorten SRF joint moment arms, thereby mitigating SRF joint moments in younger individuals (Polk, 2002; Gruss, 2007). The assumption that limb growth determines SRF moment arms and moments motivated Carrier's (1983) and Young's (2005) morphometric analyses of developmental joint mechanics. However, the data presented here failed to show a strong direct link between limb length and joint moments in growing squirrel monkeys, despite strong positive allometry of limb growth. Excluding the elbow joint, limb length never explained more than 13.2% of the variance in moment arm length (Figs. 2.7-2.10) and the product of limb length and body weight, Carrier's (1983) and Young's (2005) proxy for joint moments, never explained more than 50.4% of the variance in joint moments (Table 2.14). Compared to the other segments, forearm length was a better predictor of elbow mechanics, perhaps due to the strong positive allometry of forearm growth. Forearm length explained 11.8-27.8% of the variance in elbow moment arm length and the product of forearm length and body weight explained as much as 64.2% of the variance in elbow moments.

The current results do not necessarily invalidate Carrier's (1983) and Young's (2005) morphometric approach. Predicted joint moments (i.e., the product of limb length and body weight) consistently overestimated actual joint moments, regardless of joint, gait type or substrate. Therefore, because external joint dimensions are generally a good predictor of muscle moment arm lengths (Biewener et al., 2004), negative scaling of anatomical mechanical advantage (i.e., bony muscle lever length/limb length) should still conservatively estimate ontogenetic changes in actual, or effective, mechanical advantage. Nevertheless, the current study showed that ontogenetic changes in joint postures and weight distribution alone were sufficient to mitigate joint loading in growing squirrel monkeys. Therefore, the status of "compensatory" growth trajectories as

generalized mammalian adaptations to ontogenetic limits on locomotor performance may be suspect, at least among species characterized by similar patterns of locomotor development. Morphological adaptations to ontogenetic limits on locomotion may be more critical for animals characterized by more flexed limb postures early in life or in species where young are under extreme selective pressure to accelerate quickly to evade predation - such as the jackrabbits studied by Carrier (1983). Additional ontogenetic studies of joint mechanics in a variety of primates and other mammals would be required to test this hypothesis.

Whereas the proximal and middle limb segments typically grow with positive allometry, autopodia (i.e., hands and feet) scale to body size with negative allometry or isometry in almost all mammals yet studied. Negative allometry of hand and foot size has been interpreted as an adaptation allowing young primates to cling to their mothers and young quadrupeds in general to negotiate "adult-sized" substrates and maintain a larger, more secure base of support (Jungers and Fleagle, 1980; Raichlen, 2005b). In a recent study combining morphometric and quantitative genetic approaches, Lawler (2006) was able to show that juvenile hand and foot size were undergoing active directional selection in a population of Verreaux's sifaka (*Propithecus verreauxi*), suggesting that patterns of negative allometry are in fact adaptive. There may, however, be a cost associated with relatively larger hands and feet – by lengthening the moment arm of the SRF, longer segments may increase joint moments at the wrist and ankle. Although limb length had a minimal effect on most joint moments in the current study, I was unable to document patterns of hand and foot growth. Future studies should combine allometric analyses of these segments with the detailed kinematic and kinetic techniques used here.

2.4.5. Summary and conclusions

I sought to answer three questions in this study. First, among growing squirrel monkeys, do joint postures, SRF magnitudes, SRF orientations, SRF joint moment arms and SRF joint moments vary ontogenetically? Second, what proportion of the ontogenetic variance in moment arm length can be attributed to limb growth? Finally, how well does the product of limb length and body weight predict actual variation in joint moment magnitudes? Following previous studies, I hypothesized that joint posture and loading would remain isometric over development and limb length and body weight would explain a large part of the variation in joint moment arm lengths and moments. Contrary to my hypotheses, joint postures changed significantly during development, with older and larger squirrel monkeys using more crouched limb postures compared to the stiffer, more upright gaits of younger monkeys. Although joint moment arm lengths tended to remain isometric over development, size-related increases in limb excursions and joint flexion resulted in relatively longer joint moment arms in four of the twenty-four joint by gait by substrate comparisons examined. In nearly half of the twenty-four comparisons, ontogenetic changes in moment arm lengths, combined with shifts in body weight distribution, led to significant size-related increases in shoulder, elbow, hip and ankle joint moments scaled to body mass. When scaled to the product of body weight and effective limb length, relative joint moments tended to remain isometric, although some significant size–related decreases in forelimb joint moments and increases in hind limb joint moments were observed, depending on gait type and substrate. In sum,

extended joint postures and shifts in weight distribution frequently allowed young squirrel monkeys to mitigate joint loading relative to older and larger individuals, even when traveling at the same absolute speed. Contrary to my predictions, anatomical limb length and body weight were consistently poor predictors of actual variation in moment arm lengths and moments, indicating the importance of incorporating kinematic and kinetic measures of locomotor development when studying the ontogeny of limb joint mechanics.

This study was the first attempt to simultaneously quantify ontogenetic changes in body size, limb length, joint posture and joint loading in any quadrupedal mammal. My results show that modeling the ontogeny of joint mechanics is a complex problem that requires simultaneous understanding of morphological, kinematic and kinetic data. For this reason, it is critical that future studies incorporate additional mammalian taxa, displaying a variety of morphological and behavioral growth trajectories, and include additional types of data, such radiographic and histological studies of skeletal and muscular development.

2.5. Tables

Table 2.1. Total number of ground strides sampled at each age (in days) and body mass (in grams) for each subject.

ID	Age	Body mass	Strides	ID	Age	Body mass	Strides
4428	120	379	14	4466	280	483	12
	127	384	4				
	131	410	4	4475	93	219	14
	139	396	2		99	221	12
	158	427	1		104	218	15
	175	445	1		112	243	13
	189	458	11		132	262	15
	204	488	12		147	286	12
	216	495	14		162	305	20
	244	510	9		181	337	16
	260	532	9		190	346	20
	272	518	11		220	353	11
	288	533	5		230	386	14
	302	535	4		247	396	13
					261	378	12
4433	156	370	2		272	430	10
4445	128	341	4	4483	74	237	6
	167	372	3		76	232	11
	180	385	4		82	251	8
	195	402	7		87	240	9
	237	409	7		96	275	8
	251	415	12		116	293	16
	268	462	8		130	316	1
	282	442	11		145	354	16
					164	370	18
4466	118	345	10		173	386	15
	140	373	9		199	361	9
	157	399	9		215	404	13
	181	447	12		229	409	13
	195	450	7		248	430	7
	225	427	8		259	442	10
	239	400	10				
	258	461	11				

Table 2.2. Total number of pole strides sampled at each age and body mass for each subject.

ID	Age	Body mass	Strides	ID	Age	Body mass	Strides
4428	153	413	22	4475	267	424	14
	167	438	20				
	209	499	16	4483	112	305	24
	224	491	8		123	312	20
	251	511	10		138	332	11
	263	520	13		158	367	20
	281	525	9		180	390	18
	293	522	7		208	387	12
					223	403	13
4433	150	375	15		241	394	9
					252	438	7
4445	145	320	4				
	160	351	4				
	177	380	3				
	202	407	10				
	214	412	8				
	244	408	7				
	262	436	6				
	275	445	13				
4466	133	380	18				
	148	383	12				
	168	410	13				
	206	447	17				
	232	423	10				
	252	446	9				
	262	453	9				
	276	474	8				
4475	128	268	23				
	143	276	30				
	155	295	22				
	175	334	11				
	198	355	17				
	237	400	16				
	253	400	16				

Table 2.3. Anatomical landmarks used to approximate joint centers of rotation in the sagittal plane.

Joint	Anatomical landmark
Shoulder	Midpoint between the acromion process of the scapula and the greater tubercle of the humerus
Elbow	Midpoint between the lateral epicondyle of the humerus and the lateral aspect of the radial head
Wrist	Radial styloid porcess
Hip	Greater trochanter of the femur
Knee	Midpoint between the lateral epicondyle of the femur and the lateral condyle of the tibia
Ankle	Lateral malleolus of the fibula

Table 2.4. Percent of cross talk between force channels, grouped by force platform and substrate.

	Force Platform 1		**Force Platform 2**	
	Runway	Pole	Runway	Pole
Vertical/Fore-aft	1% (±0.1%)	0.7% (±0.1%)	0.7% (±0.1%)	0.3% (±0.2%)
Vertical/Transverse	1.2% (±0.5%)	1.2% (±0.3%)	0.3% (±0.1%)	0.3% (±0.1%)
Fore-aft/Vertical	1.7% (±0.7%)	1.8% (±1.4%)	1.5% (±1.7%)	1.3% (±0.9%)
Fore-aft/Transverse	1.3% (±0.6%)	0.7% (±0.5%)	1.3% (±0.8%)	1.7% (±0.7%)
Transverse/Vertical	3.5% (±0.5%)	10.5% (±2.2%)	0.9% (±0.5%)	5.3% (±1.7%)
Transverse/Fore-aft	0.7% (±0.4%)	1.1% (±1.2%)	0.9% (±0.5%)	1.3% (±0.5%)

Data are presented as Mean (±SD); N runway = 40, N pole = 25.

Table 2.5. Kinematic and kinetic variables used in this study.

Variable	Units	Events	Variable	Units	Events
Segment angles			Sagittal SRF angle	degrees	PK
FL angle	degrees	TD,PK,LO	Total SRF magnitude	N	PK
Arm angle	degrees	TD,PK,LO	*Joint moment arms*		
FL angular excursion	degrees	step	Shoulder moment arm	m	PK
Arm angular excursion	degrees	step	Elbow moment arm[1]	m	PK
HL angle	degrees	TD,PK,LO	Wrist moment arm	m	PK
Thigh angle	degrees	TD,PK,LO	Hip moment arm	m	PK
HL angular excursion	degrees	step	Knee moment arm[1]	m	PK
Thigh angular excursion	degrees	step	Ankle moment arm	m	PK
Joint angles			*Joint moments*		
Elbow angle[1]	degrees	TD,MS,PK,LO	Shoulder moment	N·m	PK
Elbow yield[1]	degrees	step	Elbow moment[1]	N·m	PK
Wrist angle	degrees	PK	Wrist moment	N·m	PK
Knee angle[1]	degrees	TD,MS,PK,LO	Hip moment	N·m	PK
Knee yield[1]	degrees	step	Knee moment[1]	N·m	PK
Ankle angle	degrees	PK	Ankle moment	N·m	PK
Substrate reaction forces					
Sagittal SRF magnitude	N	PK			

See text for details of calculations. FL – forelimb, HL – hind limb, 2D – two-dimensional, 3D – three-dimensional, SRF- substrate reaction force, TD – touchdown, MS – mid-stance, PK – peak vertical force, LO – lift-off, step – calculated across a FL/HL step, stride – calculated across an entire stride.

[1] Measured both in the sagittal plane and three-dimensionally (see text for details).

Table 2.6. Accuracy of kinematic data.

	Touchdown		Mid-stance		Lift-off	
Ground						
Arm	6.9 ± 6.1% (45.6%)	-4.8 ± 3.8% (29.2%)	6.7 ± 6.0% (44.8%)	-4.4 ± 3.7 (32.3%)	7.8 ± 6.8% (44.5%)	-4.9 ± 4.2 (27.3%)
Forearm	6.5 ± 4.4% (60.2%)	-3.2 ± 2.9% (14.6%)	3.5 ± 3.0% (24.8%)	-5.3 ± 3.9% (52.3%)	4.9 ± 4.0% (43.3%)	-4.7 ± 4.5% (28.4%)
Thigh	6.3 ± 4.1% (58.8%)	-2.7 ± 2.2% (20.6%)	6.5 ± 4.1% (62.5%)	-3.2 ± 2.5% (18.8%)	4.7 ± 3.5% (32.3%)	-4.9 ± 3.6% (45.0%)
Leg	4.5 ± 3.5% (52.6%)	-3.2 ± 3.0% (26.9%)	4.2 ± 3.1% (53.4%)	-3.1 ± 2.5% (28.1%)	5.3 ± 3.7% (53.7%)	-2.9 ± 2.9% (23.5%)
Pole						
Arm	9.5 ± 5.8% (40.5%)	-6.6 ± 4.5% (47.0%)	7.8 ± 5.5% (42.9%)	-7.4 ± 4.5% (51.0%)	8.2 ± 6.1% (56.9%)	-4.8 ± 3.7% (38.2%)
Forearm	5.9 ± 4.4% (64.5%)	-4.3 ± 3.5% (23.1%)	2.5 ± 2.1% (11.9%)	-7.8 ± 4.6% (81.8%)	5.2 ± 4.3% (44.9%)	-5.4 ± 4.1% (50.3%)
Thigh	6.4 ± 3.9% (78.2%)	-2.5 ± 1.8% (17.7%)	6.5 ± 4.7% (82.5%)	-2.8 ± 2.6% (14.6%)	4.8 ± 3.3% (58.6%)	-5.0 ± 3.9% (35.0%)
Leg	4.6 ± 3.6% (53.5%)	-2.8 ± 2.4% (42.3%)	4.5 ± 3.5% (53.3%)	-4.2 ± 4.1% (43.8%)	5.7 ± 4.5% (77.8%)	-2.3 ± 2.2% (15.7%)

Cells display the average percentage difference between measured segment length and digitized segment length. Positive values indicate overestimation errors (i.e., digitized segment longer than measured segment); negative values indicate underestimation errors (i.e., digitized segment shorter than measured segment). Data are displayed as mean ± SD. Error frequency, as a percentage of total trials, is shown in parentheses.

Table 2.7. Precision of kinematic and kinetic data.

Variable	Mean	SD	Error CV	IE CV	Variable	Mean	SD	Error CV	IE CV
FL angle					Wrist angle at PK	110.0°	1.9°	1.7%	4.4%
TD	27.4°	0.9°	4.6%	15.0%	2D knee angle				
PK	-8.0°	1.4°	1.2%	320.4%	TD	130.3°	1.4°	1.1%	4.6%
LO	-50.2°	0.9°	1.6%	9.7%	MS	113.7°	1.5°	1.3%	6.7%
Arm angle					PK	110.1°	1.2°	1.0%	6.6%
TD	7.5°	1.4°	6.7%	335.2%	LO	125.2°	2.5°	2.1%	5.7%
PK	-39.9°	1.5°	2.8%	11.7%	Ankle angle at PK	93.7°	3.5 °	3.8%	6.7%
LO	-71.9°	1.6°	2.2%	7.1%	Shoulder moment arm	-0.011 m	0.0018 m	15.6%	33.4%
HL angle					2D elbow moment arm	-0.026 m	0.0016 m	6.2%	11.1%
TD	16.0°	1.3°	26.9%	29.9%	Wrist moment arm	-0.013 m	0.0014 m	10.2%	15.6%
PK	-9.9°	1.8°	1.5%	325.5%	Hip moment arm	-0.023 m	0.0035 m	13.7%	42.3%
LO	-42.1°	0.9°	2.1%	7.8%	2D knee moment arm	-0.011 m	0.0030 m	22.3%	135.5%
Thigh angle					Ankle moment arm	-0.023 m	0.0023 m	10.6%	12.3%
TD	41.2°	0.9°	2.9%	13.5%	Shoulder moment	-0.052 N·m	0.0090 N·m	15.4%	35.8%
PK	25.4°	1.2°	1.1%	37.3%	2D elbow moment	-0.130 N·m	0.0085 N·m	7.5%	20.2%
LO	-14.2°	2.4°	0.02%	47.9%	Wrist moment	-0.063 N·m	0.0070 N·m	10.9%	20.1%
2D elbow angle					Hip moment	-0.104 N·m	0.0150 N·m	14.2%	70.3%
TD	138.7°	1.7°	1.2%	2.3%	2D knee moment	-0.048 N·m	0.0120 N·m	22.2%	142.5%
MS	111.5°	1.6°	1.4%	5.0%	Ankle moment	-0.100 N·m	0.0110 N·m	11.2%	18.4%
PK	110.0°	1.9°	1.7%	4.4%					
LO	133.0°	2.1°	1.6%	5.0%					

Standard deviations (SD) and coefficients of variation (CV) summarize the average measurement variation across three replicates of 20 randomly selected trials (Error CV) and intra-experimentally (IE CV). Reported CVs are means across all individual CVs for that variable.

Table 2.8. Allometry of limb growth in *Saimiri boliviensis* (n=97).

Segment	RMA slope	- CI	+ CI	LS slope	- CI	+ CI	RMA Intercept	- CI	+ CI	r
Arm	0.624	0.555	0.700	0.512	0.439	0.584	1.166 mm	0.755 mm	1.799 mm	0.820
Forearm	0.702	0.628	0.785	0.586	0.508	0.665	0.679 mm	0.424 mm	1.086 mm	0.835
Thigh	0.555	0.497	0.619	0.467	0.406	0.528	2.093 mm	1.453 mm	3.014 mm	0.842
Leg	0.539	0.490	0.593	0.475	0.424	0.527	2.422 mm	1.722 mm	3.296 mm	0.883
Forelimb	0.616	0.560	0.677	0.545	0.487	0.603	2.363 mm	1.669 mm	3.347 mm	0.886
Hind limb	0.533	0.485	0.586	0.471	0.420	0.522	4.888 mm	3.606 mm	6.623 mm	0.883

Both Model II Reduced Major Axis (RMA) and Model I least-squares (LS) slopes are presented. Intercepts were calculated from the RMA regressions and have been antilog-transformed for ease of presentation. Lower and upper 95% confidence intervals (- CI and + CI) are provided for all estimates. Bivariate correlation coefficients for each relationship are shown in the last column.

Table 2.9. Zero-order and partial correlations for symmetrical strides on the ground.

	Speed	Froude	Mass	Mass.Speed	Mass.Froude
Forelimb angle					
Protraction (*at TD*)	-0.03	-0.03	**0.24**	**0.24**	**0.24**
	(148)	(148)	**(148)**	**(145)**	**(145)**
Peak vertical	-0.23	-0.24	0.22	**0.27**	0.26
	(58)	(58)	(58)	**(55)**	(55)
Retraction (*at LO*)	0.11	0.10	0.10	0.10	0.10
	(147)	(147)	(147)	(144)	(144)
Angular excursion	-0.01	-0.01	0.08	0.08	0.08
	(145)	(145)	(145)	(142)	(142)
Arm angle					
Protraction (*at TD*)	-0.01	-0.01	**0.17**	**0.17**	**0.17**
	(144)	(144)	**(144)**	**(141)**	**(141)**
Peak vertical	**-0.30**	**-0.33**	0.19	**0.26**	0.24
	(58)	**(58)**	(58)	**(55)**	(55)
Retraction (*at LO*)	0.10	0.09	-0.01	-0.02	-0.01
	(148)	(148)	(148)	(145)	(145)
Angular excursion	-0.10	-0.11	**0.20**	**0.21**	**0.20**
	(143)	(143)	**(143)**	**(140)**	**(140)**
Elbow angle (2-D)					
Touchdown	0.05	0.04	0.05	0.05	0.05
	(142)	(142)	(142)	(139)	(139)
Mid-stance	**-0.19**	**-0.20**	-0.06	-0.05	-0.06
	(144)	**(144)**	(144)	(141)	(141)
Peak vertical	**-0.27**	**-0.30**	0.02	0.07	0.06
	(58)	**(58)**	(58)	(55)	(55)
Liftoff	0.06	0.05	**-0.20**	**-0.20**	**-0.19**
	(143)	(143)	**(143)**	**(140)**	**(140)**
Yield	**0.30**	**0.30**	0.09	0.07	0.09
	(140)	**(140)**	(140)	(137)	(137)
Elbow angle (3-D)					
Touchdown	-0.46	-0.50	0.17	0.18	0.16
	(10)	(10)	(10)	(7)	(7)
Mid-stance	0.06	0.02	0.13	0.12	0.12
	(35)	(35)	(35)	(32)	(32)
Peak vertical	-0.18	-0.26	0.17	0.23	0.23
	(9)	(9)	(9)	(6)	(6)
Liftoff	0.41	0.40	-0.23	-0.19	-0.18
	(21)	(21)	(21)	(18)	(18)
Yield	-0.75	-0.73	-0.03	-0.08	-0.12
	(7)	(7)	(7)	(4)	(4)

Bold shading indicates significance ($p \leq 0.05$). Degrees of freedom are shown in parentheses.

Table 2.9. Continued.

	Speed	Froude	Mass	Mass.Speed	Mass.Froude
Wrist angle (peak vertical)	-0.06 (58)	-0.04 (58)	0.05 (58)	0.06 (56)	0.06 (56)
Hind limb angle					
Protraction (*at TD*)	**-0.17 (151)**	**-0.19 (151)**	**0.56 (151)**	**0.58 (148)**	**0.57 (148)**
Peak vertical	**-0.62 (37)**	**-0.63 (37)**	-0.06 (37)	0.22 (34)	0.16 (34)
Retraction (*at LO*)	**-0.19 (145)**	**-0.20 (145)**	-0.01 (145)	0.00 (142)	-0.02 (142)
Angular excursion	-0.04 (144)	-0.06 (144)	**0.54 (144)**	**0.54 (141)**	**0.54 (141)**
Thigh angle					
Protraction (*at TD*)	-0.08 (152)	-0.07 (152)	**0.38 (152)**	**0.39 (149)**	**0.38 (149)**
Peak vertical	-0.29 (38)	-0.29 (38)	0.15 (38)	0.28 (35)	0.26 (35)
Retraction (*at LO*)	**-0.48 (145)**	**-0.44 (145)**	-0.09 (145)	-0.08 (142)	-0.12 (142)
Angular excursion	**0.40 (145)**	**0.37 (145)**	**0.45 (145)**	**0.47 (142)**	**0.50 (142)**
Knee angle (2-D)					
Touchdown	-0.07 (151)	-0.11 (151)	0.04 (151)	0.05 (148)	0.04 (148)
Mid-stance	-0.12 (151)	-0.14 (151)	**-0.31 (151)**	**-0.31 (148)**	**-0.32 (148)**
Peak vertical	**-0.33 (38)**	**-0.35 (38)**	-0.30 (38)	-0.20 (35)	-0.21 (35)
Liftoff	**0.44 (145)**	**0.40 (145)**	0.12 (145)	0.11 (142)	0.15 (142)
Yield	0.10 (150)	0.08 (150)	**0.45 (150)**	**0.45 (147)**	**0.45 (147)**
Knee angle (3-D)					
Touchdown	-0.39 (21)	-0.41 (21)	0.39 (21)	0.28 (18)	0.25 (18)
Mid-stance	-0.39 (14)	-0.45 (14)	0.40 (14)	0.42 (11)	0.40 (11)
Peak vertical	**-0.99 (3)**	-0.99 (3)	0.87 (3)	--	--
Liftoff	0.42 (19)	0.37 (14)	0.14 (14)	0.27 (16)	0.28 (16)
Yield	0.30 (10)	0.34 (10)	-0.03 (10)	0.05 (7)	0.10 (7)

Table 2.9. Continued.

	Speed	Froude	Mass	Mass.Speed	Mass.Froude
Ankle angle (peak vertical)	-0.03	-0.05	-0.16	-0.16	-0.15
	(37)	(37)	(37)	(34)	(34)
Substrate reaction forces					
Sagittal forelimb SRF	**0.78**	**0.79**	-0.14	**-0.45**	**-0.37**
magnitude	**(57)**	**(57)**	(57)	**(54)**	**(54)**
Sagittal forelimb SRF angle	0.10	0.11	**-0.32**	**-0.33**	**-0.33**
	(57)	(57)	**(57)**	**(54)**	**(54)**
Total forelimb SRF	**0.79**	**0.80**	-0.14	**-0.45**	**-0.37**
magnitude	**(57)**	**(57)**	(57)	**(54)**	**(54)**
Sagittal hind limb SRF	**0.48**	**0.46**	**0.60**	**0.52**	**0.54**
magnitude	**(37)**	**(37)**	**(37)**	**(34)**	**(34)**
Sagittal hind limb SRF angle	0.22	0.24	0.06	-0.02	-0.02
	(37)	(37)	(37)	(34)	(34)
Total hind limb SRF	**0.48**	**0.46**	**0.60**	**0.52**	**0.54**
magnitude	**(37)**	**(37)**	**(37)**	**(34)**	**(34)**
Moment arms (body mass)					
Shoulder	**0.27**	**0.27**	0.03	-0.02	0.00
	(58)	**(58)**	(58)	(55)	(55)
Elbow (2-D)	-0.07	-0.09	0.03	0.04	0.04
	(58)	(58)	(58)	(55)	(55)
Elbow (3-D)	0.20	0.21	0.27	0.24	0.25
	(9)	(9)	(9)	(6)	(6)
Wrist	-0.02	-0.04	-0.15	-0.15	-0.15
	(58)	(58)	(58)	(55)	(55)
Hip	**-0.57**	**-0.57**	-0.01	0.26	0.21
	(37)	**(37)**	(37)	(34)	(34)
Knee (2-D)	**0.60**	**0.60**	0.20	-0.02	0.03
	(37)	**(37)**	(37)	(34)	(34)
Knee (3-D)	0.97	0.99	-0.71	---	---
	(3)	(3)	(3)		
Ankle	**-0.42**	**-0.43**	0.05	0.24	0.21
	(37)	**(37)**	(37)	(34)	(34)
Moment arms (limb length)					
Shoulder	**0.32**	**0.32**	0.01	-0.05	-0.03
	(58)	**(58)**	(58)	(55)	(55)
Elbow (2-D)	0.02	0.04	-0.06	-0.07	-0.06
	(58)	(58)	(58)	(55)	(55)
Elbow (3-D)	0.19	0.26	-0.06	-0.12	-0.12
	(9)	(9)	(9)	(6)	(6)
Wrist	0.07	0.07	-0.22	-0.24	-0.23
	(58)	(58)	(58)	(55)	(55)

Table 2.9. Continued.

	Speed	Froude	Mass	Mass.Speed	Mass.Froude
Moment arms (limb length)					
Hip	**-0.56**	**-0.55**	-0.02	0.23	0.18
	(37)	**(37)**	(37)	(34)	(34)
Knee (2-D)	**0.62**	**0.62**	0.24	-0.03	0.02
	(37)	**(37)**	(37)	(34)	(34)
Knee (3-D)	0.97	0.99	-0.68	---	---
	(3)	(3)	(3)		
Ankle	**-0.33**	**-0.32**	0.04	0.18	0.18
	(37)	**(37)**	(37)	(34)	(34)
Moments (body mass)					
Shoulder	**0.52**	**0.51**	0.04	-0.06	-0.03
	(58)	**(58)**	(58)	(55)	(55)
Elbow (2-D)	**0.69**	**0.67**	0.05	-0.10	-0.04
	(58)	**(58)**	(58)	(55)	(55)
Elbow (3-D)	0.60	0.62	0.34	0.24	0.29
	(9)	(9)	(9)	(6)	(6)
Wrist	**0.67**	**0.64**	-0.02	-0.19	-0.12
	(58)	**(58)**	(58)	(55)	(55)
Hip	-0.27	-0.29	**0.34**	**0.48**	**0.46**
	(37)	(37)	**(37)**	**(34)**	**(34)**
Knee (2-D)	**0.63**	**0.63**	0.28	0.08	0.13
	(37)	**(37)**	(37)	(34)	(34)
Knee (3-D)	0.82	0.87	-0.39	---	---
	(3)	(3)	(3)		
Ankle	-0.03	-0.06	**0.52**	**0.57**	**0.57**
	(37)	(37)	**(37)**	**(34)**	**(34)**
*Moments (body weight*length)*					
Shoulder	**0.51**	**0.51**	0.00	-0.13	-0.09
	(57)	**(57)**	(57)	(54)	(54)
Elbow (2-D)	**0.62**	**0.62**	-0.11	**-0.31**	**-0.26**
	(57)	**(57)**	(57)	**(54)**	**(54)**
Elbow (3-D)	0.45	0.54	-0.17	-0.34	-0.33
	(9)	(9)	(9)	(6)	(6)
Wrist	**0.75**	**0.75**	-0.14	**-0.43**	**-0.35**
	(58)	**(58)**	(58)	**(55)**	**(55)**
Hip	**-0.34**	**-0.34**	0.18	**0.36**	**0.33**
	(35)	**(35)**	(35)	**(35)**	**(35)**
Knee (2-D)	**0.64**	**0.64**	0.27	0.01	0.07
	(38)	**(38)**	(38)	(35)	(35)
Knee (3-D)	0.90	0.93	-0.52	---	---
	(3)	(3)	(3)		
Ankle	0.10	0.09	**0.48**	**0.49**	**0.48**
	(40)	(40)	**(40)**	**(37)**	**(37)**

Table 2.10. Zero-order and partial correlations for asymmetrical strides on the ground.

	Speed	Froude	Mass	Mass.Speed	Mass.Froude
Forelimb angle					
Protraction (*at TD*)	-0.01	0.02	0.03	0.03	0.00
	(422)	(409)	(422)	(419)	(406)
Peak vertical	0.00	0.02	0.03	0.00	0.02
	(116)	(115)	(116)	(113)	(112)
Retraction (*at LO*)	**-0.31**	**-0.30**	**-0.17**	-0.07	**-0.20**
	(409)	**(396)**	**(409)**	(406)	**(393)**
Angular excursion	**0.28**	**0.28**	**0.17**	0.09	**0.17**
	(384)	**(372)**	**(384)**	(381)	**(369)**
Arm angle					
Protraction (*at TD*)	**0.19**	**0.16**	**0.17**	**0.11**	**0.12**
	(412)	**(400)**	**(412)**	**(409)**	**(397)**
Peak vertical	-0.18	-0.17	-0.06	-0.07	-0.13
	(119)	(118)	(119)	(116)	(115)
Retraction (*at LO*)	**-0.13**	**-0.20**	-0.07	**0.13**	0.04
	(428)	**(415)**	(428)	**(425)**	(412)
Angular excursion	**0.28**	**0.31**	0.05	-0.05	0.03
	(393)	**(381)**	(393)	(390)	(378)
Elbow angle (2-D)					
Touchdown	**0.25**	**0.21**	**0.15**	0.07	0.10
	(408)	**(395)**	**(408)**	(405)	(392)
Mid-stance	**-0.11**	**-0.14**	-0.07	-0.04	**-0.10**
	(428)	**(414)**	(428)	(425)	**(411)**
Peak vertical	**-0.27**	**-0.24**	**-0.18**	**-0.20**	**-0.29**
	(119)	**(118)**	**(119)**	**(116)**	**(115)**
Liftoff	**0.14**	0.06	**0.21**	**0.18**	**0.18**
	(395)	(382)	**(395)**	**(392)**	**(379)**
Yield	**0.32**	**0.31**	**0.19**	0.09	**0.18**
	(400)	**(387)**	**(401)**	(397)	**(384)**
Elbow angle (3-D)					
Touchdown	0.24	0.28	0.05	0.05	0.09
	(36)	(36)	(36)	(33)	(33)
Mid-stance	-0.06	-0.11	0.06	0.06	0.04
	(110)	(110)	(110)	(107)	(107)
Peak vertical	**-0.41**	**-0.38**	-0.19	-0.27	-0.35
	(32)	**(32)**	(32)	(29)	(29)
Liftoff	**-0.40**	**-0.47**	**0.47**	**0.43**	**0.35**
	(37)	**(37)**	**(37)**	**(34)**	**(34)**
Yield	0.26	0.33	-0.01	-0.01	0.03
	(29)	(29)	(29)	(26)	(26)

Presentation of data follows Table 2.9.

Table 2.10. Continued.

	Speed	Froude	Mass	Mass.Speed	Mass.Froude
Wrist angle (peak vertical)	-0.15 (114)	-0.17 (113)	0.09 (114)	0.08 (111)	0.06 (110)
Hind limb angle					
Protraction (*at TD*)	0.05 (435)	**0.14 (435)**	-0.06 (435)	-0.08 (432)	-0.08 (432)
Peak vertical	0.26 (48)	**0.29 (48)**	0.22 (48)	0.25 (45)	0.26 (45)
Retraction (*at LO*)	-0.09 (428)	**-0.10 (428)**	0.05 (428)	0.08 (425)	0.06 (425)
Angular excursion	**0.12 (416)**	**0.24 (416)**	**-0.12 (416)**	**-0.18 (413)**	**-0.17 (413)**
Thigh angle					
Protraction (*at TD*)	0.06 (441)	**0.22 (441)**	**-0.33 (441)**	**-0.38 (441)**	**-0.38 (438)**
Peak vertical	0.02 (60)	0.10 (60)	0.10 (60)	0.11 (57)	0.12 (57)
Retraction (*at LO*)	**-0.45 (424)**	**-0.40 (424)**	**-0.22 (424)**	-0.07 (421)	**-0.18 (421)**
Angular excursion	**0.35 (422)**	**0.46 (422)**	**-0.15 (422)**	**-0.30 (419)**	**-0.24 (419)**
Knee angle (2-D)					
Touchdown	**-0.13 (431)**	**-0.30 (431)**	**0.38 (431)**	**0.46 (428)**	**0.45 (428)**
Mid-stance	**-0.14 (442)**	**-0.34 (442)**	**0.35 (442)**	**0.43 (439)**	**0.42 (439)**
Peak vertical	0.15 (59)	0.04 (59)	0.05 (59)	0.05 (56)	0.06 (56)
Liftoff	**0.37 (422)**	**0.33 (422)**	**0.18 (422)**	0.06 (419)	**0.14 (419)**
Yield	0.04 (429)	**0.10 (429)**	0.02 (429)	0.01 (426)	0.00 (426)
Knee angle (3-D)					
Touchdown	-0.09 (32)	**-0.40 (32)**	**0.66 (32)**	**0.67 (29)**	**0.62 (29)**
Mid-stance	**-0.48 (35)**	**-0.73 (35)**	**0.60 (35)**	**0.63 (32)**	**0.46 (32)**
Peak vertical	-0.31 (5)	-0.31 (5)	0.04 (5)	--	--
Liftoff	0.11 (45)	0.17 (45)	0.10 (45)	0.08 (42)	0.12 (42)
Yield	0.34 (19)	0.45 (19)	-0.07 (19)	-0.09 (16)	0.12 (16)

Table 2.10. Continued.

	Speed	Froude	Mass	Mass.Speed	Mass.Froude
Ankle angle (peak vertical)	-0.15	-0.17	0.09	0.09	0.07
	(48)	(48)	(48)	(45)	(45)
Substrate reaction forces					
Sagittal forelimb SRF	**0.50**	**0.56**	**-0.36**	**-0.40**	**-0.28**
magnitude	**(113)**	**(112)**	**(113)**	**(110)**	**(109)**
Sagittal forelimb SRF angle	-0.04	-0.06	**-0.19**	**-0.19**	-0.16
	(113)	(112)	**(113)**	**(110)**	(109)
Total forelimb SRF	**0.55**	**0.59**	**-0.36**	**-0.40**	**-0.28**
magnitude	**(113)**	**(112)**	**(113)**	**(110)**	**(109)**
Sagittal hind limb SRF	**0.71**	**0.71**	0.15	0.22	**0.33**
magnitude	**(48)**	**(48)**	(48)	(45)	**(45)**
Sagittal hind limb SRF angle	**-0.32**	**-0.37**	0.24	-0.11	-0.16
	(48)	**(48)**	(48)	(45)	(45)
Total hind limb SRF	**0.72**	**0.71**	0.15	0.22	**0.33**
magnitude	**(48)**	**(48)**	(48)	(45)	**(45)**
Moment arms (body mass)					
Shoulder	**-0.32**	**-0.37**	**0.24**	**0.23**	0.15
	(114)	**(113)**	**(114)**	**(111)**	(110)
Elbow (2-D)	**0.41**	**0.39**	0.02	0.06	0.14
	(114)	**(113)**	(114)	(111)	(110)
Elbow (3-D)	0.32	0.34	-0.09	-0.04	0.01
	(30)	(30)	(30)	(27)	(27)
Wrist	**0.32**	**0.31**	-0.07	-0.05	0.00
	(114)	**(113)**	(114)	(111)	(110)
Hip	-0.21	-0.17	**0.30**	**0.31**	**0.29**
	(49)	(49)	**(49)**	**(46)**	**(46)**
Knee (2-D)	0.14	0.14	-0.07	-0.07	-0.06
	(49)	(49)	(49)	(46)	(46)
Knee (3-D)	0.99	**0.99**	0.88	---	---
	(3)	**(3)**	(3)		
Ankle	-0.16	-0.19	0.11	0.12	0.10
	(49)	(49)	(49)	(46)	(46)
Moment arms (limb length)					
Shoulder	**-0.29**	**-0.34**	**0.25**	**0.24**	0.18
	(114)	**(113)**	**(114)**	**(111)**	(110)
Elbow (2-D)	**0.44**	**0.44**	0.02	0.06	0.18
	(114)	**(113)**	(114)	(111)	(110)
Elbow (3-D)	**0.43**	**0.43**	-0.07	-0.01	0.07
	(30)	**(30)**	(30)	(27)	(27)
Wrist	**0.43**	**0.43**	-0.06	-0.04	0.06
	(114)	**(113)**	(114)	(112)	(110)

Table 2.10. Continued.

	Speed	Froude	Mass	Mass.Speed	Mass.Froude
Moment arms (limb length)					
Hip	-0.19	-0.14	0.25	0.24	0.22
	(48)	(48)	(48)	(45)	(45)
Knee (2-D)	0.14	0.16	-0.14	-0.14	-0.12
	(48)	(48)	(48)	(45)	(45)
Knee (3-D)	0.99	0.99	0.76	---	---
	(3)	(3)	(3)		
Ankle	-0.12	-0.11	-0.02	-0.02	-0.04
	(48)	(48)	(48)	(45)	(45)
Moments (body mass)					
Shoulder	-0.11	-0.16	**0.21**	**0.21**	0.17
	(114)	(113)	**(114)**	**(111)**	(110)
Elbow (2-D)	**0.62**	**0.58**	0.10	0.18	**0.32**
	(115)	**(114)**	(115)	(112)	**(111)**
Elbow (3-D)	**0.51**	**0.51**	0.02	0.09	0.18
	(30)	**(30)**	(30)	(27)	(27)
Wrist	**0.59**	**0.56**	0.00	0.05	0.16
	(114)	**(113)**	(115)	(111)	(110)
Hip	0.13	0.14	**0.42**	**0.44**	**0.46**
	(49)	(49)	**(49)**	**(46)**	**(46)**
Knee (2-D)	**0.41**	**0.40**	0.17	0.18	0.23
	(49)	**(49)**	(49)	(46)	(46)
Knee (3-D)	0.95	0.96	0.97	---	---
	(3)	(3)	(3)		
Ankle	**0.38**	**0.33**	**0.36**	**0.39**	**0.43**
	(49)	**(49)**	**(49)**	**(46)**	**(46)**
*Moments (body weight*length)*					
Shoulder	-0.10	-0.13	0.13	0.11	0.09
	(112)	(112)	(112)	(109)	(109)
Elbow (2-D)	**0.59**	**0.61**	**-0.20**	-0.18	-0.05
	(113)	**(113)**	**(113)**	(110)	(110)
Elbow (3-D)	**0.46**	**0.51**	-0.30	-0.26	-0.18
	(31)	**(31)**	(31)	(27)	(27)
Wrist	**0.62**	**0.67**	**-0.35**	**-0.40**	**-0.25**
	(115)	**(114)**	**(115)**	**(111)**	**(110)**
Hip	0.15	0.18	**0.30**	**0.31**	**0.33**
	(46)	(46)	**(46)**	**(43)**	**(43)**
Knee (2-D)	**0.47**	**0.49**	-0.04	0.02	0.02
	(46)	**(46)**	(46)	(43)	(43)
Knee (3-D)	0.98	0.99	0.92	---	---
	(3)	(3)	(3)		
Ankle	**0.59**	**0.60**	0.10	0.13	0.21
	(48)	**(48)**	(48)	(45)	(45)

Table 2.11. Zero-order and partial for symmetrical strides on the pole.

	Speed	Froude	Mass	Mass.Speed	Mass.Froude
Forelimb angle					
Protraction (*at TD*)	**-0.20**	**-0.23**	**0.49**	**0.47**	**0.45**
	(206)	**(202)**	**(206)**	**(203)**	**(199)**
Peak vertical	**0.38**	**0.38**	0.06	0.10	0.14
	(106)	**(103)**	(106)	(103)	(100)
Retraction (*at LO*)	-0.06	-0.02	**-0.21**	**-0.23**	**-0.21**
	(223)	(219)	**(223)**	**(220)**	**(214)**
Angular excursion	-0.07	-0.12	**0.46**	**0.46**	**0.45**
	(206)	(202)	**(206)**	**(202)**	**(198)**
Arm angle					
Protraction (*at TD*)	**-0.18**	**-0.20**	**0.29**	**0.27**	**0.26**
	(208)	**(204)**	**(208)**	**(205)**	**(201)**
Peak vertical	0.17	**0.21**	**-0.22**	**-0.21**	**-0.18**
	(106)	**(103)**	**(106)**	**(103)**	**(100)**
Retraction (*at LO*)	**-0.28**	**-0.27**	-0.04	-0.10	-0.10
	(226)	**(222)**	(226)	(223)	(219)
Angular excursion	**0.16**	0.13	**0.24**	**0.28**	**0.28**
	(207)	(203)	**(207)**	**(204)**	**(200)**
Elbow angle (2-D)					
Touchdown	-0.03	-0.03	0.01	0.00	0.00
	(204)	(200)	(204)	(201)	(197)
Mid-stance	0.04	0.07	**-0.44**	**-0.44**	**-0.43**
	(217)	(213)	**(217)**	**(214)**	**(210)**
Peak vertical	-0.06	-0.03	**-0.40**	**-0.41**	**-0.43**
	(106)	(103)	**(107)**	**(103)**	**(100)**
Liftoff	**-0.34**	**-0.36**	**0.21**	**0.15**	**0.14**
	(223)	**(219)**	**(223)**	**(220)**	**(216)**
Yield	-0.05	-0.09	**0.46**	**0.46**	**0.45**
	(203)	(199)	**(203)**	**(200)**	**(196)**
Elbow angle (3-D)					
Touchdown	0.28	0.25	-0.21	-0.05	-0.06
	(17)	(17)	(17)	(14)	(14)
Mid-stance	0.05	0.06	**-0.42**	**-0.42**	**-0.40**
	(92)	(90)	**(92)**	**(89)**	**(87)**
Peak vertical	0.26	**0.21**	**-0.49**	**-0.49**	**-0.43**
	(43)	**(41)**	**(43)**	**(40)**	**(39)**
Liftoff	-0.14	-0.16	-0.18	**-0.31**	**-0.33**
	(46)	(46)	(46)	**(43)**	**(43)**
Yield	-0.10	-0.15	0.45	**0.57**	**0.56**
	(15)	(15)	(15)	**(12)**	**(12)**

Presentation of data follows Table 2.9.

Table 2.11. Continued.

	Speed	Froude	Mass	Mass.Speed	Mass.Froude
Wrist angle (peak vertical)	-0.14 (106)	-0.12 (103)	0.14 (106)	0.12 (103)	0.10 (100)
Hind limb angle					
Protraction (*at TD*)	**-0.51 (225)**	**-0.50 (225)**	**0.49 (225)**	**0.46 (222)**	**0.43 (222)**
Peak vertical	**-0.57 (91)**	**-0.56 (90)**	-0.03 (91)	0.17 (88)	0.12 (87)
Retraction (*at LO*)	-0.02 (222)	-0.01 (222)	**-0.25 (222)**	**-0.26 (219)**	**-0.26 (219)**
Angular excursion	**-0.38 (221)**	**-0.39 (221)**	**0.51 (221)**	**0.49 (218)**	**0.46 (218)**
Thigh angle					
Protraction (*at TD*)	**-0.14 (228)**	-0.10 (226)	**0.25 (228)**	**0.23 (225)**	**0.24 (223)**
Peak vertical	**-0.43 (93)**	**-0.41 (92)**	0.13 (93)	**0.30 (90)**	**0.26 (89)**
Retraction (*at LO*)	**-0.19 (223)**	**-0.16 (221)**	-0.09 (223)	**-0.14 (220)**	**-0.14 (218)**
Angular excursion	0.06 (223)	0.060 (221)	**0.27 (223)**	**0.29 (220)**	**0.30 (218)**
Knee angle (2-D)					
Touchdown	**-0.41 (225)**	**-0.44 (225)**	**0.21 (225)**	**0.14 (222)**	0.10 (222)
Mid-stance	-0.11 (226)	**-0.13 (226)**	**-0.32 (226)**	**-0.35 (223)**	**-0.37 (223)**
Peak vertical	**-0.37 (93)**	**-0.40 (92)**	**-0.31 (93)**	**-0.23 (90)**	**-0.26 (89)**
Liftoff	**0.19 (221)**	**0.17 (221)**	-0.06 (221)	-0.02 (218)	-0.01 (218)
Yield	**-0.30 (226)**	**-0.32 (226)**	**0.66 (226)**	**0.64 (222)**	**0.62 (222)**
Knee angle (3-D)					
Touchdown	**-0.32 (43)**	**-0.31 (43)**	**-0.44 (43)**	**-0.62 (40)**	**-0.64 (40)**
Mid-stance	-0.14 (26)	-0.17 (26)	-0.31 (26)	-0.35 (23)	-0.39 (23)
Peak vertical	**-0.70 (16)**	**-0.71 (16)**	-0.44 (16)	-0.33 (13)	-0.39 (13)
Liftoff	-0.24 (16)	-0.25 (16)	-0.04 (16)	-0.06 (13)	-0.06 (13)
Yield	-0.10 (22)	-0.05 (22)	-0.08 (22)	-0.10 (19)	-0.09 (19)

Table 2.11. Continued.

	Speed	Froude	Mass	Mass.Speed	Mass.Froude
Ankle angle (peak vertical)	**-0.49**	**0.49**	**-0.30**	-0.19	**-0.22**
	(91)	**(90)**	**(91)**	(88)	**(87)**
Substrate reaction forces					
Sagittal forelimb SRF	**0.80**	**0.83**	**-0.37**	**-0.48**	**-0.38**
magnitude	**(106)**	**(103)**	**(106)**	**(103)**	**(100)**
Sagittal forelimb SRF angle	**-0.48**	**-0.49**	0.02	-0.04	-0.09
	(107)	**(104)**	(107)	(103)	(100)
Total forelimb SRF	**0.80**	**0.83**	**-0.37**	**-0.48**	**-0.38**
magnitude	**(106)**	**(103)**	**(106)**	**(103)**	**(100)**
Sagittal hind limb SRF	**0.58**	**0.58**	**0.38**	**0.28**	**0.33**
magnitude	**(91)**	**(90)**	**(91)**	**(88)**	**(87)**
Sagittal hind limb SRF angle	**0.49**	**0.51**	0.04	-0.12	-0.07
	(91)	**(90)**	(91)	(88)	(87)
Total hind limb SRF	**0.58**	**0.58**	**0.38**	**0.28**	**0.33**
magnitude	**(91)**	**(90)**	**(91)**	**(88)**	**(87)**
Moment arms (body mass)					
Shoulder	-0.08	-0.07	-0.03	-0.04	-0.06
	(106)	(103)	(106)	(103)	(100)
Elbow (2-D)	0.05	0.01	**0.34**	**0.34**	**0.37**
	(106)	(103)	**(106)**	**(103)**	**(100)**
Elbow (3-D)	0.05	-0.01	**0.64**	**0.66**	**0.65**
	(42)	(40)	**(42)**	**(39)**	**(37)**
Wrist	0.16	0.16	-0.13	-0.11	-0.08
	(106)	(103)	(106)	(103)	(100)
Hip	**-0.46**	**-0.44**	-0.02	0.13	0.10
	(91)	**(90)**	(91)	(88)	(87)
Knee (2-D)	**0.54**	**0.53**	**0.21**	0.08	0.11
	(91)	**(90)**	**(91)**	(88)	(87)
Knee (3-D)	-0.18	-0.18	0.09	0.16	0.14
	(16)	(16)	(16)	(13)	(13)
Ankle	0.20	**0.22**	0.17	0.12	0.14
	(91)	**(90)**	(91)	(88)	(87)
Moment arms (limb length)					
Shoulder	-0.03	-0.02	-0.07	-0.08	-0.09
	(106)	(103)	(106)	(103)	(100)
Elbow (2-D)	0.13	0.10	**0.26**	**0.28**	**0.31**
	(106)	(103)	**(106)**	**(103)**	**(100)**
Elbow (3-D)	0.13	0.05	**0.64**	**0.66**	**0.66**
	(42)	(40)	**(42)**	**(39)**	**(37)**
Wrist	**0.24**	**0.23**	-0.15	-0.13	-0.09
	(106)	**(103)**	(106)	(103)	(100)

Table 2.11. Continued.

	Speed	Froude	Mass	Mass.Speed	Mass.Froude
Moment arms (limb length)					
Hip	**-0.44**	**-0.41**	0.00	0.14	0.11
	(91)	**(90)**	(91)	(88)	(87)
Knee (2-D)	**0.53**	**0.52**	**0.21**	0.08	0.12
	(91)	**(90)**	**(91)**	(88)	(87)
Knee (3-D)	-0.14	-0.13	0.02	0.07	0.06
	(16)	(16)	(16)	(13)	(13)
Ankle	**0.23**	**0.27**	0.17	0.12	0.14
	(91)	**(90)**	(91)	(88)	(87)
Moments (body mass)					
Shoulder	**0.31**	**0.33**	-0.15	-0.12	-0.10
	(106)	**(103)**	(106)	(103)	(100)
Elbow (2-D)	**0.72**	**0.71**	0.06	**0.38**	**0.46**
	(106)	**(103)**	(106)	**(103)**	**(100)**
Elbow (3-D)	**0.69**	**0.67**	0.22	**0.40**	**0.48**
	(42)	**(40)**	(42)	**(40)**	**(38)**
Wrist	**0.71**	**0.72**	**-0.20**	-0.17	-0.06
	(106)	**(103)**	**(106)**	(104)	(101)
Hip	-0.09	-0.07	**0.28**	**0.32**	**0.32**
	(91)	(90)	**(91)**	**(88)**	**(87)**
Knee (2-D)	**0.57**	**0.57**	**0.22**	0.08	0.12
	(91)	**(90)**	**(91)**	(88)	(87)
Knee (3-D)	-0.05	-0.06	0.23	0.25	0.25
	(16)	(16)	(16)	(13)	(13)
Ankle	**0.54**	**0.53**	**0.52**	**0.46**	**0.50**
	(91)	**(90)**	**(91)**	**(88)**	**(88)**
*Moments (body weight*length)*					
Shoulder	**0.31**	**0.34**	**-0.29**	**-0.28**	**-0.26**
	(106)	**(103)**	**(106)**	**(103)**	**(100)**
Elbow (2-D)	**0.72**	**0.74**	-0.18	-0.14	-0.02
	(106)	**(103)**	(106)	(103)	(100)
Elbow (3-D)	**0.64**	**0.65**	-0.05	0.03	0.13
	(42)	**(40)**	(42)	(39)	(37)
Wrist	**0.79**	**0.81**	**-0.27**	**-0.31**	-0.18
	(106)	**(103)**	**(106)**	**(103)**	(100)
Hip	-0.18	-0.16	0.11	0.17	0.16
	(91)	(90)	(91)	(88)	(87)
Knee (2-D)	**0.56**	**0.56**	**0.23**	0.09	0.13
	(91)	**(90)**	**(91)**	(88)	(87)
Knee (3-D)	-0.10	-0.10	0.10	0.13	0.13
	(16)	(16)	(16)	(13)	(13)
Ankle	**0.52**	**0.51**	**0.39**	**0.30**	**0.34**
	(91)	**(90)**	**(91)**	**(88)**	**(87)**

Table 2.12. Zero-order and partial correlations for asymmetrical strides on the pole.

	Speed	Froude	Mass	Mass.Speed	Mass.Froude
Forelimb angle					
Protraction (*at TD*)	-0.11	**-0.15**	**0.13**	**0.19**	**0.18**
	(295)	**(291)**	**(295)**	**(292)**	**(288)**
Peak vertical	-0.02	-0.02	-0.08	-0.08	-0.06
	(159)	(157)	(159)	(156)	(154)
Retraction (*at LO*)	**-0.19**	**-0.17**	**-0.27**	**-0.22**	**-0.22**
	(310)	**(306)**	**(310)**	**(307)**	**(303)**
Angular excursion	0.07	0.03	**0.31**	**0.31**	**0.31**
	(288)	(284)	**(288)**	**(285)**	**(281)**
Arm angle					
Protraction (*at TD*)	**-0.19**	**-0.18**	**-0.20**	**-0.13**	**-0.14**
	(286)	**(282)**	**(286)**	**(283)**	**(279)**
Peak vertical	**-0.24**	**-0.19**	**-0.52**	**-0.48**	**-0.48**
	(163)	**(161)**	**(163)**	**(160)**	**(158)**
Retraction (*at LO*)	**-0.23**	**-0.21**	**-0.27**	**-0.20**	**-0.21**
	(313)	**(309)**	**(313)**	**(310)**	**(306)**
Angular excursion	0.05	0.03	0.06	0.04	0.04
	(282)	(278)	(282)	(279)	(275)
Elbow angle (2-D)					
Touchdown	**-0.21**	**-0.17**	**-0.39**	**-0.34**	**-0.35**
	(283)	**(279)**	**(283)**	**(279)**	**(275)**
Mid-stance	**-0.30**	**-0.25**	**-0.50**	**-0.43**	**-0.44**
	(305)	**(301)**	**(305)**	**(302)**	**(298)**
Peak vertical	**-0.30**	**-0.24**	**-0.66**	**-0.61**	**-0.62**
	(163)	**(161)**	**(163)**	**(160)**	**(158)**
Liftoff	**-0.14**	**-0.16**	-0.01	0.05	0.05
	(306)	**(302)**	(306)	(303)	(299)
Yield	**0.16**	**0.13**	**0.20**	**0.15**	**0.16**
	(281)	**(277)**	**(281)**	**(278)**	**(274)**
Elbow angle (3-D)					
Touchdown	0.16	0.08	0.07	0.10	0.10
	(47)	(47)	(47)	(44)	(44)
Mid-stance	-0.10	-0.08	**-0.36**	**-0.34**	**-0.33**
	(150)	(147)	**(150)**	**(147)**	**(144)**
Peak vertical	-0.10	-0.09	**-0.49**	**-0.49**	**-0.46**
	(77)	(75)	**(77)**	**(74)**	**(72)**
Liftoff	0.13	0.08	0.14	0.15	0.15
	(74)	(74)	(74)	(71)	(71)
Yield	0.06	0.02	0.19	0.20	0.19
	(43)	(43)	(43)	(40)	(40)

Presentation of data follows Table 2.9.

Table 2.12. Continued.

	Speed	Froude	Mass	Mass.Speed	Mass.Froude
Wrist angle (peak vertical)	0.03 (159)	0.03 (157)	**0.29 (159)**	**0.31 (156)**	**0.29 (154)**
Hind limb angle					
Protraction (*at TD*)	**0.20 (311)**	**0.22 (309)**	**0.31 (311)**	**0.25 (308)**	**0.26 (306)**
Peak vertical	-0.02 (92)	-0.03 (92)	0.19 (92)	**0.25 (92)**	**0.23 (92)**
Retraction (*at LO*)	**-0.17 (307)**	**-0.15 (304)**	**-0.37 (307)**	**-0.33 (304)**	**-0.34 (301)**
Angular excursion	**0.28 (299)**	**0.29 (297)**	**0.47 (299)**	**0.40 (296)**	**0.42 (294)**
Thigh angle					
Protraction (*at TD*)	**0.25 (321)**	**0.32 (318)**	**0.14 (321)**	0.05 (318)	0.05 (315)
Peak vertical	0.14 (97)	0.16 (97)	**0.27 (97)**	**0.23 (97)**	**0.22 (97)**
Retraction (*at LO*)	**-0.26 (302)**	**-0.25 (299)**	**-0.32 (302)**	**-0.24 (299)**	**-0.26 (296)**
Angular excursion	**0.32 (302)**	**0.36 (299)**	**0.28 (302)**	**0.18 (299)**	**0.19 (296)**
Knee angle (2-D)					
Touchdown	**-0.16 (310)**	**-0.25 (308)**	**0.22 (310)**	**0.32 (307)**	**0.32 (305)**
Mid-stance	**-0.27 (316)**	**-0.35 (316)**	**-0.30 (316)**	**-0.21 (313)**	**-0.22 (313)**
Peak vertical	**-0.35 (97)**	**-0.43 (97)**	**-0.22 (97)**	-0.02 (94)	-0.02 (94)
Liftoff	**0.15 (301)**	**0.15 (298)**	0.05 (301)	-0.01 (298)	0.00 (295)
Yield	**0.17 (306)**	**0.17 (306)**	**0.51 (306)**	**0.49 (303)**	**0.49 (303)**
Knee angle (3-D)					
Touchdown	-0.17 (36)	-0.29 (36)	-0.12 (36)	-0.07 (33)	-0.06 (33)
Mid-stance	-0.27 (33)	**-0.40 (33)**	-0.27 (33)	-0.16 (30)	-0.11 (30)
Peak vertical	-0.07 (9)	-0.07 (9)	0.19 (9)	0.41 (6)	0.33 (6)
Liftoff	-0.09 (9)	0.00 (9)	-0.63 (9)	-0.63 (6)	-0.63 (6)
Yield	0.05 (21)	0.11 (21)	-0.01 (21)	-0.02 (18)	-0.03 (18)

Table 2.12. Continued.

	Speed	Froude	Mass	Mass.Speed	Mass.Froude
Ankle angle (peak vertical)	-0.15	**-0.22**	-0.08	0.00	0.02
	(92)	**(92)**	(92)	(89)	(89)
Substrate reaction forces					
Sagittal forelimb SRF	**0.32**	**0.34**	-0.07	**-0.31**	**-0.22**
magnitude	**(159)**	**(157)**	(159)	**(156)**	**(154)**
Sagittal forelimb SRF angle	0.11	0.12	0.12	0.07	0.08
	(159)	(157)	(159)	(156)	(156)
Total forelimb SRF	**0.32**	**0.34**	-0.07	**-0.31**	**-0.22**
magnitude	**(159)**	**(157)**	(159)	**(156)**	**(154)**
Sagittal hind limb SRF	**0.40**	**0.47**	0.20	-0.04	0.00
magnitude	**(91)**	**(91)**	(91)	(88)	(88)
Sagittal hind limb SRF angle	-0.11	-0.11	-0.21	-0.19	**-0.21**
	(91)	(91)	(91)	(88)	**(88)**
Total hind limb SRF	**0.40**	**0.47**	0.20	-0.04	0.00
magnitude	**(91)**	**(91)**	(91)	(88)	(88)
Moment arms (body mass)					
Shoulder	-0.05	-0.06	0.00	0.03	0.02
	(159)	(157)	(159)	(156)	(154)
Elbow (2-D)	**0.37**	**0.32**	**0.51**	**0.41**	**0.44**
	(159)	**(157)**	**(159)**	**(156)**	**(154)**
Elbow (3-D)	**0.23**	0.18	**0.40**	**0.36**	**0.37**
	(74)	(72)	**(74)**	**(74)**	**(69)**
Wrist	0.03	0.04	**-0.21**	**-0.26**	**-0.24**
	(159)	(157)	**(159)**	**(156)**	**(154)**
Hip	-0.13	-0.14	0.07	0.18	0.15
	(92)	(92)	(92)	(89)	(89)
Knee (2-D)	**0.30**	**0.32**	0.09	-0.10	-0.07
	(92)	**(92)**	(92)	(89)	(89)
Knee (3-D)	0.09	0.01	0.20	0.36	0.45
	(8)	(8)	(8)	(5)	(5)
Ankle	-0.04	-0.04	0.09	0.14	0.12
	(92)	(92)	(92)	(89)	(89)
Moment arms (limb length)					
Shoulder	-0.09	-0.10	0.01	0.05	0.03
	(159)	(157)	(159)	(156)	(154)
Elbow (2-D)	**0.26**	**0.23**	**0.44**	**0.37**	**0.38**
	(159)	**(157)**	**(159)**	**(156)**	**(154)**
Elbow (3-D)	0.15	0.11	**0.36**	**0.34**	**0.33**
	(74)	(72)	**(74)**	**(71)**	**(69)**
Wrist	0.00	0.01	**-0.19**	**-0.21**	**-0.20**
	(159)	(157)	**(159)**	**(159)**	**(159)**

Table 2.12. Continued.

	Speed	Froude	Mass	Mass.Speed	Mass.Froude
Moment arms (limb length)					
Hip	-0.14	-0.14	0.04	0.14	0.11
	(92)	(92)	(92)	(89)	(89)
Knee (2-D)	**0.30**	**0.34**	0.11	-0.08	-0.05
	(92)	**(92)**	(92)	(89)	(89)
Knee (3-D)	-0.01	-0.08	0.10	0.33	0.39
	(8)	(8)	(8)	(5)	(5)
Ankle	-0.06	-0.11	0.02	0.06	0.02
	(92)	(92)	(92)	(89)	(89)
Moments (body mass)					
Shoulder	0.14	0.12	0.14	0.08	0.11
	(159)	(157)	(159)	(156)	(154)
Elbow (2-D)	**0.55**	**0.50**	**0.53**	**0.37**	**0.44**
	(159)	**(157)**	**(159)**	**(156)**	**(154)**
Elbow (3-D)	**0.60**	**0.55**	**0.43**	**0.36**	**0.46**
	(74)	**(72)**	**(74)**	**(71)**	**(69)**
Wrist	**0.34**	**0.32**	0.00	-0.19	-0.11
	(159)	**(157)**	(159)	(156)	(154)
Hip	0.07	0.06	**0.22**	**0.22**	**0.22**
	(92)	(92)	**(92)**	**(89)**	**(89)**
Knee (2-D)	**0.29**	**0.32**	0.08	-0.12	-0.08
	(92)	**(92)**	(92)	(89)	(89)
Knee (3-D)	0.28	0.27	0.35	0.29	0.28
	(8)	(8)	(8)	(5)	(5)
Ankle	**0.42**	**0.44**	**0.40**	**0.21**	**0.24**
	(92)	**(92)**	**(92)**	**(89)**	**(89)**
*Moments (body weight*length)*					
Shoulder	-0.02	-0.02	-0.1	-0.1	-0.09
	(159)	(157)	(159)	(156)	(154)
Elbow (2-D)	**0.41**	**0.40**	**0.23**	0.05	0.12
	(159)	**(157)**	**(159)**	(156)	(154)
Elbow (3-D)	**0.48**	**0.51**	0.07	0.07	0.04
	(74)	**(72)**	(74)	(71)	(71)
Wrist	**0.37**	**0.37**	-0.07	**-0.28**	**-0.20**
	(159)	**(157)**	(159)	**(156)**	**(154)**
Hip	0.00	0.01	0.12	0.15	0.13
	(92)	(92)	(92)	(89)	(89)
Knee (2-D)	**0.27**	**0.31**	0.04	-0.14	-0.12
	(92)	**(92)**	(92)	(89)	(89)
Knee (3-D)	0.14	0.14	0.22	0.28	0.22
	(8)	(8)	(8)	(4)	(4)
Ankle	**0.30**	**0.36**	0.16	0.00	0.00
	(92)	**(92)**	(92)	(89)	(89)

Table 2.13. Direct and indirect influences of limb length on joint moment arm lengths across the ontogenetic sample.

Shoulder Moment Arm		**Elbow Moment Arm**		**Hip Moment Arm**		**Knee Moment Arm**	
Symmetrical ground		*Symmetrical ground*		*Symmetrical ground*		*Symmetrical ground*	
Forelimb length		Forearm length		Hind limb length		Leg length	
Direct	0.100	Direct	0.343	Direct	0.230	Direct	0.059
Indirect	-0.001	Indirect	0.027	Indirect	-0.028	Indirect	0.208
Total	0.099	Total	0.370	Total	0.202	Total	0.267
Asymmetrical ground		*Asymmetrical ground*		*Asymmetrical ground*		*Asymmetrical ground*	
Forelimb length		Forearm length		Hind limb length		Leg length	
Direct	0.119	Direct	0.467	Direct	0.201	Direct	0.159
Indirect	-0.014	Indirect	0.106	Indirect	-0.003	Indirect	0.058
Total	0.105	Total	0.573	Total	0.198	Total	0.217
Symmetrical pole		*Symmetrical pole*		*Symmetrical pole*		*Symmetrical pole*	
Forelimb length		Forearm length		Hind limb length		Leg length	
Direct	0.238	Direct	0.331	Direct	0.179	Direct	0.025
Indirect	-0.040	Indirect	0.177	Indirect	-0.049	Indirect	0.302
Total	0.198	Total	0.508	Total	0.130	Total	0.327
Asymmetrical pole		*Asymmetrical pole*		*Asymmetrical pole*		*Asymmetrical pole*	
Forelimb length		Forearm length		Hind limb length		Leg length	
Direct	0.264	Direct	0.301	Direct	0.141	Direct	0.083
Indirect	-0.087	Indirect	0.322	Indirect	-0.039	Indirect	0.210
Total	0.177	Total	0.623	Total	0.102	Total	0.293

Direct effects, equivalent to the path coefficients shown in Figures 2.7-2.10, quantify the influence of limb length on joint moment arm lengths, independent of all postural variables. Indirect effects quantify the influence of limb length solely attributable to correlations between limb length and angular variables (see Section 2.2.6 for details on calculation). Total effects (i.e., sum of direct and indirect effects) quantify the total correlation between limb length and moment arm length.

Table 2.14. Least-squares regressions of joint moments on the product of body weight and anatomical limb length below each joint, grouped by gait and substrate.

	Shoulder moment		**Elbow moment**		**Hip moment**		**Knee moment**	
	Slope	R^2	Slope	R^2	Slope	R^2	Slope	R^2
Symmetrical ground	0.083 ± 0.076	0.245	0.301 ± 0.164	0.199	0.356 ± 0.161	0.381	0.321 ± 0.279	0.143
Asymmetrical ground	0.009 ± 0.018	0.397	0.666 ± 0.139	0.448	0.407 ± 0.136	0.449	0.298 ± 0.202	0.164
Symmetrical pole	0.044 ± 0.023	0.127	0.343 ± 0.152	0.162	0.301 ± 0.096	0.302	0.205 ± 0.139	0.089
Asymmetrical pole	0.145 ± 0.040	0.504	0.794 ± 0.094	0.642	0.246 ± 0.129	0.137	0.284 ± 0.176	0.103

Table 2.15. Scaling of limb growth in primates.

Species	Segment	Exponent	Pattern	r	Reference
Propithecus tattersalli (Golden-crowned sifaka)	Forelimb	0.319 ± 0.022	I	0.979	Ravosa et al. (1993)
	Hand	0.289 ± 0.021	NA	0.977	
	Hind limb	0.305 ± 0.018	NA	0.984	
	Foot	0.286 ± 0.025	NA	0.966	
Propithecus diadema (Diademed sifaka)	Forelimb	0.383 ± 0.012	PA	0.996	Ravosa et al. (1993)
	Hand	0.338 ± 0.009	I	0.997	
	Hind limb	0.397 ± 0.013	PA	0.996	
	Foot	0.308 ± 0.012	NA	0.994	
Propithecus verreauxi (Verreaux's sifaka)	Arm	0.381	NA	0.656	Lawler (2006)[1]
	Forearm	0.344	NA	0.755	
	Hand	0.286	NA	0.735	
	Thigh	0.344	NA	0.755	
	Leg	0.332	NA	0.663	
	Foot	0.250	NA	0.721	
Saimiri boliviensis (Bolivian squirrel monkey)	Arm	0.624 ± 0.073	PA	0.820	This study
	Forearm	0.702 ± 0.079	PA	0.835	
	Thigh	0.555 ± 0.061	PA	0.842	
	Leg	0.539 ± 0.052	PA	0.883	
	Forelimb	0.616 ± 0.058	PA	0.886	
	Hind limb	0.533 ± 0.051	PA	0.883	
Cebus albifrons (White-fronted capuchin monkey)	Humerus	0.546 ± 0.093	PA	--	Jungers and Fleagle (1980)[2]
	Radius	0.627 ± 0.171	PA	--	
	Hand	0.378 ± 0.122	I	--	
	Femur	0.614 ± 0.152	PA	--	
	Tibia	0.611 ± 0.117	PA	--	
	Foot	0.422 ± 0.105	I	--	

Except where indicated, allometric exponents were calculated from reduced major axis regressions of segment length on body mass. 95% confidence intervals on the exponents and correlation coefficients (r) are shown where available. PA: positive allometry; NA: negative allometry; I: isometry. Common names for each species are shown in parentheses.

[1] Although these authors did not provide confidence intervals on calculated exponents, the scaling relationships are indicated to be significant at the α=0.05 level.

[2] Parameters calculated using least-squares regression

Table 2.15. Continued

Species	Segment	Exponent	Pattern	r	Reference
Cebus apella (Tufted capuchin monkey)	Humerus	0.472 ± 0.112	PA	--	Jungers and Fleagle (1980)[2]
	Radius	0.528 ± 0.069	PA	--	
	Hand	0.302 ± 0.164	I	--	
	Femur	0.542 ± 0.138	PA	--	
	Tibia	0.501 ± 0.129	PA	--	
Papio cynocephalus (Yellow baboon)	Forelimb	0.319 ± 0.029	I	0.926	Raichlen (2005)
	Hind limb	0.363 ± 0.037	I	0.910	
Chlorocebus aethiops (Vervet monkey)	Arm	0.389 ± 0.029	PA	0.962	(Turner et al., 1997)
	Forearm	0.389 ± 0.028	PA	0.965	
	Hand	0.301 ± 0.024	NA	0.956	
	Thigh	0.402 ± 0.028	PA	0.968	
	Leg	0.388 ± 0.027	PA	0.966	
	Foot	0.288 ± 0.024	NA	0.954	
Hylobates lar (White-handed gibbon)	Humerus	0.368	PA	--	Jungers and Cole (1992)[1]
	Radius	0.410	PA	--	
	Femur	0.353	I	--	
	Tibia	0.372	PA	--	
Pan troglodytes (Chimpanzee)	Humerus	0.39 ± 0.04	I	0.92	Hartwig-Scherer and Martin (1992)
	Femur	0.41 ± 0.04	PA	0.92	
Gorilla gorilla (Gorilla)	Humerus	0.41 ± 0.03	PA	0.99	Hartwig-Scherer and Martin (1992)
	Femur	0.42 ± 0.04	PA	0.98	
Pongo pygmaeus (Orangutan)	Humerus	0.41 ± 0.02	PA	0.99	Hartwig-Scherer and Martin (1992)
	Femur	0.42 ± 0.03	PA	0.99	

Table 2.16. Scaling of limb growth in non-primate mammals.

Species	Segment	Exponent	r	Pattern	Reference
Monodelphis domesticus (Gray short-tailed opossum)	Humerus	0.39	--	PA	Lammers and German (2002)[1]
	Radius	0.37	--	I	
	Metacarpal III	0.25	--	NA	
	Femur	0.44	--	PA	
	Tibia	0.39	--	PA	
	Metatarsal III	0.32	--	I	
Trichosurus vulpecula (Brushtail opossum)	Humerus	0.365	0.842	I	Lentle et al. (2006)[1]
	Radius	0.461	0.802	I	
	Ulna	0.400	0.853	PA	
	Femur	0.451	0.868	PA	
	Tibia	0.469	0.864	PA	
	Fibula	0.461	0.869	PA	
Macropus eugenii (Tammar wallaby)	Humerus	0.352	0.984	I	Lentle et al. (2006)[1]
	Radius	0.457	0.962	PA	
	Ulna	0.403	0.975	PA	
	Femur	0.546	0.950	PA	
	Tibia	1.252	0.826	PA	
	Fibula	0.543	0.986	PA	
Chinchilla lanigera (Chinchilla)	Humerus	0.33	--	I	Lammers and German (2002)[1]
	Radius	0.28	--	NA	
	Metacarpal III	0.21	--	NA	
	Femur	0.40	--	PA	
	Tibia	0.37	--	PA	
	Metatarsal III	0.23	--	NA	
Oryctolagus cuniculus (Domestic white rabbit)	Humerus	0.38	--	PA	Lammers and German (2002)[1]
	Radius	0.41	--	PA	
	Metacarpal III	0.34	--	I	
	Femur	0.42	--	PA	
	Tibia	0.42	--	PA	
	Metatarsal III	0.36	--	I	

Presentation of data as in Table 15.

[1]Although these authors did not provide confidence intervals on calculated exponents, the scaling relationships are indicated to be significant at the α=0.05 level.

Table 2.16. Continued.

Species	Segment	Exponent	r	Pattern	Reference
Lepus californicus (Jackrabbit)	Humerus	0.368 ± 0.026	0.984	PA	Carrier (1983)
	Radius	0.402 ± 0.022	0.987	PA	
	Metacarpal III	0.290 ± 0.017	0.948	NA	
	Femur	0.418 ± 0.026	0.974	PA	
	Tibia	0.468 ± 0.028	0.983	PA	
	Metatarsal III	0.339 ± 0.018	0.967	I	
Rattus norvegicus (Domestic white rat)	Humerus	0.42	--	PA	Lammers and German (2002)[1]
	Radius	0.33	--	I	
	Metacarpal III	0.16	--	NA	
	Femur	0.53	--	PA	
	Tibia	0.41	--	PA	
	Metatarsal III	0.18	--	NA	
Galea musteloides (Cui)	Humerus	0.304 ± 0.010	0.969	NA	Schilling and Petrovitch (2006)
	Radius	0.268 ± 0.013	0.934	NA	
	Hand	0.246 ± 0.016	0.866	NA	
	Femur	0.373 ± 0.011	0.977	PA	
	Tibia	0.300 ± 0.008	0.979	NA	
	Metatarsals	0.235 ± 0.007	0.970	NA	
Felis domesticus (Domestic cat)	Ulna	0.411 ± 0.069	0.979	PA	Carrier (1983)
	Metacarpal	0.342 ± 0.052	0.983	I	
	Metatarsal	0.415 ± 0.067	0.960	PA	
Tupaia glis (Tree shrew)	Humerus	0.380 ± 0.030	0.854	PA	Schilling and Petrovitch (2006)
	Radius	0.300 ± 0.020	0.899	NA	
	Hand	0.205 ± 0.020	0.760	NA	
	Femur	0.471 ± 0.035	0.865	PA	
	Tibia	0.354 ± 0.026	0.867	I	
	Metatarsals	0.263 ± 0.030	0.660	NA	
Sus domesticus (Domestic pig)	Humerus	0.286	0.98	NA	Liu et al. (1999)[1]
	Radius	0.293	0.99	NA	
	Femur	0.323	0.99	NA	
	Tibia	0.313	0.99	NA	
Ovibos moschatus (Muskox)	Femur	0.26 ± 0.02	--	NA	Heinrich et al. (1999)

2.6. Figures

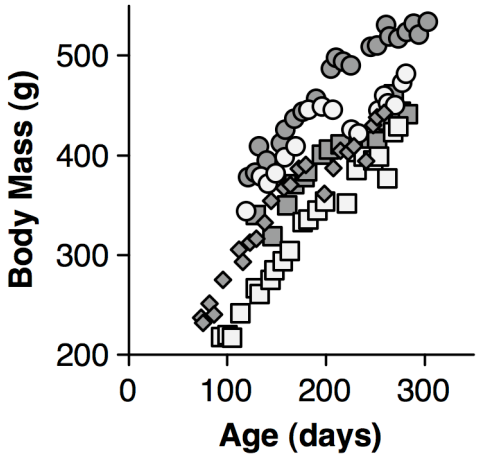

Figure 2.1. Body mass plotted against age for all infant *Saimiri boliviensis*.
Body mass increased as a linear function of age in all infants. Shaded circles = Animal 4428 (R^2=0.924); white diamonds = Animal 4433; shaded squares = Animal 4445 (R^2=0.860); white circles = Animal 4466 (R^2=0.739); white squares = Animal 4475 (R^2=0.970); shaded diamonds = Animal 4483 (R^2=0.908). The coefficient of determination was not computed for Animal 4433 due to limited participation (see text).

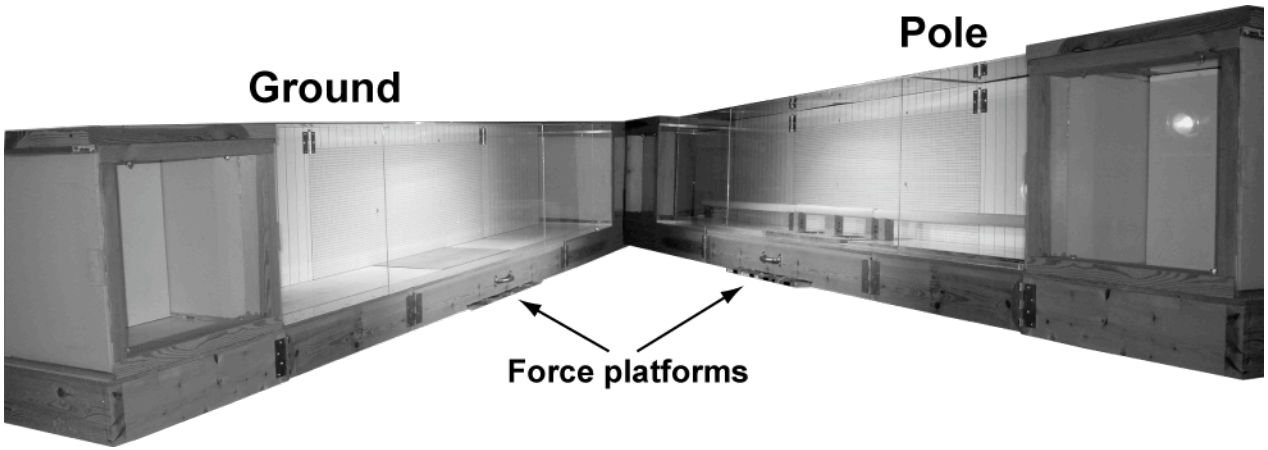

Figure 2.2. Illustration of the runway used for all locomotor experiments.
The runway is shown in both the flat ground and elevated pole configurations. See text for details on design and construction.

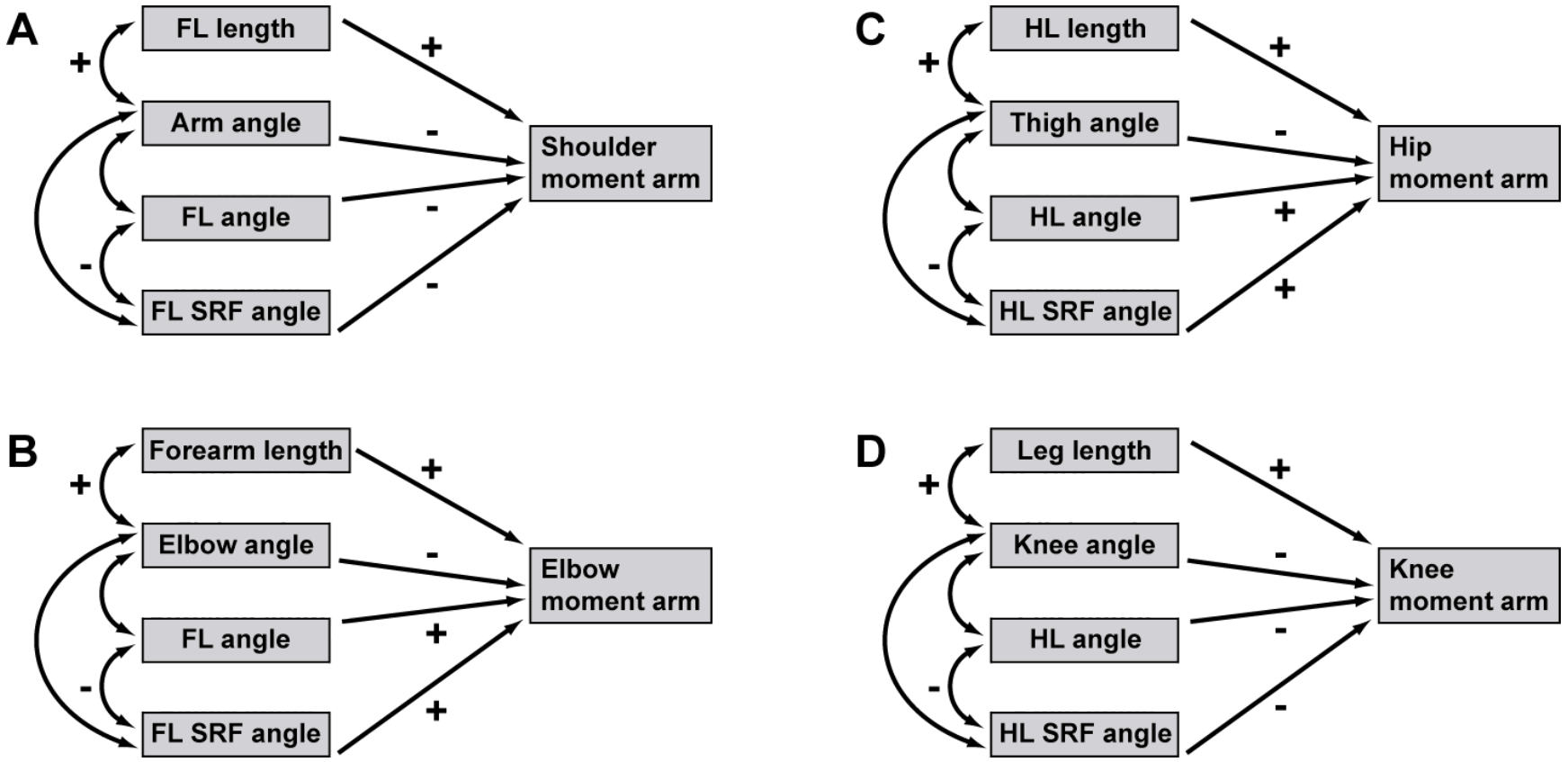

Figure 2.3. Schematic of the diagrams used for path analyses.
Paths are shown for shoulder (A), elbow (B), hip (C), and knee (D) joints. Single-headed arrows indicate a directed causal link between predictor variables and moment arm lengths. Double-headed arrows indicate an undirected correlation between predictor variables. + and – symbols indicate the predicted direction of the relationship.

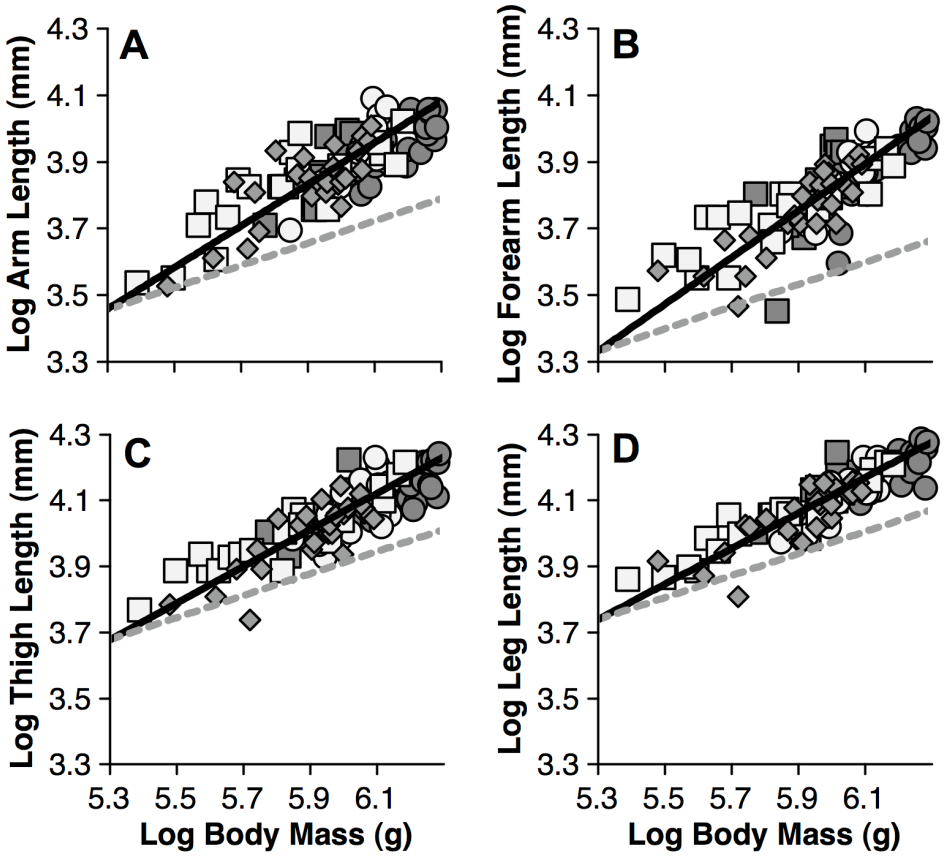

Figure 2.4. Allometry of limb growth in *Saimiri boliviensis*.
Data are presented for each segment, separated by individual (symbols as in Fig. 2.1). Black lines illustrate calculated RMA slopes for each segment (computed across individuals). Dashed gray lines indicate isometry. Graphs are plotted on the same scale to indicate absolute differences in segment length. All segment lengths scaled to body mass with strong positive allometry.

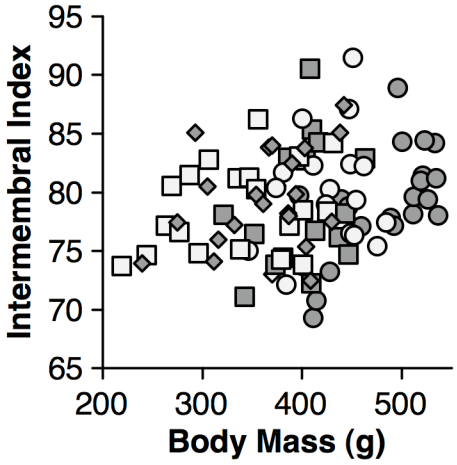

Figure 2.5. Ontogenetic changes in the intermembral index (forelimb length/hind limb length*100%) in *Saimiri boliviensis*.
Data are separated by individual (symbols follow Fig. 2.1). The intermembral index showed a slight, but significant, increase across the ontogenetic sample.

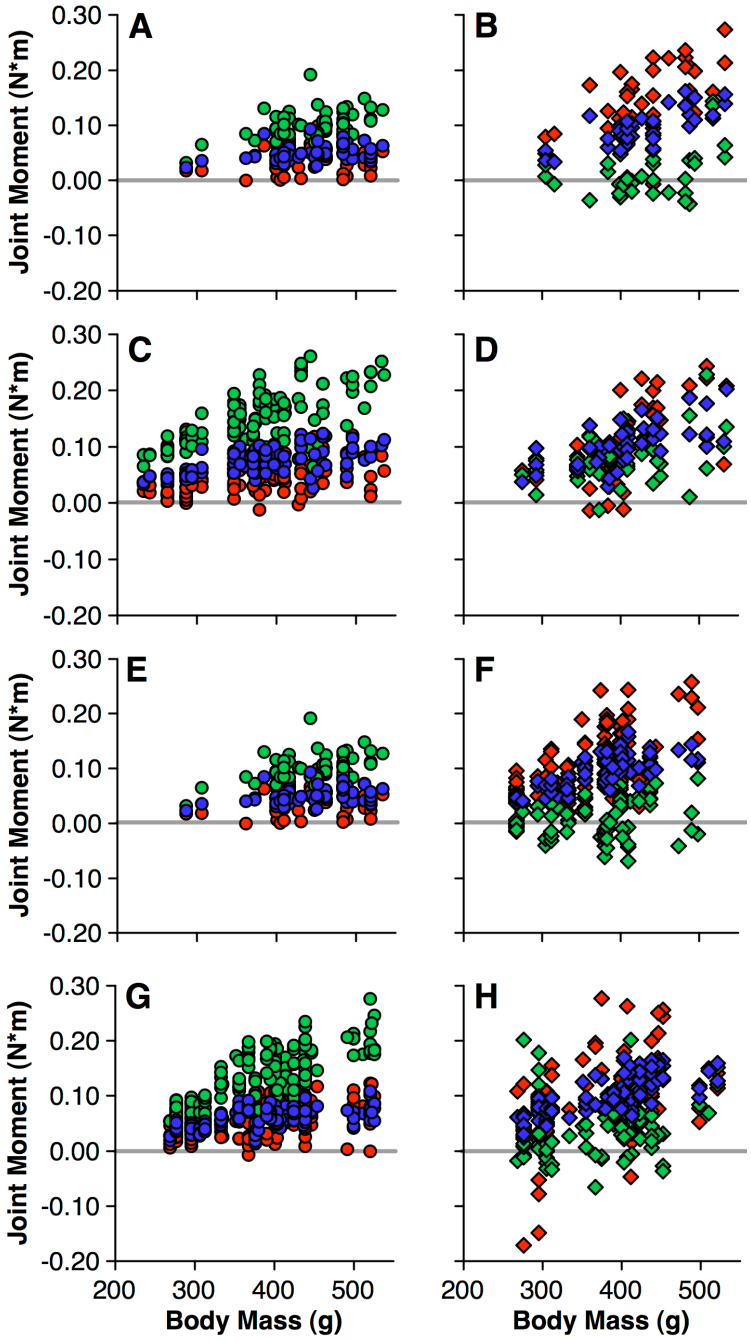

Figure 2.6. Scatter plots of absolute joint moment magnitudes versus body mass. Data are shown for symmetrical gaits on the ground (A and B), asymmetrical gaits on the ground (C and D), symmetrical gaits on the pole (E and F), and asymmetrical gaits on the pole (G and H). Forelimb joint moments are represented by circles (red=shoulder, green=elbow, blue=wrist) and graphed in the left-hand panels. Hind limb joint moments are represented by squares (red=hip, green=knee, blue=ankle) and graphed in the right-hand panels. The gray horizontal bar indicates the division between positive flexing moments and negative extending moments. Note that, with the exception of the knee joint, most joints in both limbs primarily experienced flexing moments.

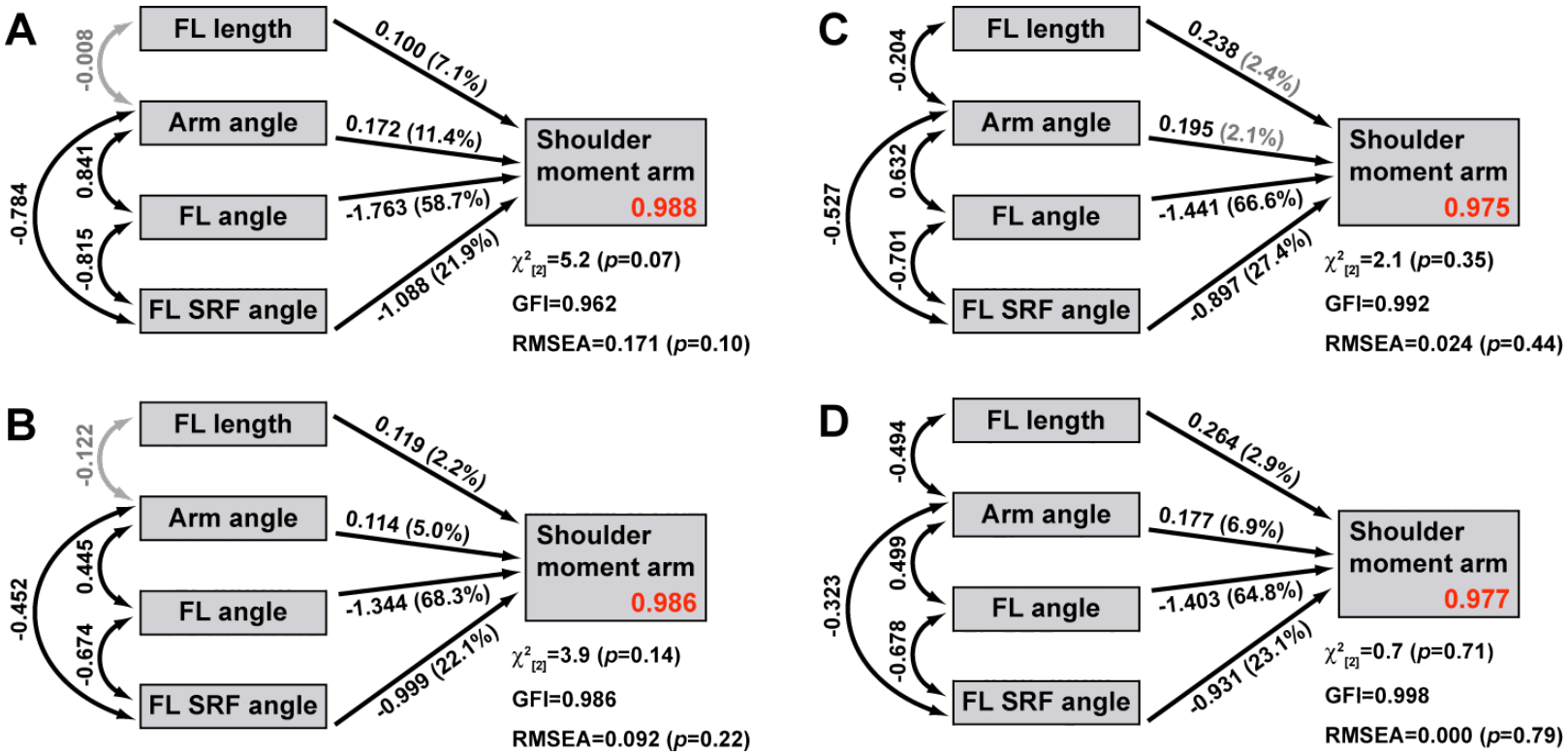

Figure 2.7. Path analyses of the influences of limb length, posture, and SRF direction on shoulder joint moment arm lengths. Paths are shown for symmetrical (A) and asymmetrical (B) strides on the ground and symmetrical (C) and asymmetrical (D) strides on the pole. Values in parentheses next to the path coefficients show the percentage of moment arm length variance explained by each predictor variable, as determined by hierarchical partitioning. Values shaded in gray were not significant at the α=0.05 level. Measures of model fit are also presented for each subgroup (see text for details). Total R^2 for the entire model, including all the direct and indirect effects of each predictor variable, is shown in bold red text in the moment arm box.

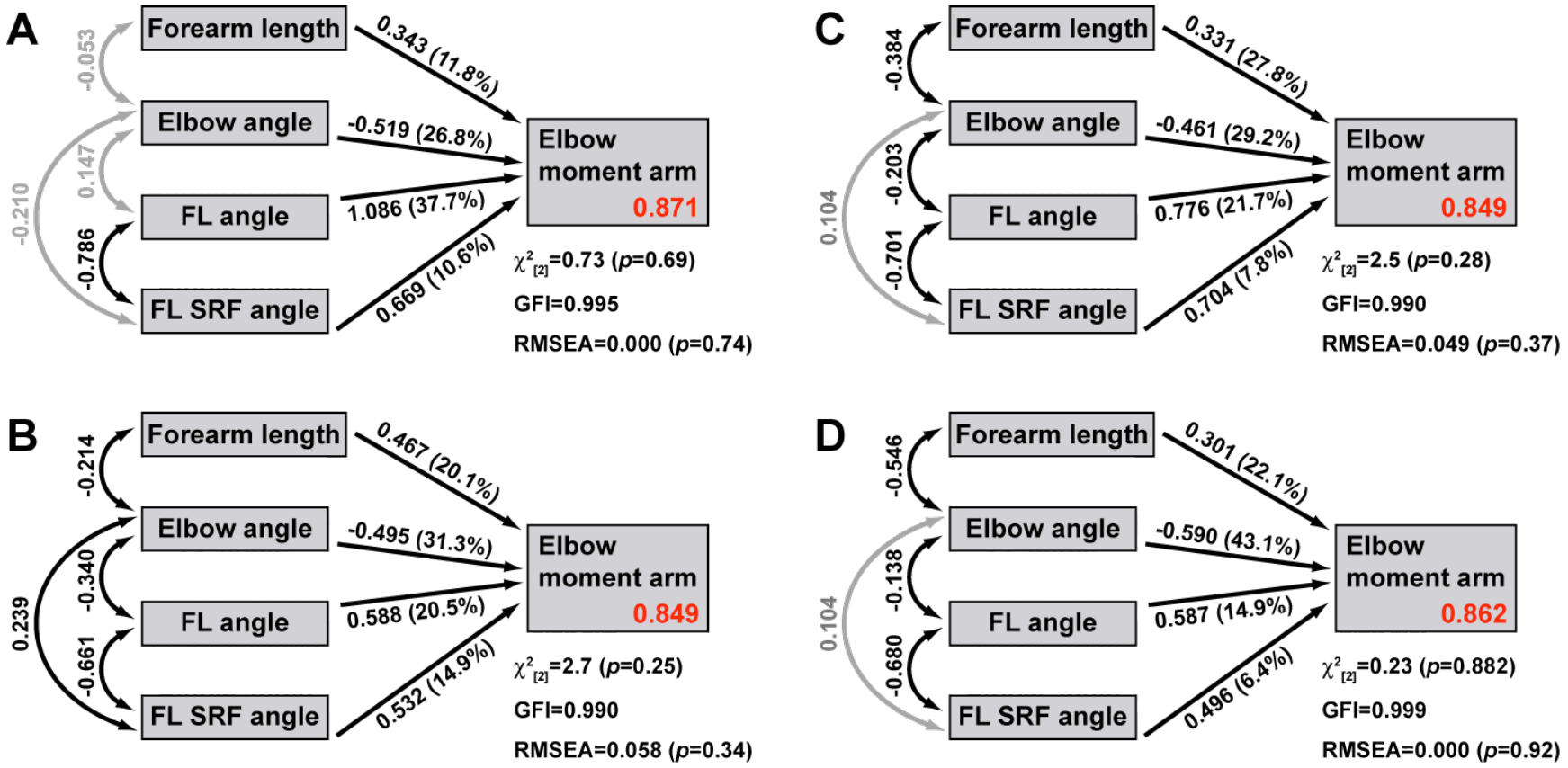

Figure 2.8. Path analyses of the influences of limb length, posture, and SRF direction on elbow joint moment arm lengths. Paths are shown for symmetrical (A) and asymmetrical (B) strides on the ground and symmetrical (C) and asymmetrical (D) strides on the pole. Presentation of data follows Figure 2.7.

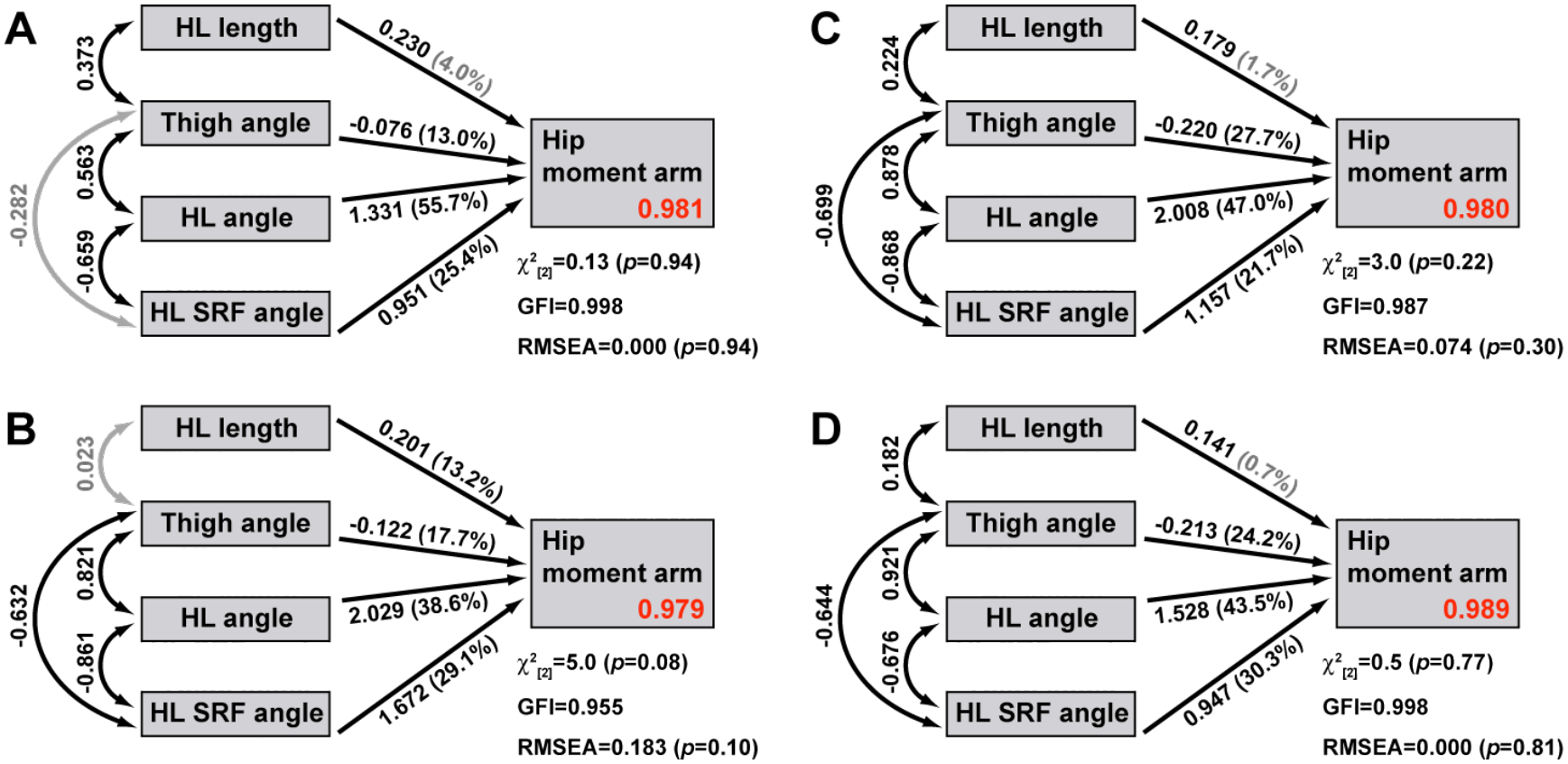

Figure 2.9. Path analyses of the influences of limb length, posture, and SRF direction on hip joint moment arm lengths. Paths are shown for symmetrical (A) and asymmetrical (B) strides on the ground and symmetrical (C) and asymmetrical (D) strides on the pole. Presentation of data follows Figure 2.7.

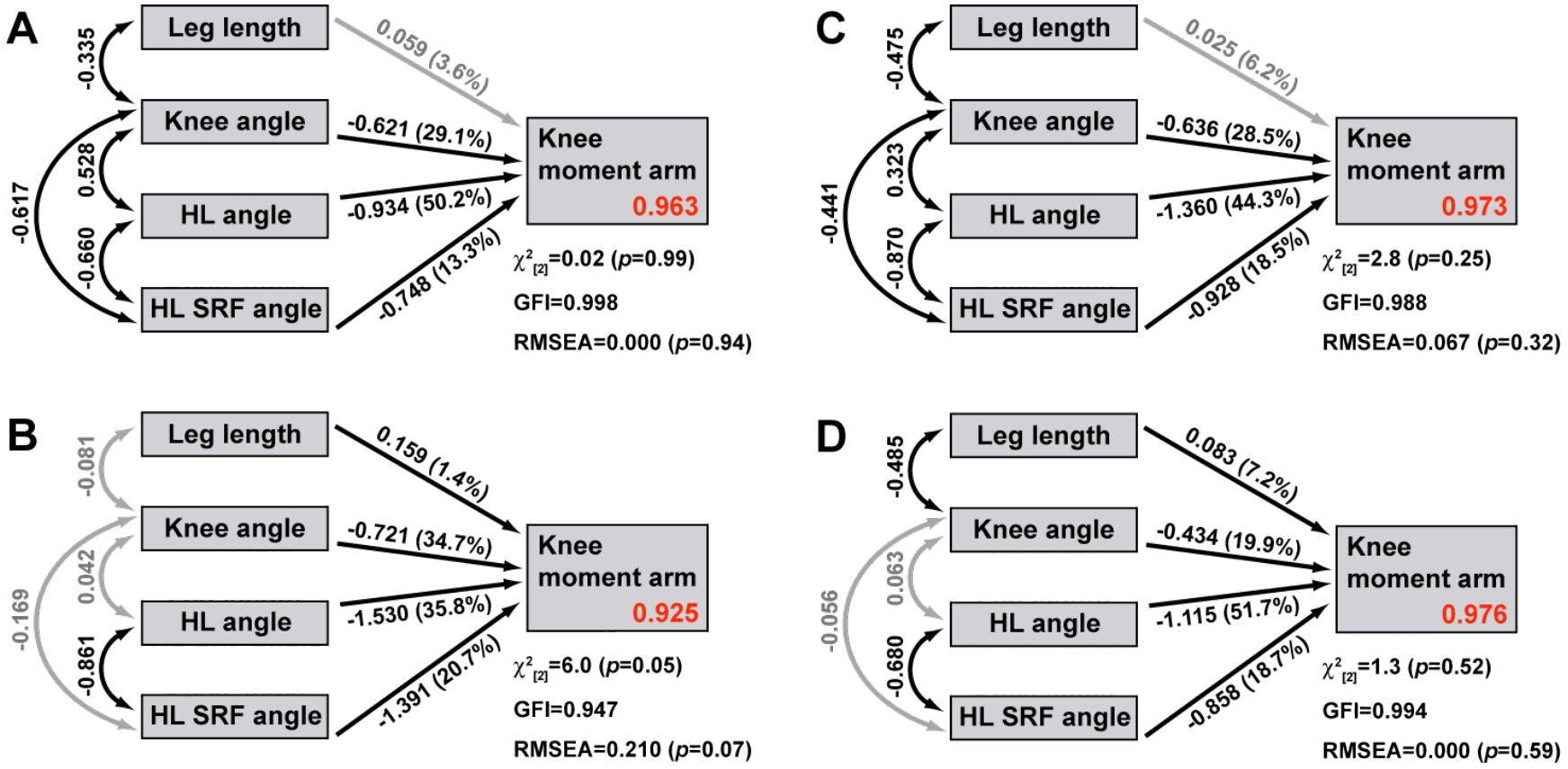

Figure 2.10. Path analyses of the influences of limb length, posture, and SRF direction on knee joint moment arm lengths. Paths are shown for symmetrical (A) and asymmetrical (B) strides on the ground and symmetrical (C) and asymmetrical (D) strides on the pole. Presentation of data follows Figure 2.7.

Chapter 3: Substrate Determines Asymmetrical Gait Dynamics in Marmosets (*Callithrix jacchus*) and Squirrel Monkeys (*Saimiri boliviensis*)

3.1. Introduction

Arboreal locomotion may be compromised by two sources of instability: toppling moments around the long axis of the branch and branch sway (Napier, 1967; Cartmill, 1985; Demes et al., 1990; Schmitt, 1994, 1999; Stevens, 2003; Lammers and Biknevicius, 2004). Both problems are exacerbated as 1) substrate diameter decreases relative to body size and 2) locomotor speed increases. On a relatively wide branch, an animal can counter the potential for toppling moments by distributing the limbs transversely, thereby broadening the base of support (Rose, 1973; Cartmill, 1985). In this way, locomotion on wide arboreal supports can be functionally indistinguishable from terrestrial locomotion (Jenkins, 1974). However, as branch size decreases relative to body size, all points of foot contact become effectively collinear (Cartmill, 1985), minimizing the base of support and increasing the potential for disruptive toppling moments. Similarly, the average bending stress in a supporting branch varies directly with magnitude of the bending moment, which is proportional to body mass, and indirectly with the branch's second moment of area, which is proportional to branch diameter (assuming a circular cross-section). Therefore, branch deflection and branch sway also increase as branch size decreases relative to body size. Finally, traveling at higher speeds generally increases the forces exerted on the substrate. Greater force magnitudes should increase both the shear forces beneath the hands and feet and the bending moments applied to the substrate, intensifying the potential for toppling moments and branch sway. In sum, arboreally stability is generally increased by minimizing both the forces exerted on substrate and the vertical movement of the center of mass (COM).

Studies of skeletal pathology indicate that injury from falling may account for the greatest incidence of long bone trauma in free-ranging primate populations (Schultz, 1944; Bramblett, 1967; Buikstra, 1975; Lovell, 1990; Lovell, 1991; Jurmain, 1997; Carter et al., 2008). Such studies suggest that primates should be under strong selective pressure to manifest morphological and behavioral mechanisms that increase stability on arboreal substrates. Morphological adaptations permitting primates to counteract disruptive toppling moments include divergent first manual and pedal rays (particularly the hallux), well-developed flexor and rotator musculature in the distal limbs, frictional skin on the volar surfaces of the hands and feet, and long tails that can be used statically as counterbalances or dynamically to generate stabilizing angular momentum (Cartmill, 1972, 1979; Boinski, 1989; Lemelin, 1999; Hamrick, 2001; Larson and Stern, 2006; Lemelin and Schmitt, 2007). Additionally, many primates and other arboreal mammals increase joint flexion when moving arboreally (Napier, 1967; Taylor, 1970; Rose, 1973; Schmitt, 2003c; Stevens, 2003), reducing the distance between the COM and the substrate, shortening the toppling gravitational moment arm. Primates use a variety of behavioral mechanisms to mitigate arboreal instability, including longer substrate contact times (i.e., duty factors), larger limb angular excursions, greater limb joint yield over a step, increased stride lengths, and lower stride frequencies (Rose, 1973; Alexander and Maloiy, 1984; Reynolds, 1987; Demes et al., 1990; Schmitt, 1994; Larson, 1998; Schmitt, 1999; Larson et al., 2000; Larson et al., 2001; Schmitt, 2003c; Stevens, 2003;

Larney and Larson, 2004; Schmitt and Hanna, 2004). Together, these behavioral modifications decrease the potential for disruptive branch sway by facilitating a more compliant gait, thereby reducing peak forces and minimizing the vertical displacement of the COM. Morphological adaptations permitting limb compliance are more ambiguous, although several authors have identified skeletal features permitting greater joint mobility and limb compliance (Fleagle, 1977; Larson, 1993; Larson, 2007). Additionally, long distally heavy limbs may be considered primate "exaptations" facilitating long stride lengths and low stride frequencies (Alexander et al., 1979; Polk et al., 2000; Raichlen, 2004a, 2005a; Raichlen et al., 2007).

Our understanding of how primates adapt locomotor behaviors to increase arboreal stability comes almost exclusively from studies of symmetrical gait dynamics (i.e., walking and running). Few studies have examined the dynamics of asymmetrical gaits in primates (but see Vilensky, 1980; Vilensky and Patrick, 1985; Vilensky and Gankiewicz, 1986; Hurov, 1987; Vilensky et al., 1990; Kimura, 1992; Demes et al., 1994; Franz et al., 2005; Hanna et al., 2006; Raichlen et al., 2007). Nevertheless, asymmetrical gaits constitute an important element of most primates' locomotor repertoires, particularly in smaller-bodied taxa. In a symmetrical gait, each forelimb is temporally paired with a hind limb and footfalls of contralateral fore- and hind limb pairs (e.g., right and left hind limbs) are evenly spaced in time (Hildebrand, 1965, 1966, 1967; Gambaryan, 1974; Sukhanov, 1974; Hildebrand, 1976). By contrast, during asymmetrical gaits, forelimbs are paired together and hind limbs are paired together and the footfalls of contralateral fore- and hind limb pairs are unevenly spaced in time (Howell, 1944; Gambaryan, 1974; Hildebrand, 1977, 1980; Renous et al., 2004)[2]. Asymmetrical gaits are typically used at higher speeds and are associated with greater substrate forces (Demes et al., 1994; Franz et al., 2005; Hanna et al., 2006). Despite the potential for increased forces to exacerbate arboreal instability, no previous study has explicitly focused on how primates might modify asymmetrical gait dynamics to ensure stability on arboreal substrates.

3.1.1. Specific aims and hypotheses

This study focused on asymmetrical gait dynamics in ontogenetic samples of common marmosets (*Callithrix jacchus*, L. 1758) and Bolivian (i.e., black-capped) squirrel monkeys (*Saimiri boliviensis*, Geoffroy and Blainville 1834) moving on terrestrial and simulated arboreal substrates. Despite belonging to the same family of platyrrhine monkeys, the Cebidae, marmosets and squirrel monkeys differ in many aspects of their ecology, anatomy and locomotor behavior. Marmosets are among the smallest platyrrhine primates, with an average adult body mass of 320 grams (Smith and Jungers, 1997). They are primarily found in sub-Amazonian Brazil and the eastern edge of Bolivia (Digby et al., 2007). Although no study has exclusively focused on the positional behavior of common marmosets, previous studies of other closely-related callitrichine genera have suggested that asymmetrical gaits represent a substantial portion

[2] Actually, symmetrical gaits are more properly viewed as the small subset of all possible asymmetrical gaits in which forelimb and hind limb leads (i.e., duration between successive touchdowns) are approximately equal to 50% of stride duration (Hildebrand, 1977; Renous et al., 2004).

of the locomotor repertoire, accounting for 33-50% of arboreal travel among tamarins and Goeldi's monkeys (Fleagle and Mittermeier, 1980; Garber, 1991; Rosenberger and Stafford, 1994; Stafford et al., 1996). Marmosets and other callitrichines are unique among extant primates in having claws, rather than nails, on every digit but the hallux. Clawed digits are often interpreted as an adaptation to gumnivory, enabling callitrichines (and particularly marmosets) to grip onto large vertical tree trunks while feeding on tree exudates (Sussman and Kinzey, 1984; Garber, 1992; Hamrick, 1998). An adaptive shift away from a fine-branch foraging environment, often understood to be the fundamental adaptive niche for primates (Cartmill, 1972, 1974b; Rasmussen, 1990; Sussman, 1991; Schmitt and Lemelin, 2002), has also affected marmoset autopodial anatomy. Compared to other small-bodied cebids, marmosets are characterized by relatively narrow apical pads with poorly developed papillary ridges, laterally-compressed terminal manual phalanges, and a relatively short hallux marked by limited mobility and diminished intrinsic adductor musculature (Beattie, 1927; Midlo, 1934; Hamrick, 1998). These derived changes in marmoset autopodial morphology should limit stability and efficiency when moving and foraging in a small branch environment (Hamrick, 1998; Schmitt, 2003a).

Bolivian squirrel monkeys natively inhabit the upper Amazon basin of Peru, southwest Brazil and Bolivia (Boinski, 1999; Jack, 2007). Although not as small as marmosets, squirrel monkeys are still among the smallest anthropoid primates, with an average adult body mass of 811 grams (Smith and Jungers, 1997). Several researchers have studied the locomotor behavior of captive and free-ranging squirrel monkeys (Prost and Sussman, 1969; Fleagle and Mittermeier, 1980; Fleagle et al., 1981; Vilensky and Patrick, 1985; Boinski, 1989; Fontaine, 1990; Vilensky, 1994; Youlatos, 1999; Arms et al., 2002; Schmidt, 2005). Both in captivity (Fontaine, 1990; Arms et al., 2002) and the wild (Fleagle and Mittermeier, 1980; Fleagle et al., 1981; Boinski, 1989; Youlatos, 1999), arboreal quadrupedalism represents the predominant mode of locomotion. Fontaine (1990) found that asymmetrical gaits accounted for 16% of all quadrupedal locomotion in semi-captive free-ranging Bolivian squirrel monkeys. Unlike marmosets, squirrel monkeys frequently feed and travel in a fine-branch niche (Fleagle et al., 1981; Boinski, 1989) and are characterized by better developed grasping morphology and abilities than callitrichines (Costello and Fragaszy, 1988; Janson and Boinski, 1992; Hamrick, 1998; but see Lemelin and Grafton, 1998).

In the current study, I tested three general hypotheses. First, locomotion on arboreal substrates should be associated with greater challenges to stability. Therefore, marmosets and squirrel monkeys using asymmetrical gaits on arboreal substrates should attempt to increase stability by decreasing vertical forces and reducing the vertical displacement of the COM. Previous studies of primate symmetrical gait kinematics suggest a variety of strategies that might effect these changes. Based on this previous research, I formulated and tested the following three predictions. First, relative forelimb and hind limb stance phase durations (i.e., duty factors) should be greater on arboreal substrates. Because total vertical impulse across all limbs during a stride must equal the product of body weight and stride duration, extending limb stance phase durations without changing velocity necessarily reduces peak vertical force magnitudes (McMahon, 1985; Farley, 1991; Schmitt, 1994, 1999; Schmidt, 2005). Second, monkeys traveling on arboreal substrates should favor limb sequence patterns that limit whole-body aerial

phases and increase total contact time with the substrate during the stride. Increasing net substrate contact duration limits the vertical oscillation of the COM and reduces peak vertical force by distributing impulse more evenly across the stride (Hutchinson et al., 2003; Biknevicius et al., 2004; Ruina et al., 2005; Hutchinson et al., 2006; Schmitt et al., 2006; Walter and Carrier, 2007). Therefore, a) forelimb and hind limb lead durations (i.e., phasing between the limb contacts) should be greater on arboreal substrates, and b) animals should choose lead sequences and gait types that maximize substrate contact. Third, monkeys should use shorter and more frequent strides on arboreal substrates. This prediction is somewhat counterintuitive, as previous research on symmetrical gaits has argued that primates reduce branch sway and promote stability by *increasing* stride length and *decreasing* stride frequency (e.g., Demes et al., 1990). However, longer strides during asymmetrical gaits are primarily achieved with the use of extended aerial phases and marked by large vertical oscillations of the COM (Dagg, 1973; Heglund et al., 1974; Hurov, 1987; Gasc, 1993; Schilling and Hackert, 2006). Therefore, short strides without pronounced aerial phases should decrease COM movement and increase arboreal stability.

My second hypothesis was that due to their derived autopodial anatomy and retreat from the fine-branch foraging niche (Sussman and Kinzey, 1984; Garber, 1992), marmosets should experience greater instability when using asymmetrical gaits on arboreal substrates than squirrel monkeys. As such, the specific kinematic and kinetic changes detailed above should be more pronounced among marmosets than among squirrel monkeys. Specifically, differences between arboreal and ground locomotion should be greater for marmosets than for squirrel monkeys.

Finally, because both toppling moments and branch sway are exacerbated as body size increases relative to branch diameter, older and larger individuals within each species should experience greater challenges to stability than younger and smaller individuals. Therefore, across species, instability and the need for kinematic and kinetic compensation should increase with body size during pole locomotion but not during ground locomotion. Specifically, once gait parameters are scaled to body size (see Section 3.2.3 below), ontogenetic increases in size should be associated with decreased peak vertical forces, decreased vertical COM displacements, increased limb and net substrate contact durations, decreased stride lengths and increased stride frequencies, and the rate of size-related changes in these parameters should always be greater during locomotion on the pole.

3.2. Methods

3.2.1. Animal subjects

Research took place at two National Institutes of Health Primate Research Centers. A total of 34 marmoset experiments were conducted at the Southwest National Primate Research Center (SNPRC: San Antonio, TX) from May to July 2006. A total of 99 squirrel monkey experiments were conducted at the Center for Neotropical Primate Research and Resources (CNPRR: Mobile, AL) from August 2006 to March 2007. Both primate centers support long-established breeding colonies and have ample experience facilitating external research projects. Veterinary technicians from each center assisted with animal care, management and motivation during the experiments. Institutional

Animal Care and Use Committees (IACUC) at Stony Brook University, the SFBR and the CNPRR approved all procedures prior to the beginning of this research.

Five marmosets, two young juveniles (one male and one female), one older male juvenile, and two adults (one male and one female) comprised the marmoset sample. The marmosets were housed in family groups of 6-9 individuals in cages that were large relative to body size (1.52m x 1.42m x 0.62m) and included a variety of flat and "arboreal" supports (e.g., dried branches and PVC pipe). The two young juveniles (Animals 707 and 708) were twins from the same litter and ranged in age from 85 to 139 days and in body mass from 143 to 201 grams (mean: 184 grams). The older juvenile (Animal 597) ranged in age from 258 to 320 days and in body mass from 314 to 349 grams (mean: 327 grams). The adult marmosets, Animals 114 and 452, were aged 12.2 years and 2.4 years, respectively, and had a mean body mass of 326 grams. To better illustrate ontogenetic changes in body size, body mass has been plotted against age for all marmosets and squirrel monkeys in Figure 3.1.

FIGURE 3.1 HERE

Five female infant-juvenile squirrel monkeys comprised the squirrel monkey sample. An additional squirrel monkey (Animal 4433) participated in two experiments but had to be withdrawn from the study due to an unrelated tail injury. The squirrel monkeys ranged in age from 74-302 days and body mass from 218-535 grams (29-71% of adult size; mean: 367 grams). Because the intense and frequent infant interaction required for this research might have placed undue stress on mother-infant relationships, all of squirrel monkeys were chosen from a cohort that had been hand-reared by veterinary staff, following perinatal rejection by their birth mothers. The use of hand-reared individuals also insured that animals would be well habituated to veterinary staff, therefore facilitating locomotor training. After weaning at 1-2 months of age, hand-reared infants were integrated into social groups of 15-30 individuals and fostered onto surrogate mothers. Social groups were housed in large 1.5m x 2.1m x 4.5m enclosures with 35-40 linear meters of perches and substrates for free-ranging locomotor activity. Previous research at the CNPRR has suggested that during the first 45 days of life, nursery-reared infants have reduced strength and balance when compared to dam-reared peers. Such developmental delays are likely the result of restricted environmental interaction while in the nursery (Williams, 2004). Nevertheless, because all of the infants in this study were nursery-reared under similar conditions, developmental delays relative to dam-reared infants should not be a confounding factor.

Although my samples included infant and juvenile animals, purely maturational effects should have little impact on the results and conclusions of this study. Compared to other primates, both marmosets and squirrel monkeys are markedly precocial in their behavioral development. Marmoset mothers provide very little assistance to their newborn infant, rarely even carrying the infants and limiting their parental investment to nursing (Ross, 1991). Fathers and older siblings are therefore the primary infant carriers (Schradin and Anzenberger, 2001). Grappling and suckling reflexes are well developed at birth (Missler et al., 1992) and newborns who are unable to grip often fall to their deaths. Marmoset infants typically begin to venture off of their carriers at around two weeks of age. From that point, other locomotor skills develop rapidly. The full locomotor repertoire is usually present by the three months of age, when the infants begin

the process of weaning, body mass starts to rapidly increase, adult-like limb proportions are reached and synaptic density in the visual cortex peaks (Missler et al, 1992).

Squirrel monkey development proceeds on a similar pace (see Chapter 2). Following an extended gestation period, squirrel monkeys are born with a brain that is already 60% of adult size and essentially ceases to grow after two months of life (Elias, 1977; Hartwig, 1995). Infants engage in independent locomotion within the first month, begin foraging independently after seven weeks, are weaned by four months of age, and are completely independent from their mothers by eight months of age (Elias, 1977; Kaack et al., 1979; Boinski and Fragaszy, 1989; Fragaszy et al., 1991).

In sum, the fast pace of marmoset and squirrel monkey locomotor development should minimize the influence of age *per se* on the kinematic and kinetic parameters studied here, particularly after data are size-adjusted (see Section 3.2.3). Moreover, focusing on the locomotion of younger, smaller-bodied squirrel monkeys diminished the size disparity the squirrel monkey and marmoset samples, thus partially controlling for potential species-level allometric influences on locomotor behavior.

3.2.2. Data collection

Marmosets and squirrel monkeys were filmed as they traversed a linear runway. Depending on experimental condition (e.g., ground vs. pole), monkeys traversed either the flat runway floor or a 2.5 cm diameter PVC pipe elevated 10.7 cm above the surface of the runway. Both substrates were coated with a mixture of polyurethane and non-skid paint additive (Behr Process Corporation, Santa Ana, CA) in order to increase traction. See Chapter 2 for additional details of runway construction.

I used a Motionmeter 1000 high-speed digital video camera (Redlake MASD Incorporated, San Diego, CA) to film all locomotor sequences. For the first three marmoset experiments, the camera was electronically shuttered at a rate of 1/1250 sec and operated at 125 Hz. For all subsequent experiments, the camera was shuttered at a rate of 1/2500 sec and operated at 250 Hz. These filming speeds were sufficient to prevent aliasing of cyclic locomotor data (e.g., stride lengths and durations: Polk et al., 2005). Composite video output from the camera was converted to digital video using a Canopus ADVC-55 Analog-Digital converter (Canopus Corporation, San Jose, CA) and stored on an Apple Macintosh Powerbook computer (Apple Incorporated, Cupertino, CA) for later processing.

3.2.2.1. Kinematic data collection

Differing regulations at the two primate centers necessitated changes in the experimental procedure used with each species. During marmoset data collection, animals were placed inside the runway and allowed to move freely about. Unlike the procedure used with squirrel monkeys (see below), no reflective markers were placed on the animals. A scale was placed in one of the enclosures at the end of the runway and used to record body mass *ad libitum* during the experiment. Animals were motivated to move back and forth across the substrate with food rewards (e.g., raisins and grapes) and coaxing by veterinary staff. Experiments lasted for no more than 30 minutes and animals were returned to their home cages once the experiment had ended.

Prior to the beginning of each squirrel monkey experiment, individuals were weighed and the skin over the approximate center of rotation of the shoulder and the hip

was shaved and marked with retro-reflective tape (3M Corporation, St. Paul, MN). During data collection, squirrel monkeys were placed in one of the enclosed boxes at the end of the runway. A veterinary technician stood at the opposite end of the runway and verbally coaxed the monkey across. After crossing the runway, monkeys were given 60 seconds of rest before the beginning of the next trial. Experiments consisted of 12-30 such trials and lasted for no more than 30 minutes. Once the experiment was over, reflective markers were removed and the monkey was returned to its social group.

Video files from each marmoset and squirrel monkey experiment were imported into the MATLAB DLT Dataviewer 2 digitizing platform (Hedrick, 2007) for coding on a trial-by-trial basis. Individual strides were identified based on the cyclic action of a reference limb (i.e., first touchdown to second touchdown of the left hind limb). Within each stride, touchdown events for each of the four limbs were recognized as the first frame in which the limb contacted the substrate whereas lift-off events were recognized as the first frame following touchdown in which the limb did not contact the substrate. Individual steps (i.e., stance phases) lasted from limb touchdown to lift-off. In order to calculate average locomotor speed, the X (horizontal) and Y (vertical) coordinates of a standard reference marker were recorded across the entire video clip. The nose was used as a reference marker for marmoset trials whereas the shoulder or the hip marker, depending on marker visibility, was used for squirrel monkey trials. The force platforms were used as calibration objects to transform raw pixel coordinates into meters (combined length of force platforms: 0.6096m).

3.2.2.2. Kinetic data collection

Two force platforms, placed in series, were used to measure peak vertical forces and the vertical displacement of the COM. The platforms were located in the center of the runway, allowing monkeys to reach steady speeds of locomotion prior to contact. During the simulated arboreal trials, PVC segments (30.5 cm long and 2.5 cm in diameter) were attached to each force platform via bolts secured directly to the platform frame. The platforms were custom built for this study, following the design of Heglund (1981), Biewener and Full (1992), and Riskin et al. (2005). The platforms measured forces in three orthogonal directions: vertical, fore-aft (cranio-caudal) and mediolateral (transverse). Voltage output from each channel was routed through a National Instruments (Austin, TX) SC-2345 chassis and recorded using a LabView virtual instrument running on a notebook computer. Cross-talk between force channels was generally low, ranging between 0.3% and 3.5% without the pole segment and 0.3% and 10.5% when the pole segment was attached.

Kinetic and kinematic data were synchronized via a 3.3V square-wave pulse, generated by the master-slave port of the Redlake camera, that was routed separately to a bank of LEDs positioned on the back wall of the runway and to the notebook computer via the SC-2345 chassis. This circuit was normally interrupted by means of a handheld switch. During each trial, the switch was briefly closed, simultaneously illuminating the LEDs in the video frame and changing the shape of the square wave in the data file. Using this procedure, it was possible to synchronize video and kinetic data to a resolution of four to eight milliseconds (depending on video frame rate).

Following the recommendations of Biewener and Full (1992), the platforms were calibrated daily by regressing applied weights against measured changes in raw voltage

output from the instrument. Calibration regressions consistently yielded coefficients of determination (i.e., R^2) greater than 0.999, indicating a linear relationship between applied force and voltage output. See Chapter 2 for additional details on force platform construction and calibration.

Force data from each trial were imported into a custom-written MATLAB program (Mathworks, Natick, MA) where the raw voltages were transformed into Newtons and corrected for cross-talk. Force traces from each channel were smoothed using a zero-lag fourth-order Butterworth low pass filter with a cut-off frequency of 30 Hz for the marmosets and 25 Hz for the larger squirrel monkeys. Baseline drift during and between trials was corrected by sampling the average values of unloaded periods immediately prior to and following platform contact and subtracting these values from the force traces.

3.2.3. Dependent variables

Processed video and force platform data were used to calculate a total of 14 gait parameters (Table 3.1). All computations were performed using customized MATLAB routines.

TABLE 3.1 HERE

3.2.3.1. Speed

For each species, I calculated average locomotor speed from the displacement of the standard reference marker (see above). I used a zero-lag fourth-order low pass Butterworth filter with a cut-off frequency of 10 Hz to correct marker trajectories for digitizing noise. This cutoff frequency was selected as optimal using a residual analysis procedure described by Winter (1990). I used the piecewise cubic interpolation function of MATLAB to interpolate over gaps of missing data ≤ 10 frames (i.e., 40-80ms, depending on frame rate). Linear least-squares regressions of corrected displacement data on time were used to estimate overall horizontal and vertical velocity across each stride. Total speed was calculated as the resultant magnitude of horizontal and vertical velocities. However, because vertical velocity was essentially zero when averaged across an entire stride, resultant velocity is tantamount to horizontal velocity. In order to ensure that only steady-speed locomotion was examined, trials in which the coefficient of determination (i.e., R^2) of reference marker position against time was less than 0.99 were discarded. To control for differences in body mass across the sample, Froude number (Alexander, 1984; Hof, 1996; Polk, 2002; Bullimore and Donelan, 2008) was calculated as:

$$\frac{u}{\sqrt{gh}}$$

where u is velocity, g is gravitational acceleration ($9.81 ms^{-2}$) and h is the cube root of body mass. Note that this quantity is actually the square root of the "original" Froude number (i.e., $u^2(gh)^{-1}$) introduced by Alexander and Jayes (1983). However, both forms of the Froude number are dimensionless ratios and adjust for body size effects on locomotor speed.

3.2.3.2. Vertical force and COM displacement

Vertical forces and COM displacement were only measured for strides in which the animal's body weight was completely supported by the force platforms. I measured peak vertical force as the maximum vertical force applied to the substrate by the COM during the course of the stride. The vertical displacements of the COM were calculated from force profiles using standard methods (Cavagna, 1975; Cavagna et al., 1977). After subtracting body weight from the vertical force vector to control for gravitational acceleration, the force vector was divided by body mass to calculate the instantaneous acceleration of the COM. The acceleration vector was then integrated with respect to stride duration in order to obtain instantaneous velocity and then integrated again to obtain the instantaneous position of the COM. Because only steady-speed, linear locomotion was examined, the integration constant for velocity calculations was defined such that mean vertical velocity equaled zero across the stride. The integration constant for position calculations was set to zero. Total vertical displacment of the COM during each stride were measured as the net amplitude of the position vector (i.e., difference between lowest and highest positions). To control for differences in body size, peak vertical forces were scaled to body weight and COM displacement was scaled to the cube root of body mass.

3.2.3.3. Temporal gait variables

To ensure that only asymmetrical strides were examined, stride symmetry was calculated as the percentage of stride duration separating the touchdowns of the right and left hind limbs (Hildebrand, 1976, 1977). Strides in which symmetry was between 43.75% and 56.25% were designated symmetrical and not included in the dataset.

Stride length (in meters) was measured as the resultant horizontal and vertical distance traversed by the reference marker (i.e., nose, shoulder or hip) from the beginning to the end of the stride. Stride frequency (in Hz) was measured as the reciprocal of stride duration, where stride duration was defined as the time in seconds elapsed from the beginning to the end of the stride. Following Hof (1996) stride length was scaled to the cube root of body mass whereas stride frequency was scaled to the quotient of gravitational acceleration and the cube root of body mass (i.e., g/h).

Several variables were used to describe the duration of substrate contact during each stride. Limb duty factor was defined as the proportion of a stride that each limb was in stance phase (i.e., contact duration/stride duration). Mean forelimb, mean hind limb and mean overall duty factor were calculated separately for each stride in the dataset. Additionally, because forelimb pairs and hind limb pairs operate as a combined functional unit during asymmetrical gaits (e.g., Walter and Carrier, 2007), relative forelimb and hind limb contact duration was calculated as the proportion of stride duration either or both limbs in the pair were in contact with the substrate. Mean limb pair contact duration was calculated as the average of forelimb and hind limb contact durations. Forelimb and hind limb lead durations were measured as the time elapsed between the touchdowns of the trailing and leading limbs in each pair[3]. Following

[3] Although trailing and leading limbs are formally defined with reference to position (e.g., Dagg, 1973; Hildebrand, 1977; Vilensky et al., 1990), the trailing limb usually contacts the substrate prior to the leading limb.

Hildebrand (1977), lead durations were scaled to the absolute contact durations. Finally, relative net substrate contact duration (i.e., total duration of contact by one or more limbs, scaled to stride duration) was calculated as the sum of relative forelimb and hind limb contact duration, minus the proportion of stride time forelimb and hind limb contact periods overlapped.

3.2.3.4. Gait classifications

Following Hildebrand (1977), strides were placed into discrete gait categories based on the temporal association of limb contact within forelimb and hind limb pairs. Gaits were classified as bounds when forelimb touchdowns were simultaneous and hind limb touchdowns were simultaneous, as half-bounds when forelimb touchdowns were separated in time and hind limb touchdowns were simultaneous, as crutch walks when forelimb touchdowns were simultaneous and hind limb touchdowns were separated, and as gallops/canters when both forelimb and hind limb touchdowns were separated. However, because perfect simultaneity of gait events is rarely discernible in locomotor studies (e.g., Polk et al., 2005), "simultaneous" touchdowns were identified when lead durations were less than or equal to 10% of limb contact duration (Hildebrand, 1977). Canters were classified as the subset of gallops lacking whole-body aerial phases.

3.2.4. Precision of kinematic data

To estimate precision (e.g., reliability: Sokal and Rohlf, 1995) in the current dataset, 20 randomly selected trials from each species were coded three times on different days. As a metric of precision, coefficients of variation (i.e., standard deviation/mean*100%) were calculated for each variable and compared to the amount of variation within each experiment from which the randomly selected trials were drawn. Means, standard deviations and coefficients of variation for each parameter are presented in Table 3.2 for marmosets and Table 3.3 for squirrel monkeys. For marmosets, coefficients of variation ranged from 2.5% to 21.7% with an overall mean value of 7.3% and a median value of 4.2%. For squirrel monkeys, coefficients of variation ranged from 1.4% to 8.3% with mean value of 3.4% and a median value of 3.5%. Variables with high coefficients of variation typically had low mean values (e.g., forelimb and hind limb lead durations). When lead durations are excluded, all remaining variables have coefficients of variation under 10% for marmoset trials and 5% for squirrel monkey trials. Moreover, variation due to measurement error was consistently minor compared to levels of intra-experimental variation. Overall, these results indicate that the precision of the experimental procedures used here remains within tolerable limits.

TABLE 3.2 HERE

TABLE 3.3 HERE

3.2.5. Statistical analyses

Because none of the raw continuous variables examined here followed a normal distribution, all data were Box-Cox transformed (Box and Cox, 1964; Sokal and Rohlf, 1995) prior to analysis. The Box-Cox family of power transformations takes the general form

$$Y_T = \frac{(Y^\lambda - 1)}{\lambda}$$

when the parameter λ is not equal to zero and

$$Y_T = \ln Y$$

when λ is equal to zero (where Y is the original data vector and Y_T is the transformed data vector). The value of λ which yields the best transformation to normality is that which maximizes the log-likelihood function

$$L = -\frac{df}{2}\ln s_T^2 + (\lambda - 1)\frac{df}{n}\sum \ln Y$$

where df is the degrees of freedom for the data vector, s^2_T is the variance of the transformed data vector, and n is sample size (Sokal and Rohlf, 1995). The optimal values of λ for all variables in the current dataset were found using a customized iterative procedure written in MATLAB 7.1 (Mathworks, Natick, MA). In order to ensure data were amenable to logarithmic transformation, I added one to all variables that could include zero as possible values (i.e., lead durations). Box-Cox transformation yielded normal distributions for most, but not all, variables across the four species-by-substrate groups. Therefore, for comparisons in which the data for at least one of the groups were non-normally distributed, parametric tests were supplemented by non-parametric analyses of rank-transformed data (Huitema, 1980; Conover and Iman, 1981). In all cases, non-parametric tests corroborated parametric results, indicating that statistical procedures were robust to deviations from normality.

I used two-way analyses of covariance (ANCOVA) to test for substrate and species differences in asymmetrical gait dynamics, specifying substrate and species as factors in the analysis and Froude number as the covariate. Pearson product-moment correlations indicated that most gait variables were significantly associated with Froude number across species-by-substrate categories (see Results section below), thus justifying the use of ANCOVA. Nevertheless there were several tests in which the dependent variable was not correlated with Froude number in all conditions or in which regression slopes were significantly heterogeneous among groups. In these situations, Froude numbers across species and substrates were collapsed into three discrete categories: lowest Froude number through the 33rd percentile of the distribution, 33rd percentile through 66th percentile and 66th percentile through the highest Froude number. Substrate and species differences were then tested using three-way analyses of variance (ANOVA), specifying substrate, species and speed category as factors. Finally, I used two-way ANOVA to test for differences in variables not correlated with speed, specifying substrate and species as factors. I used Dunn-Sidák adjusted t-tests of group means (or least-squares means following ANCOVA) to test for significant post-hoc differences between ground and pole locomotion in each species. The species-by-substrate interaction term in the overall ANOVA/ANCOVA was used to test for species-level differences in the *magnitude* of substrate-related changes.

I used a combination of multiple regression and ANCOVA to test whether size-related changes in asymmetrical gait parameters differed by substrate within each species. Because ontogenetic changes in body size could potentially influence locomotor mechanics across substrates for a variety of reasons (see Chapter 2), this procedure allowed me to test for size-related changes specifically associated with substrate type. First, multiple regressions of each parameter on Froude number and body mass were used to quantify the independent relationship between gait mechanics and body size, controlling for Froude number. Second, homogenous slope tests (i.e., the first part of a

standard ANCOVA) were used to test if patterns of size-related change differed by substrate. An iterative process was used to build the proper covariate-by-factor interaction terms for each homogenous slope test (Quinn and Keough, 2002). First, tests were carried out using the fully specified model, with all interaction terms included (i.e., mass-by-substrate, Froude number-by-substrate, Froude number-by-mass-by-substrate). Then, any non-significant significant interaction terms including Froude number were removed from the model and all statistics were recalculated.

I used G-tests of independence (Sokal and Rohlf, 1995) to test for proportional differences in gait type between substrates. Tests were performed separately for each species. Standardized residuals, calculated as the differences between observed and expected cell counts divided by the square-root of the expected cell counts (Haberman, 1978), were compared to assess the magnitude of substrate-related changes. Like other standardized scores, standardized residuals are approximately distributed with a mean of zero and a standard deviation of one, permitting scale-free comparisons. All transformations and statistical tests were performed using SPSS 11 for Macintosh (SPSS Inc, Chicago, IL, USA)

3.3. Results

A total of 998 strides were analyzed, including 76 marmoset and 499 squirrel monkey strides on the ground and 81 marmoset and 342 squirrel monkey strides on the pole. A subset of 231 strides was available for kinetic analyses, including 21 marmoset and 95 squirrel monkey strides on the ground and 23 marmoset and 92 squirrel monkey strides on the pole.

3.3.1. Relative support size

Following Stevens (2003; 2007), the support size index, calculated as the quotient of pole diameter and the cube root of body mass (in kilograms), was used as a measure of relative support size for the pole condition. The support size index for the pole used in this study ranged from 3.56 to 4.78 for the marmoset sample, with a mean of 4.07, and from 3.08 to 4.15 for the squirrel monkey sample, with a mean of 3.53 (data for individual monkeys are shown in Table 3.4). Values for both species fell between Stevens' (2003, 2007) recommendations of 2.5 for "small" substrates and 10 for "large" substrates, indicating that the 2.5 cm diameter pole represented a small to medium sized arboreal support relative to both species' body mass. Support size indices were significantly larger in marmosets ($t_{[129]}$=8.45, p<0.001), suggesting that, all else being equal, locomotion on the pole segment should pose greater biomechanical challenges for squirrel monkeys.

TABLE 3.4 HERE

3.3.2. Substrate and species differences in gait dynamics

Species means, separated by substrate, are presented for each kinematic and kinetic variable in Table 3.5, along with data on the magnitude and direction of substrate differences within species, species differences within substrates, and interaction effects across species and substrates. Percentage differences between species and substrates are calculated relative to the larger value. Interaction effects from the overall

ANOVA/ANCOVA were used to test the prediction that marmosets would alter locomotory patterns between substrates to a greater extent than squirrel monkeys.

TABLE 3.5 HERE

Marmosets moved significantly faster during ground locomotion than during pole locomotion ($t_{[155]}$=3.90, p<0.001; Fig. 3.2). By contrast, Froude number did not differ by substrate for squirrel monkeys ($t_{[839]}$=1.73, p=0.08). Marmosets moved significantly faster than squirrel monkeys during ground locomotion ($t_{[573]}$=2.38, p=0.018), but significantly slower than squirrel monkeys during pole locomotion ($t_{[573]}$=2.31, p=0.021). As suggested by the above patterns, the interaction effect in the overall ANOVA was significant ($F_{[1,994]}$=10.98, p=0.001), indicating that substrate differences in Froude number were greater in marmosets than in squirrel monkeys.

FIGURE 3.2 HERE

Across species and substrates, most variables were significantly correlated with Froude number (Table 3.6). Only two variables, relative vertical COM displacement and relative forelimb lead duration, were not significantly correlated with Froude number across the four species by substrate conditions. Relative vertical COM displacement was only correlated with Froude number during ground strides in marmoset, whereas relative forelimb lead duration was only correlated with Froude number during ground strides in both species. Parametric and non-parametric correlations yielded congruent results, indicating that results were robust to deviations from normality.

TABLE 3.6 HERE

Both marmosets and squirrel monkeys significantly reduced relative peak vertical forces when traveling on pole (Fig. 3.3), even after controlling for the effects of speed (*Callithrix*: $t_{[42]}$=4.81, p<0.001; *Saimiri*: $t_{[185]}$=4.36, p<0.001). On the ground, relative peak vertical forces (in body weight units) were significantly greater for marmosets than for squirrel monkeys ($t_{[114]}$=4.63, p<0.001). By contrast, relative peak vertical forces did not differ between two species during pole locomotion ($t_{[113]}$=1.26, p=0.209). The interaction effect was significant, indicating that substrate differences in relative peak vertical force were greater in marmosets than in squirrel monkeys ($F_{[1,225]}$=9.21, p<0.01).

FIGURE 3.3 HERE

Marmosets and squirrel monkeys significantly reduced the relative vertical displacement of the COM when traveling on the pole (*Callithrix*: $t_{[42]}$=4.75, p<0.001; *Saimiri*: $t_{[185]}$=7.05, p<0.001; Fig. 3.4). On the ground, relative vertical COM displacement was significantly greater in marmosets than in squirrel monkeys ($t_{[114]}$=2.58, p=0.011). Relative vertical COM displacement did not differ between species during pole locomotion ($t_{[113]}$=0.94, p=0.351). The interaction effect was not significant, indicating that marmosets and squirrel monkeys showed similar reductions in COM movement when locomoting on the pole ($F_{[1,227]}$=0.80, p=0.230).

FIGURE 3.4 HERE

Both species significantly increased forelimb duty factor (*Callithrix*: $t_{[155]}$=10.35, p<0.001; *Saimiri*: $t_{[839]}$=6.24, p<0.001), hind limb duty factor (*Callithrix*: $t_{[155]}$=6.24, p<0.001; *Saimiri*: $t_{[839]}$=5.72, p<0.001) and mean duty factor (*Callithrix*: $t_{[155]}$=9.84, p<0.001; *Saimiri*: $t_{[839]}$=6.30, p<0.001) during locomotion on the pole (Fig. 3.5). Across limbs, squirrel monkeys displayed significantly greater duty factors than marmosets during ground locomotion (forelimb: $t_{[573]}$=10.29, p<0.001; hind limb: $t_{[573]}$=3.09, p=0.002; mean: $t_{[573]}$=7.58, p<0.001). By contrast, during pole locomotion, forelimb

duty factor ($t_{[421]}$=1.88, p=0.060) and mean duty factor ($t_{[421]}$=0.71, p=0.476) did not significantly differ between species, and hind limb duty factor was greater in marmosets ($t_{[421]}$=2.87, p=0.004). Interaction effects were significant across limbs, indicating that substrate differences in duty factor were consistently greater in marmosets than in squirrel monkeys (forelimb: $F_{[1,992]}$=48.85, p<0.001; hind limb: $F_{[1,992]}$=11.85, p=0.01; mean: $F_{[1,992]}$=42.22, p<0.001).

FIGURE 3.5 HERE

Both species significantly increased relative forelimb lead duration (*Callithrix*: $t_{[155]}$=3.46, p<0.001; *Saimiri*: $t_{[839]}$=17.86, p<0.001) and relative hind limb lead duration (*Callithrix*: $t_{[155]}$=4.49, p<0.001; *Saimiri*: $t_{[839]}$=15.98, p<0.001) when traveling on the pole (Fig. 3.6). Across limbs, relative lead durations were greater in squirrel monkeys than in marmosets, both on the ground (forelimb: $t_{[573]}$=9.44, p<0.001; hind limb: $t_{[573]}$=9.74, p<0.001) and the pole (forelimb: $t_{[421]}$=9.36, p<0.001; hind limb: $t_{[421]}$=12.56, p<0.001). Interaction effects were significant across limbs (forelimb: $F_{[1,992]}$=16.13, p<0.001; hind limb: $F_{[1,993]}$=5.17, p=0.023). However, in contrast to the most other gait parameters examined, changes in relative lead durations were greater in squirrel monkeys than in marmosets.

FIGURE 3.6 HERE

Increases in limb duty factors and lead durations resulted in significant increases in relative forelimb (*Callithrix*: $t_{[155]}$=6.76, p<0.001; *Saimiri*: $t_{[839]}$=19.41, p<0.001), hind limb (*Callithrix*: $t_{[155]}$=6.81, p<0.001; *Saimiri*: $t_{[839]}$=18.28, p<0.001) and mean limb pair contact durations (*Callithrix*: $t_{[155]}$=8.02, p<0.001; *Saimiri*: $t_{[839]}$=21.51, p<0.001) during locomotion on the pole (Fig. 3.7). Relative contact durations were consistently longer in squirrel monkeys than in marmosets, both on the ground (forelimb: $t_{[573]}$=8.74, p<0.001; hind limb: $t_{[573]}$=9.77, p<0.001; mean: $t_{[573]}$=11.44, p<0.001) and on the pole (forelimb: $t_{[421]}$=10.49, p<0.001; hind limb: $t_{[421]}$=10.81, p<0.001; mean: $t_{[421]}$=13.01, p<0.001). Across limbs, interaction effects were not significant, indicating that substrate-related changes in limb contact durations were similar across species (forelimb: $F_{[1,993]}$=0.079, p=0.118; hind limb: $F_{[1,993]}$=0.207, p=0.105; mean: $F_{[1,992]}$=42.22, p<0.001).

FIGURE 3.7 HERE

For both species, substrate differences in relative lead durations were also manifested by significant categorical changes in discrete gait types (*Callithrix*: $G_{[4]}$=46.75, p<0.001; *Saimiri*: $G_{[4]}$=243.49, p<0.001; Fig. 3.8). Examination of standardized residuals revealed that substrate differences were primarily due to substantial increases in the frequency of canters used during pole locomotion. On the ground, canters accounted for 11.8% of marmoset gaits and 36.5% of squirrel monkey gaits. By contrast, when animals were traveling on the pole, canters accounted for 49.4% of marmoset gaits and 84.8% of squirrel monkey gaits. In marmosets, an increase in the frequency of canters was accompanied by decreases in the frequency of half-bounds and bounds and slight increases in the frequency of gallops and crutch walks. In squirrel monkeys, all gaits other than canters decreased in frequency during pole locomotion.

FIGURE 3.8 HERE

As predicted, a shift towards more asynchronous, "grounded" asymmetrical gaits, such as the canter, resulted in significant increases in relative net substrate contact duration in both species (*Callithrix*: $t_{[155]}$=9.99, p<0.001; *Saimiri*: $t_{[839]}$=13.55, p<0.001; Fig. 3.9). Relative substrate contact duration was consistently greater in squirrel

monkeys than in marmosets, both on the ground ($t_{[573]}$=11.76, p<0.001) and on the pole ($t_{[421]}$=5.86, p<0.001). The interaction effect was significant, indicating that the magnitude of substrate differences in relative net substrate contact duration was greater in marmosets than in squirrel monkeys ($F_{[1,992]}$=17.21, p<0.001).

FIGURE 3.9 HERE

Finally, in both marmosets and squirrel monkeys, locomotion on the pole was associated with a decrease in relative stride length (*Callithrix*: $t_{[154]}$=9.18, p<0.001; *Saimiri*: $t_{[766]}$=11.64, p<0.001) and an increase in relative stride frequency (*Callithrix*: $t_{[155]}$=11.37, p<0.001; *Saimiri*: $t_{[839]}$=11.80, p<0.001; Fig. 3.10). On both substrates, marmosets used relatively shorter (Ground: $t_{[526]}$=6.78, p<0.001; Pole: $t_{[394]}$=13.64, p<0.001) and more frequent (Ground: $t_{[573]}$=8.57, p<0.001; Pole: $t_{[394]}$=13.67, p<0.001) strides than squirrel monkeys. Interaction effects for both variables were significant, indicating that the magnitude of substrate-related change was again greater in marmosets than in squirrel monkeys (Relative stride length: $F_{[1,919]}$=12.66, p<0.001; Relative stride frequency: $F_{[1,992]}$=13.18, p<0.001).

FIGURE 3.10 HERE

3.3.3. Ontogenetic differences in asymmetrical gait dynamics

Results from multiple regression analyses of each gait parameter on body mass, controlling for Froude number, are shown in Table 3.7. Across substrates, both marmosets and squirrel monkeys showed significant size-related changes in Froude number, although the direction of change differed between species. Marmosets moved at significantly slower Froude numbers as body size increased, regardless of substrate. By contrast, squirrel monkeys traveling on both substrates moved at significantly faster Froude numbers as size increased. In both species, Froude number changed with body mass at a statistically similar rate across substrates.

TABLE 3.7 HERE

Among marmosets, peak vertical forces did not significantly vary with body size on either substrate. By contrast, larger squirrel monkeys significantly decreased relative peak vertical forces on both substrates, and the rate of size-related decrease was greater during pole locomotion. Larger marmosets showed a non-significant decrease in relative vertical COM displacements during ground locomotion and a non-significant increase in COM displacements during pole locomotion. Therefore, the mass-by-substrate interaction was marginally significant (p=0.046), despite non-significant slopes. As body size increased, squirrel monkeys showed non-significant decreases in vertical COM displacements on both substrates, with no significant substrate differences in the rate of change.

Both species frequently showed significant size-related changes in limb and net substrate contact patterns, although few of these changes accorded with my predictions. As predicted, larger marmosets used significantly greater forelimb and mean duty factors, regardless of substrate, and the rate of increase was always significantly greater during pole locomotion. Hind limb duty factor in marmosets was unassociated with body size on either substrate and mass-by-substrate interactions were not significant. Contradicting predictions, larger squirrel monkeys significantly decreased forelimb duty factor on both substrates, and the rate of decrease was significantly greater during pole locomotion. Nevertheless, size-related changes in hind limb duty factor corroborated my predictions,

with hind limb duty factor independent of size on the ground and significantly increasing with size on the pole, resulting in a highly significant mass-by-substrate interaction. An increase in forelimb duty factor resulted in greater mean duty factor on the ground, whereas opposite size-related trends in forelimb and hind limb duty factors during pole locomotion caused mean duty factor to remain constant as body size increased. The mass-by-substrate interaction for mean duty factor was not significant within squirrel monkeys.

Marmosets showed non-significant increases in relative forelimb lead durations during ground locomotion and non-significant decreases in forelimb lead durations during pole locomotion, resulting in a marginally significant mass-by-substrate interaction (p=0.035). By contrast, relative hind limb lead durations tended to become shorter as size increased (although the decrease was only significant during pole locomotion) and the mass-by-substrate interaction was not significant. In squirrel monkeys, patterns were similar across limbs but varied by substrate. During ground locomotion, relative forelimb and hind limb lead durations significantly increased with size. On the pole, however, increases in body size were associated with significant decreases in relative forelimb and hind limb lead durations. As expected given such divergent substrate-related changes, mass-by-substrate interactions were highly significant for both forelimb and hind limb relative lead durations.

In marmosets, variation in relative limb contact durations was largely independent of body size, although significant increases in relative forelimb contact durations were evident during ground locomotion. Stasis of relative limb contact durations likely resulted from simultaneous size-related increases in duty factor and decreases in lead duration. No significant mass-by-substrate interactions were observed. Squirrel monkeys again showed contrasting patterns on the ground and the pole. Whereas forelimb, hind limb and mean contact durations significantly increased with size during ground locomotion, limb contact durations significantly decreased with size during locomotion on the pole. Again, mass-by-substrate interactions were highly significant across all contact durations.

Both marmosets and squirrel monkeys showed significant size-related increases in relative net substrate contact duration during locomotion on the ground. By contrast, relative substrate contact duration was independent of size when both species were traveling on the pole. The mass-by-substrate interaction was significant in squirrel monkeys but not in marmosets.

Finally, both species showed significant, though divergent, size-related changes in relative stride lengths and frequencies. Across substrates, marmosets used relatively shorter strides at higher frequencies as size increased, and rates of change for both parameters were greater on the pole. By contrast, across substrates larger squirrel monkeys used significantly longer strides at lower frequencies. There were no significant mass-by-substrate interactions for either parameter.

3.4. Discussion

3.4.1. Effects of substrate on asymmetrical gait dynamics

The results of this study emphatically demonstrate that marmosets and squirrel monkeys alter locomotor dynamics when using asymmetrical gaits on simulated arboreal substrates. Specifically, when traveling on the pole, both species significantly increased

duty factors, relative lead durations and relative limb pair contact durations. Relatively longer leads and contact durations led to an increase in the prevalence of more "grounded" asymmetrical gaits, such as canters and gallops, and a corresponding decrease in more acrobatic gaits, such as bounds and half-bounds. As a result of these qualitative shifts in gait type, relative net substrate contact durations also significantly increased during locomotion on the pole. Finally, both species used relatively shorter and more frequent strides when traveling on the pole. Collectively, these kinematic adjustments permitted marmosets and squirrel monkeys to significantly limit peak vertical forces and COM displacements, theoretically increasing arboreal stability.

Additionally, adjustments to asymmetrical gait dynamics were generally more pronounced in marmosets, as predicted based on their derived autopodial anatomy and retreat from the fine-branch foraging niche (Beattie, 1927; Midlo, 1934; Sussman and Kinzey, 1984; Garber, 1992; Hamrick, 1998). In fact, marmosets consistently exhibited greater kinematic and kinetic adjustments to pole locomotion, despite being smaller relative to support size (Table 3.4). Compared to squirrel monkeys, marmosets were characterized by significantly greater substrate differences in Froude number, peak vertical forces, duty factors, net substrate contact durations, stride lengths and stride frequencies. By contrast, squirrel monkeys showed significantly greater substrate-related changes in relative lead durations. Interestingly, the magnitude of substrate differences in relative limb pair contact durations did not differ between species. Because limb pair contact durations are a product of individual limb duty factors and the lead durations separating limb contacts, statistically similar substrate-related changes in limb pair contact durations suggests that marmosets and squirrel monkeys were using alternative strategies to achieve a similar goal. Specifically, marmosets increased limb pair contact durations via increases in duty factor whereas squirrel monkeys achieved the same result via increases in lead durations. The difference in strategy likely results from a difference in body size: short lead durations should permit the forelimbs and hind limbs of the smaller marmosets to function as a unit, generating forces simultaneously and increasing power outputs despite absolutely shorter limbs (Gambaryan, 1974; Hildebrand, 1977; Walter and Carrier, 2007).

Comparisons between species within each substrate frequently demonstrated significant differences during ground locomotion but similarity during pole locomotion. For instance, when traveling on the ground marmosets exhibited significantly greater peak vertical forces and COM displacements and significantly shorter forelimb and mean duty factors. None of these parameters significantly varied between species during pole locomotion. Lack of variation between species during locomotion on the pole is consistent with increased stability constraints on narrow substrates, limiting kinematic and kinetic flexibility despite differences in ecology and anatomy. Nevertheless, other species-level differences were consistent across substrates. On both the ground and the pole, squirrel monkeys used longer lead and limb contact durations and used a higher percentage of "grounded" gaits, such as gallops and canter. Although squirrel monkeys took longer and less frequent strides than marmosets, they also exhibited relatively longer net substrate contact periods, suggesting that increases in stride length likely resulted from greater limb excursions, rather than an increase in potentially disruptive whole-body aerial phases (e.g., Demes et al., 1990). Together, these data suggest that squirrel monkeys were using more compliant asymmetrical gait kinematics (McMahon, 1985;

McMahon et al., 1987; Ruina et al., 2005), a finding consistent with the squirrel monkeys' greater exploitation of the fine-branch arboreal niche. Compliant walking, characterized by increased joint excursion and substrate contact durations, has been shown to be a hallmark of arboreal locomotion in primates and other mammals (Larson et al., 2000; Larson et al., 2001; Larney and Larson, 2004; but see Chapter 4), allowing these animals to increase stability while simultaneously mitigating joint and bone loading (Schmitt, 1994, 1999). The role of compliance during primate asymmetrical locomotion has yet to be explored, but will surely prove to be an interesting area for future research.

Recent research has also suggested that marmosets and squirrel monkeys differ in several aspects of symmetrical gait dynamics. Schmitt (2003a; also J.W. Young, unpublished data) found that marmoset walking mechanics are unique among primates and more similar to non-primate mammals, a difference he attributed to a reduction in the time spent foraging in a terminal fine-branch environment. Whereas most primates use diagonal sequence (DS) footfall patterns when walking and running (in which hind foot touchdowns are followed by contralateral forefoot touchdowns: Hildebrand, 1967), marmosets use a predominance of trots and lateral sequence (LS) patterns (in which hind foot touchdowns are followed by ispilateral forefoot touchdowns). Additionally, marmosets use retracted arm postures at touchdown and generate greater peak vertical forces on their forelimbs, whereas most primates use protracted arm postures at touchdown and generate greater peak vertical forces on their hind limbs (Demes et al., 1994; Larson et al., 2000). Early studies suggested that squirrel monkeys, like marmosets, differ from most other primates in using LS footfall patterns when walking and running (e.g., Prost and Sussman, 1969; Vilensky and Patrick, 1985; Vilensky, 1994). However, Prost and Sussman (1969) based their conclusions on five strides collected from one monkey, whereas monkeys in Vilensky's studies (Vilensky and Patrick, 1985; Vilensky, 1994) were filmed while walking on flat treadmills. Recent work with larger numbers of animals moving on more naturalistic substrates indicates that DS gaits predominate (i.e., Schmidt, 2005; J. W. Young unpublished data). Like most other primates, mature squirrel monkeys also use protracted arm postures at touchdown and support their body weight on their hind limbs (Schmidt, 2005; but see Chapter 4).

3.4.2. Effects of body size on asymmetrical gait dynamics

Compared to the effects of substrate, size-related influences on asymmetrical gaits dynamics were more ambiguous. Because the potential for arboreal instability is exacerbated as body size increases relative to substrate diameter, I predicted that ontogenetic gains in body mass would necessitate kinematic and kinetic adjustment when animals were traveling on the pole but have less effect on ground locomotion. As predicted, squirrel monkeys significantly decreased peak vertical forces as size increased and did so a greater rate during locomotion on the pole. By contrast, marmosets maintained similar peak forces with ontogenetic increases in body mass. As predicted, older and larger marmosets tended to use greater duty factors, particularly during pole locomotion, although increases in hind limb duty factor were not significant. By contrast, duty factors largely decreased with body size in squirrel monkeys. Lead and limb pair contact durations were generally unassociated with body size in marmosets on both substrates. In direct contradiction to my predictions, older and larger squirrel monkeys

increased lead and contact durations on the ground and decreased lead and contact durations on the pole. In both species, net substrate contact durations significantly increased with size when monkeys were traveling on the ground, but remained constant during pole locomotion. Finally, as predicted, older and larger marmosets used significantly shorter and more frequent strides, particularly when traveling on the pole. By contrast, squirrel monkeys directly contradicted predictions, exhibiting significant increases in stride length and decreases in stride frequency as body size increased.

In sum, specific size-related adjustments to gait parameters varied between species, with marmosets generally showing a greater number of changes in the predicted direction than squirrel monkeys. However, it is unlikely that the majority of the observed kinematic and kinetic changes in either species were a response to size-related instability *per se*. Marmosets tended to exhibit similar adjustments on both the ground and the pole, as indicated by pervasive non-significant mass-by-substrate interactions. In squirrel monkeys, substrate-related differences in gait parameters frequently directly contradicted predictions, with greater kinematic and kinetic "adjustments" evident during ground locomotion. It may be that within the range of body sizes encompassed in this study (143-346 grams in marmosets and 218-535 grams in squirrel monkeys), the biomechanical challenges posed by a 2.5 cm diameter pole remained fairly constant. Indeed, the support size index varied from 3.56-4.78 for marmosets and 3.08-4.15 for squirrel monkeys, far less than the range of 2.5-10 recommended by Stevens (2003; 2007) for small to large supports. Future ontogenetic and comparative studies, encompassing a wider array of body sizes and support diameters, may find more consistent evidence for purely size-related adjustments to asymmetrical gait dynamics on arboreal substrates.

3.4.3. Summary and conclusions

Previous discussions of primate locomotion evolution have almost exclusively focused on symmetrical gait dynamics (e.g., Hildebrand, 1967; Prost, 1969; Kimura et al., 1979; Vilensky and Larson, 1989; Schmitt, 1994; Larson, 1998; Schmitt, 1999; Larson et al., 2000; Larson et al., 2001; Cartmill et al., 2002; Schmitt and Lemelin, 2002; Lemelin et al., 2003; Schmitt, 2003c, 2003a; Larney and Larson, 2004; Schmitt and Hanna, 2004; Schmitt and Lemelin, 2004; Shapiro and Raichlen, 2005; Schmitt et al., 2006; Cartmill et al., 2007a; Lemelin and Schmitt, 2007). Nevertheless, laboratory studies have demonstrated that asymmetrical gaits typify rapid locomotion in nearly all the major primate clades, from cheirogaleids to great apes (e.g., Vilensky, 1980; Vilensky and Patrick, 1985; Hurov, 1987; Vilensky et al., 1990; Kimura, 1992; Demes et al., 1994; Polk, 2001; Arms et al., 2002; Franz et al., 2005; Schmitt et al., 2006). Although few field studies have specifically reported instances of galloping or bounding in free-ranging primates (but see Morbeck, 1976; Rose, 1977; Fleagle and Mittermeier, 1980; Garber, 1991), the lacuna may be primarily methodological: most studies of positional behavior lump asymmetrical gaits under the general rubric of "quadrupedal running" or even simply "quadrupedal locomotion", suggesting the need for greater precision of behavioral categories (e.g., Hunt et al., 1996). Nevertheless, even if asymmetrical gaits are rather infrequent and contribute little to overall travel *time*, they may still account for a substantial proportion of overall travel *distance*, perhaps a more ecologically and

physiologically relevant metric when comparing locomotor behaviors (Fleagle and Mittermeier, 1980; Full, 1989; Arms et al., 2002).

Several lines of evidence suggest that asymmetrical gaits have represented an important component of primates' locomotor repertoires throughout their evolutionary history. First, among non-cursorial Eutherian mammals, asymmetrical gaits are typically used more frequently as body size decreases (Dagg, 1973; Hildebrand, 1977), and ancestral primates are most often reconstructed as small-bodied, arboreal quadrupeds (Cartmill, 1972; Martin, 1990; Gebo, 2004; but see Soligo and Martin, 2006). Second, recently discovered Paleocene and Eocene fossil postcrania indicate morphological adaptation to bounding locomotion among several Plesiadapiforms (Bloch and Boyer, 2007), arguably the closest Archontan outgroup to Euprimates (Bloch and Boyer, 2002; Silcox, 2007). Finally, several of the early Euprimate traits associated with leaping, such as long and dorso-ventrally tall lumbar vertebral bodies, broadened ilia, shortened ischia, relatively long hind limbs and elongated tarsals (Gregory, 1920; Dagosto, 1993, 2007), could also have facilitated bounding and galloping.

In sum, understanding the dynamics of primate asymmetrical gaits may be critical to understanding primate locomotor ecology and evolution in general. The results of this study illustrate that 1) symmetrical gaits are not the only stable way to travel arboreally and 2) small-bodied primates utilize specific kinematic and kinetic adaptations that should increase stability when using asymmetrical gaits on arboreal substrates. Future work should explore primate asymmetrical gait dynamics across a greater range of taxa, body sizes and substrates.

Also, although beyond the scope of the current paper, it would be interesting to compare asymmetrical gait dynamics between primates and other mammals, particularly given the established uniqueness of primate walking (Larson, 1998; Schmitt and Lemelin, 2002). Most non-primate mammals studied to date exhibit predictable, discontinous kinematic and kinetic changes when transitioning from symmetrical to asymmetrical gaits (Heglund et al., 1974; Farley, 1991; Vilensky et al., 1991; but see Iriarte-Diaz et al., 2006). For instance, when using symmetrical gaits, most mammals increase speed by increasing both stride frequency and stride length. However, past the trot-gallop (i.e., symmetrical-asymmetrical) transition point, speed is only increased via extensions of stride length, whereas stride frequency tends to remain constant. Interestingly, the data presented here indicate that marmosets and squirrel monkeys, unlike other mammals, continue to increase both stride length and stride frequency with speed during asymmetrical gaits. Vilensky (1980) obtained similar results for rhesus macaques (*Macaca mulatta*). It may be that primates, which typically do not use a running trot (Demes et al., 1990; Demes et al., 1994; Preuschoft and Günther, 1994; Schmitt et al., 2006), transition to asymmetrical gaits at lower speeds and stride frequencies than other mammals. Indeed, marmosets and squirrel monkeys used asymmetrical gaits at Froude numbers as low as 0.5 (0.25 as calculated by Alexander and Jayes, 1983), whereas most mammals transition to asymmetrical gaits at Froude numbers of 2 to 3 (Alexander and Jayes, 1983). Again, however, a broader survey of primate asymmetrical gait dynamics, encompassing greater taxonomic and morphological variation, would be required to test this hypothesis.

3.5. Tables

Table 3.1. Kinematic and kinetic variables calculated in this study.

Variable	Raw units	Scaling factor
Speed	m/s	$(gh)^{-0.5}$
Peak vertical force	N	bw
Vertical COM displacement	m	h
FL/HL/mean duty factors	s	t_s
FL/HL lead durations	s	t_c
FL/HL/mean contact durations	s	t_s
Whole body substrate contact duration	s	t_s
Stride length	m	h
Stride frequency	Hz ($1/t_s$)	$(g/h)^{-0.5}$

Specific names for scaled variables are shown in parentheses (i.e., duty factor).

Abbreviations – FL: forelimb, HL: hind limb, g: gravitational acceleration, h: cube root of body mass, bw: body weight, t_s: stride duration, t_c: contact duration

Table 3.2. Precision of marmoset gait data.

	Error variation			Intra-experimental variation		
Variable	**Mean**	**SD**	**CV**	**Mean**	**SD**	**CV**
Speed	1.7 m/s	0.052 m/s	2.5%	1.7 m/s	0.22 m/s	13.2%
Stride duration	0.21 s	0.0055 s	3.2%	0.22 s	0.023 s	10.6%
Stride length	0.35 m	0.014 m	4.0%	0.35 m	0.043 m	11.5%
Left HL duty factor	0.36	0.012	3.4%	0.39	0.045	12.0%
Left FL duty factor	0.30	0.012	4.3%	0.32	0.043	13.8%
Right HL duty factor	0.36	0.014	4.3%	0.38	0.038	10.5%
Right HL duty factor	0.30	0.011	3.9%	0.32	0.048	15.4%
FL lead duration	0.042 s	0.0025 s	16.6%	0.046 s	0.0181 s	58.4%
HL lead duration	0.013 s	0.0015 s	21.7%	0.015 s	0.0102 s	104.8%
FL contact duration	0.10 s	0.0053 s	7.9%	0.11 s	0.0221 s	21.0%
HL contact duration	0.09 s	0.0060 s	8.7%	0.09 s	0.0210 s	21.7%

Standard deviations (SD) and coefficients of variation (CV) summarize the average amount of measurement variation across three replicates of 20 randomly selected trials (error variation) or within the experiments from which the trials were drawn (intra-experimental variation). Reported CVs are means across all CVs for that variable.

Table 3.3. Precision of squirrel monkey gait data.

	Error variation			Intra-experimental variation		
Variable	**Mean**	**SD**	**CV**	**Mean**	**SD**	**CV**
Speed	1.7 m/s	0.026 m/s	1.7%	1.7 m/s	0.25 m/s	15.8%
Stride duration	0.31 s	0.0043 s	1.4%	0.29 s	0.030 s	9.8%
Stride length	0.50 m	0.0097 m	1.9%	0.48 m	0.059 m	12.2%
Left HL duty factor	0.37	0.0099	2.6%	0.38	0.045	11.6%
Left FL duty factor	0.33	0.013	4.0%	0.34	0.037	11.0%
Right HL duty factor	0.36	0.014	3.6%	0.38	0.050	12.7%
Right HL duty factor	0.32	0.013	4.2%	0.34	0.042	12.1%
FL lead duration	0.072 s	0.0050 s	8.3%	0.077 s	0.037 s	52.9%
HL lead duration	0.060 s	0.0016 s	3.7%	0.071 s	0.042 s	65.8%
FL contact duration	0.17 s	0.0073 s	4.4%	0.17 s	0.048 s	27.2%
HL contact duration	0.17 s	0.0036 s	2.2%	0.18 s	0.053 s	28.8%

Presentation of data follows Table 3.2.

Table 3.4. Support size indices (substrate diameter ÷ bodymass$^{0.33}$) for each monkey, separated by species.

	Mean	Median	Range
Callithrix jacchus			
114	3.65	3.65	3.64-3.67
452	3.59	3.58	3.56-3.67
597	3.62	3.61	3.59-3.68
707	4.54	4.58	4.36-4.78
708	4.32	4.28	4.27-4.61
Saimiri boliviensis			
4428	3.22	3.16	3.08-3.45
4433	3.47	3.47	3.47-3.48
4445	3.44	3.37	3.23-3.66
4466	3.34	3.30	3.24-3.56
4475	3.72	3.71	3.31-4.15
4483	3.62	3.53	3.28-4.07

Table 3.5. Substrate and species differences in asymmetrical gait dynamics.

Variable	*Callithrix*		*Saimiri*		Substrate		Species		Interaction
	G	P	G	P	*Callithrix*	*Saimiri*	G	P	
Froude number	2.23 ±0.127 (76)	1.85 ±0.118 (81)	2.06 ±0.049 (499)	2.01 ±0.059 (342)	**G > P (16.9%)**	G = P (2.7%)	**Cj > Sb (7.4%)**	**Cj < Sb (7.8%)**	**Cj > Sb**
Relative peak vertical force (bw)	2.12 ±0.150 (21)	1.75 ±0.102 (23)	1.84 ±0.054 (95)	1.68 ±0.047 (92)	**G > P (20.8%)**	**G > P (6.2%)**	**Cj > Sb (17.0%)**	Cj = Sb (1.6%)	**Cj > Sb**
Relative vertical COM displacement	0.250 ±0.053 (21)	0.132 ±0.022 (23)	0.185 ±0.017 (95)	0.121 ±0.010 (92)	**G > P (47.2%)**	**G > P (34.6%)**	**Cj > Sb (25.9%)**	Cj = Sb (8.2%)	Cj = Sb
Forelimb duty factor	0.291 ±0.007 (76)	0.344 ±0.008 (81)	0.334 ±0.003 (499)	0.353 ±0.004 (342)	**G < P (15.8%)**	**G < P (5.5%)**	**Cj < Sb (12.6%)**	Cj = Sb (2.5%)	**Cj > Sb**
Hind limb duty factor	0.361 ±0.008 (76)	0.400 ±0.009 (81)	0.370 ±0.003 (499)	0.386 ±0.004 (342)	**G < P (10.5%)**	**G < P (4.0%)**	**Cj < Sb (2.4%)**	**Cj > Sb (3.6%)**	**Cj > Sb**
Mean duty factor	0.327 ±0.006 (76)	0.373 ±0.007 (81)	0.352 ±0.003 (499)	0.370 ±0.004 (342)	**G < P (13.0%)**	**G < P (4.8%)**	**Cj < Sb (7.2%)**	Cj = Sb (0.8%)	**Cj > Sb**

Reported values were adjusted for body size differences (Section 3.2.3). Means ± standard errors and sample sizes (in parentheses) are reported for each species on each substrate. Percentage differences between substrates and species (calculated relative to the larger value) are shown in parentheses beneath each comparison. Bold print indicates a significant species or substrate difference ($p \leq 0.05$).

Table 3.5. Continued.

Variable	*Callithrix*		*Saimiri*		Substrate Difference		Species Difference		Interaction
	G	P	G	P	*Callithrix*	*Saimiri*	G	P	
Relative forelimb lead duration	0.338 ±0.029 (76)	0.402 ±0.025 (81)	0.386 ±0.010 (499)	0.518 ±0.010 (342)	**G < P (16.6%)**	**G < P (25.5%)**	**Cj < Sb (12.6%)**	**Cj < Sb (22.5%)**	**Cj < Sb**
Relative hind limb lead duration	0.097 ±0.032 (76)	0.201 ±0.030 (81)	0.267 ±0.012 (499)	0.420 ±0.014 (342)	**G < P (39.1%)**	**G < P (36.6%)**	**Cj < Sb (63.7%)**	**Cj < Sb (52.2%)**	**Cj < Sb**
Relative forelimb contact duration	0.419 ±0.023 (76)	0.537 ±0.026 (81)	0.530 ±0.010 (499)	0.706 ±0.015 (342)	**G < P (22.3%)**	**G < P (24.9%)**	**Cj < Sb (20.9%)**	**Cj < Sb (23.9%)**	Cj = Sb
Relative hind limb contact duration	0.377 ±0.019 (76)	0.473 ±0.024 (81)	0.497 ±0.010 (499)	0.681 ±0.018 (342)	**G < P (19.4%)**	**G < P (24.1%)**	**Cj < Sb (27.0%)**	**Cj < Sb (30.5%)**	Cj = Sb
Relative mean contact duration	0.396 ±0.017 (76)	0.507 ±0.021 (81)	0.517 ±0.009 (499)	0.695 ±0.015 (342)	**G < P (21.5%)**	**G < P (25.6%)**	**Cj < Sb (23.4%)**	**Cj < Sb (27.0%)**	Cj = Sb
Relative substrate contact duration	0.771 ±0.027 (76)	0.979 ±0.030 (81)	0.954 ±0.012 (499)	1.099 ±0.016 (342)	**G < P (21.8%)**	**G < P (13.1%)**	**Cj < Sb (19.2%)**	**Cj < Sb (10.9%)**	**Cj > Sb**

Table 3.5. Continued.

Variable	*Callithrix*		*Saimiri*		Substrate Difference		Species Difference		Interaction
	G	P	G	P	*Callithrix*	*Saimiri*	G	P	
Relative stride length	0.614 ±0.018 (76)	0.505 ±0.015 (80)	0.702 ±0.008 (452)	0.631 ±0.009 (316)	**G > P (15.6%)**	**G > P (10.1%)**	**Cj < Sb (12.6%)**	**Cj < Sb (20.0%)**	**Cj > Sb**
Relative stride frequency	0.324 ±0.009 (76)	0.402 ±0.010 (81)	0.286 ±0.003 (499)	0.319 ±0.004 (342)	**G < P (24.2%)**	**G < P (10.3%)**	**Cj > Sb (11.7%)**	**Cj > Sb (20.6%)**	**Cj > Sb**

Table 3.6. Correlations between gait variables and Froude number.

	Callithrix		*Saimiri*	
	Ground	**Pole**	**Ground**	**Pole**
Relative peak vertical force	**0.938 (0.905)**	**0.589 (0.617)**	**0.506 (0.601)**	**0.419 (0.361)**
Relative vertical COM displacement	**0.444 (0.462)**	-0.096 (-0.111)	0.134 **(0.207)**	0.035 (0.075)
FL duty factor	**-0.694 (-0.688)**	**-0.739 (-0.751)**	**-0.764 (-0.767)**	**-0.759 (-0.760)**
HL duty factor	**-0.595 (-0.596)**	**-0.741 (-0.755)**	**-0.776 (-0.790)**	**-0.730 (-0.727)**
Mean duty factor	**-0.692 (-0.703)**	**-0.800 (-0.814)**	**-0.804 (-0.814)**	**-0.808 (-0.812)**
Relative FL lead duration	**-0.622 (-0.628)**	0.070 (0.071)	**-0.170 (-0.147)**	0.006 (-0.003)
Relative HL lead duration	**-0.607 (-0.500)**	**-0.448 (-0.433)**	**-0.149 (-0.152)**	**-0.201 (-0.206)**
Relative FL contact duration	**-0.858 (-0.863)**	**-0.621 (-0.685)**	**-0.583 (-0.577)**	**-0.586 (-0.568)**
Relative HL contact duration	**-0.691 (-0.682)**	**-0.771 (-0.753)**	**-0.535 (-0.536)**	**-0.565 (-0.570)**
Relative mean contact duration	**-0.843 (-0.884)**	**-0.767 (-0.781)**	**-0.612 (-0.625)**	**-0.625 (-0.622)**
Relative substrate contact duration	**-0.819 (-0.882)**	**-0.723 (-0.768)**	**-0.551 (-0.617)**	**-0.223 (-0.244)**
Relative stride length	**0.722 (0.737)**	**0.842 (0.850)**	**0.790 (0.808)**	**0.742 (0.745)**
Relative stride frequency	**0.823 (0.761)**	**0.744 (0.732)**	**0.580 (0.569)**	**0.613 (0.574)**

Spearman rank correlations are shown in parentheses. Bold print indicates a significant correlation coefficient ($p \leq 0.05$).

Table 3.7. Multiple regressions of asymmetrical gait parameters on body mass, controlling for Froude number.

	Callithrix			*Saimiri*		
	Ground (β)	**Pole (β)**	**Difference**	**Ground (β)**	**Pole (β)**	**Difference**
Froude number	**-5.26±1.898**	**-4.43±1.036**	NS	**1.58±0.570**	**1.59±0.5873**	NS
Relative peak vertical force (bw)	0.172±0.3624	0.202±0.9977	NS	**-0.374±0.3481**	**-0.764±0.2422**	*
Relative vertical COM displacement	-4.72±5.123	3.26±6.324	*	-2.64±2.672	-0.574±2.593	NS
FL duty factor	**1.56±0.7910**	**1.83±0.7389**	*	**-0.299±0.1669**	**-0.782±0.2122**	***
HL duty factor	0.190±0.9249	0.511±0.6021	NS	-0.145±0.1791	**0.530±0.2132**	***
Mean duty factor	**0.826±0.7940**	**1.17±0.5528**	*	**-0.230±0.1598**	-0.122±0.1887	NS
Relative FL lead duration	0.278±1.154	-1.28±1.508	*	**1.54±0.3528**	**-0.716±0.3766**	***
Relative HL lead duration	-0.392±0.4134	**-0.660±0.5913**	NS	**1.32±0.1921**	**-0.626±0.1838**	***
Relative FL contact duration	**1.23±0.5768**	0.416±0.8849	NS	**0.664±0.2265**	**-1.19±0.2589**	***
Relative HL contact duration	-0.440±1.206	-0.467±0.9631	NS	**2.11±0.3525**	**-0.555±0.3868**	***
Relative mean contact duration	0.781±0.7938	0.117±0.7956	NS	**1.38±0.2509**	**-0.979±0.2872**	***
Relative net substrate contact duration	**0.648±0.5916**	0.298±0.5417	NS	**0.615±0.1694**	0.084±0.2194	**
Relative stride length	**-0.715±0.5780**	**-0.796±0.3376**	***	**0.645±0.1374**	**0.617±0.1628**	NS
Relative stride frequency	**0.659±0.4988**	**0.941±0.3906**	*	**-0.724±0.1066**	**-0.656±0.1363**	NS

Partial regression slopes (β±95% CI) are presented for each parameter on body mass, controlling for Froude number. Froude number comparisons are bivariate regressions on body mass. Bold print indicates the regression was significant ($p \leq 0.05$). Results from slope comparisons are shown in the "difference" column for each species (*: $p \leq 0.05$; **: $p \leq 0.01$; ***: $p \leq 0.001$; NS: not significant).

3.6. Figures

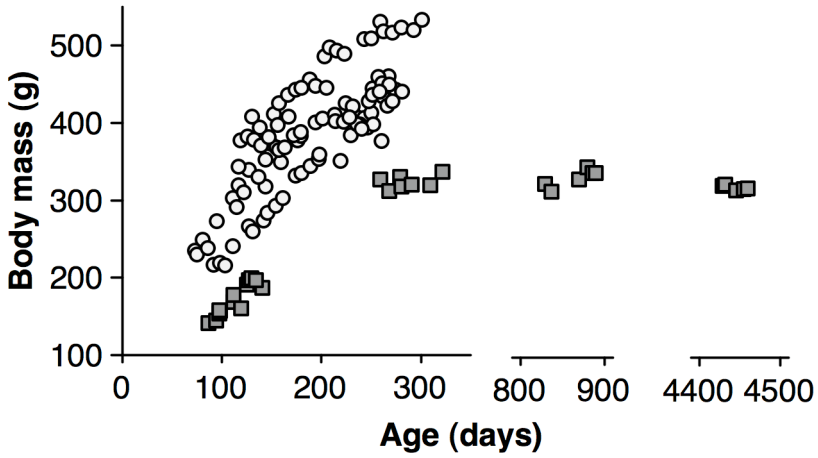

Figure 3.1. Body mass plotted against age for all marmosets and squirrel monkeys. Marmosets are represented by gray squares and squirrel monkeys by white circles. For ease of presentation, body masses for the two adult marmosets (Animals 114 and 452) have been plotted on broken axes.

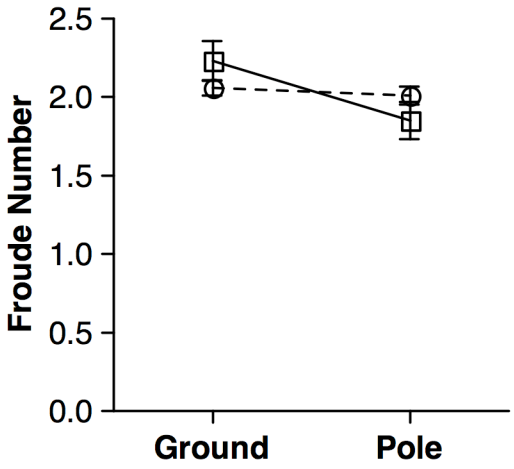

Figure 3.2. Species and substrate differences in Froude number.
Symbols correspond to species means on each substrate; error bars represent standard errors. Marmosets are represented by squares connected with the solid line and squirrel monkeys by circles connected with the dashed line. Marmosets significantly reduced Froude numbers when traveling on the pole, whereas squirrel monkeys moved at similar Froude numbers across substrates.

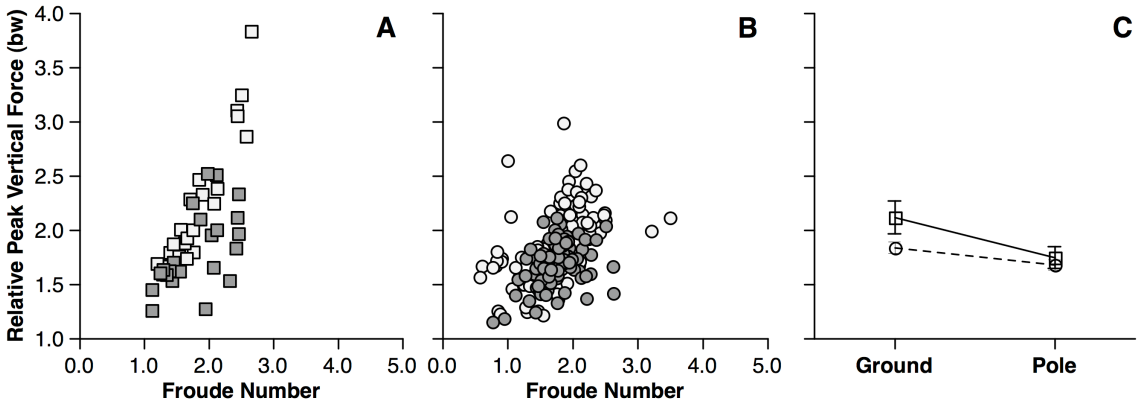

Figure 3.3. Species and substrate differences in relative peak vertical forces. Relative peak vertical forces are plotted against Froude number for marmosets in (A) and for squirrel monkeys in (B). White symbols represent ground strides; gray symbols represent pole strides. (C) Least-squares means for each species on each substrate. Symbols follow Figure 3.2. Marmosets and squirrel monkeys significantly reduced peak vertical forces when traveling on the pole, even after controlling for Froude number.

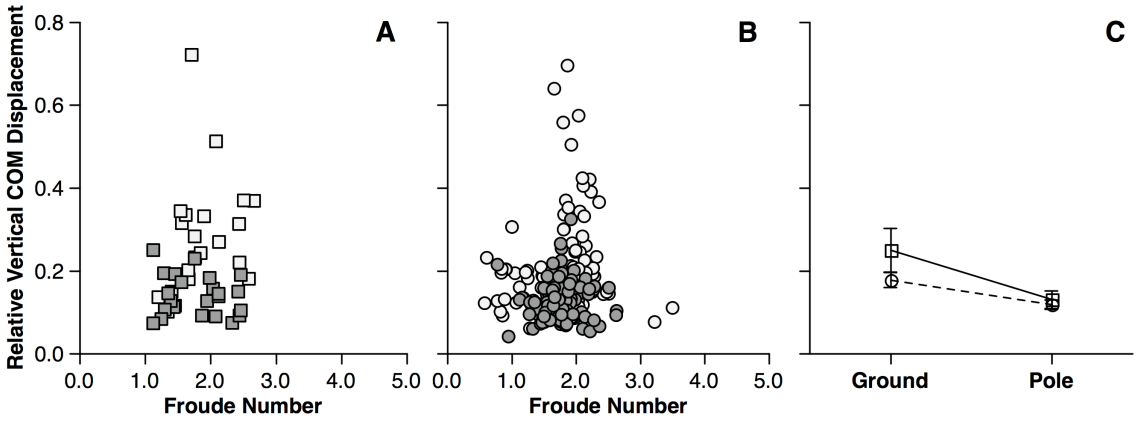

Figure 3.4. Species and substrate differences in the relative vertical displacement of the COM.
Relative vertical COM displacement is plotted against Froude number for marmosets in (A) and for squirrel monkeys in (B). Species means on each substrate are shown in (C). A least-squares corrected mean is shown for marmoset strides on the ground, as vertical COM displacement was significantly correlated with Froude number in this condition. Symbols follow Figure 3.2 and 3.3.

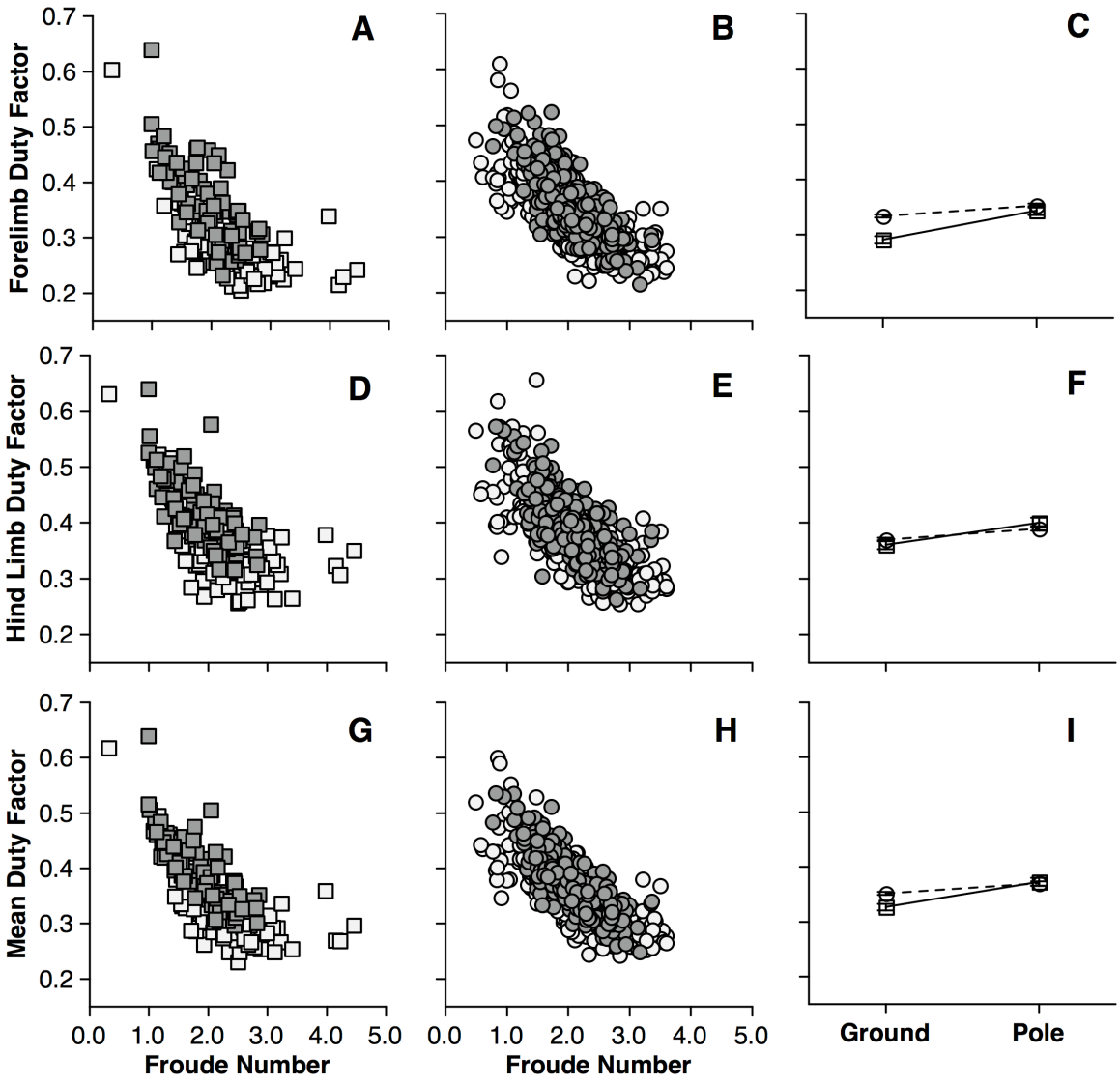

Figure 3.5. Species and substrate differences in limb duty factors.
Duty factors are plotted against Froude number for marmosets in (A), (D) and (G) and for squirrel monkeys in (B), (E) and (H). Least-squares means for each species on each substrate are shown in (C), (F) and (I). Symbols follow Figure 3.2 and 3.3. Marmosets and squirrel monkeys significantly increased forelimb, hind limb and mean duty factor when traveling on the pole, even after controlling for Froude number.

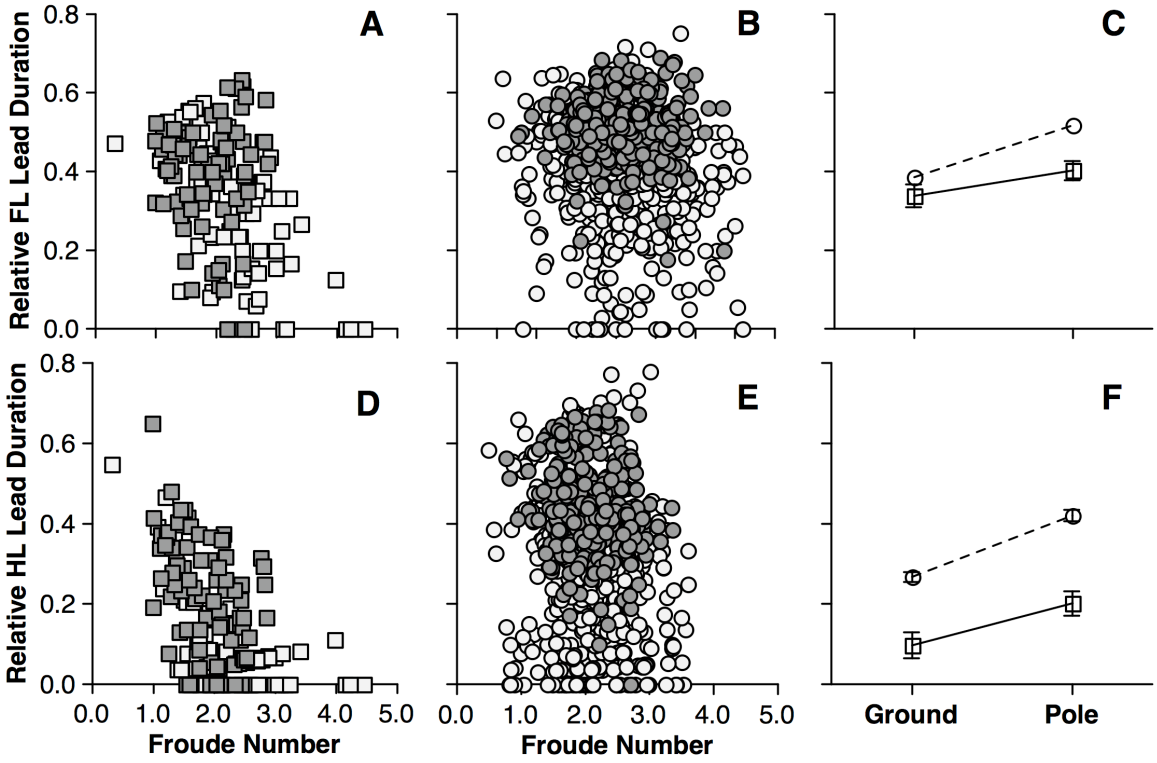

Figure 3.6. Species and substrate differences in relative lead durations.
Lead durations are plotted against Froude number for marmosets in (A) and (D) and for squirrel monkeys in (B) and (E). Least-squares means for each species on each substrate are shown in (C) and (F). Uncorrected means are shown for forelimb lead durations on the pole, as this parameter was not correlated with Froude number in either species (Table 3.6). Symbols follow Figure 3.2 and 3.3. Marmosets and squirrel monkeys significantly increased relative forelimb and hind limb lead durations when traveling on the pole, even after controlling for Froude number.

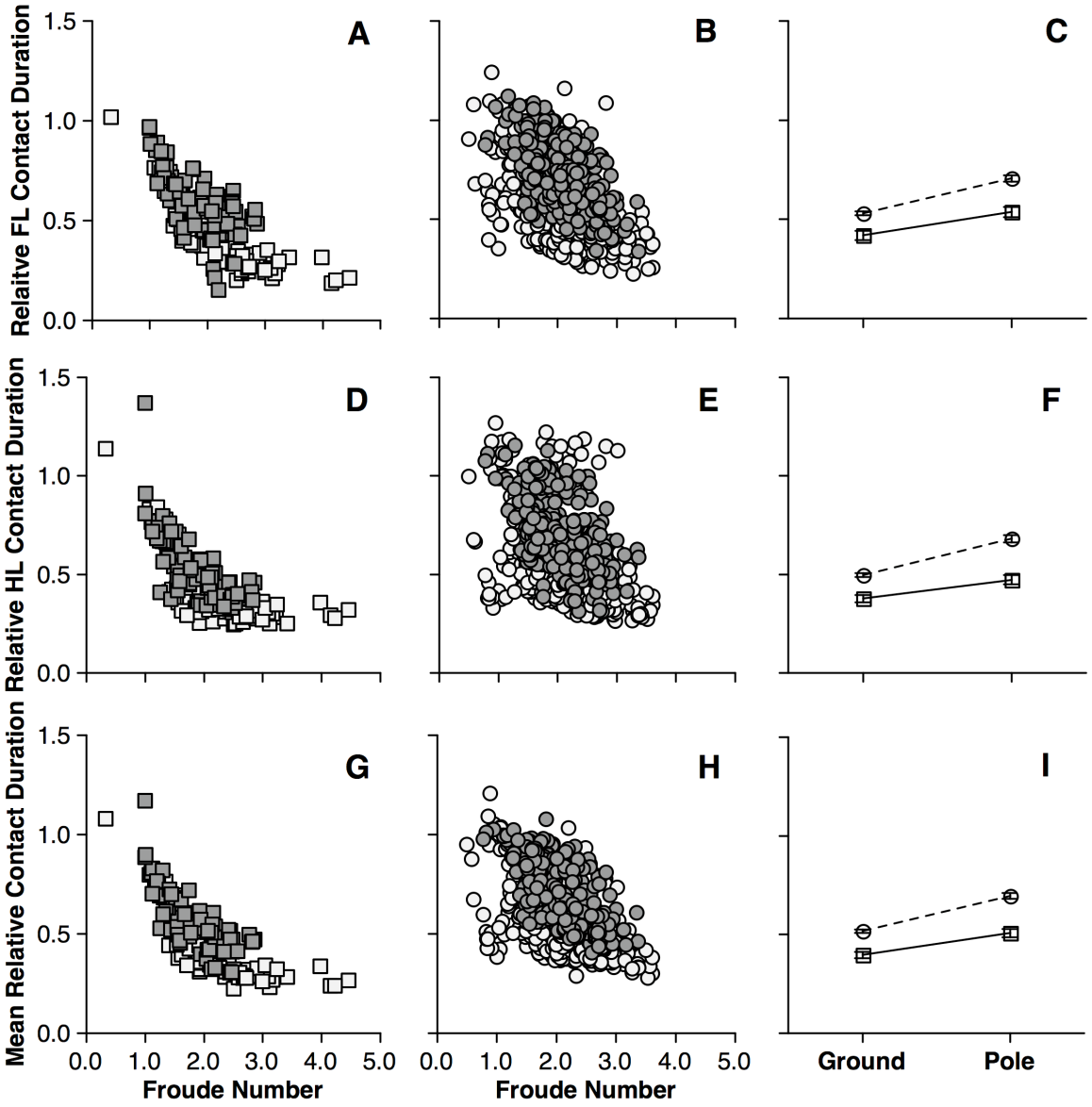

Figure 3.7. Species and substrate differences in relative limb contact durations. Relative contact durations are plotted against Froude number for marmosets in (A), (D) and (G) and for squirrel monkeys in (B), (E) and (H). Least-squares means for each species on each substrate are shown in (C), (F) and (I). Symbols follow Figure 3.2 and 3.3. Marmosets and squirrel monkeys significantly increased forelimb, hind limb and mean relative contact durations when traveling on the pole, even after controlling for Froude number.

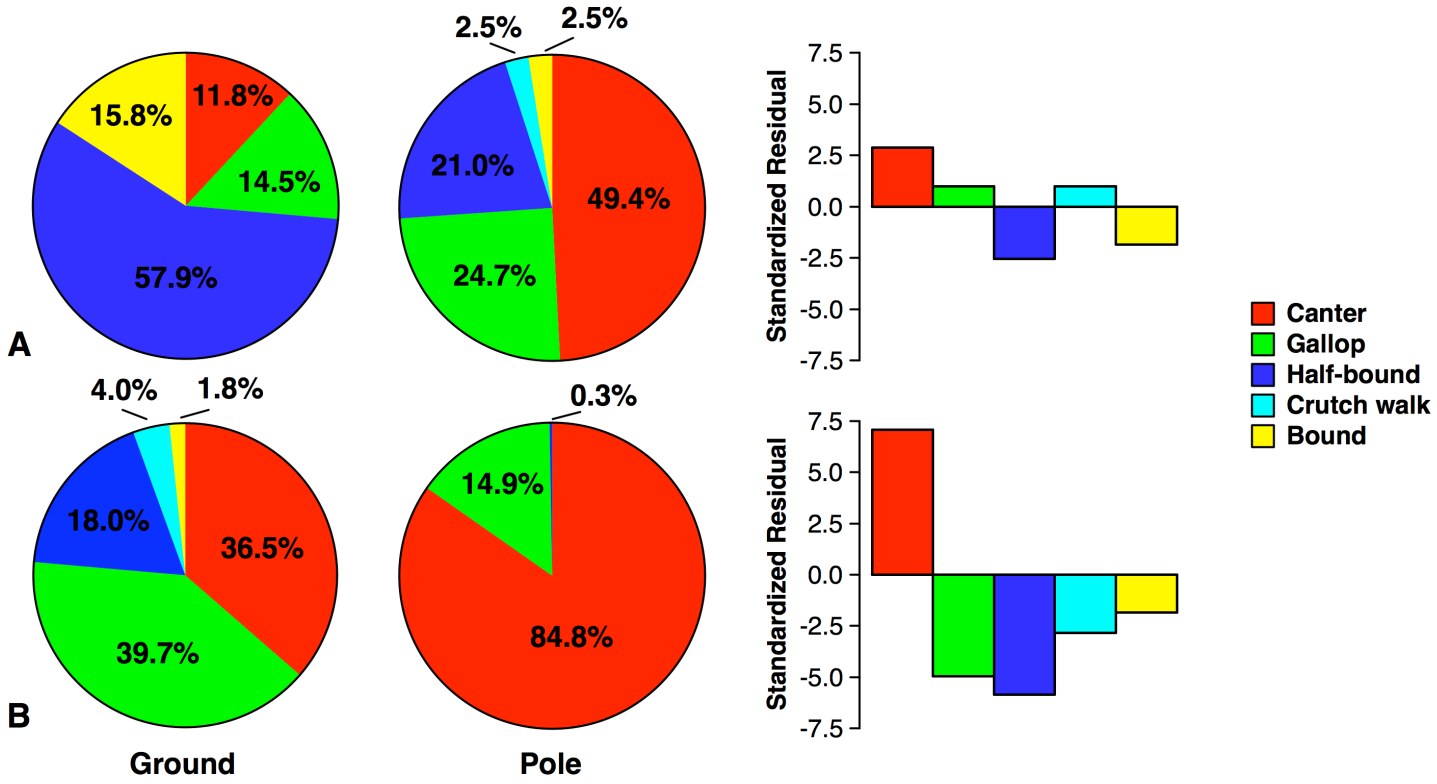

Figure 3.8. Substrate differences in gait use in marmosets (A) and squirrel monkeys (B).
Pie charts in left-hand panels depict the proportional distribution of gaits used during ground locomotion. Pie charts in center panels indicate the proportional distribution of gait used during pole locomotion. Bar charts in right-hand panels depict standardized residuals (i.e., differences between observed and expected counts on the pole scaled to the square root of the expected counts: Haberman, 1978). When traveling on the pole, marmosets increased their use of canters, gallops and crutch walks and used fewer bounds and half-bounds. Squirrel monkeys substantially increased their use of canters when traveling on the pole, decreasing the use of all other gaits.

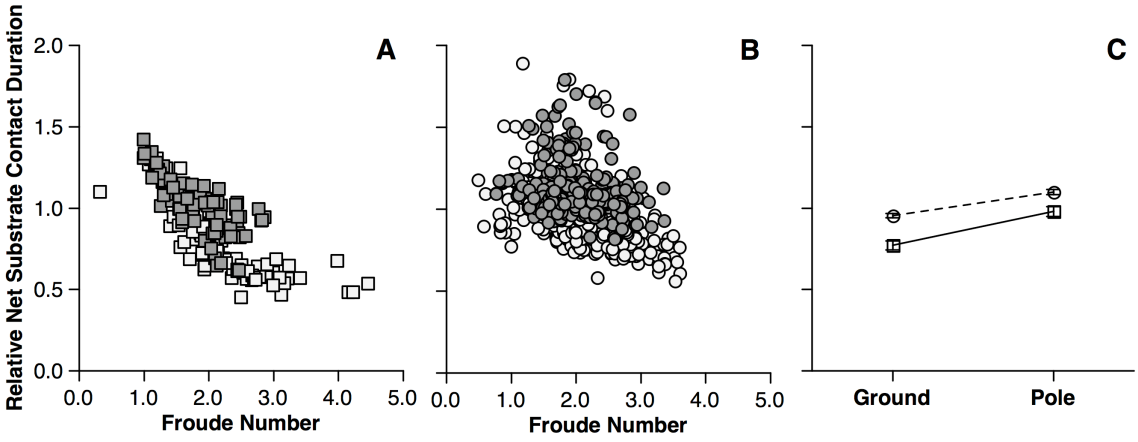

Figure 3.9. Species and substrate differences in relative net substrate contact durations.
Relative net substrate contact duration is plotted against Froude number for marmosets in (A) and for squirrel monkeys in (B). Least-squares means for each species on each substrate are shown in (C). Symbols follow Figure 3.2 and 3.3. Marmosets and squirrel monkeys significantly increased relative net substrate contact durations when traveling on the pole, even after controlling for Froude number.

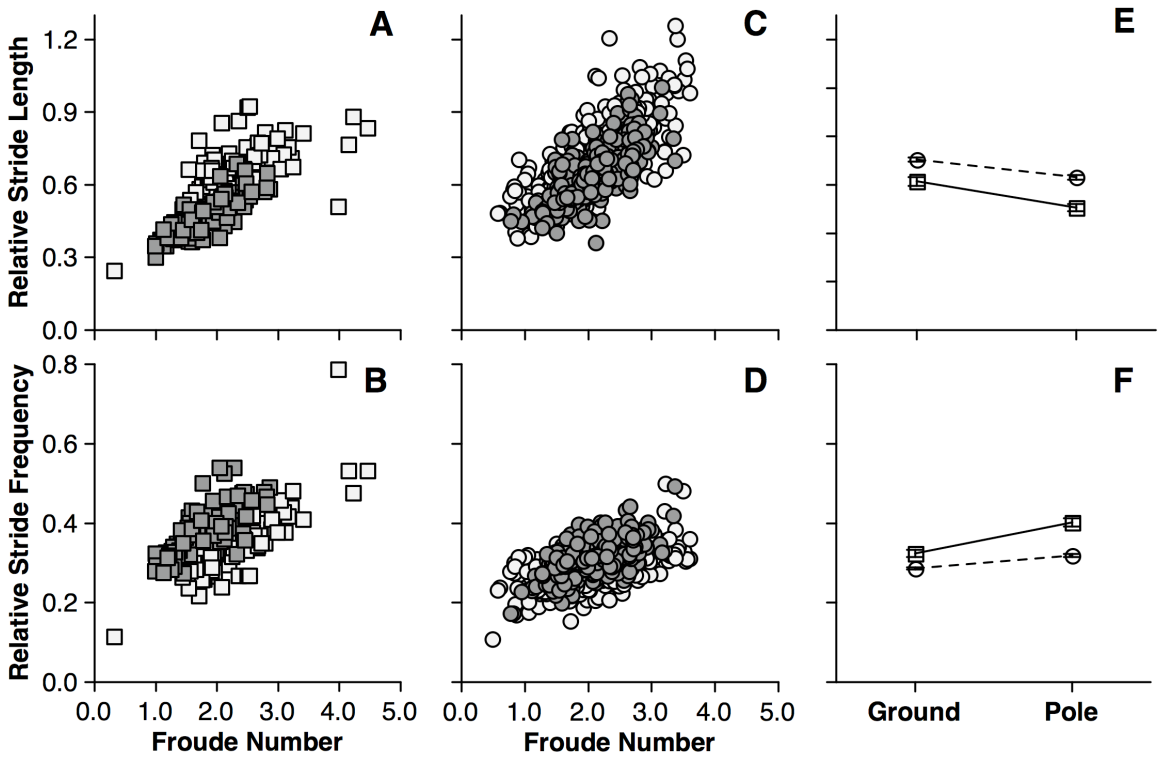

Figure 3.10. Species and substrate differences in relative stride length and relative stride frequency.
Relative stride length and relative stride frequency are plotted against Froude number for marmosets in (A) and (D) and for squirrel monkeys in (B) and (E). Least-squares corrected mean stride length and mean stride frequency for each species on each substrate are shown in (C) and (F). Symbols follow Figure 3.2 and 3.3. Marmosets and squirrel monkeys significantly used significantly shorter and more frequent strides when traveling on the pole, even after controlling for Froude number.

Chapter 4. Ontogeny of Limb Force Distribution in Squirrel Monkeys (*Saimiri boliviensis*): Implications for Understanding Primate Locomotor Kinetics

4.1. Introduction

The distribution of peak vertical forces between the forelimbs and the hind limbs has often been cited as one of the key traits distinguishing primate quadrupedal locomotion from that of other mammals (Larson, 1998; Schmitt and Lemelin, 2002; Schmitt, 2003b). Whereas most mammals generate greater peak vertical forces with their forelimbs, primates typically generate greater peak vertical forces with their hind limbs (Kimura et al., 1979; Reynolds, 1985a, 1985b; Kimura, 1992; Demes et al., 1994; Polk, 2001; Schmitt and Lemelin, 2002; Schmitt, 2003a; Li et al., 2004; Schmitt and Hanna, 2004; Schmitt and Lemelin, 2004; Franz et al., 2005; Hanna et al., 2006; Raichlen et al., 2007; Wallace and Demes, 2007)[4]. A shift from "forelimb dominant" to "hind limb dominant" locomotion has been presented as an adaptive strategy that permitted basal primates to emancipate their forelimbs from a weight-bearing function, thus facilitating foraging and locomotion in the potentially unstable "fine-branch niche" (Cartmill, 1974b, 1974a; Schmitt, 1994, 1999; Cartmill et al., 2002; Schmitt and Lemelin, 2002). In support of this hypothesis, *Caluromys philander*, a South American marsupial known to exploit the "fine-branch niche" (Julienlaferriere and Atramentowicz, 1990), converges on the primate pattern of greater hind limb loading (Schmitt and Lemelin, 2002; Lemelin and Schmitt, 2007). By contrast, common marmosets (*Callithrix jacchus*), platyrrhine primates that show many specializations for movement on large vertical substrates, differ from most primates in generating greater peak vertical forces on their forelimbs (Schmitt 2003a). Additionally, more terrestrially-adapted primates, such as patas monkeys (*Erythrocebus patas*) and baboons (*Papio* spp), tend to distribute peak forces more evenly between the forelimbs and hind limbs (Kimura et al., 1979; Reynolds, 1985b; Demes et al., 1994; Polk, 2001), further suggesting that hind limb dominance in limb force distribution is associated with committed arboreality. Reduction of forelimb loading has also been argued to be a precursor to the evolution of hominin bipedalism (Kimura et al., 1979; Reynolds, 1985b; Kimura, 1987). Despite the importance of hind limb dominance in limb force distribution to theories of primate and human locomotor evolution, the biomechanical bases for peak limb force distribution remain controversial.

The simplest model attributes primates' unique mode of limb loading to differences in the position of the whole-body center of mass (COM) relative to the hands and feet (Rollinson and Martin, 1981; Lemelin and Schmitt, 2004; Raichlen et al., 2007). Indeed, natural and experimental variation COM position has been shown to significantly

[4] Many authors have discussed patterns of peak limb force distribution in terms of "weight-support", asserting that primates differ from other mammals in supporting a greater proportion of body weight on the hind limbs. However, this association is not necessarily valid. Impulse, calculated as the area under the force-time curve, is a better metric of each limb's contribution weight support, as the total impulse across a stride must sum to body weight times contact duration (Bertram et al., 1997; Lee et al., 2004). Nevertheless, provided forelimb and hind limb duty factors do not differ greatly, patterns of peak force distribution should be a reliable and valid indicator of impulse distribution and weight support.

affect limb force distribution in primates and other mammals (Bertram et al., 2000; Lee et al., 2004; Lemelin and Schmitt, 2004; Young et al., 2007). Although morphological studies have found that the whole-body COM in most adult primates is near, or even anterior to, the transverse midline of the trunk (Reynolds, 1974; Wells and DeMenthon, 1987; Turnquist and Wells, 1994; Crompton et al., 1996; Raichlen et al., 2007; Young et al., 2007), behavioral adjustments in joint kinematics have the potential for altering force distribution between limb pairs, even in the absence of morphological variation. For example, provided the whole-body COM is ventral to a line connecting the forelimb and hind limb centers of rotation – a condition likely to characterize most primates – changes in effective forelimb and hind limb lengths should theoretically shift body weight towards the longer pair of limbs (Stern, 1975). Similarly, Raichlen et al. (2007) recently found that the average position of the hands and feet relative to the whole-body COM accurately predicted patterns of body weight support in a sample of walking chimpanzees. Raichlen et al. (2007) also reviewed evidence showing that primates, as an order, tend to show more protracted hind limb positions and less retracted forelimb positions than other quadrupedal mammals (see also Larson et al., 2000; Larson et al., 2001), suggesting that all primates tend to place their hind limbs closer to the COM than their forelimbs.

Reynolds (1985a) presented an alternative model of primate limb force distribution. Citing his own unpublished data, Reynolds (1985a) argued that, in most primates, the average position of the feet during walking is not sufficiently protracted to generate the observed patterns of forelimb-hind limb peak force distribution. Expanding on biomechanical theory first developed by Gray (1944) and Barclay (1953), Reynolds (1985a) instead proposed that primates actively redistribute body weight to their hind limbs *via* the selective activation of retractor muscles on a protracted hind limb during early stance phase. Reynolds (1985a) argued that if the hind limb were sufficiently protracted at the moment of muscle activation, the braking impulse resulting from the limb functioning as a cranially-displaced strut should sufficiently negate any propulsive impulse imparted by the rectractor musculature, thus ensuring that the net horizontal impulse was low. In support of Reynolds' (1985a) hypothesis, Reynolds (1987) and Larson et al. (2001) found that primates exhibit pronounced degrees of hind limb protraction at touchdown, higher than any other mammalian group with the exception of marsupials. Electromyographic (EMG) studies have also presented data congruent with Reynolds' (1985a) hypothesis. Kimura et al. (1979) and Ishida et al. (1985) found that in several species of anthropoid primates, the long head of *m. biceps femoris*, an important hind limb retractor, was active across the initial half of stance phase during walking, as Reynolds (1985a) predicted. The long head of *m. biceps femoris* has also been shown to be active in orangutans (*Pongo pygmaeus*) during the latter half of swing phase and the first half of stance phase (Stern and Susman, 1981). More recently, Larson and Stern (2008) found that hip retractor muscles were active across the first two-thirds of stance phase during walking in an eclectic sample of prosimian and catarrhine primates. Interestingly, the great apes, which tended to show the highest levels of retractor activity, also exhibit the greatest degree hind limb dominance in force distribution (Kimura, 1979; Reynolds, 1985b; Demes et al., 1994).

Nevertheless, recent data and biomechanical theory have challenged Reynolds' (1985a) hypothesis. As Raichlen et al. (2007) note, according to Reynold's (1985a) own

calculations, net propulsive impulse across the stride would never sum to zero – even if the hind limb were highly protracted at the moment of peak force. Therefore, locomotion would not be strictly steady-state and measures of limb force distribution would be complicated by unbalanced pitching torques around the COM (Gray, 1944). Also, Reynold's (1985a) mechanism applies solely to limb force distribution during walking. Primates, however, tend to generate greater peak vertical forces on the hind limbs across all gaits, including ambling (i.e., "grounded running": Wallace and Demes, 2007) and galloping (Kimura, 1992; Demes et al., 1994; Hanna et al., 2006).

Schmitt and colleagues (Schmitt, 1994, 1998, 1999; Schmitt and Hanna, 2004) have also challenged Reynold's (1985a) model, asserting that although primates tend to significantly reduce forelimb loading when walking on simulated branches, there is no evidence that hind limb protraction significantly differs between terrestrial and arboreal substrates. Instead, these authors argue that primates mitigate forelimb loading by adopting more "compliant" limb kinematics, marked by augmented forelimb angular excursions, prolonged substrate contact durations and pronounced elbow flexion from touchdown to mid-stance. Experimental studies have shown that the use of compliant kinematics allows human runners to significantly reduce vertical forces at mid-stance while maintaining net impulse and velocity (McMahon et al., 1987). In support of Schmitt's (1994,1998,1999) model of primate limb force distribution, Larney and Larson (2004) found that primates exhibit substantially more joint yield than other quadrupedal mammals, particularly at the elbow.

4.1.1. Specific aims and predictions

In the current study, I employed morphological, kinematic and kinetic variation in a mixed longitudinal sample of growing Bolivian squirrel monkeys (*Saimiri boliviensis*, Geoffroy and Blainville 1834) as a model system to explore the biomechanical bases for primates' unique mode of limb force distribution. Bolivian squirrel monkeys are small-bodied platyrrhine primates that natively inhabit the upper Amazon basin of Peru, southwest Brazil and Bolivia (Boinski, 1999; Jack, 2007). They frequently feed and travel in the "fine-branch" arboreal environment (Fleagle et al., 1981; Boinski, 1989), making this an excellent species in which to probe the association between limb force distribution, biomechanics and locomotor ecology. To document fully the growing squirrel monkeys' locomotor repertoires, I studied both symmetrical and asymmetrical gaits on terrestrial and simulated arboreal substrates (i.e., an elevated pole).

I used the ontogenetic squirrel monkey data set to evaluate two previously developed models of primate and mammalian limb force distribution: the COM Position model (Gray, 1944; Raichlen et al., 2007) and the Compliant Limb model (Schmitt, 1994, 1998, 1999). In a previous study of this sample (Chapter 2), I found that the relative magnitude of resultant forelimb forces (scaled to body weight) significantly declined as size increased during development, whereas relative hind limb forces tended to increase with size. Therefore, I predicted that growing monkeys should transition from forelimb dominant infants to hind limb dominant juveniles and adults (see Schmidt, 2005 for data on limb force distribution in adult squirrel monkeys). The COM Position and Compliant Limb models each support specific hypotheses of how gait mechanics should change during ontogeny to produce the observed differences in limb force distribution. Note,

however, that the two models are not mutually exclusive: primates could conceivably use a combination of strategies to redistribute forces between the limbs.

The COM Position model argues that limb force distribution is determined by the average position of the whole-body COM relative to the average position of the hands and feet. According to this model, a variety of morphological and kinematic changes could prompt an ontogenetic shift from forelimb dominated to hind limb dominated locomotion, including: a caudal translation of whole-body COM position, an increase in effective hind limb length relative to effective forelimb length, a decrease in forelimb retraction at peak vertical force and on average across a step, an increase hind limb protraction at peak vertical force and on average across a step, or a combination of these strategies.

The Compliant Limb model predicts that reductions in peak loading should be associated with increases in substrate contact durations, limb excursions, and limb yield from touchdown to mid-stance. According to this model, ontogenetic increases in relative hind limb forces should be associated with an increase in compliant forelimb kinematics, a decrease in compliant hind limb kinematics, or a combination of the two strategies.

4.2. Methods

4.2.1 Animal subjects

A total of 100 experiments, consisting of 58 ground experiments and 42 simulated arboreal experiments, were conducted at the Center for Neotropical Primate Research and Resources (CNPRR: Mobile, AL) from August 2006 to March 2007. The CNPRR supports a long-established squirrel monkey breeding colony and staff members have ample experience facilitating external research projects. Veterinary technicians assisted with animal care, management and motivation during experiments. Institutional Animal Care and Use Committees (IACUC) at Stony Brook University and the CNPRR approved all procedures prior to the beginning of this research.

Five female squirrel monkeys comprised the sample for these experiments. Collectively, the monkeys ranged in age from 76-302 days and body mass from 218-535 grams (29-71% of adult body size). An additional individual (Animal 4433) participated in one pole experiment but had to be withdrawn from the study due to an unrelated tail injury. All of the infants were chosen from a cohort that had been initially hand-reared by veterinary staff, following perinatal rejection by their birth mothers. Using hand-reared infants minimized any undue stress that might have been placed upon early mother-infant relationships. Additionally, all nursery-reared individuals were well habituated to veterinary staff, thus facilitating locomotor training. Additional details of sample composition and husbandry are discussed in Section 2.2.1.

Because body mass was linearly related to age in all individuals (see Fig. 2.1), body mass, rather than chronological age, was used as the primary independent variable in all ontogenetic analyses. Moreover, as a result of the precocial nature of squirrel monkey behavioral development (Elias, 1977; Kaack et al., 1979; Boinski and Fragaszy, 1989; Fragaszy et al., 1991; Hartwig, 1995; Chapter 2), size should have a stronger effect on locomotor mechanics than age *per se* (e.g., Schilling, 2005).

Sample information on individual monkeys is provided in Tables 4.1 and 4.2, including the number of forelimb and hind limb steps analyzed at each age and body

mass. Summaries of ground steps are provided in Table 4.1 and summaries of pole steps are provided in Table 4.2.

TABLE 4.1 HERE
TABLE 4.2 HERE

4.2.2. Data collection and processing

Squirrel monkeys were filmed as they traversed a linear runway. Depending on experimental condition (e.g., ground vs. pole), monkeys traversed either the flat runway floor or a 2.5 cm diameter PVC pipe elevated 10.7 cm above the surface of the runway. Both substrates were coated with a mixture of polyurethane and non-skid paint additive (Behr Process Corporation, Santa Ana, CA) in order to increase traction. See Chapter 2 for additional details of runway construction.

I used a Motionmeter 1000 high-speed digital video camera (Redlake MASD Incorporated, San Diego, CA) to film all locomotor sequences. The camera was electronically shuttered at a rate of 1/2500s and operated at 250 Hz. Across the entire sample, the average stride duration was 0.333 seconds (83.3 frames) and average forelimb and hind limb stance phase durations were 0.134 seconds (33.5 frames) and 0.149 seconds (37.24 frames), respectively. Therefore, the filming speed used in data collection should have been sufficient to identify cyclic locomotor data (e.g., touchdown and lift-off events) with minimal aliasing bias (i.e., Polk et al., 2005). Composite video output from the camera was converted to digital video using a Canopus ADVC-55 Analog-Digital converter (Canopus Corporation, San Jose, CA) and stored on an Apple Macintosh Powerbook computer (Apple Incorporated, Cupertino, CA) for later processing.

4.2.2.1. Kinematic data

Prior to the beginning of each experiment, individuals were weighed and the skin over the approximate center of rotation of the shoulder, elbow, wrist, hip, knee and ankle joints was shaved and marked with retro-reflective tape (3M Corporation, St. Paul, MN). Anatomical landmarks used in identifying joint centers of rotation are listed in Table 2.3. Segment lengths were measured with sliding digital calipers as the distance between the centers of the relevant landmarks. Total forelimb and hind limb lengths were computed as the sum of adjacent limb segments. None of the above procedures required the use of anesthesia.

During data collection, individuals were placed in an enclosed box at one end of the runway. A veterinary technician stood at the opposite end of the runway and verbally coaxed the monkey across. After crossing, monkeys were given 60 seconds of rest before the beginning of the next trial. Experiments consisted of 12-30 such trials and lasted for no more than 30 minutes. Once the experiment was over, reflective markers were removed and the monkey was returned to its social group.

Video files from each experiment were imported into the MATLAB DLT Dataviewer 2 digitizing platform (Hedrick, 2007) for coding on a trial-by-trial basis. Using this software, the X (horizontal) and Y (vertical) coordinates of all landmarks were recorded at three events during a single forelimb and hind limb step (i.e., stance phase) within each stride: touchdown (the first frame that a limb made contact with the substrate), mid-stance (frame in which the shoulder/hip marker was most directly above

the wrist/ankle marker) and lift-off (the final frame before the limb left the substrate). This convention for identifying lift-off events will tend to underestimate actual stance phase durations. However, at a filming speed of 250Hz, error magnitudes could never exceed 4 ms, or approximately 3% of average forelimb and hind limb stance phase durations. For steps in which peak vertical forces were available for the limbs facing the camera, joint markers and the position of the fifth metapodial head were digitized in the frame most closely corresponding to the moment of peak vertical force. Due to the small size of the young monkeys, reflective markers could not be attached to the skin overlying the metacarpal and metatarsal heads. Therefore, the position of these landmarks was estimated to be at the base of the fifth manual/pedal ray. Strides were identified based on the cyclic action of a reference limb (e.g., first touchdown to second touchdown of the left hind limb). To calculate average locomotor speed, the coordinates of either the shoulder or the hip marker, depending on marker visibility, were recorded across the entire video clip. The force platforms were used as calibration objects to transform raw pixel coordinates into meters (combined length of force platforms: 0.6096m).

4.2.2.1. Kinetic data

Two force platforms, placed in series, were used to measure peak vertical limb forces. The platforms were located in the center of the runway, allowing monkeys to reach steady speeds of locomotion prior to contact. During the simulated arboreal trials, PVC segments (30.5 cm long and 2.5 cm in diameter) were attached to each force platform via bolts secured directly to the platform frame. The platforms were custom-built for this study, following the designs of Heglund (1981), Biewener and Full (1992), and Riskin et al. (2005). The platforms registered displacement in three orthogonal directions: vertical, fore-aft (cranio-caudal) and mediolateral (transverse). Voltage output from each channel was routed through a National Instruments (Austin, TX) SC-2345 chassis and recorded using a LabView virtual instrument running on a notebook computer. Following the recommendations of Biewener and Full (1992), the platforms were calibrated daily by regressing known weights against measured changes in raw voltage output. Calibration regressions consistently yielded coefficients of determination (i.e., R^2) greater than 0.999, indicating a linear relationship between applied force and voltage output. Cross-talk between force channels was generally low, ranging between 0.3% and 3.5% without the pole segment and 0.3% and 10.5% when the pole segment was attached (see Table 2.4 for detailed information on the average amount of cross-talk between specific channels). Additional details of force platform construction and calibration are discussed in Section 2.2.2.2.

Force data from each trial were imported into MATLAB (Mathworks, Natick, MA) where the raw voltages were transformed into force units and corrected for cross-talk. Force traces from each channel were smoothed using a zero-lag fourth-order Butterworth low pass filter with a cut-off frequency of 25 Hz. Baseline drift during and between trials was corrected by sampling the average values of unloaded periods immediately prior to and following platform contact and subtracting these values from the force traces. Kinetic and kinematic data were synchronized via a 3.3V square-wave pulse, generated by the master-slave port of the Redlake camera, that was routed separately to a bank of LEDs positioned on the back wall of the runway and to the notebook computer via the SC-2345 chassis. This circuit was interrupted by means of a

handheld switch. During each trial, the switch was briefly closed, simultaneously illuminating the LEDs in the video frame and changing the shape of the square wave in the data file. Using this procedure, it was possible to synchronize video and kinetic data to a resolution of four milliseconds.

4.2.3. Outcome variables

4.2.3.1. Speed

I calculated average locomotor speed from the displacement of the hip or shoulder marker (see Section 4.2.2.1 above). I used a zero-lag fourth-order low pass Butterworth filter with a cut-off frequency of 10 Hz to correct marker trajectories for digitizing noise. This cutoff frequency was selected as optimal using a residual analysis procedure described by Winter (1990). The piecewise cubic interpolation function of MATLAB was used to interpolate over gaps of missing data ≤ 10 frames (i.e., 40ms). Corrected displacement data were linearly regressed against time (in milliseconds) to estimate overall horizontal and vertical velocity across each stride. Total speed was calculated as the resultant magnitude of horizontal and vertical velocities. However, because vertical velocity was essentially zero when averaged across an entire stride, resultant velocity is tantamount to horizontal velocity. In order to ensure that only steady-speed locomotion was examined, trials in which the coefficient of determination (i.e., R^2) of reference marker position against time was less than 0.99 were discarded. To control for differences in body mass across the sample, Froude number (Alexander, 1984; Hof, 1996; Polk, 2002; Bullimore and Donelan, 2008) was calculated as:

$$\frac{u}{\sqrt{gh}}$$

where u is velocity, g is gravitational acceleration ($9.81 ms^{-2}$) and h is the cube root of body mass. Note that this quantity is actually the square root of the "original" Froude number (i.e., $u^2(gh)^{-1}$) introduced by Alexander and Jayes (1983). However, both forms of the Froude number are dimensionless ratios and correct for body size effects on locomotor speed.

4.2.3.2. Peak vertical limb forces

Peak vertical forelimb and hind limb forces were defined as the maximum vertical force exerted during periods of single-limb contact. Single-limb force platform contacts began when a limb contacted the force platform in isolation and ended when the limb either left the platform or another limb touched down. Forelimb contacts were usually the first contacts on the force platform, whereas hind limb contacts were usually the last contacts. Because the squirrel monkeys frequently placed limbs in close proximity when walking and running or used short lead times when galloping and bounding, obtaining isolated single-limb contacts was often difficult. Trials with overlapping limb contacts on a single force platform were retained only when peak vertical force was clearly identifiable and the vertical force trace had returned to 50% of the peak value prior to rising again with subsequent limb contacts in the case of forelimb contacts, or began its rise at no more than 50% of the former vertical force peak in the case of hind limb contacts. When multiple single-limb contacts were available across the two force platforms, individual fore- and hind limb peak forces were averaged across the stride. To

adjust for differences in body size across the ontogenetic sample, peak vertical forelimb and hind limb forces were divided by body weight.

Following Demes et al. (1994) and subsequent authors (Schmitt and Lemelin, 2002; Schmitt, 2003a; Schmitt and Hanna, 2004; Schmitt and Lemelin, 2004; Schmidt, 2005; Hanna et al., 2006) the ratio of peak forelimb force to peak hind limb force, or "Vpk ratio", was used as a metric of limb force distribution. Vpk ratios greater than one indicate that forelimb peak forces were greater; values less than one indicate that hind limb peak forces were greater; a Vpk ratio of one indicates that forelimb and hind limb forces were equal. Vpk ratios were calculated in two ways. First, when successive forelimb and hind limb contacts were available, Vpk ratios were computed on a stride-by-stride basis. Second, average experiment-wise Vpk ratios for each monkey at each sampled body mass were computed as the ratio of mean forelimb peak vertical force to mean hind limb peak vertical force for that experiment. If peak vertical forces were significantly correlated with Froude number within a given experiment, least-squares corrected means, evaluated at mean Froude number, were used in lieu of arithmetic means when calculating experiment-wise Vpk ratios.

To estimate the precision (e.g., reliability: Sokal and Rohlf, 1995) of peak force measurements, peak limb forces from 20 randomly selected trials were measured on three separate occasions. As a metric of precision, coefficients of variation (standard deviation as a percentage of the mean) were calculated across the three replications for each trial and compared to the average amount of "intra-experimental" variation within the experiments from which the randomly selected trials were drawn. Coefficients of variation for forelimb peak vertical force ranged from 0.00-3.54% with a mean of 0.36% and a median of 0.02%. Coefficients of variation for peak hind limb vertical force ranged from 0.00-3.53% with a mean of 0.36% and a median of 0.02%. Variance associated with measurement error was minimal compared with the average level of peak force variation within an experiment, where forelimb peak force coefficients of variation ranged from 5.6-36.0%, with a mean of 15.7% and a median of 14.7%, and hind limb coefficients of variation ranged from 1.8-38.6%, with a mean of 15.4% and a median of 12.0%. Measurement error associated with the kinematic variables examined in this study (e.g., joint angles and duty factors) has been previously investigated (Tables 2.7 and 3.3) and found to be sufficiently minimal to maintain adequate precision.

4.2.3.3. Anatomical and effective intermembral indices

To assess the relationship between relative limb length and force distribution, I calculated intermembral indices (IMI: forelimb length as a percentage of hind limb length) in two ways. First, anatomical IMI for each individual at each body mass was calculated from the ratio of anatomically measured forelimb and hind limb lengths. Second, "effective" IMI during a stride was calculated from the ratio of effective forelimb and hind limb lengths at mid-stance. Effective limb length was calculated as the Euclidean distance between the most shoulder/hip and the wrist/ankle. Relative effective limb lengths were calculated by dividing effective limb lengths by the cube root of body mass.

4.2.3.4. Whole-body COM position

A geometric model (Crompton et al., 1996; Raichlen, 2004a) was used to estimate whole-body COM position during locomotion from sagittal-view video clips. Images of the monkeys at the moment of peak forelimb or peak hind limb force, captured from video and rendered as TIFF files, were imported into NIH ImageJ (Rasband, 1997-2007) for measurement. Using ImageJ, I measured the length of the trunk, the tail and each forelimb and hind limb segment facing the video camera, as well as the sagittal diameter of each segment at approximately 25%, 50% and 75% of segment length. Transverse segment diameters (i.e. minor axes) were assumed to be proportional to one-half the sagittal diameter (i.e., major axes). Similar 1:2 ratios of minor to major axis diameters have been observed in other primates (i.e., *Erythrocebus patas* and *Callithrix jacchus*: J.W. Young, unpublished data). Also, the assumed ratio of transverse to sagittal segment diameters heuristically supported, as it was that which provided the best estimate of whole-body mass *via* the geometric model. Raw pixel coordinates were converted into centimeters using the force platforms as calibration objects.

The length and diameters of the forelimb and hind limb facing away from the camera were assumed to match those of the measured limbs. The positions of obscured limb segments were reconstructed in following manner. First, the X- and Y-coordinates at the tip of the 3rd digit on the obscured limb were measured. Then, assuming the proximal joint (i.e., shoulder or hip) of the obscured forelimb or hind limb was positioned identically to that of the visible limb, the angular difference between the two limbs was calculated (i.e., protraction or retraction or the obscured limb relative to the visible limb). Then, the X- and Y-coordinates describing the measured lengths and diameters of the visible limb segments were mathematically rotated to match the overall position of the obscured limb by multiplying the coordinate matrix by the following transformation matrix:

$$\begin{bmatrix} \cos(\alpha) & -\sin(\alpha) \\ \sin(\alpha) & \cos(\alpha) \end{bmatrix}$$

where α equals the angular difference between the visible and obscured limbs. This calculation makes the simplifying assumption that the intralimb angles (i.e., elbow angle or ankle angle) in the obscured limb equaled those of the visible limb.

The trunk, tail and limb segments were modeled as columns with ellipsoidal cross-sections that changed dimensions along the length of the column. Measurements of segment diameters were fit to second-order polynomial equations describing the change in cross-sectional profile along the length of the segment. The coefficients generated from the polynomial equations were then used to estimate segment volumes and centroid locations following formulae provided by Raichlen (2004). Because the density of terrestrial vertebrates is approximately equal to one (Schmidt-Nielsen, 1975), segment volumes and segment masses are equivalent quantities, as are centroid positions and centers of mass. The head was modeled as an ellipsoid with the COM at the midpoint. Head length was measured from inion to prosthion and head height from gonion to bregma. Head width was assumed to be equal to one-half of head length. Whole-body COM position was then calculated as the mean of all segmental COM positions weighted by segment mass.

Whole-body COM was measured in a total of 58 video frames and 26 trials, encompassing the entire range of body mass variation present in the sample. The validity

of the COM measurements was assessed by comparing estimated total body mass to empirically measured body mass. Estimated body and measured body mass were highly correlated (R^2=0.96). The slope of a least-squares regression of actual mass on estimated mass was not significantly different from one and the intercept was not significantly different from zero (Fig. 4.1). The reliability of the whole-body COM estimates was assessed by repeatedly measuring five randomly selected video frames five times each. Coefficients of variations from these replications ranged from 3.5-6.0% for estimated body mass, with a mean of 4.7% and a median of 4.8%, and 4.2-10.2% for whole-body COM position, with a mean of 6.8% and median of 5.4%. Across the ontogenetic sample, CVs for estimated body mass and COM position were 19.7% and 17.5%, respectively, indicating that variation due to measurement error was therefore consistently less than biological variation.

FIGURE 4.1 HERE

4.2.3.5. Joint kinematics

All angular kinematic measurements were limited to the sagittal plane. Forelimb and hind limb angles were calculated as the two-dimensional vector angles between the relevant limb segment and a vertical line through the proximal pivot (i.e., hip/shoulder). Forelimbs and hindlimbs at touchdown (protraction) and lift-off (retraction) were defined by lines joining the shoulder/hip to the wrist/ankle, whereas limbs measured at peak vertical force were defined by a line joining the proximal pivot to the metapodial head. Positive segment angles indicate protraction; negative segment angles indicate retraction. Segmental angular excursion was calculated as the absolute value of the difference between protraction and retraction angles. Average forelimb and hind limb angle, necessary for computing the average position of the hands and feet across a step (see below), was defined as the mean of protraction and retraction angles, following Raichlen et al. (2007). This calculation assumes that limb angular velocity is constant during stance phase.

Joint angles (e.g., elbow or knee angle) were calculated as the two-dimensional vector angles between the relevant limbs segments (e.g., arm and forearm or thigh and leg). Following Larney and Larson (2004), elbow and knee joint yields were calculated as the difference between joint angles at touchdown and at mid-stance. Positive values indicate the joint became more flexed between the two events; negative values indicate the joint became more extended.

Hand and foot position, as a percentage of the horizontal distance from the hip to the shoulder (i.e., "effective trunk length"), was computed trigonometrically from limb angle, limb length, trunk angle and trunk length. Hand and foot positions were calculated at the moment of peak vertical force and on average across the stride (i.e., mean of positions at limb touchdown and lift-off). Values greater than 100% indicate that the segment was in front of the shoulder, whereas negative values indicate that the hand/foot was behind the hip.

4.2.3.6. Gait variables

To distinguish between symmetrical and asymmetrical strides, stride symmetry was calculated as the absolute duration between the touchdowns of the right and left hind limbs expressed as a percentage of total stride duration (Hildebrand, 1966, 1977). Strides

in which symmetry was between 43.75% and 56.25% were designated symmetrical. All other strides were designated asymmetrical.

Contact duration was defined as the amount of time elapsed between limb touchdown and lift-off. Duty factor, or relative contact duration, was defined as the proportion of a stride that each limb was in stance phase (i.e., contact duration/stride duration). Mean forelimb and mean hind limb duty factor were calculated separately for each stride in the dataset. Additionally, a "duty factor ratio" was computed as the ratio of forelimb duty factor to hind limb duty factor.

4.2.4. Statistical analyses

Few of the variables examined here followed a normal distribution across all gaits and substrates. Therefore, most data were transformed prior to analysis. Most variables were Box-Cox transformed (Box and Cox, 1964; Sokal and Rohlf, 1995). The Box-Cox family of power transformations takes the general form

$$Y_T = \frac{(Y^\lambda - 1)}{\lambda}$$

when the parameter λ is not equal to zero and

$$Y_T = \ln Y$$

when λ is equal to zero (where Y is the original data vector and Y_T is the transformed data vector). The value of λ which yields the best transformation to normality is that which maximizes the log-likelihood function

$$L = -\frac{df}{2}\ln s_T^2 + (\lambda - 1)\frac{df}{n}\sum \ln Y$$

where df is the degrees of freedom for the data vector, s^2_T is the variance of the transformed data vector, and n is sample size (Sokal and Rohlf, 1995). The optimal values of λ for all variables in the current dataset were found using an iterative procedure written in MATLAB. In addition to the Box-Cox transformation, both the standard logarithmic and the arcsine transformation (Sokal and Rohlf, 1995) were tested. In order to ensure data were amenable to transformation, I added a constant to all variables including negative numbers or zero as possible values. Constants ranged from 1 to 100, depending on the range of the target variable. The efficacy of each transformation was evaluated by examining normal probability plots (i.e., quantile-quantile plots) of raw and transformed distributions and Durbin-Watson statistics of residuals from linear least-squares regressions of raw and transformed data against Froude number and body mass. The transformation chosen was that which best approximated normality for both the raw data and residual error. In total, 24 of the 33 variables examined in this study were transformed using one of the procedures listed above. Specific transformations for each variable are listed in Table 4.3.

TABLE 4.3 HERE

To increase statistical power, data from individual monkeys were combined to create mixed longitudinal samples for all analyses (Cock, 1966). Regression analyses were used to test for 1) significant speed- and size-related changes in all kinematic and kinetic parameters and 2) association between peak force data and any predictor variables specified by the COM Position and the Compliant Limb models. First, I used linear least-squares regressions to explore bivariate associations between each dependent variable and Froude number and body mass, respectively. Multiple regressions were then

used to investigate the independent influence of body mass and Froude number on each outcome variable, controlling for the effects of the other independent variable. Multiple regressions were also used to test for predicted associations between specific gait parameters and patterns of peak force distribution, controlling for the influence of speed and body mass. All regression analyses were performed using SPSS 11.0 for Macintosh (SPSS Inc, Chicago, IL, USA). Regressions were calculated separately for each gait-by-substrate grouping. Throughout the presentation of the results, I frequently use the following abbreviations when referring to the four gait-by-substrate groups: SG (symmetrical ground strides); SP (symmetrical pole strides); AG (asymmetrical ground strides); AP (asymmetrical pole strides).

4.3. Results

A total of 1,249 strides were analyzed, including 165 symmetrical strides on the ground, 244 symmetrical strides on the pole, 498 asymmetrical strides on the ground, and 342 asymmetrical strides on the pole. Peak force data were available for a subset of 852 strides, including 105 symmetrical strides on the ground (96 forelimb steps and 81 hind limb steps), 185 symmetrical strides on the pole (178 forelimb steps and 158 hind limb steps), 275 asymmetrical strides on the ground (250 forelimb steps and 109 hind limb steps), and 287 asymmetrical strides on the pole (276 forelimb steps and 206 hind limb steps). Across the ontogenetic sample, walks (i.e., mean duty factor greater than 0.5) represented 61.8% of symmetrical gaits on the ground and 38.2% of symmetrical gaits on the pole. Running (i.e., mean duty factor less than or equal to 0.5) represented 29.2% of symmetrical gaits on the ground and 70.8% of symmetrical gaits on the pole. Canters and gallops were the most common asymmetrical gaits used, representing 76.2% of all asymmetrical gaits on the ground and 99.7% of all asymmetrical gaits on the pole. Bounds, half-bounds and crutch-walks were comparatively rare, representing 1.8%, 18% and 4% of all asymmetrical gaits on the ground, respectively. Half-bounds represented 0.3% all asymmetrical gaits on the pole. Bounds and crutch walks were not observed during pole locomotion (also see Figure 3.8).

4.3.1. Speed

Froude number ranged from 0.22-2.15 when squirrel monkeys were using symmetrical strides on the ground, 0.41-2.70 when squirrel monkeys were using symmetrical strides on the pole, 0.48-3.59 when squirrel monkeys were using asymmetrical strides on the ground, and 0.76-3.35 when squirrel monkeys were using asymmetrical strides on the pole. Froude number was significantly associated with body mass in all gait-by-substrate conditions except for symmetrical strides on the ground ($r=0.04$, $p=0.59$). Larger animals moved at significantly slower relative speeds when using symmetrical strides on the pole ($r=-0.31$, $p<0.001$). By contrast, Froude number was weakly, but significantly, positively correlated with body mass when animals were using asymmetrical gaits on both substrates (AG: $r=0.21$, $p<0.001$; AP: $r=0.25$, $p<0.001$). The wide overlap of Froude numbers across symmetrical and asymmetrical gaits seems to be typical of primates, who, unlike other mammals, do not show abrupt gait transitions at set physiological speeds (Heglund et al., 1974).

4.3.2. Limb force distribution

Results from regression analyses of peak force data on Froude number and body mass are presented in Table 4.4, grouped by gait and substrate. Forelimb and hind limb peak vertical forces significantly increased with Froude number across all gaits and substrates. During symmetrical gaits, forelimb peak vertical forces increased with Froude number at a greater rate than hind limb peak vertical forces, regardless of substrate (SG: $F_{[1,174]}$=15.1, p<0.001; SP: $F_{[1,332]}$=67.6, p<0.001). By contrast, during asymmetrical gaits on the ground hind limb peak vertical forces increased at a greater rate, whereas during asymmetrical gaits on the pole forelimb and hind limb peak vertical force increased at a statistically similar rate (AG: $F_{[1,355]}$=14.7, p<0.001; AP: $F_{[1,478]}$=3.0, p=0.084). As a result of these inter-limb differences in speed-force relationships, Vpk ratio, calculated as the quotient of forelimb peak vertical force and hind limb peak vertical force, increased with Froude number during symmetrical gaits, remained static during asymmetrical gaits on the ground, and slightly decreased during asymmetrical gaits on the pole. However, after statistically controlling for the effects of body mass *via* multiple regression, only the speed-related increases in Vpk ratio observed for symmetrical gaits remained statistically significant.

TABLE 4.4 HERE

As documented previously (Chapter 2), forelimb peak vertical forces generally decreased with size, whereas hind limb peak vertical forces increased. Although not all of these trends were significant when peak force data were regressed on body mass alone, multiple regression revealed significant decreases in forelimb peak vertical forces and increases in hind limb peak vertical forces across the entire sample when the effects of Froude number were appropriately controlled (Figs. 4.2 and 4.3). Divergent size-related changes in forelimb and hind limb peak vertical forces resulted in significant declines in Vpk ratio as body mass increased ontogenetically, irrespective of gait or substrate (Fig. 4.4). Increases in peak vertical hind limb forces tended to outpace decreases in peak vertical fore limb forces (note the different slopes in Table 4.4) suggesting that declines in Vpk ratio over development may principally reflect changes in hind limb gait mechanics.

FIGURE 4.2 HERE
FIGURE 4.3 HERE
TABLE 4.4 HERE

Size-related changes in limb force distribution are even more evident when average experiment-wise Vpk ratios are regressed against body mass (Table 4.5; Fig. 4.4). These regressions indicate that, in general, squirrel monkeys tended to transition to hind limb dominance at smaller sizes when using symmetrical gaits, regardless of substrate. Within each gait, transitions to hind limb dominance occurred at smaller body sizes during ground locomotion, although this difference was only significant for symmetrical gaits. Gait and substrate exerted similar influences on the timing of the transition to hind limb dominance, whether body size at the transition point was evaluated as the smallest body mass at which average Vpk ratios were less than 1.0 or on the basis of predictive regression equations (Table 4.5).

TABLE 4.5 HERE
FIGURE 4.4 HERE

4.3.3. Testing the COM Position model

According to the COM Position model, the horizontal distances between the whole-body COM and hands and feet determine the distribution of vertical impulse and peak vertical forces between the limbs. The relative position of the hands and feet could, in turn, be influenced by limb geometry (i.e., anatomical and effective limb lengths) and limb angular kinematics, both at the moment of peak vertical force and on average across a step. Below I present data on 1) size-related changes in each of these parameters during ontogeny and 2) associations between each parameter and peak limb force distribution during growth. For the sake of completeness, I present the results of both simple bivariate regressions of each parameter on speed and body mass independently and multiple regressions on the linear combination of Froude number and body mass. However, when discussing size-related changes in gait parameters and specific associations between the parameters and limb force distribution, I limit my discussion to the results obtained from multiple regression.

4.3.3.1. Whole-body COM Position

Whole-body COM position moved caudally as size increased during growth, shifting from approximately 40% of trunk length (from the shoulders to the hips) at the smallest body size to approximately 60% of trunk length at the largest body size (Fig. 4.6). The caudal translation of whole-body COM position resulted from ontogenetic decreases in relative head and forelimb mass (Figs. 4.7A and 4.7D) and simultaneous increases in relative hind limb mass (Figs. 4.7E). Over development, the head decreased from about 30% of total body mass to about 18% and the forelimb from about 6% of total body mass to about 2%. By contrast, the hind limb increased from about 5% of total body mass to about 12%. Relative trunk mass tended to increase during growth, although this trend was not statistically significant (Fig. 4.7B). Relative tail mass did not significantly change during growth (Fig. 4.7C).

FIGURE 4.6 HERE

FIGURE 4.7 HERE

An inadequately sized sample of whole-body COM measurements prevented testing the relationship between COM position and Vpk ratios within each gait-by-substrate category. Therefore, because Vpk ratios showed similar declines with increasing body mass across gaits and substrates (Table 4.4), average experiment-wise Vpk ratios were pooled across conditions and regressed against estimates of whole-body COM position for each available body mass. As predicted in the COM Position model, average Vpk ratios significantly declined as the whole-body COM moved caudally with increasing body mass (Fig. 4.8). Overall, whole-body COM position explained 57% of the variance in average Vpk ratios over development.

FIGURE 4.8 HERE

4.3.3.2. Anatomical IMI

As reviewed previously (Section 2.3.1) all forelimb and hind limb segments (i.e., arm, forearm, thigh and leg) grew with strong positive allometry across the ontogenetic squirrel monkey sample. Forelimb segments, particularly the forearm, grew with stronger positive allometry than hind limb segments, resulting in a weak, but significant, positive correlation between anatomical IMI and body mass ($r=0.25$, $p=0.014$; Fig. 2.5).

Across the ontogenetic sample, IMIs were consistently less than 100, indicating hind limb length always exceeded forelimb length. Among monkeys older than eight months of age, the age at which juvenile squirrel monkeys in the wild become fully independent (Boinski, 1989; Boinski and Fragaszy, 1989), the mean IMI was 79.9. This value closely matches values previously reported for adult squirrel monkeys (79.1: Jungers, 1985; 79: Napier and Napier, 1985; 80: Fleagle, 1999).

4.3.3.3. Effective IMI

Results from regression analyses of relative effective limb lengths at mid-stance and effective IMIs against Froude number and body mass are presented in Table 4.6. Relative effective forelimb length significantly increased with body mass in most gait-by-substrate conditions, particularly during ground locomotion. Only during asymmetrical gaits on the pole did relative effective forelimb length remain ontogenetically static. By contrast, relative effective hind limb length substantially increased only during asymmetrical gaits on ground, marginally increased during symmetrical gaits on the ground, and remained static during all pole locomotion. As a result of the divergent intermembral differences in relative effective limb length across conditions, effective IMI increased marginally with body mass during symmetrical gaits on the ground, substantially decreased with mass during asymmetrical gaits on the ground, and remained static during locomotion on the pole.

TABLE 4.6 HERE

In sum, allometric changes in joint postures attenuated ontogenetic increases in anatomical IMI, resulting in variable patterns of effective forelimb and hind limb "growth" across gaits and substrates. Nevertheless, after controlling for the influence of body mass and speed *via* multiple regression, effective IMI was found to be unassociated with Vpk ratios during symmetrical gaits and negatively correlated with Vpk ratios during asymmetrical gaits (Table 4.7 and Fig. 4.9). Both of these patterns contradict the predictions of the COM Position model that force distribution changes with interlimb length proportions.

TABLE 4.7 HERE

FIGURE 4.9 HERE

4.3.3.4. Forelimb and hind limb kinematics

Results from regression analyses of forelimb angular kinematics on Froude number and body mass are presented in Table 4.8. As size increased during growth, squirrel monkeys tended to increase forelimb protraction at touchdown across all conditions except asymmetrical strides on the ground, and forelimb retraction at liftoff across all conditions except symmetrical strides on the ground. Because increases in protraction and retraction angles were generally of similar magnitude, average forelimb angles (i.e., the average of protraction and retraction angles) remained static as size increased in most conditions, as did forelimb angles at peak vertical force. During symmetrical strides on the ground, average forelimb angle and forelimb angle at peak vertical force showed slight size-related increases, with average forelimb angles transitioning from retracted to more neutral positions and forelimb angles at peak vertical force from neutral to more protracted positions.

TABLE 4.8 HERE

Results from regression analyses of hind limb angular kinematics on Froude number and body mass are presented in Table 4.9. Older, larger monkeys used significantly more protracted hind limb postures at touchdown during all gait-by-substrate conditions except for asymmetrical gaits on the ground, where hind limb protraction angle showed a non-significant decrease with increasing body size. Hind limb retraction at lift-off did not change with body size during ground locomotion, but significantly increased with body size when monkeys were traveling on the pole, regardless of gait type. Average hind limb angle increased with body size when monkeys were using symmetrical strides on either substrate, transitioning from a retracted to a more neutral position as size increased. By contrast, average hind limb angles remained ontogenetically static during asymmetrical strides on both substrates. Hind limb angle at peak vertical force tended to increase across all gaits and substrates, transitioning from retracted positions among the smallest monkeys to more protracted positions as monkeys grew. However, these trends were only significant during symmetrical strides on the ground and asymmetrical strides on the pole.

TABLE 4.9 HERE

4.3.3.5. Hand and foot position

Results from regression analyses of hand and foot position (relative to trunk length) on Froude number and body mass are presented in Table 4.10. Ontogenetic changes in hand and foot position generally paralleled trends in forelimb and hind limb angular kinematics. Across all body sizes, gaits and substrates, the forelimbs tended to be in a slightly protracted position at peak vertical force. Thus, hand position at peak vertical force, as a percentage of trunk length from the hips to the shoulders, was always slightly greater than 100%, indicating that the hand was in front of the shoulder (Mean hand position - SG: 107.7±1.87%; SP: 102.7±1.31%; AG: 104.1±1.01%; AP: 102.8±0.86%). There was a significant size-related increase during symmetrical gaits on the ground, with hands of larger monkeys in more craniad positions. Hand position at peak vertical force did not change with size in any other gait-by-substrate condition. On average across a step, monkeys tended to place their forelimbs in retracted positions with the hands significantly behind the shoulders (SG: 88.8±0.54%; SP: 91.9±0.48%; AG: 84.9±0.78%; AP: 91.5±0.92%). There were significant, but divergent, size-related trends when monkeys were traveling on the ground, with larger monkeys placing their hands in more craniad positions during symmetrical gaits and more caudad positions during asymmetrical gaits.

INSERT TABLE 4.10

At peak vertical hind limb force, the feet were slightly in front of the hips during symmetrical gaits and in a more neutral position, directly beneath the hips, during asymmetrical gaits, regardless of substrate (SG: 7.1±4.76%; SP: 13.0±2.77%; AG: 3.4±0.78%; AP: 3.4±4.31%). As observed with the hind limb angular data, foot position at peak vertical force tended to increase (i.e., move cranially) as size increased ontogenetically. This trend, however, was only significant during asymmetrical gaits on the pole. On average across a step, monkeys tended to have hind limbs in retracted positions, with the feet significantly behind the hips (SG: -10.7±0.85%; SP: -9.1±0.74%; AG: -9.3±0.64%; AP: -11.5±0.83%). Average foot position moved significantly craniad with ontogenetic increases in body size when monkeys were using symmetrical gaits on

the ground, whereas average foot positions did not change with body size during symmetrical gaits on the pole. By contrast, average foot positions during asymmetrical gaits became more caudad as size increased, although the trend was only significant when monkeys were traveling on the ground.

Results from multiple regressions of peak vertical limb forces against relative hand and foot positions at peak vertical force and on average across a step are presented in Table 4.11, grouped by gait and substrate. In direct contradiction to the predictions of the COM Position model, hand position and peak vertical forelimb forces were significantly positively correlated when monkeys were using asymmetrical gaits, indicating that forces increased as the hand was moved farther away from the COM (Fig. 4.10). Hand position at peak vertical force was unassociated with peak vertical forelimb forces during symmetrical gaits. In accordance with the predictions of the COM Position model, average hand position was negatively associated with peak vertical forelimb force across gaits and substrates. However, this trend was only significant for asymmetrical strides on the ground (Fig. 4.11). As predicted in the COM Position model, across all gaits and substrates foot position at peak vertical force was significantly positively correlated with hind limb peak vertical force magnitudes, indicating that hind limb forces increased as squirrel monkeys placed their feet closer to the COM (Fig. 4.12). Average foot position across a step also tended to be positively associated with peak vertical hind limb forces, although this trend was only significant during asymmetrical gaits on the pole (Fig. 4.13).

TABLE 4.11 HERE
FIGURE 4.10 HERE
FIGURE 4.11 HERE
FIGURE 4.12 HERE
FIGURE 4.13 HERE

4.3.4. Testing the Compliant Limb model

The Compliant Limb model predicts that greater use of compliant limb kinematics, marked by longer duty factors, greater angular excursion and increased mid-joint yield, has the potential to mitigate peak vertical forces and alter force distribution between the limbs. To evaluate these predictions, I present data below on 1) size-related changes in each of these compliant gait parameters during ontogeny and 2) associations between each parameter and peak limb forces during growth.

4.3.4.1. Duty factor

Results from regression analyses of forelimb duty factor, hind limb duty factor and duty factor ratio on Froude number and body mass are presented in Table 4.12. As documented in previous studies of primate locomotion (e.g., Vilensky and Patrick, 1985; Polk, 2001; Young et al., 2007), forelimb and hind limb duty factors were highly negatively correlated with locomotor speed. After appropriately controlling for the effects of speed, forelimb duty factor was found to decrease with increasing size across all gaits and substrates. By contrast, hind limb duty factor increased with size during locomotion on the pole and remained static during locomotion on the ground. As a result of these divergent ontogenetic trajectories in forelimb and hind limb duty factors,

forelimb over hind limb duty factor ratios significantly declined with body size across all gaits and substrates with the exception of asymmetrical gaits on the pole.

TABLE 4.12 HERE

Results from multiple regression analyses of peak vertical limb forces regressed against the linear combination of Froude number, body mass and the relevant duty factor are presented in Table 4.13. Results from multiple regression analyses of Vpk ratios regressed against Froude number, body mass and duty factor ratio are presented in Table 4.14. According to the Compliant Limb Model, peak limb forces should be inversely proportional to duty factor and, therefore, Vpk ratios should be also be inversely proportional to duty factor ratios (i.e., greater duty factor ratios indicate relatively longer forelimb duty factors and, theoretically, lower peak forelimb forces). After holding Froude number and body mass constant, peak vertical forelimb force was found to be negatively associated with forelimb duty factor in all conditions except for symmetrical gaits on the ground, where there was a non-significant positive association between forelimb force and duty factor (Fig. 4.14). Similarly, across all conditions, hind limb peak forces tended to decrease with increasing duty factor, although this trend was only significant for locomotion on the pole (Fig. 4.15). In sum, forelimb and hind limb duty factors exhibited the predicted relationships with peak vertical limb forces. Nevertheless, Vpk ratios were independent of duty factor ratios in three of the four gait-by-substrate conditions. Moreover, though duty factor ratios were significantly associated with Vpk ratios during symmetrical gaits on the ground, the association was positive, a direct contradiction to one of the predictions of the Compliant Limb model (Fig. 4.16).

TABLE 4.13 HERE

TABLE 4.14 HERE

FIGURE 4.14 HERE

FIGURE 4.15 HERE

FIGURE 4.16 HERE

4.3.4.2. Limb angular excursion

Results from regression analyses of forelimb and hind limb angular excursions on Froude number and body mass are presented in Table 4.15. As reviewed in Section 4.3.3.4, forelimb protraction angles increased with body mass in all conditions except for asymmetrical strides on the ground and forelimb retraction angles increased with body mass during all conditions except for symmetrical strides on the ground. Similarly, hind limb protraction angles increased with body size during all conditions except for asymmetrical strides on the ground and hind limb retraction angles increased during all locomotion on the pole. As a result, total forelimb angular excursion increased with body size across all gaits and substrates, although the increase was not significant for symmetrical strides on the ground. Total hind limb angular excursion increased with body size during symmetrical strides on the ground and during all locomotion on the pole. During asymmetrical strides on the ground, decreases in protraction angles at touchdown and retraction angles at lift-off resulted in significant size-related declines in hind limb angular excursion.

TABLE 4.15 HERE

Results from multiple regression analyses of peak vertical forelimb and hind limb forces on the linear combination of Froude number, body mass and the angular excursion

of the relevant limb are shown in Table 4.16, grouped by gait and substrate. On the Compliant Limb model, increased limb angular excursion should be associated with lower peak vertical forces. However, after controlling for the influence of Froude number and body mass, neither forelimb nor hind limb angular excursion were found to be significantly associated with peak vertical force magnitudes in any of the four gait-by-substrate conditions (Figs. 4.17 and 4.18).

TABLE 4.16 HERE
FIGURE 4.17 HERE
FIGURE 4.18 HERE

4.3.4.3. Elbow and knee kinematics

Results from regression analyses of elbow angular kinematics on Froude number and body mass are presented in Table 4.17. Elbow angles at touchdown remained static during symmetrical gaits, marginally increased with body mass during asymmetrical gaits on the pole, and substantially decreased with body mass during asymmetrical gaits on the pole. Elbow flexion at mid-stance remained static during ground locomotion, but significantly increased with size during locomotion on the pole, perhaps as a mean of increasing stability among larger animals (Napier, 1967; Schmitt, 2003c; Stevens, 2003). As a result of these ontogenetic size-related changes in elbow posture, elbow yield from touchdown to liftoff significantly increased with body mass in all conditions except for symmetrical strides on the ground.

TABLE 4.17 HERE

Results from regression analyses of knee angular kinematics on Froude number and body mass are presented in Table 4.18. Knee angle at touchdown tended to increase with body size across gaits and substrates, although this trend was only significant during asymmetrical strides. By contrast, knee angle at mid-stance significantly decreased with body size during symmetrical gaits on either substrate and during asymmetrical strides on the pole, but significantly increased with body size during asymmetrical strides on the ground. Significant increases in mid-stance knee flexion resulted in greater knee yield as body size increased for all conditions except asymmetrical strides on the ground, where knee yield was independent of body size.

TABLE 4.18 HERE

Results from multiple regressions of forelimb/hind limb peak vertical forces on Froude number, body mass, and the relevant joint yield are presented in Table 4.19, grouped by gait and substrate. According to the Compliant Limb model, increases in yield should be concomitant with lower peak vertical limb forces. However, once the effects of speed and body mass were controlled, elbow yield was found to have no independent association with peak vertical forelimb forces in the ontogenetic squirrel monkey sample (Fig. 4.19). Similarly, knee yield was unassociated with peak vertical hind limb forces in all conditions except for asymmetrical strides on the ground, where peak vertical force and knee yield were positively correlated, in direct contradiction to the predictions of the Compliant Limb model (Fig 4.20).

TABLE 4.19 HERE
TABLE 4.20 HERE

4.4. Discussion

Bolivian squirrel monkeys exhibit significant ontogenetic variation in limb force distribution, transitioning from forelimb dominant infants to hind limb dominant juveniles and adults (i.e., Schmidt, 2005) over the first 10 months of life. Across gaits and substrates, ontogenetic changes in limb force distribution resulted from decreases in forelimb peak vertical forces and simultaneous increases in hind limb peak vertical forces. Although the current study is the first to examine the ontogeny of limb force distribution in a detailed biomechanical context, previous work by Kimura (1987; 2000) and Biknevicius et al. (1997) corroborates some of the findings presented here. Kimura (1987; 2000) examined the ontogeny of vertical force distribution in chimpanzees and Japanese macaques. The typical primate pattern of hind limb dominance during locomotion was evident in chimpanzees throughout development and in macaques from three months of age onwards. Prior to this age, infant macaques distributed vertical peak forces equally between the forelimbs and hind limbs. Interestingly, during the first year of life, standing chimpanzees supported more body weight on their forelimbs than their hind limbs. Kimura (1987) argued that the ontogenetic change in static body weight support resulted from decreasing relative head mass in the growing chimpanzees and the corresponding caudal shift in whole-body COM position. The finding that infant chimpanzees are forelimb dominant when standing but hind limb dominant when walking implies that chimpanzees must use a dynamic mechanism to redistribute forces between then hands and feet during locomotion. Recent work by Raichlen et al. (2007) supports this view – on average across a step, adult chimpanzees position their hind limbs in significantly protracted postures, thus kinematically redistributing body weight away from the forelimbs towards the hind limbs. Previous research has also shown that ontogenetic changes in limb force distribution are not limited to primates. In a longitudinal study of growing domestic dogs, Biknevicius et al. (1997) found that relative forelimb peak vertical forces remained static across growth whereas relative hind limb peak vertical forces significantly increased with body mass, a difference the authors attributed to developmental changes in body composition.

4.4.1. Are ontogenetic changes in limb force distribution determined by COM Position?

The COM Position model predicts that limb force distribution varies as a function of the horizontal distance between the COM vector (i.e., the center of gravity) and the center of pressure of the hands and feet (Gray, 1944; Rollinson and Martin, 1981; Lemelin and Schmitt, 2004; Raichlen et al., 2007). According to this model, any shift in morphology or kinematics that decreases the average distance between the feet and COM or increases in the average distance between the hands and the COM has the potential to redistribute body weight and peak forces from the forelimbs to the hind limbs.

In support of the COM Model, increasing hind limb dominance over squirrel monkey development was concomitant with a caudal translation of the whole-body COM, which moved from 40% of horizontal trunk length from the shoulders to the hip among the youngest and smallest monkeys to 60% of horizontal trunk length among the oldest and largest monkeys. This shift in COM position resulted from significant decreases in relative head and forelimb mass and significant increases in relative hind limb mass. Previous studies have documented similar caudal shifts in whole-body COM position and changes in relative segment masses in growing rhesus macaques (Grand,

1977, 1983; Turnquist and Wells, 1994) and yellow baboons (Raichlen, 2004b; Shapiro and Raichlen, 2007a). Overall, the caudal translation of the whole-body COM explained nearly 60% of the variation in average experiment-wise Vpk ratios in the ontogenetic squirrel monkey sample.

According to the COM Position model, Vpk ratios vary directly with effective IMI, such that proportional decreases in effective forelimb length should reduce peak vertical forelimb forces (Stern, 1975). Clearly, most ontogenetic changes in IMI among the squirrel monkeys examined here belie this prediction: anatomical IMI increased during development whereas effective IMI did not change during locomotion on the pole and increased during symmetrical gaits on the ground. As predicted in the COM Position model, effective IMI significantly declined with increasing body size when monkeys were using asymmetrical strides on the ground, a pattern that likely resulted from significant increases in mid-stance elbow flexion and knee extension as animals grew. However, multiple regressions controlling for the influence of speed and body mass showed that effective IMI was unrelated to Vpk ratio during symmetrical gaits and *inversely* proportional to Vpk ratio during asymmetrical gaits, a direct contradiction of one of the predictions of the COM position model.

If limb force distribution is determined by relative COM position, decreases in peak vertical forelimb forces and increases in peak vertical hind limb forces should be associated with greater cranial displacement of both hand and foot positions, increasing the distance between the hands and COM and decreasing the distance between the feet and COM. In support of the COM Position model, during symmetrical gaits on the ground, average hand position, hand position at peak vertical forelimb force and average foot position significantly increased (i.e., became more cranially displaced) as body size increased. Similarly, foot position at peak vertical hind limb force tended to increase with mass across conditions, although the trend was only significant for asymmetrical gaits on the pole. Interestingly, during asymmetrical gaits, average foot position and foot position at peak vertical force became increasingly caudad with increasing body mass, in contradiction to the predictions COM Position model – although the trend was only significant for ground locomotion. The caudal average position of the hands and feet during asymmetrical gaits may account for the comparatively shallow declines in Vpk ratio with increasing body mass and the relatively late transitions to hind limb dominance (i.e., average Vpk ratio < 1) when compared to symmetrical gaits (Tables 4.4 and 4.5 and Figs. 4.4 and 4.5).

Partial regressions of peak limb forces on hand and foot positions, controlling for the influence of Froude number and body mass, also provided support for the COM Position model in some, though not all, cases. Forelimb force magnitudes tended to increase with more cranial hand positions at peak vertical force, in opposition to the predictions of the COM Position model, although the trend was only significant during locomotion on the pole. In support of the model, increasing force magnitudes were associated with relatively caudal average hand positions and relatively cranial average foot positions, although these trends were significant in only a few cases. Finally, across all gaits and substrates, hind limb force magnitudes significantly increased with more cranial positions of the foot at peak vertical force, as predicted by the COM model.

4.4.2. Are ontogenetic changes in limb force distribution determined by limb compliance?

According to the Compliant Limb Model (Schmitt, 1994, 1998, 1999; Schmitt and Hanna, 2004), an ontogenetic transition to greater hind limb dominance in limb force distribution should result from increased forelimb compliance, decreased hind limb compliance, or a combination of these strategies. Following Schmitt and colleagues, I evaluated forelimb and hind limb compliance on the basis of three parameters: duty factor, limb angular excursion and mid-joint yield.

In direct contradiction to the predictions of the Compliant Limb model, once the effects of speed were held constant *via* multiple regression, forelimb duty factors were found to decrease with increasing body mass, whereas hind limb duty factors were found to increase in all conditions except asymmetrical gaits on the ground. As a result, the duty factor ratio significantly declined across all conditions except asymmetrical gaits on the ground. Partial regressions controlling for speed and body mass demonstrated that peak vertical forelimb and hind limb forces were negatively associated with duty factors across limbs in most of the gait-by-substrate conditions, as expected in the Compliant Limb model. However, a negative correlation between peak force and duty factor is not a unique prediction of the Compliant Limb model. Over a stride, similar-sized animals moving at similar speeds must produce identical vertical impulses in order to support body weight (Cavagna et al., 1977; Bertram et al., 1997). Because impulse is equal to the area under the force-time curve, shorter stance durations (i.e., duty factors) necessarily require higher peak forces in order to maintain impulse. Also, if the ontogenetic transition to hind limb dominated force distribution resulted from relative shifts in forelimb and hind limb duty factors in the manner predicted by the Compliant Limb model, Vpk ratios should be negatively associated with duty factor ratios. However, once the effects of speed and mass had been held constant, duty factor ratios were found to be unassociated with Vpk ratios during symmetrical gaits on both substrates and asymmetrical gaits on the pole, and *positively* associated with Vpk ratios during asymmetrical gaits on the ground.

Ontogenetic changes in limb angular excursions and mid-joint yield also failed to provide consistent support for the Compliant Limb model. Forelimb and hind limb angular excursion and elbow and knee yield significantly increased with body mass in most of the gait-by-substrate conditions examined, indicating that growing squirrel monkeys were increasing compliance across all limbs. If growing squirrel monkeys were specifically adjusting limb compliance to reduce forelimb loading at larger body sizes, one would instead expect measures of forelimb compliance to increase with size and measures of hind limb compliance to remain static, or even decrease. Reduced limb excursions and extended joint postures among younger and smaller monkeys more likely served to mitigate external joint moments and to increase muscle mechanical advantage, thus facilitating locomotor performance early in life when the musculoskeletal system is underdeveloped and predation risk is relatively high (see Chapter 2). Finally, partial regressions controlling for speed and body mass failed to demonstrate a predictive relationship between peak vertical limb forces and either limb excursions or mid-joint yields in almost every gait-by-substrate condition examined. Only during asymmetrical gaits on the ground was a compliance measure, knee yield, significantly associated with peak vertical force. However, the association was between knee yield and peak vertical hind limb force was positive – a direct contradiction of the Compliant Limb model.

4.4.3. Summary and conclusions

This study used longitudinal data on somatic growth and locomotor development in Bolivian squirrel monkeys as a model system to address the biomechanical bases of "hind limb dominance" in primate limb force distribution. Two previously developed models of primate locomotor kinetics were evaluated: the COM Position model (Gray, 1944; Rollinson and Martin, 1981; Lemelin and Schmitt, 2004; Raichlen et al., 2007) and the Compliant Limb model (Schmitt, 1994; 1998; 1999; Schmitt and Hanna, 2004). The data presented here provide greater support for the COM position model of limb force distribution. Ontogenetic decreases in peak forelimb forces and increases in peak hind limb forces were concomitant with a caudal translation in the whole-body COM and, in general, cranial shifts in average hand positions, average foot positions, and foot positions at peak vertical force. In contrast, very little support was found for the Compliant Limb model of limb force distribution. Larger monkeys tended to use more compliant gait kinematics across all limbs, not just in the forelimbs as would have been predicted by the model. Moreover, many common measures of limb compliance were unassociated with peak force magnitudes once the influence of speed and body mass had been statistically controlled.

It should be stressed that my results are strictly valid only in the context of ontogenetic changes in squirrel monkey limb force distribution. I was able to show that relatively simple parameters, such as the whole-body COM position and hand and foot placement, could explain a significant proportion of the variation in limb force distribution in growing monkeys. Nevertheless, this study is not a demonstrative proof that the COM Position model explains force distribution across primates and other mammals. In support of the general explanatory power of the COM Position model, Raichlen et al. (2007) have recently presented convincing evidence that 1) relative COM position explains weight distribution in walking chimpanzees and that 2) primates, as an order, typically adopt more protracted hind limb postures and more retracted fore limb postures than other mammalian quadrupeds. Additional data, however, on COM positions and patterns of hand and foot placement in an expanded primate and non-primate mammalian sample are needed to further corroborate the COM Position model.

It should also be emphasized that this study is also not necessarily a refutation of the Compliant Limb model. In a series of publications, Schmitt (1994, 1998, 1999) has amply demonstrated that many primates adopt compliant forelimb kinematics as a means of mitigating forelimb joint moments and simultaneously maintaining stability when walking arboreally. However, despite the potential of the Compliant Limb model to address important biomechanical adaptations to locomotion on narrow arboreal substrates, data on COM movements and limb excursions in primates and other mammals challenge the argument that limb compliance is necessarily a primate "adaptation" to mitigate limb loading or maintain stability.

The hallmark and presumptive benefit of compliant gait kinematics is a reduction in the vertical excursion of the COM. A flat COM should allow an arboreal animal to reduce branch sway and maintain greater stability (Demes et al., 1990). There is, however, a cost associated with maintaining a flat COM. Across a broad multitude of animals, the efficient exchange of forward kinetic and gravitational potential energy during walking (i.e., inverted pendular mechanics) has been shown to be the primary means of reducing external work and possibly minimizing the metabolic cost of transport

(Cavagna et al., 1977; Heglund et al., 1982; Full, 1989; Farley and Ko, 1997; Griffin and Kram, 2000; Reilly and Biknevicius, 2003; Griffin et al., 2004). The efficiency with which kinetic and potential energy are exchanged during a stride is usually evaluated as "percent recovery", with 100% recovery indicating a complete (i.e., perfectly efficient) transfer of energy and 0% indicating that no energy was exchanged (Cavagna et al., 1976; Heglund et al., 1982).

If primates indeed maintain a flatter COM than other quadrupedal mammals, one would expect fluctuations in forward kinetic energy among walking primates to be much greater than fluctuations in gravitational potential energy, limiting the possibility for energy exchange and thus reducing percent recovery. Nevertheless, recent research has shown that percent recovery among quadrupedal primates differs little from values reported for other mammalian quadrupeds (Schmitt et al., 2007; Schmitt et al., 2008; J. W. Young, unpublished data). Rather, it is likely that greater limb yield in primates, which dampen vertical oscillations of the COM, is balanced by increased limb angular excursions, which augment vertical oscillations of the COM. The net result is that over a stride, vertical COM excursions should be comparable between primates and other similar sized quadrupedal mammals. This leads to an interesting prediction: if quadrupedal mammals strive to maintain similar relative vertical COM excursions, limb yield over a step should vary as a direct function of limb excursion across all mammals. Figure 4.21 is a schematic illustration of this model, showing two idealized forelimbs of equal length, one with limited angular excursion (45º: Figure 4.21A) and one with more pronounced angular excursion (60º: Figure 4.21B). For the purposes of this model, I have made the simplifying assumptions that shoulder height at lift-off equals shoulder height at touchdown, limb excursion is symmetrical about mid-stance (i.e., protraction angles equal retraction angles) and the arm and forearm are equal in length (i.e., the elbow joint is located in the center of the combined limb). In order for shoulder height at mid-stance to shoulder height at touchdown, the limb with reduced excursion would have to flex the elbow joint to 135º at mid-stance. By contrast, the limb showing a more exaggerated amount of excursion would have to flex the elbow joint to 108º - a difference in limb yield of 27º. A similar mechanical relationship would apply to hind limb excursion and knee yield. Data from this study and previous studies corroborate the hypothesis that mid-joint yield varies as a direct function of limb angular excursion. Across gaits and substrates within the ontogenetic squirrel monkey sample, stride-to-stride variation in elbow and knee yield was significantly positively associated with forelimb and hind limb angular excursion, even after controlling for the influence of speed and body mass on joint kinematics via multiple regression (Figs. 4.22 and 4.23). Moreover, research by Larson and colleagues (Larson et al., 2000; Larson et al., 2001; Larney and Larson, 2004) suggests that fore limb and hind limb angular excursions predict mid-joint yield across several mammalian groups, including primates, marsupials, carnivores, rodents and artiodactyls (Fig 4.24). In sum, augmented levels of knee and elbow yield among primates may be a by-product of increased levels of forelimb and hind limb angular excursion, rather than an independent locomotor adaptation.

FIGURE 4.22 HERE

FIGURE 4.23 HERE

FIGURE 4.24 HERE

Future research should examine the ontogeny of locomotor kinetics in other primates and non-primate quadrupeds. Previous research with macaques, chimpanzees and dogs suggests that ontogenetic changes in limb force distribution may be common among mammals (Kimura, 1987; Biknevicius et al., 1997; Kimura, 2000), highlighting the potential for additional studies of locomotor development to provide insight into the biomechanical bases of limb force distribution. Finally, it is critical that future studies of primate locomotion move away from characterizing single limb forces at single points in time. Holistic descriptions of impulse development across all four limbs over entire strides (e.g., Bertram et al., 1997) will be crucial to understanding how primates and other mammals dynamically adjust limb forces to cope with locomotor demands.

4.5. Tables

Table 4.1. Total number of ground steps sampled at each age (in days) and body mass (in grams) for each subject.

ID	Age	Mass	FL steps	HL steps	ID	Age	Mass	FL steps	HL steps
4428	120	379	3	2	4475	93	219	2	2
	127	384	3	4		99	221	5	0
	131	410	2	2		104	218	12	0
	175	445	1	0		112	243	2	1
	189	458	7	6		132	262	10	1
	204	488	7	5		147	286	12	1
	216	495	10	4		162	305	12	2
	244	510	4	5		181	337	4	0
	260	532	4	3		190	346	13	7
	272	518	9	7		220	353	7	1
	288	533	3	3		230	386	7	5
	302	535	1	2		247	396	5	2
						261	378	10	0
4445	118	321	5	7		272	430	7	0
	128	341	1	1					
	167	372	2	1	4483	76	232	6	0
	180	385	1	1		87	240	3	0
	195	402	1	1		96	275	6	3
	237	409	2	3		116	293	11	5
	251	415	8	7		130	316	1	1
	268	462	3	2		145	354	6	4
	282	442	4	6		164	370	12	2
						173	386	11	2
4466	118	345	3	4		199	361	5	4
	140	373	7	6		215	404	7	4
	157	399	8	6		229	409	11	10
	181	447	6	4		248	430	6	3
	195	450	5	3		259	442	6	6
	225	427	4	3					
	239	400	6	6		**Total steps:**		**346**	**190**
	258	461	9	5					
	269	451	8	6					
	280	483	10	9					

FL steps: number of forelimb steps; HL steps: number of hind limb steps.

Table 4.2. Total number of pole steps sampled at each age (in days) and body mass (in grams) for each subject.

ID	Age	Mass	FL steps	HL steps	ID	Age	Mass	FL steps	HL steps
4428	153	413	14	16	4475	198	355	16	15
	167	438	18	18		237	400	17	17
	209	499	15	13		253	400	14	15
	224	491	7	3		267	424	14	13
	251	511	6	3					
	263	520	9	3	4483	112	305	22	19
	281	525	4	3		123	312	21	18
	293	522	7	6		138	332	9	5
						158	367	15	5
4433	150	375	14	13		180	390	15	6
						208	387	4	3
4445	145	320	3	2		223	403	11	11
	160	351	4	4		241	394	6	2
	177	380	3	2		252	438	7	4
	202	407	8	4					
	214	412	2	3		**Total steps:**		**454**	**364**
	244	408	1	1					
	262	436	7	4					
	275	445	7	5					
4466	133	380	13	16					
	148	383	11	11					
	168	410	11	8					
	206	447	12	4					
	232	423	8	5					
	252	446	7	1					
	262	453	5	2					
	276	474	5	3					
4475	128	268	22	22					
	143	276	27	26					
	155	295	22	21					
	175	334	11	9					

Presentation of data follows Table 4.1.

Table 4.3. Procedures used to transform sample data.

Variable	Procedure	Constant	λ	Variable	Procedure	Constant	λ
Body mass	Box-Cox	--	1.298	Foot position			
Froude number	Logarithmic	--	--	Peak vertical	Box-Cox	100	1.028
				Average	--	--	--
FL Vpk	--	--	--				
HL Vpk	--	--	--	FL duty factor	Logarithmic	--	--
Vpk ratio	Box-Cox	--	-0.049	HL duty factor	Logarithmic	--	--
				Duty factor ratio	Box-Cox	--	-0.299
FL angle							
Touchdown	--	--	--	Elbow angle			
Peak vertical	Box-Cox	90	1.843	Touchdown	Arc-sine	--	--
Retraction	Logarithmic	90	--	Mid-stance	Arc-sine	--	--
Excursion	Box-Cox	--	1.131	Yield	Box-Cox	90	1.129
Average	--	--	--				
				Knee angle			
HL angle				Touchdown	Box-Cox	--	2.384
Touchdown	--	--	--	Mid-stance	Arc-sine	--	--
Peak vertical	Arc-sine	--	--	Yield	--	--	--
Retraction	Logarithmic	90	--				
Excursion	Box-Cox	--	1.522	Effective FL length	Box-Cox	--	0.571
Average	Arc-sine	--	--	Effective HL length	Box-Cox	--	3.394
				Effective IMI	--	--	--
Hand position							
Peak vertical	--	--	--				
Average	Logarithmic	--	--				

The parameter λ is provided for all Box-Cox transformations (see Section 4.2.4 for clarification). FL: forelimb, HL: hind limb.

Table 4.4. Regression analyses of peak vertical force (Vpk) data on Froude number and body mass.

		Froude number			Body Mass			Froude number + Body Mass				
	N	R^2	β	Sig	R^2	β	Sig	R^2	Froude (β_1)	Sig	Mass (β_2)	Sig
Forelimb Vpk												
SG	96	0.67	0.44±0.062	***	0.06	-0.76±0.614	*	0.74	0.44±0.056	***	-0.80±0.322	***
SP	178	0.79	0.51±0.039	***	0.09	-1.50±0.697	***	0.81	0.50±0.039	***	-0.59±0.328	***
AG	250	0.28	0.34±0.069	***	0.07	-0.91±0.434	***	0.37	0.36±0.064	***	-1.11±0.357	***
AP	276	0.26	0.39±0.078	***	0.00	-0.18±0.377	NS	0.30	0.43±0.079	***	-0.66±0.329	***
Hind limb Vpk												
SG	81	0.11	0.16±0.105	***	0.24	1.38±0.580	***	0.31	0.14±0.093	**	1.29±0.531	***
SP	158	0.22	0.21±0.064	***	0.20	1.53±0.489	***	0.46	0.23±0.054	***	1.69±0.405	***
AG	109	0.44	0.62±0.135	***	0.03	0.91±0.947	NS	0.52	0.67±0.126	***	1.50±0.677	***
AP	206	0.25	0.51±0.121	***	0.22	1.89±0.489	***	0.35	0.39±0.121	***	1.34±0.480	***
Vpk ratio												
SG	73	0.20	0.37±0.176	***	0.30	-2.44±0.873	***	0.55	0.41±0.135	***	-2.58±0.715	***
SP	151	0.19	0.28±0.093	***	0.31	-2.56±0.613	***	0.48	0.25±0.075	***	-2.44±0.540	***
AG	84	0.01	0.07±0.179	NS	0.20	-2.04±0.877	***	0.21	-0.02±0.166	NS	-2.06±0.909	***
AP	195	0.04	-0.20±0.149	**	0.21	-1.91±0.525	***	0.21	-0.03±0.144	NS	-1.87±0.562	***

Bivariate least-squares regression slopes (β) of Vpk data on Froude number and body mass and partial regression slopes (β_1 and β_2) from multiple regressions of Vpk data on the linear combination of Froude number and body mass are shown for all gait-by-substrate groups. 95% confidence intervals and significance levels are shown for each slope (*: $p \leq 0.05$; **: $p \leq 0.01$; ***: $p \leq 0.001$; NS: not significant). Regressions were calculated on transformed variates. Slopes are therefore provided as an index of the direction and relative magnitude of the reported associations, not as a precise descriptor of the linear relationship between variables.

Table 4.5. Size-related changes in average experiment-wise Vpk ratios during ontogeny.

	N	R^2	Slope (β)	Sig	Intercept (α)	Sig	Body mass at Vpk ≤ 1.0			
							Smallest	Predicted average	Lower CI	Upper CI
SG	32	0.37	$-1.72\pm0.083 \times 10^{-3}$	***	1.61±0.347	***	286 g	352.0 g	296.6 g	370.4 g
SP	30	0.61	$-3.35\pm0.104 \times 10^{-3}$	***	2.44±0.409	***	380 g	430.0 g	413.4 g	455.5 g
AG	40	0.32	$-2.05\pm0.097 \times 10^{-3}$	***	1.91±0.394	***	341 g	442.8 g	404.4 g	504.7 g
AP	37	0.41	$-1.88\pm0.077 \times 10^{-3}$	***	1.96±0.312	***	407 g	512.5 g	506.2 g	562.0 g

Slopes and intercepts (± 95% CI) from least-squares regressions of average Vpk ratios on body mass are shown for each gait-by-substrate group. The earliest and predicted average body mass (with 95% CIs) at which monkeys transitioned to hind limb dominance (i.e., Vpk ratio < 1.0) are also shown. Confidence intervals on predicted body masses were calculated following Sokal and Rohlf (1995).

Table 4.6. Regression analyses of relative effective limb lengths and effective intermembral index (IMI) on Froude number and body mass.

		Froude number			Body Mass			Froude number + Body Mass				
	N	R^2	β	Sig	R^2	β	Sig	R^2	Froude (β_1)	Sig	Mass (β_2)	Sig
Effective FL length												
SG	150	0.01	-0.02±0.041	NS	0.05	0.43±0.301	***	0.07	-0.03±0.040	NS	0.44±0.300	**
SP	217	0.06	-0.05±0.024	***	0.05	0.38±0.231	***	0.15	-0.04±0.025	**	0.28±0.238	*
AG	447	0.00	-0.01±0.026	NS	0.12	0.51±0.128	***	0.12	-0.01±0.025	NS	0.52±0.131	***
AP	318	0.06	0.08±0.036	***	0.02	0.21±0.158	**	0.07	0.07±0.037	***	0.13±0.159	NS
Effective HL length												
SG	156	0.02	-0.07±0.086	NS	0.03	0.59±0.596	NS	0.04	-0.07±0.086	NS	0.60±0.593	*
SP	227	0.07	-0.11±0.049	***	0.03	0.66±0.485	**	0.08	-0.09±0.051	***	0.40±0.493	NS
AG	452	0.00	-0.05±0.069	NS	0.36	2.37±0.295	***	0.40	-0.14±0.055	***	2.51±0.293	***
AP	321	0.00	0.02±0.088	NS	0.00	0.13±0.378	NS	0.00	0.02±0.091	NS	0.11±0.392	NS
Effective IMI												
SG	150	0.00	-0.91±2.972	NS	0.03	23.2±22.03	NS	0.03	-1.05±2.972	NS	23.6±22.09	*
SP	213	0.01	-1.14±1.797	NS	0.01	13.5±17.18	NS	0.01	-0.79±1.879	NS	11.3±18.00	NS
AG	433	0.00	1.54±2.554	NS	0.13	-51.6±12.70	***	0.14	3.38±2.409	**	-54.8±12.81	***
AP	314	0.03	5.32±3.481	**	0.01	16.1±15.28	**	0.04	4.69±3.587	*	11.0±15.54	NS

Data presented as in Table 4.4.

Table 4.7. Multiple regressions of Vpk ratio on Froude number, body mass and effective IMI.

	N	R^2	Froude (β_1)	Sig	Mass (β_2)	Sig	Effective IMI (β_3)	Sig
SG	69	0.46	0.39±0.069	***	-2.16±0.883	***	-2.91±6.978†	NS
SP	135	0.50	0.26±0.084	***	-2.66±0.560	***	-3.90±4.155†	NS
AG	80	0.29	0.03±0.163	NS	-2.46±0.935	***	-9.30±5.928†	**
AP	186	0.24	-0.03±0.145	NS	-1.87±0.583	***	-5.96±4.159†	**

Data presented as in Table 4.4. $^{\dagger} \times 10^{-3}$

Table 4.8. Regression analyses of forelimb angular data on Froude number and body mass.

		Froude number			Body Mass			Froude number + Body Mass				
	N	R^2	β	Sig	R^2	β	Sig	R^2	Froude (β_1)	Sig	Mass (β_2)	Sig
Touchdown												
SG	151	0.01	-0.03±0.063	NS	0.07	0.76±0.460	***	0.08	-0.04±0.061	NS	0.77±0.460	***
SP	206	0.05	-0.05±0.032	**	0.24	1.11±0.273	***	0.24	-0.02±0.030	NS	1.05±0.285	***
AG	426	0.00	-0.01±0.068	NS	0.00	0.12±0.353	NS	0.00	-0.01±0.069	NS	0.14±0.360	NS
AP	297	0.01	-0.09±0.091	*	0.02	0.37±0.372	*	0.04	-0.13±0.094	**	0.51±0.382	**
Lift-off												
SG	151	0.02	0.05±0.055	NS	0.00	0.15±0.394	NS	0.03	0.05±0.056	NS	0.16±0.391	NS
SP	224	0.00	-0.01±0.032	NS	0.03	-0.42±0.303	**	0.04	-0.02±0.033	NS	-0.49±0.316	**
AG	412	0.07	-0.17±0.061	***	0.03	-0.55±0.322	***	0.08	-0.16±0.062	***	-0.40±0.318	*
AP	312	0.02	-0.09±0.076	*	0.07	-0.81±0.318	***	0.08	-0.04±0.076	NS	-0.76±0.328	***
Average												
SG	148	0.00	0.61±1.337	NS	0.06	15.4±9.815	**	0.07	0.52±1.301	NS	15.3±9.837	**
SP	205	0.03	-1.02±0.793	*	0.02	6.99±7.481	NS	0.04	-1.02±0.829	*	6.99±7.761	NS
AG	388	0.04	-3.47±1.679	***	0.01	-8.66±8.750	NS	0.04	-3.26±1.707	***	-5.58±8.754	NS
AP	290	0.04	-3.82±2.130	***	0.02	-11.0±8.831	*	0.05	-3.35±2.202	**	-7.36±9.031	NS
Peak vertical												
SG	59	0.06	-253±261.3	NS	0.04	1533±3396	NS	0.13	-300±258.0	*	1899±1821	*
SP	107	0.12	194±99.08	***	0.00	286±1050	NS	0.14	210±101.0	***	742±1001.8	NS
AG	131	0.01	66.8±143.5	NS	0.00	-87.4±691.7	NS	0.01	66.0±147.6	NS	-18.8±709.1	NS
AP	170	0.00	-64.9±160.2	NS	0.01	-423±668.6	NS	0.01	-37.1±168.5	NS	-374±705.3	NS

Data presented as in Table 4.4.

Table 4.9. Regression analyses of hind limb angular data on Froude number and body mass.

		Froude number			Body Mass			Froude number + Body Mass				
	N	R^2	β	Sig	R^2	β	Sig	R^2	Froude (β_1)	Sig	Mass (β_2)	Sig
Touchdown												
SG	155	0.03	-2.58±2.277	*	0.32	57.4±13.15	***	0.36	-2.74±1.854	**	57.7±12.84	***
SP	226	0.29	-5.88±1.210	***	0.25	52.1±12.05	***	0.42	-4.72±1.147	***	39.1±11.08	***
AG	439	0.00	1.35±2.230	NS	0.00	-7.87±12.4	NS	0.01	1.72±2.275	NS	-9.84±12.67	NS
AP	312	0.03	6.62±4.233	**	0.10	50.8±17.65	***	0.10	3.62±4.247	NS	46.4±18.33	***
Lift-off												
SG	149	0.06	-0.05±0.032	**	0.01	0.15±0.228	NS	0.07	-0.05±0.032	**	0.15±0.222	NS
SP	223	0.00	-0.01±0.023	NS	0.06	-0.41±0.214	***	0.07	-0.01±0.023	NS	-0.47±0.223	***
AG	431	0.00	-0.03±0.033	NS	0.00	0.06±0.176	NS	0.01	-0.03±0.033	NS	0.09±0.179	NS
AP	309	0.01	-0.05±0.044	*	0.14	-0.65±0.181	***	0.14	-0.01±0.044	NS	-0.64±0.188	***
Average												
SG	148	0.06	0.01±0.005	**	0.23	0.10±0.031	***	0.29	0.01±0.004	**	0.10±0.030	***
SP	222	0.24	0.02±0.002	***	0.07	0.06±0.027	***	0.25	0.01±0.003	***	0.03±0.025	*
AG	419	0.00	0.001±0.01	NS	0.00	-0.004±0.03	NS	0.00	0.00±0.002	NS	-0.005±0.03	NS
AP	300	0.01	0.01±0.010	NS	0.01	0.04±0.038	NS	0.02	0.01±0.010	NS	0.03±0.040	NS
Peak vertical												
SG	42	0.31	-0.04±0.017	***	0.04	0.08±0.118	NS	0.42	-0.04±0.017	***	0.13±0.095	*
SP	94	0.28	-0.05±0.017	***	0.00	0.003±0.15	NS	0.29	-0.05±0.017	***	0.06±0.132	NS
AG	58	0.00	-0.01±0.028	NS	0.03	0.10±0.152	NS	0.04	-0.01±0.028	NS	0.11±0.155	NS
AP	99	0.00	-0.003±0.03	NS	0.04	0.14±0.147	NS	0.05	-0.03±0.039	NS	0.14±0.169	*

Data presented as in Table 4.4

Table 4.10. Regression analyses of hand and foot positions on Froude number and body mass.

		Froude number			Body Mass			Froude number + Body Mass				
	N	R^2	β	Sig	R^2	β	Sig	R^2	Froude (β_1)	Sig	Mass (β_2)	Sig
Hand position												
Peak vertical												
SG	56	0.07	-6.52±6.646	NS	0.05	39.2±47.54	NS	0.14	-7.72±6.541	*	49.1±46.36	*
SP	96	0.11	4.04±2.382	**	0.00	5.22±24.77	NS	0.12	4.37±2.438	**	14.8±23.97	NS
AG	108	0.00	1.47±4.149	NS	0.00	0.95±19.19	NS	0.00	1.60±4.278	NS	2.61±19.74	NS
AP	148	0.00	-0.95±3.922	NS	0.01	-10.2±16.29	NS	0.01	-0.06±4.209	NS	-10.1±17.56	NS
Average												
SG	109	0.00	0.001±0.21	NS	0.12	0.31±0.159	***	0.12	-0.002±0.02	NS	0.31±0.160	**
SP	147	0.03	0.01±0.009	*	0.02	-0.08±0.087	NS	0.04	0.008±0.01	NS	-0.05±0.090	NS
AG	280	0.01	-0.03±0.030	*	0.06	-0.34±0.154	***	0.07	-0.02±0.030	NS	-0.32±0.158	***
AP	210	0.02	-0.04±0.043	NS	0.06	-10.4±0.175	***	0.06	-0.02±0.045	NS	-0.30±0.186	**
Foot position												
Peak vertical												
SG	36	0.41	-27.6±11.72	***	0.02	38.9±89.16	NS	0.44	-28.0±11.66	***	48.2±80.00	NS
SP	91	0.27	-28.8±9.838	***	0.00	18.2±89.16	NS	0.29	-29.7±9.898	***	50.4±76.41	NS
AG	52	0.00	2.43±15.46	NS	0.03	57.0±88.85	NS	0.04	4.12±15.54	NS	60.1±90.74	NS
AP	92	0.00	-3.91±18.76	NS	0.03	66.7±81.53	NS	0.05	-15.1±21.18	NS	99.6±93.33	*
Average												
SG	109	0.15	-6.36±2.847	***	0.14	44.7±20.58	***	0.32	-6.86±2.561	***	48.4±18.43	***
SP	148	0.26	-4.99±1.390	***	0.09	30.7±15.85	***	0.28	-4.50±1.441	***	16.5±14.86	*
AG	313	0.00	0.26±1.958	NS	0.00	-2.21±10.54	NS	0.00	0.38±2.026	NS	-2.74±10.91	NS
AP	181	0.00	-0.19±3.874	NS	0.02	15.6±15.54	*	0.02	-1.26±3.975	NS	16.9±16.12	*

Data presented as in Table 4.4.

Table 4.11. Multiple regressions of peak vertical limb force magnitudes on Froude number, body mass and hand/foot position.

	N	R^2	Froude (β_1)	Sig	Mass (β_2)	Sig	Position (β_3)	Sig
Hand position								
Peak vertical								
SG	55	0.81	0.50±0.074	***	-1.40±0.517	***	0.84±2.974†	NS
SP	96	0.86	0.49±0.051	***	-0.81±0.472	***	5.69±4.020†	**
AG	108	0.69	0.43±0.104	***	-0.76±0.478	**	1.23±4.687†	NS
AP	148	0.57	0.40±0.103	***	-0.64±0.432	**	7.22±4.019†	**
Average								
SG	64	0.77	0.46±0.069	***	-0.81±0.474	***	-3.79±6.326†	NS
SP	106	0.81	0.52±0.051	***	-0.38±0.379	*	-6.78±8.131†	NS
AG	152	0.35	0.31±0.076	***	-1.08±0.458	***	-4.64±4.017†	*
AP	178	0.27	0.38±0.099	***	-0.64±0.432	**	-3.07±3.348†	NS
Foot position								
Peak vertical								
SG	36	0.51	0.31±0.121	***	0.43±0.644	NS	4.80±2.788†	***
SP	91	0.58	0.29±0.153	***	1.15±0.455	***	2.06±1.125†	**
AG	52	0.62	0.31±0.076	***	1.16±0.905	*	4.15±2.813†	**
AP	91	0.39	0.45±0.175	***	0.64±0.785	NS	2.08±1.715†	*
Average								
SG	52	0.20	0.10±0.134	NS	1.01±0.788	*	1.78±8.245†	NS
SP	89	0.50	0.26±0.071	***	1.66±0.514	***	3.89±5.534†	NS
AG	63	0.64	0.72±0.146	***	1.54±0.910	***	5.13±6.999†	NS
AP	123	0.31	0.35±0.163	***	1.12±0.641	***	5.80±5.662†	*

Data presented as in Table 4.4. † $\times 10^{-3}$

Table 4.12. Regression analyses of forelimb and hind limb duty factors and duty factor ratio on Froude number and body mass.

		Froude number			Body Mass			Froude number + Body Mass				
	N	R^2	β	Sig	R^2	β	Sig	R^2	Froude (β_1)	Sig	Mass (β_2)	Sig
FL duty factor												
SG	165	0.67	-0.36±0.039	***	0.02	-0.44±0.489	NS	0.67	-0.36±0.039	***	-0.33±0.282	*
SP	244	0.81	-0.36±0.022	***	0.03	0.66±0.475	**	0.83	-0.37±0.022	***	-0.43±0.211	***
AG	498	0.58	-0.38±0.029	***	0.07	-0.68±0.221	***	0.58	-0.37±0.029	***	-0.29±0.029	***
AP	342	0.56	-0.51±0.047	***	0.19	-1.24±0.273	***	0.64	-0.46±0.045	***	-0.75±0.190	***
HL duty factor												
SG	165	0.76	-0.34±0.030	***	0.00	0.09±0.433	NS	0.76	-0.34±0.030	***	0.19±0.216	NS
SP	244	0.86	-0.40±0.020	***	0.13	1.47±0.486	***	0.86	-0.39±0.021	***	0.34±0.201	**
AG	498	0.58	-0.39±0.029	***	0.04	0.56±0.230	***	0.59	-0.39±0.030	***	-0.14±0.155	NS
AP	342	0.55	-0.43±0.042	***	0.00	-0.05±0.262	NS	0.58	-0.45±0.042	***	0.42±0.178	***
Duty factor ratio												
SG	165	0.01	-0.02±0.026	NS	0.14	-0.46±0.181	***	0.14	-0.02±0.025	NS	-0.46±0.180	***
SP	244	0.05	0.04±0.020	***	0.24	-0.78±0.176	***	0.25	0.02±0.191	NS	-0.74±0.184	***
AG	498	0.00	0.01±0.023	NS	0.01	-0.12±0.122	NS	0.01	0.02±0.024	NS	-0.13±0.125	NS
AP	342	0.03	-0.08±0.048	**	0.32	-1.10±0.170	***	0.32	-0.08±0.041	NS	-1.08±0.175	***

Data presented as in Table 4.4. FL: forelimb, HL: hind limb.

Table 4.13. Multiple regressions of peak vertical limb force magnitudes on Froude number, body mass and duty factor.

	N	R^2	Froude (β_1)	Sig	Mass (β_2)	Sig	Duty Factor (β_3)	Sig
FL duty factor								
SG	96	0.75	-0.02±0.193	***	-0.73±0.331	***	0.17±0.204	NS
SP	178	0.82	0.07±0.110	***	-0.73±0.333	***	-0.29±0.186	**
AG	250	0.39	0.53±0.238	***	-1.17±0.354	**	-0.28±0.200	**
AP	276	0.36	0.15±0.178	***	-1.05±0.346	**	-0.47±0.176	***
HL duty factor								
SG	81	0.34	0.50±0.096	***	1.25±0.525	***	-0.39±0.434	NS
SP	158	0.49	0.39±0.081	***	0.74±0.399	***	-0.38±0.228	***
AG	109	0.53	0.27±0.092	***	1.49±0.675	***	-0.26±0.386	NS
AP	206	0.39	0.22±0.109	***	1.46±0.472	***	-0.50±0.285	***

Data presented as in Table 4.4.

Table 4.14. Multiple regressions of Vpk ratio on Froude number, body mass and duty factor ratio.

	N	R^2	Froude (β_1)	Sig	Mass (β_2)	Sig	Duty Factor (β_3)	Sig
SG	73	0.63	0.40±0.122	***	-1.94±0.719	***	1.10±0.534	***
SP	151	0.48	0.25±0.076	***	-2.26±0.605	***	0.21±0.327	NS
AG	84	0.23	0.04±0.169	NS	-2.08±0.901	***	0.34±0.428	NS
AP	195	0.21	0.03±0.144	NS	-1.92±0.661	***	-0.05±0.306	NS

Data presented as in Table 4.4.

Table 4.15. Regression analyses of forelimb and hind limb angular excursion on Froude number and body mass.

		Froude number			Body Mass			Froude number + Body Mass				
	N	R^2	β	Sig	R^2	β	Sig	R^2	Froude (β_1)	Sig	Mass (β_2)	Sig
FL excursion												
SG	148	0.02	-5.01±5.555	NS	0.01	23.0±42.28	NS	0.03	-5.01±5.555	NS	24.6±41.98	NS
SP	205	0.01	-2.52±3.388	NS	0.21	107±28.27	***	0.21	0.90±3.163	NS	109±29.62	***
AG	388	0.06	11.0±4.361	***	0.03	42.3±22.68	***	0.08	9.86±4.395	***	33.0±22.54	**
AP	290	0.00	2.72±7.307	NS	0.10	82.5±28.43	***	0.10	-2.77±7.191	NS	82.5±29.49	***
HL excursion												
SG	148	0.00	-2.35±22.38	NS	0.24	461±133.2	***	0.24	-3.25±19.54	NS	461±133.6	***
SP	222	0.16	-48.5±14.91	***	0.27	610±134.1	***	0.34	-33.3±13.83	***	519±133.5	***
AG	419	0.01	20.1±17.37	*	0.01	-119±95.12	*	0.04	26.2±17.64	**	-151±96.66	**
AP	300	0.05	81.6±39.38	***	0.21	703±156.4	***	0.22	41.6±37.10	*	655±161.1	***

Data presented as in Table 4.4.

Table 4.16. Multiple regressions of peak vertical limb force magnitudes on Froude number, body mass and forelimb/hind limb angular excursion.

	N	R^2	Froude (β_1)	Sig	Mass (β_2)	Sig	Excursion (β_3)	Sig
FL excursion								
SG	90	0.77	0.45±0.055	***	-0.98±0.390	***	2.80±15.92†	NS
SP	150	0.80	0.51±0.043	***	-0.58±0.408	**	0.43±17.29†	NS
AG	210	0.37	0.34±0.071	***	-1.05±0.384	***	12.3±16.56†	NS
AP	243	0.27	0.39±0.084	***	-0.64±0.359	***	-8.09±13.24†	NS
HL excursion								
SG	77	0.34	0.13±0.094	**	1.41±0.579	***	-1.15±6.562†	NS
SP	146	0.47	0.24±0.064	***	1.72±0.495	***	0.24±4.393†	NS
AG	93	0.54	0.66±0.136	***	1.42±0.835	***	4.85±7.046†	NS
AP	187	0.31	0.36±0.125	***	1.23±0.586	***	1.51±3.889†	NS

Data presented as in Table 4.4. $^{\dagger} \times 10^{-4}$

Table 4.17. Regression analyses of elbow angular data on Froude number and body mass.

		Froude number			Body Mass			Froude number + Body Mass				
	N	R^2	β	Sig	R^2	β	Sig	R^2	Froude (β_1)	Sig	Mass (β_2)	Sig
Touchdown												
SG	145	0.00	0.002±0.01	NS	0.00	0.01±0.062	NS	0.00	0.002±0.01	NS	0.01±0.065	NS
SP	204	0.00	0.00±0.006	NS	0.00	0.001±0.05	NS	0.00	0.00±0.006	NS	0.00±0.057	NS
AG	412	0.03	0.01±0.007	***	0.02	0.05±0.035	**	0.04	0.01±0.007	***	0.04±0.035	*
AP	285	0.02	-0.02±0.014	*	0.14	-0.18±0.051	***	0.14	-0.002±0.05	NS	-0.18±0.054	***
Mid-stance												
SG	147	0.04	-0.01±0.011	*	0.01	-0.04±0.082	NS	0.04	-0.01±0.011	*	-0.03±0.081	NS
SP	217	0.00	0.003±0.01	NS	0.19	-0.22±0.060	***	0.20	-0.004±0.01	NS	-0.23±0.063	***
AG	432	0.02	-0.01±0.007	***	0.01	-0.03±0.041	NS	0.02	-0.01±0.008	*	-0.03±0.042	NS
AP	308	0.05	-0.03±0.015	***	0.25	-0.30±0.059	***	0.25	-0.01±0.015	NS	-0.28±0.061	***
Yield												
SG	143	0.10	9.88±5.139	***	0.01	24.5±41.11	NS	0.10	9.71±5.153	***	24.5±39.45	NS
SP	203	0.00	-1.90±4.086	NS	0.21	127±34.45	***	0.21	2.15±3.797	NS	134±35.94	***
AG	404	0.08	16.6±5.291	***	0.04	54.8±28.06	***	0.10	15.1±5.345	***	39.9±27.59	**
AP	284	0.02	11.0±8.957	*	0.04	64.8±36.06	***	0.05	6.45±9.370	NS	56.1±38.16	**

Data presented as in Table 4.4.

Table 4.18. Regression analyses of knee angular data on Froude number and body mass.

		Froude number			Body Mass			Froude number + Body Mass				
	N	R^2	β	Sig	R^2	β	Sig	R^2	Froude (β_1)	Sig	Mass (β_2)	Sig
Touchdown												
SG	155	0.01	-1.69±3.51†	NS	0.01	15.4±24.3†	NS	0.02	-1.73±3.51†	NS	15.6±24.3†	NS
SP	226	0.16	-6.30±1.88†	***	0.04	29.8±19.5†	**	0.17	-5.90±1.96†	***	13.5±18.9†	NS
AG	434	0.03	-5.30±2.90†	***	0.14	64.9±15.1†	***	0.21	-8.21±2.68†	***	74.6±14.8†	***
AP	311	0.04	-7.10±3.73†	***	0.05	33.2±16.0†	***	0.13	-10.0±3.71†	***	45.2±16.0†	***
Mid-stance												
SG	155	0.02	-0.01±0.013	NS	0.07	-0.15±0.088	**	0.09	-0.01±0.013	NS	-0.15±0.088	***
SP	227	0.01	-0.005±0.01	NS	0.10	-0.20±0.079	***	0.13	-0.01±0.009	**	-0.24±0.082	***
AG	445	0.04	-0.02±0.012	***	0.12	0.23±0.059	***	0.18	-0.03±0.011	***	0.27±0.058	***
AP	318	0.06	-0.03±0.016	***	0.09	-0.19±0.066	***	0.12	-0.03±0.016	***	-0.16±0.067	***
Yield												
SG	154	0.01	2.57±3.413	NS	0.23	71.5±20.76	***	0.25	2.29±2.999	NS	71.1±20.68	***
SP	226	0.12	-5.58±1.984	***	0.44	102±15.39	***	0.46	-2.79±1.623	***	94.3±15.70	***
AG	432	0.00	1.37±2.965	NS	0.03	2.93±16.39	NS	0.00	1.31±3.037	NS	1.39±16.78	NS
AP	307	0.01	4.98±5.019	NS	0.27	99.3±18.63	***	0.27	-1.46±4.507	NS	101±19.39	***

Data presented as in Table 4.4. $^{\dagger} \times 10^3$

Table 4.19. Multiple regressions of peak vertical limb force magnitudes on Froude number, body mass and elbow/knee yield.

	N	R^2	Froude (β_1)	Sig	Mass (β_2)	Sig	Yield (β_3)	Sig
Elbow yield								
SG	87	0.76	0.44±0.058	***	-0.11±0.389	***	10.20±17.98†	NS
SP	147	0.80	0.51±0.045	***	-0.43±0.410	*	-4.89±14.63†	NS
AG	223	0.39	0.35±0.069	***	-1.09±0.380	***	8.73±14.35†	NS
AP	238	0.22	0.38±0.093	***	-0.64±0.374	***	-3.42±17.98†	NS
Knee yield								
SG	79	0.34	0.13±0.093	**	1.10±0.617	***	2.90±4.32††	NS
SP	148	0.47	0.24±0.590	***	1.67±0.539	***	0.75±3.64††	NS
AG	101	0.55	0.66±0.127	***	1.37±0.752	***	3.84±3.46††	*
AP	194	0.34	0.40±0.127	***	1.17±0.615	***	1.05±3.24††	NS

Data presented as in Table 4.4. $^{\dagger} \times 10^{-4}$; $^{\dagger\dagger} \times 10^{-3}$

4.6. Figures

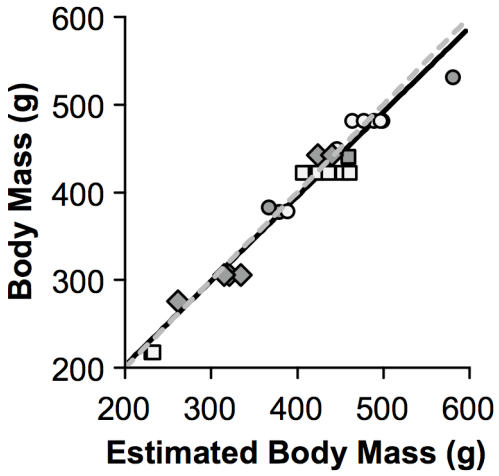

Figure 4.1. Validation of the geometric model used to calculate whole-body COM position.
Estimated body mass from the model is plotted against measured body mass. The solid black line represents a least-squares regression through the data (R^2=0.96; slope: 0.96 ± 0.085; intercept: 0.009 ± 0.035; $p<0.001$; N=26). The dashed gray line represents the line of equality. Symbols for individual monkeys follow Figure 2.1.

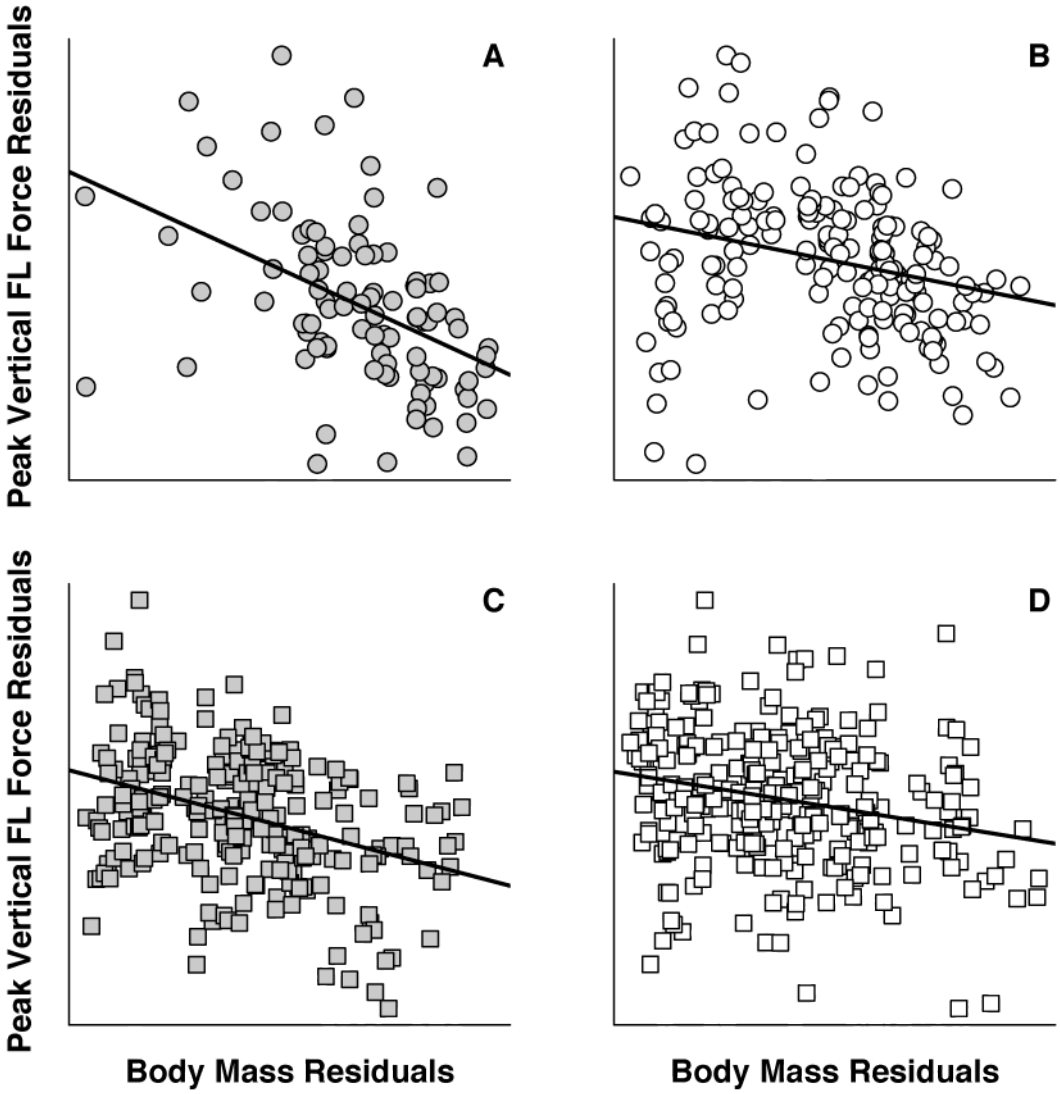

Figure 4.2. Partial regression plots of peak vertical forelimb force against body mass.

Data are shown for A) symmetrical strides on the ground (shaded circles), B) symmetrical strides on the pole (white circles), C) asymmetrical strides on the ground (shaded squares) and D) asymmetrical strides on the pole (white squares). To control for the influence of speed on locomotor kinetics, residuals from least-squares regressions of peak vertical forelimb forces on Froude number have been plotted against residuals from body mass regressed against Froude number. Solid black lines therefore depict the partial regression slope of peak vertical forelimb force on body mass, controlling for speed.

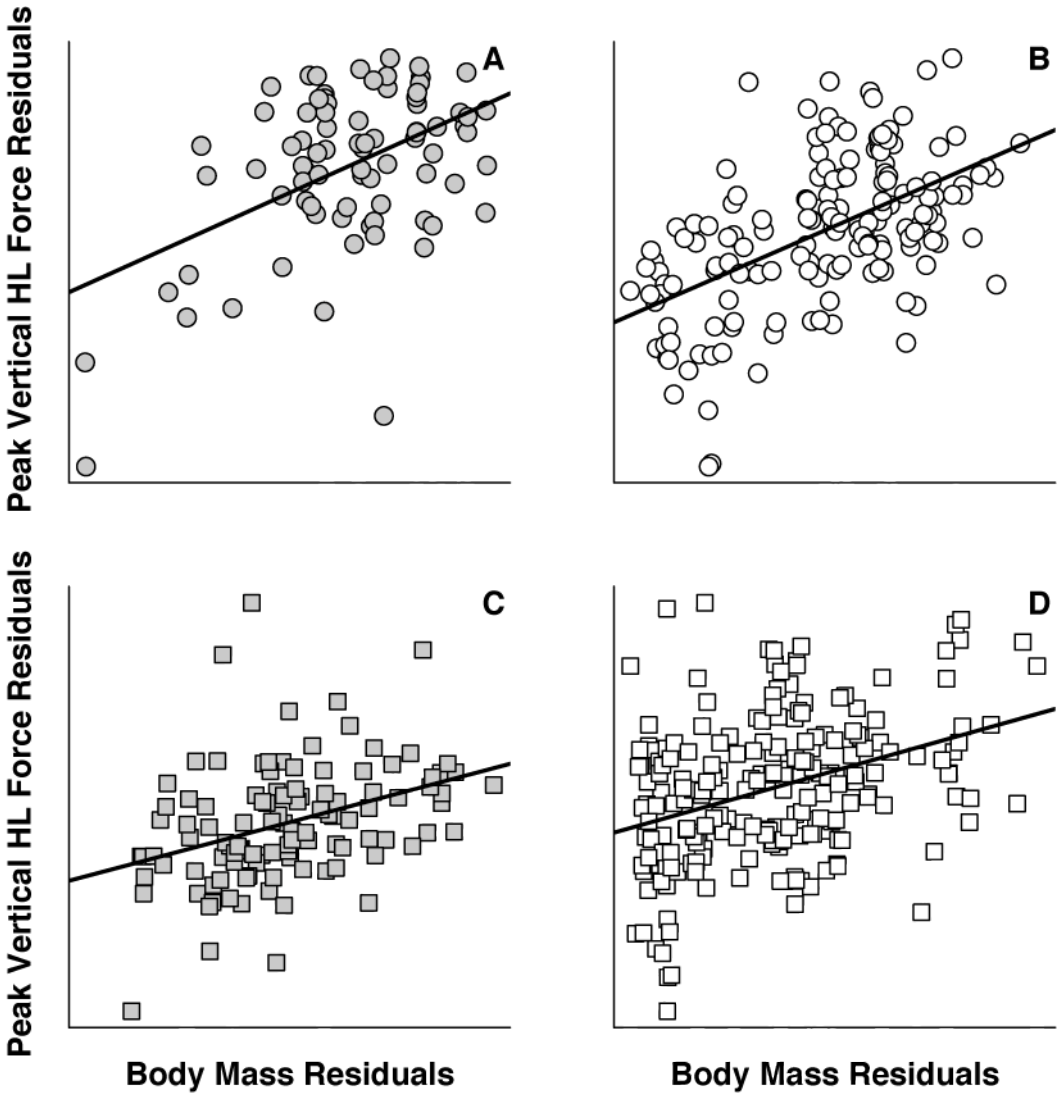

Figure 4.3. Partial regression plots of peak vertical hind limb force against body mass.

Data are shown for A) symmetrical strides on the ground, B) symmetrical strides on the pole, C) asymmetrical strides on the ground and D) asymmetrical strides on the pole. Symbols and presentation of data follow Figure 4.2.

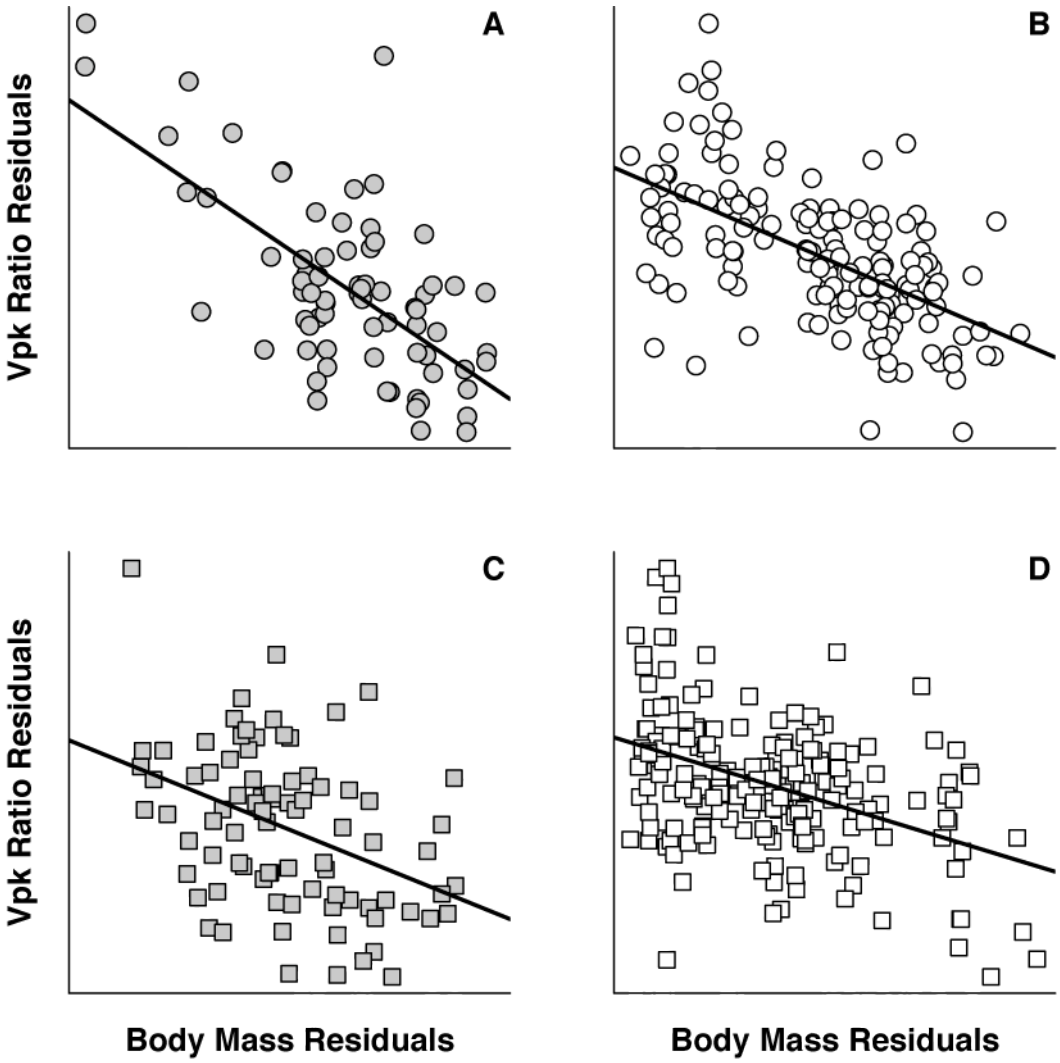

Figure 4.4. Partial regression plots of Vpk ratios against body mass.
Data are shown for A) symmetrical strides on the ground, B) symmetrical strides on the pole, C) asymmetrical strides on the ground and D) asymmetrical strides on the pole. Symbols and presentation of data follow Figure 4.2.

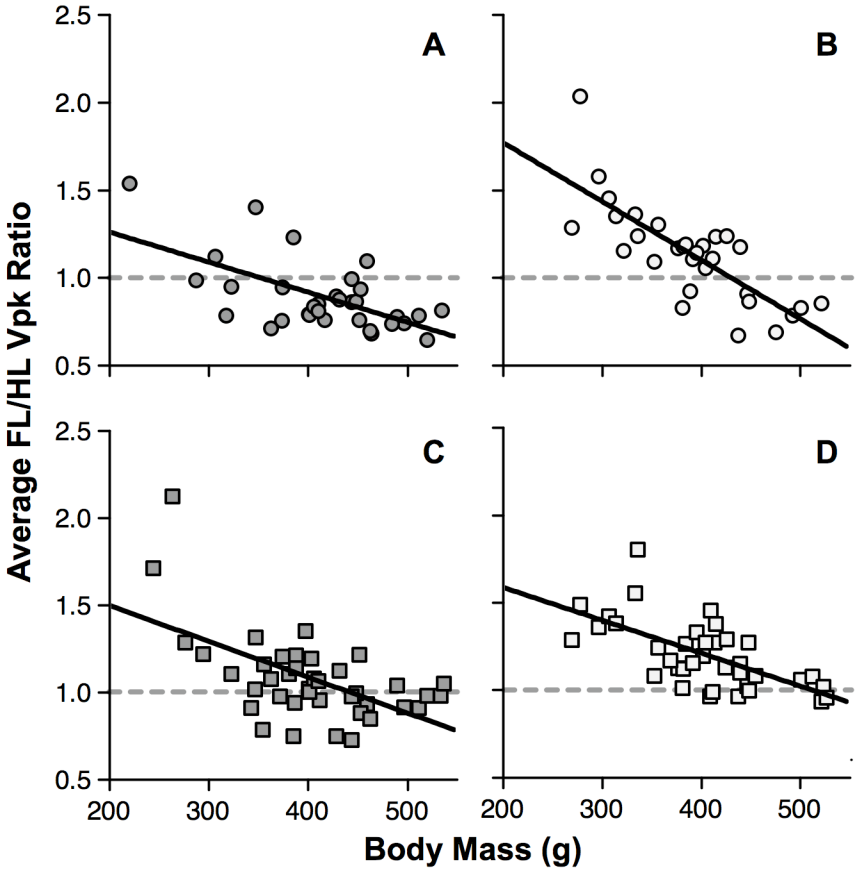

Figure 4.5. Average experiment-wise Vpk ratios plotted against body mass.
Data are shown for A) symmetrical strides on the ground, B) symmetrical strides on the pole, C) asymmetrical strides on the ground and D) asymmetrical strides on the pole. Solid black lines depict least-squares regression slopes for each relationship. Dashed horizontal lines indicate a Vpk ratio of 1, where forelimb and hind limb forces are equal. Symbols follow Figure 4.2.

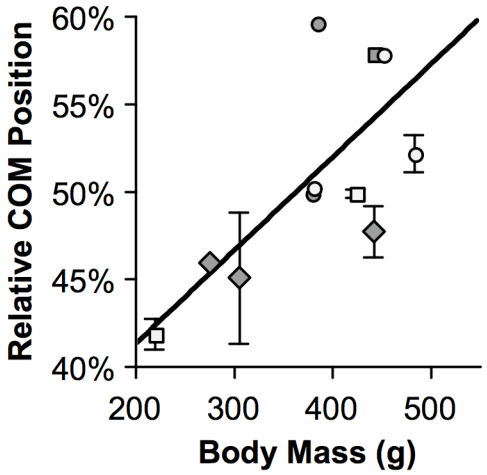

Figure 4.6. Relative whole-body COM position plotted against body mass.
COM of mass position is expressed as a percentage of horizontal trunk length from the shoulders to the hips. The black line depicts a least-squares linear regression of COM position on body mass ($y=0.0531x + 30.76$; $R^2=0.59$; $p=0.004$). Error bars, depicting one standard error, are shown to indicate the amount of variability in estimated COM position at each body mass. Regressions, however, were calculated from average COM position at each body mass (N=12). Symbols for individual monkeys follow Figure 2.1.

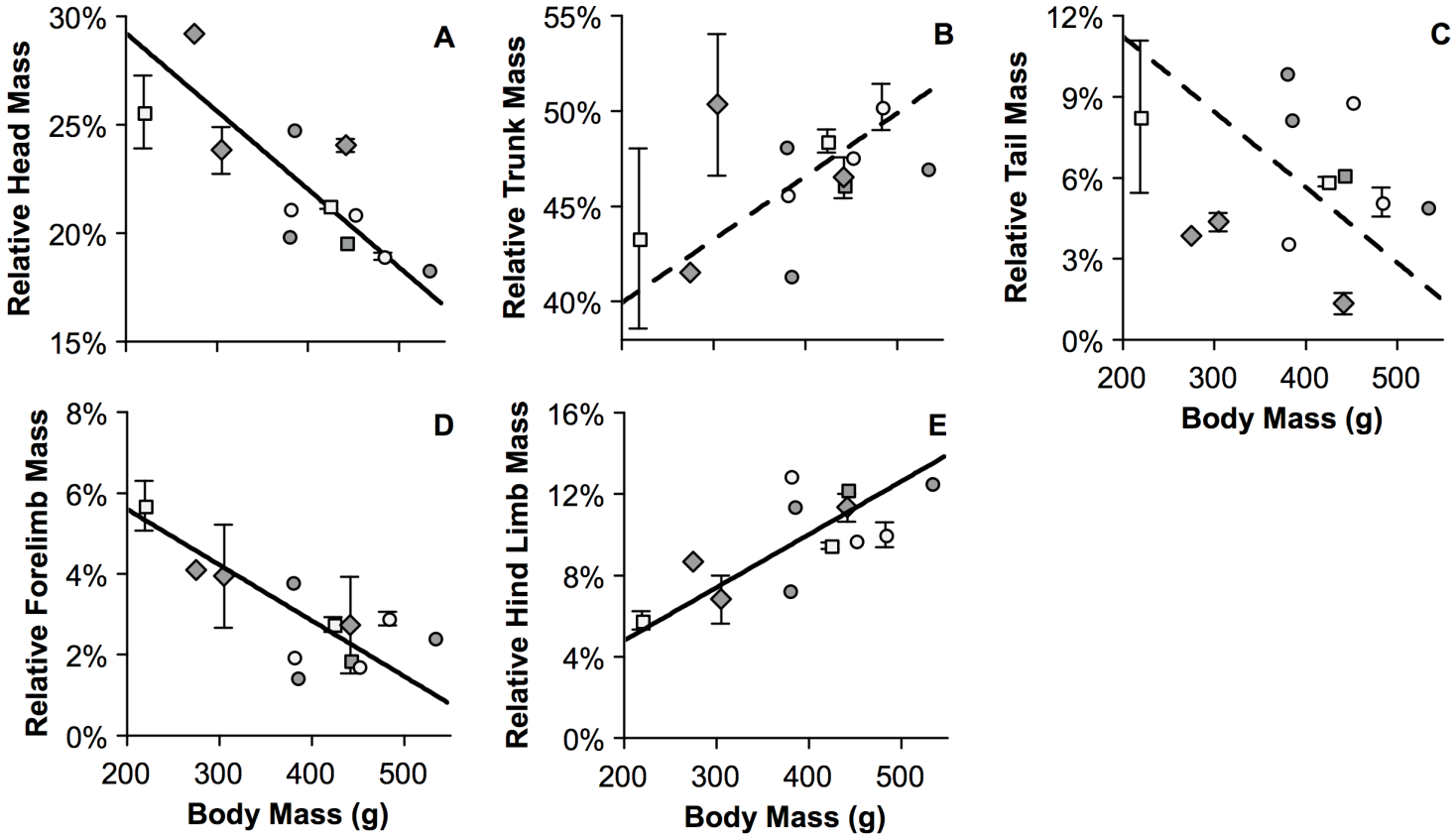

Figure 4.7. Ontogenetic changes in relative segment masses, as estimated from the geometric model.
Fitted lines, depicting Model II RMA regressions, and shown to indicate trends in the data (head: y=-0.036x + 36.4, R^2=0.62, p=0.002; trunk: y=0.033x + 33.3, R^2=0.21, NS; tail: y=-0.038x + 16.8, R^2=0.02, NS; forelimb: y=-0.014x + 8.35, R^2=0.54, p=0.006; hind limb: y=0.026x - 0.42, R^2=0.51, p=0.01). Error bars depict one standard error. Regressions were calculated from average segment mass at each body mass (N=12). Dashed lines indicate the regression was not significant. Symbols for individual monkeys follow Figure 2.1.

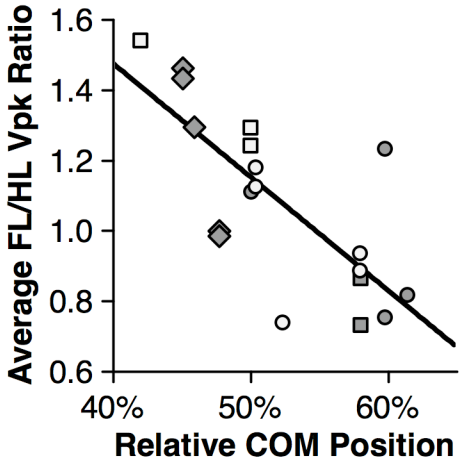

Figure 4.8. Average experiment-wise Vpk ratios plotted against whole-body COM position.
COM position is expressed as percentage of horizontal trunk length from the shoulders to the hips. The fitted line depicts a least-squares regression through the data ($y=-0.0323x + 2.77$; $R^2=0.57$; $p<0.001$). Symbols for individual monkeys follow Figure 2.1.

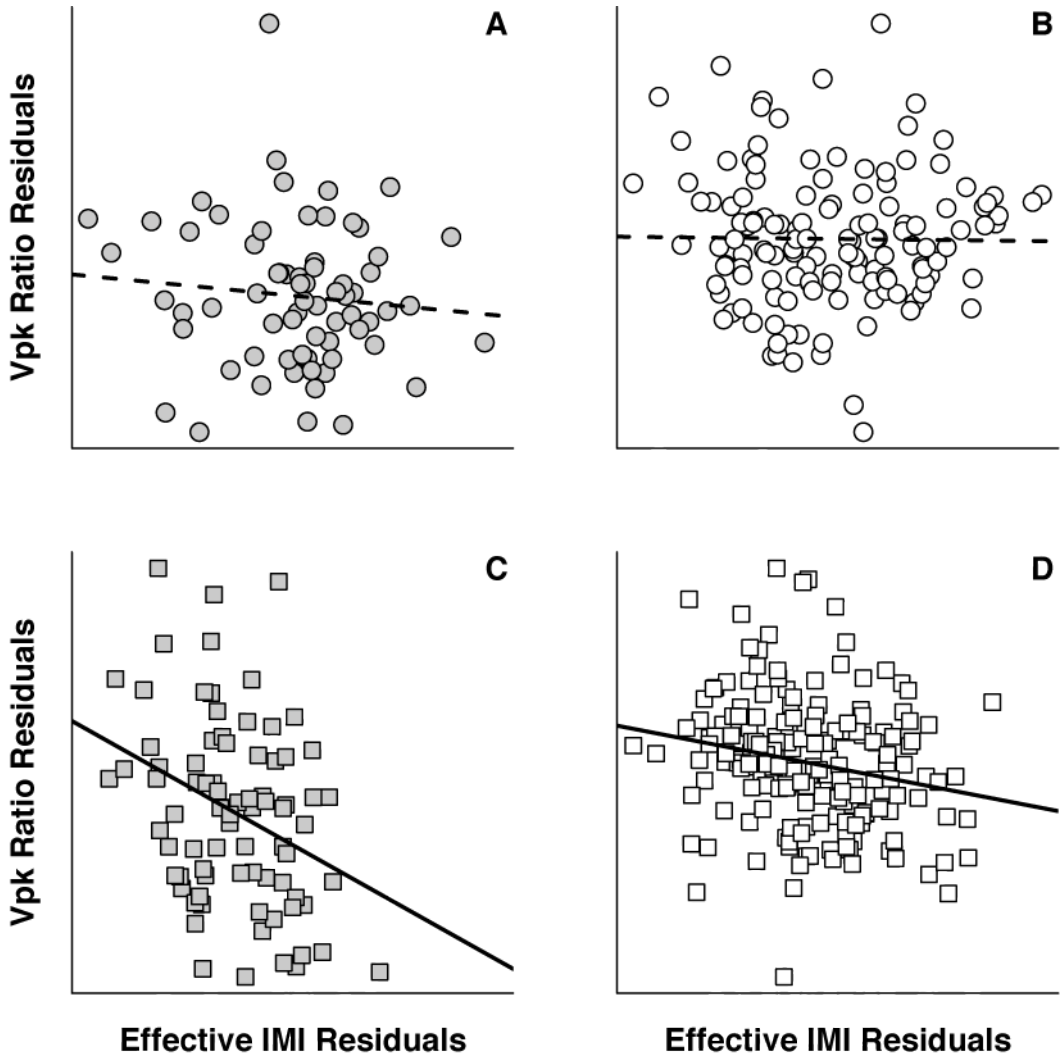

Figure 4.9. Partial regression plots of Vpk ratio against effective IMI.
Data are presented for A) symmetrical strides on the ground, B) symmetrical strides on the pole, C) asymmetrical strides on the ground and D) asymmetrical strides on the pole. To control for the influence of speed and body size on locomotor mechanics, residuals from least-squares regressions of Vpk ratios on Froude number and body mass have been plotted against residuals from effective IMI regressed against Froude number and body mass. Fitted lines therefore depict the partial regression slope of Vpk ratios against effective IMI, controlling for speed and mass. Dashed lines indicate the partial regression was not significant. Symbols follow Figure 4.2.

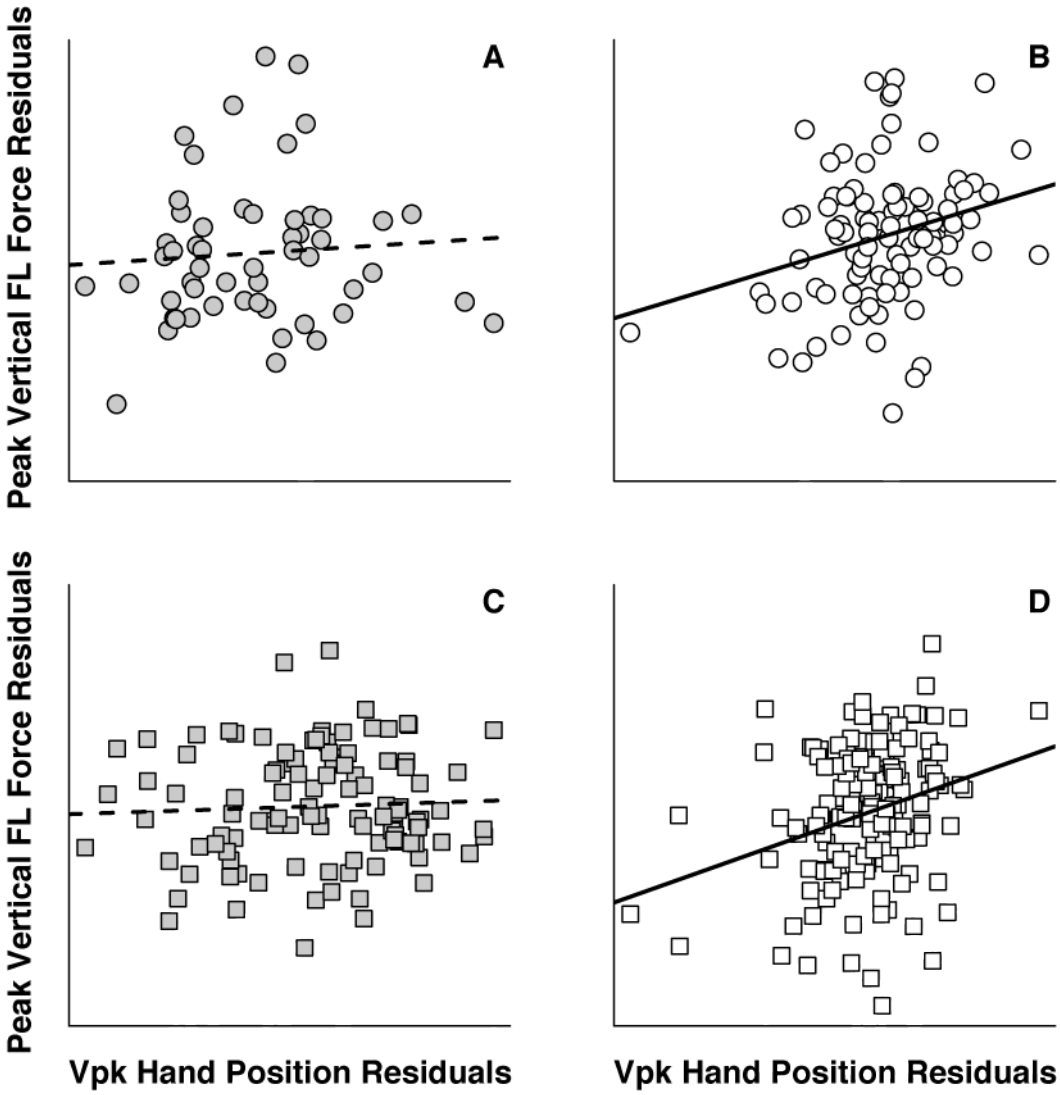

Figure 4.10. Partial regression plots of peak vertical forelimb force against hand position at peak vertical force.
Data are presented for A) symmetrical strides on the ground, B) symmetrical strides on the pole, C) asymmetrical strides on the ground and D) asymmetrical strides on the pole. The positive X-axis indicates increasing distance between the hand and the COM. Symbols and presentation of data follow Figure 4.9.

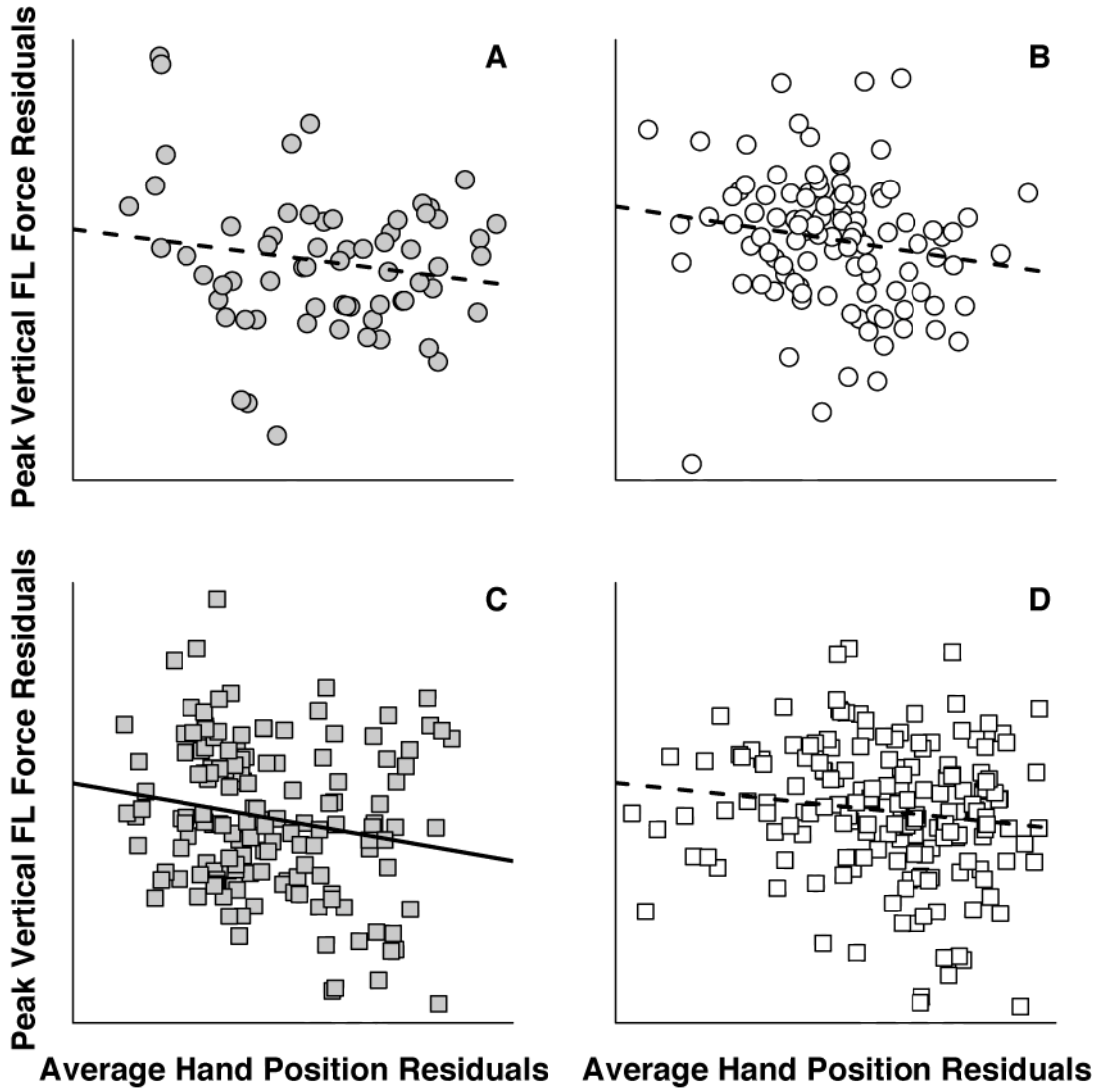

Figure 4.11. Partial regression plots of peak vertical forelimb force against average hand position over a step.
Data are presented for A) symmetrical strides on the ground, B) symmetrical strides on the pole, C) asymmetrical strides on the ground and D) asymmetrical strides on the pole. The positive X-axis indicates increasing distance between the hand and the COM. Symbols and presentation of data follow Figure 4.9.

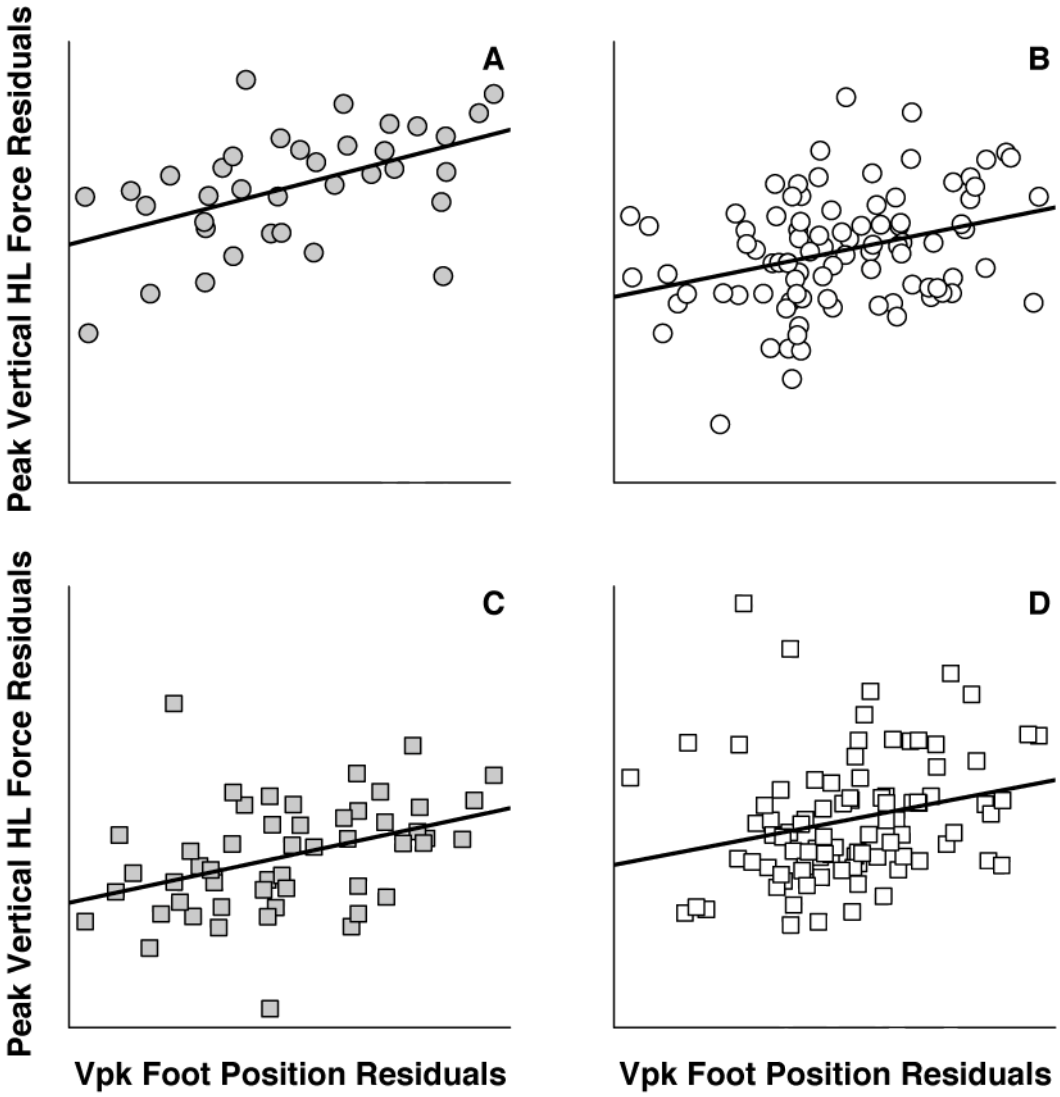

Figure 4.12. Partial regression plots of peak vertical hind limb force against foot position at peak vertical force.
Data are presented for A) symmetrical strides on the ground, B) symmetrical strides on the pole, C) asymmetrical strides on the ground and D) asymmetrical strides on the pole. The positive X-axis indicates decreasing distance between the foot and the COM. Symbols and presentation of data follow Figure 4.9.

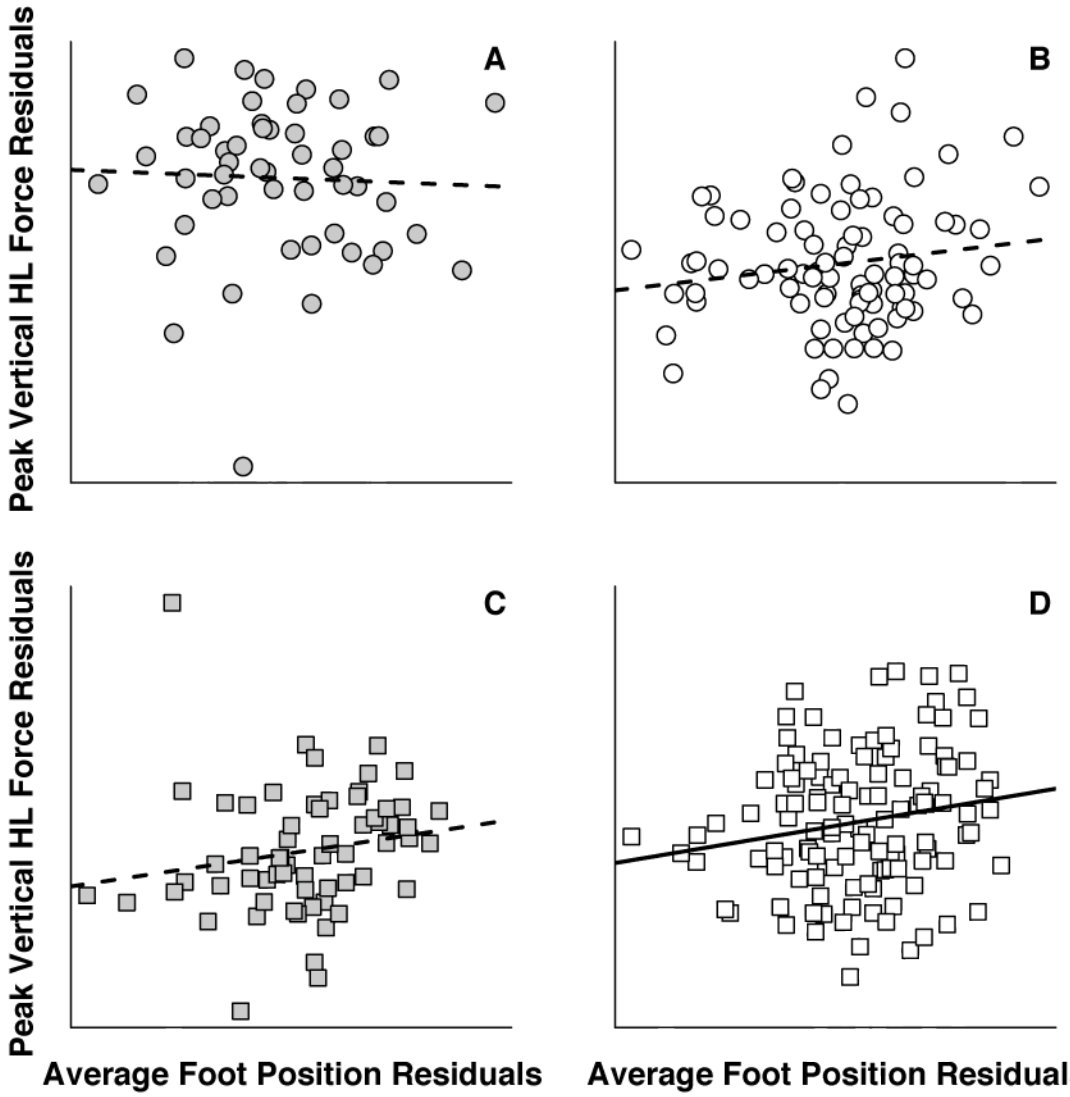

Figure 4.13. Partial regression plots of peak vertical hind limb force against average foot position over a step.
Data are presented for A) symmetrical strides on the ground, B) symmetrical strides on the pole, C) asymmetrical strides on the ground and D) asymmetrical strides on the pole. The positive X-axis indicates decreasing distance between the foot and the COM. Symbols and presentation of data follow Figure 4.9.

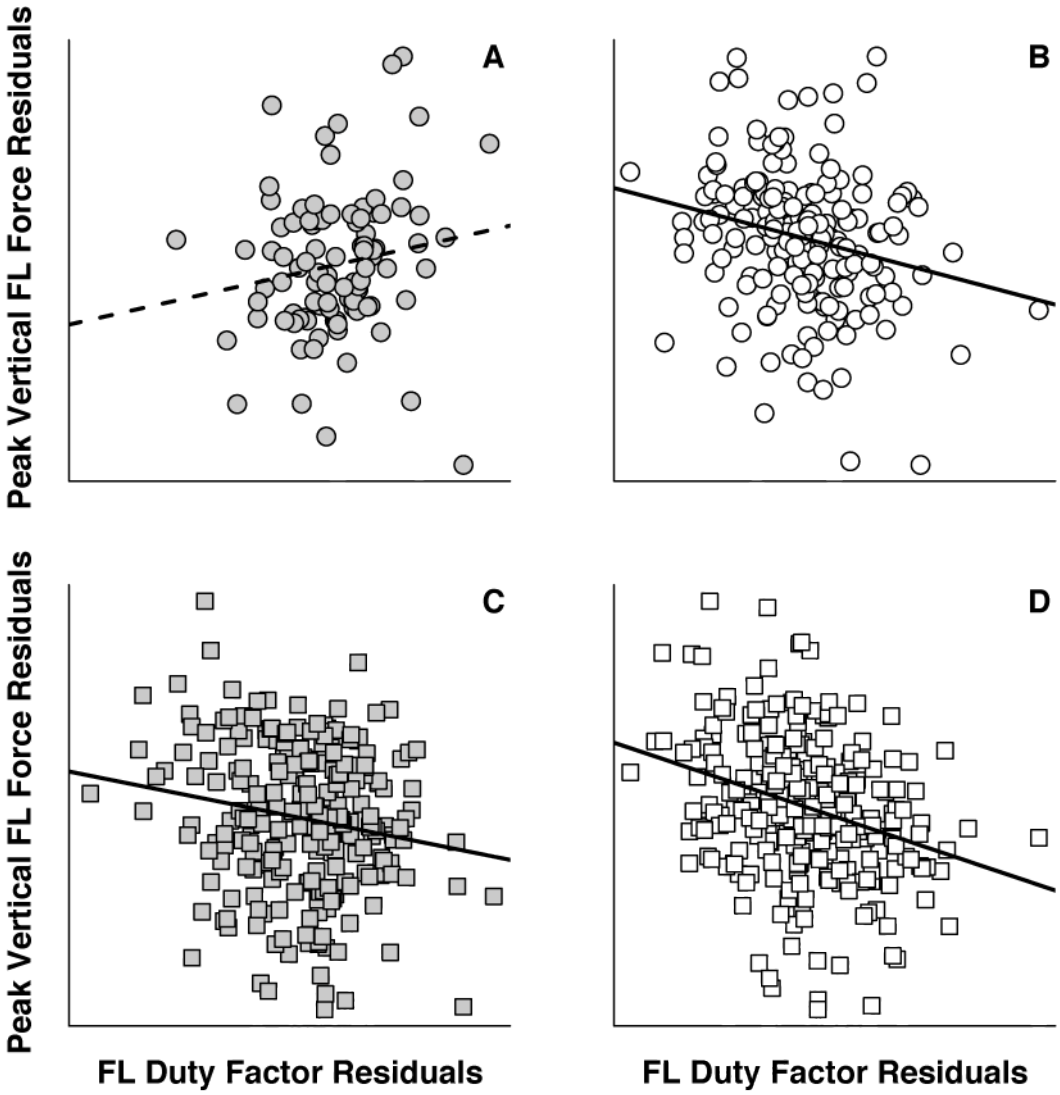

Figure 4.14. Partial regression plots of peak vertical forelimb force against forelimb duty factor.
Data are presented for A) symmetrical strides on the ground, B) symmetrical strides on the pole, C) asymmetrical strides on the ground and D) asymmetrical strides on the pole. Symbols and presentation of data follow Figure 4.9.

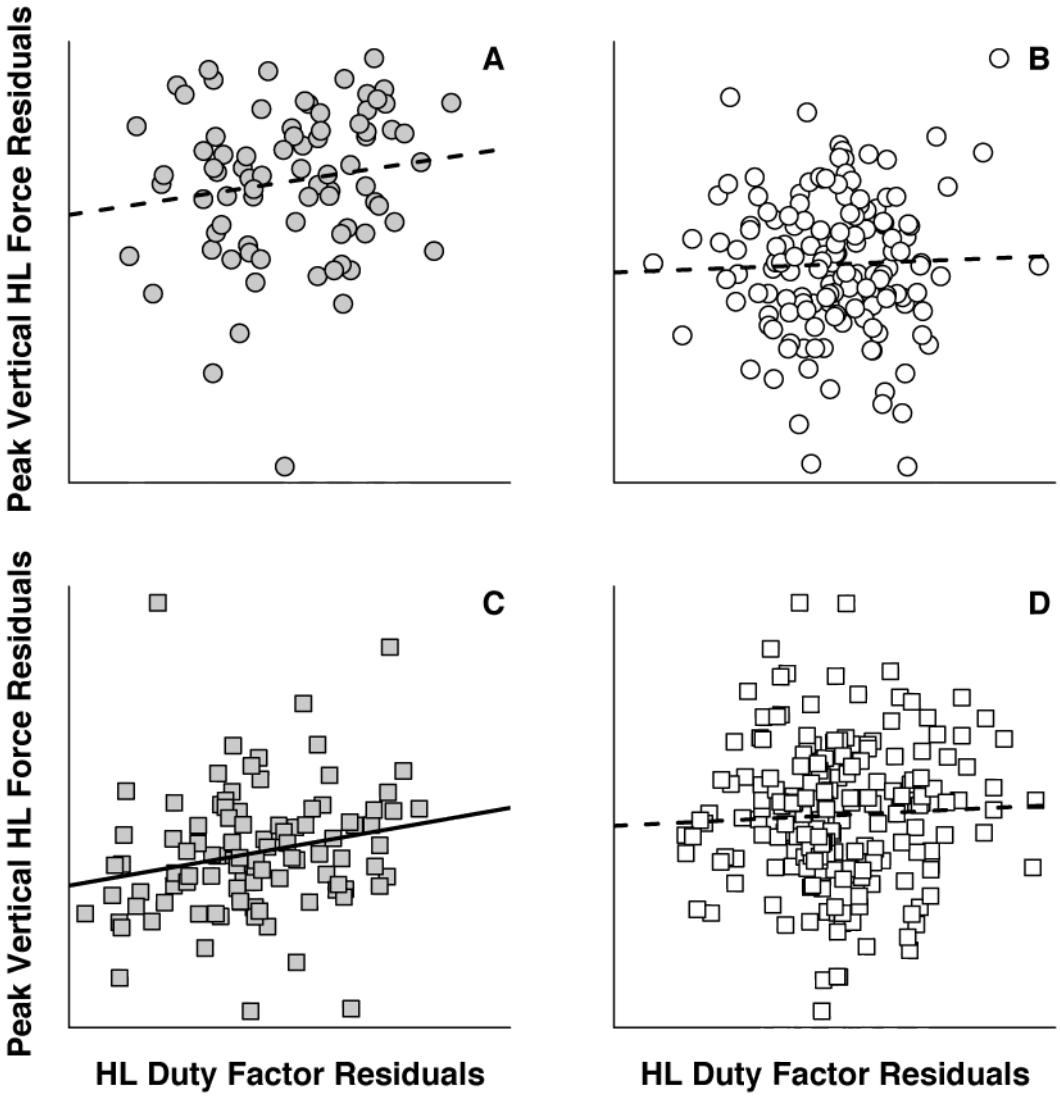

Figure 4.15. Partial regression plots of peak vertical hind limb force against hind limb duty factor.
Data are presented for A) symmetrical strides on the ground, B) symmetrical strides on the pole, C) asymmetrical strides on the ground and D) asymmetrical strides on the pole. Symbols and presentation of data follow Figure 4.9.

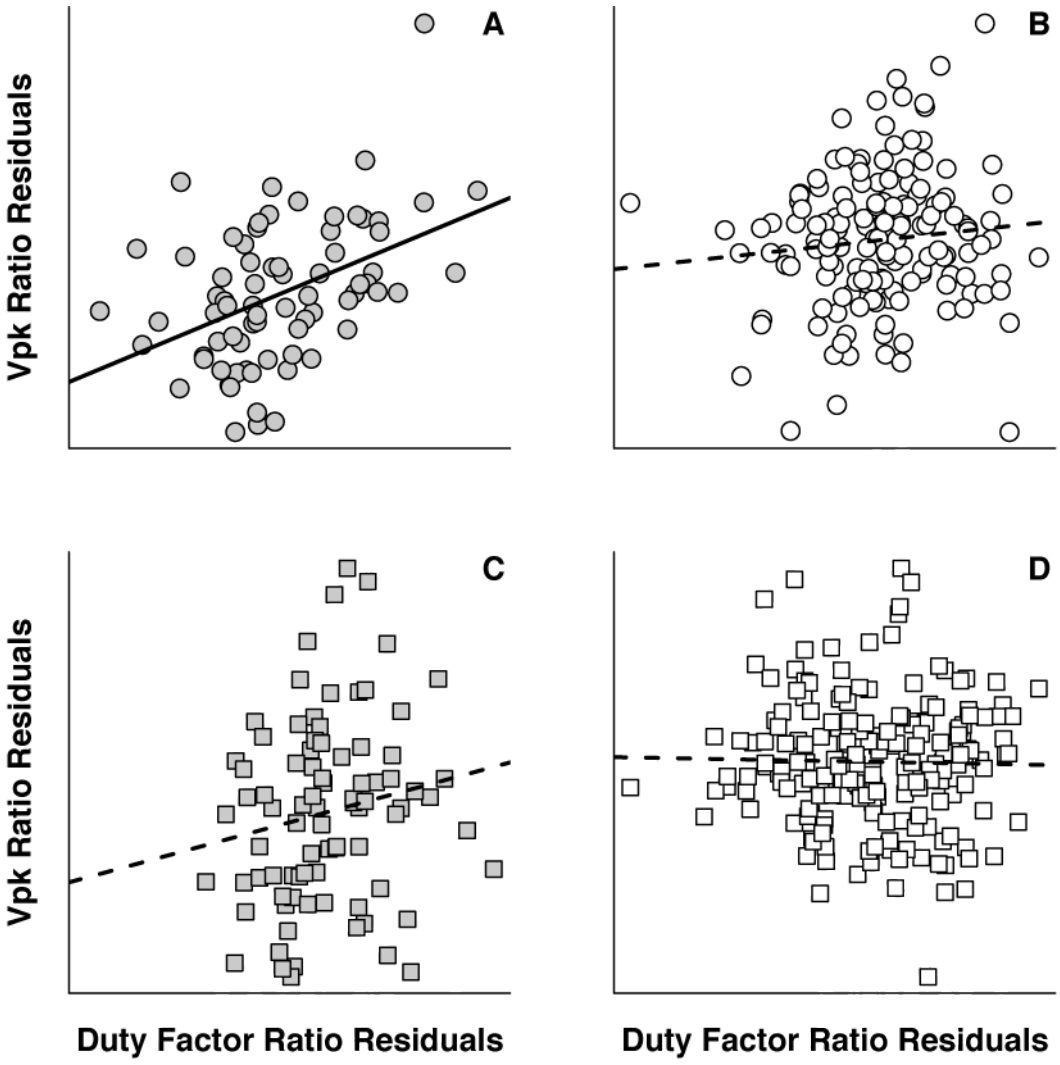

Figure 4.16. Partial regression plots of Vpk ratio against duty factor ratio.
Data are presented for A) symmetrical strides on the ground, B) symmetrical strides on the pole, C) asymmetrical strides on the ground and D) asymmetrical strides on the pole. Symbols and presentation of data follow Figure 4.9.

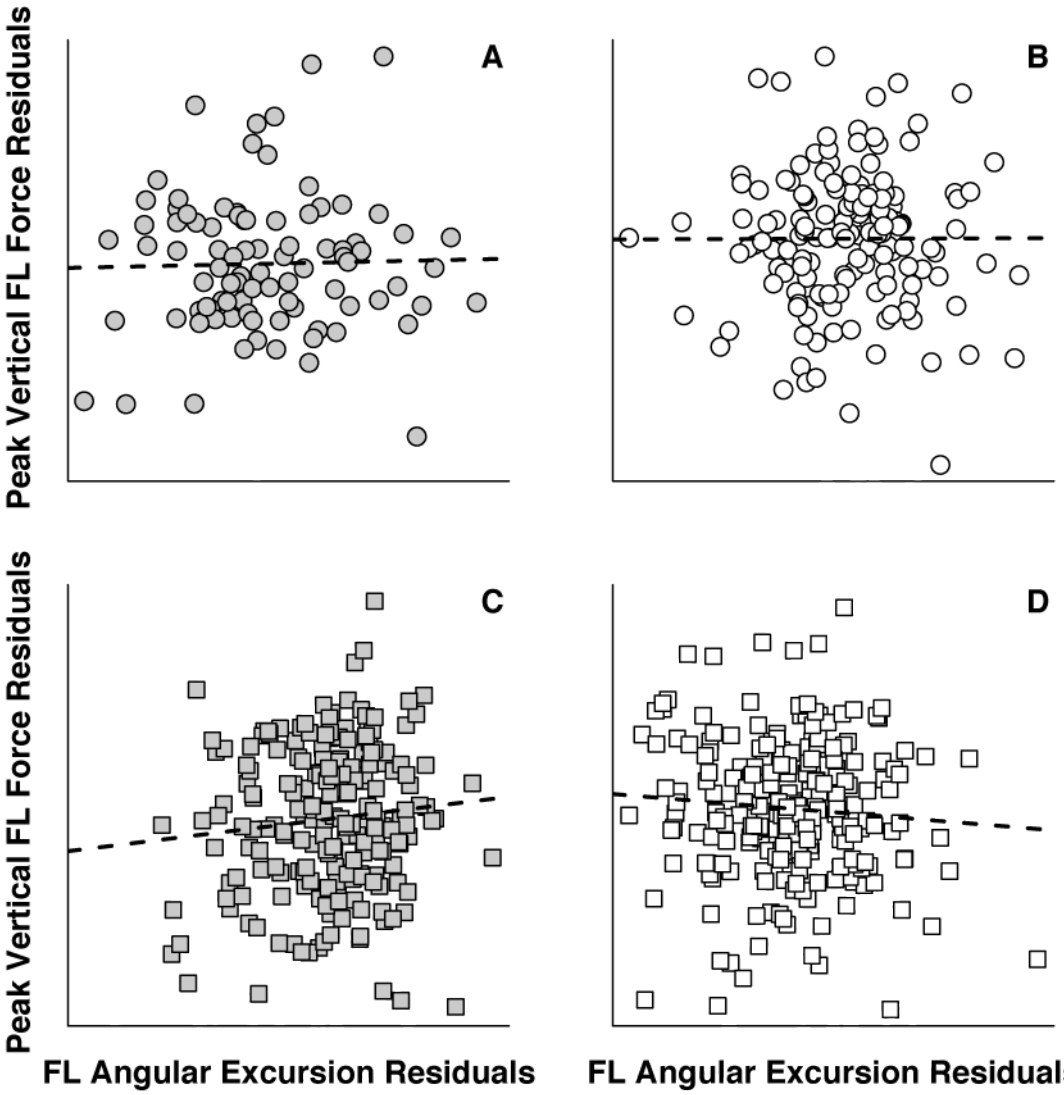

Figure 4.17. Partial regression plots of peak vertical forelimb force against forelimb angular excursion.
Data are presented for A) symmetrical strides on the ground, B) symmetrical strides on the pole, C) asymmetrical strides on the ground and D) asymmetrical strides on the pole. Symbols and presentation of data follow Figure 4.9.

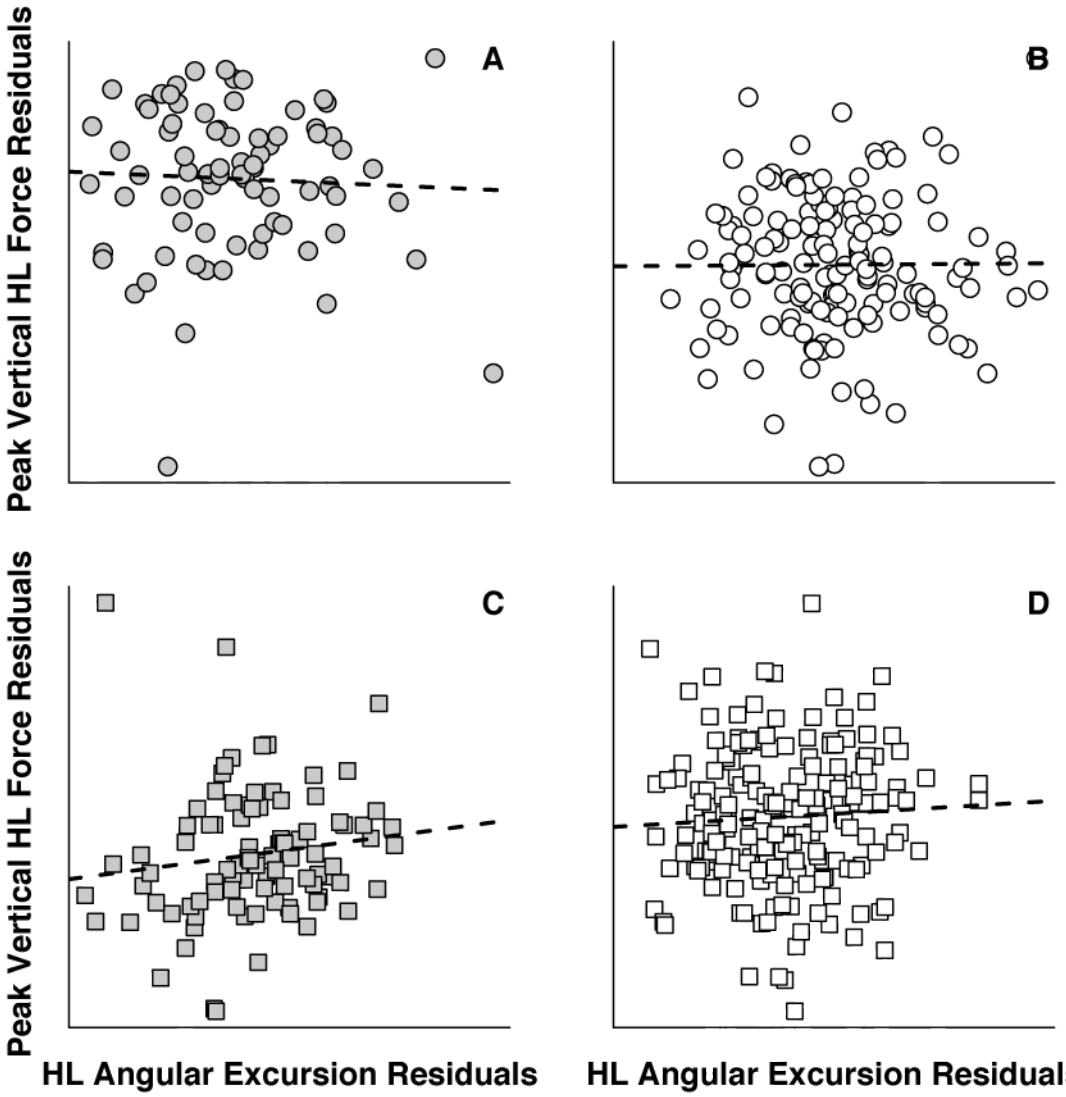

Figure 4.18. Partial regression plots of peak vertical hind limb force against hind limb angular excursion.
Data are for A) symmetrical strides on the ground, B) symmetrical strides on the pole, C) asymmetrical strides on the ground and D) asymmetrical strides on the pole. Symbols and presentation of data follow Figure 4.9.

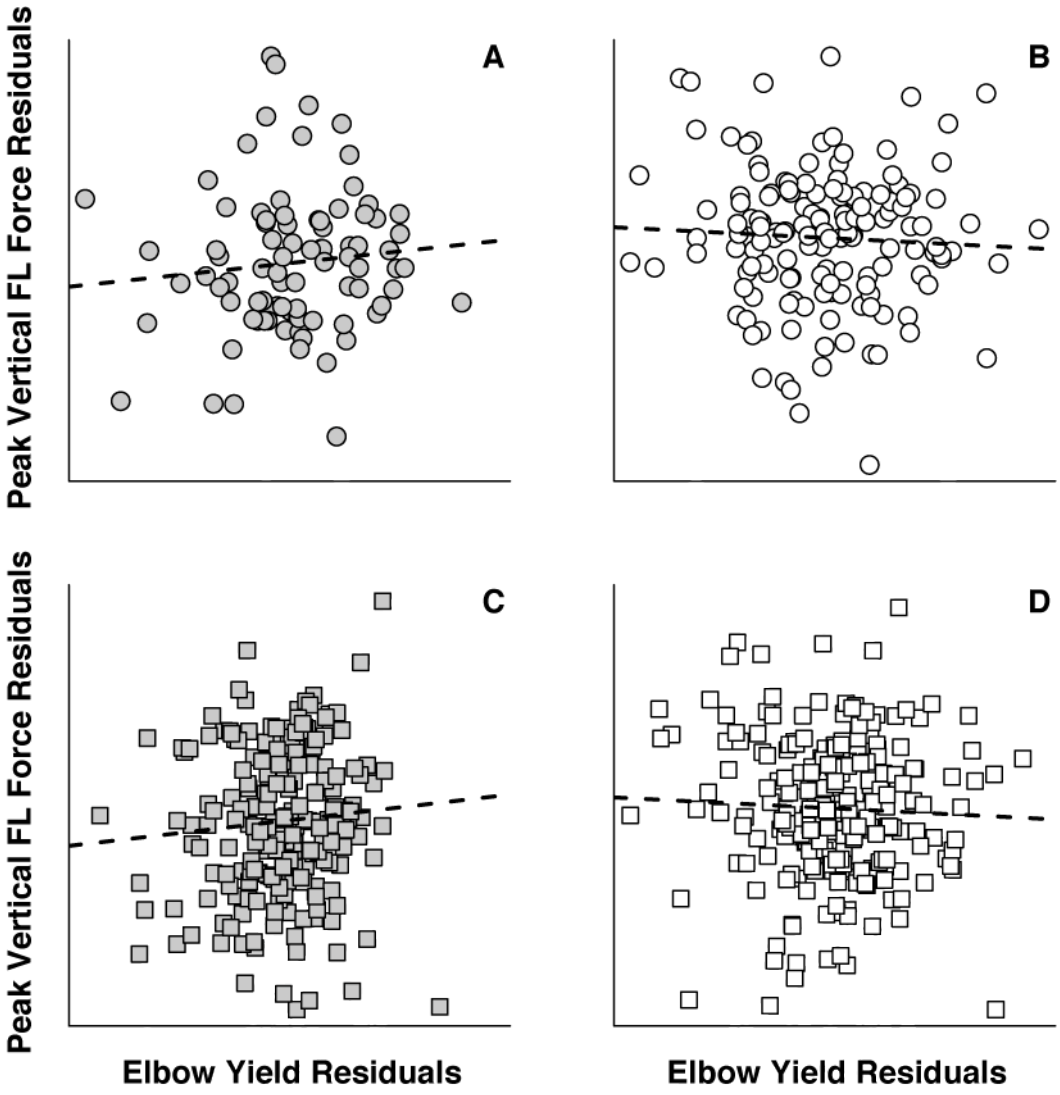

Figure 4.19. Partial regression plots of peak vertical forelimb force against elbow yield.
Data are presented for A) symmetrical strides on the ground, B) symmetrical strides on the pole, C) asymmetrical strides on the ground and D) asymmetrical strides on the pole. Symbols and presentation of data follow Figure 4.9.

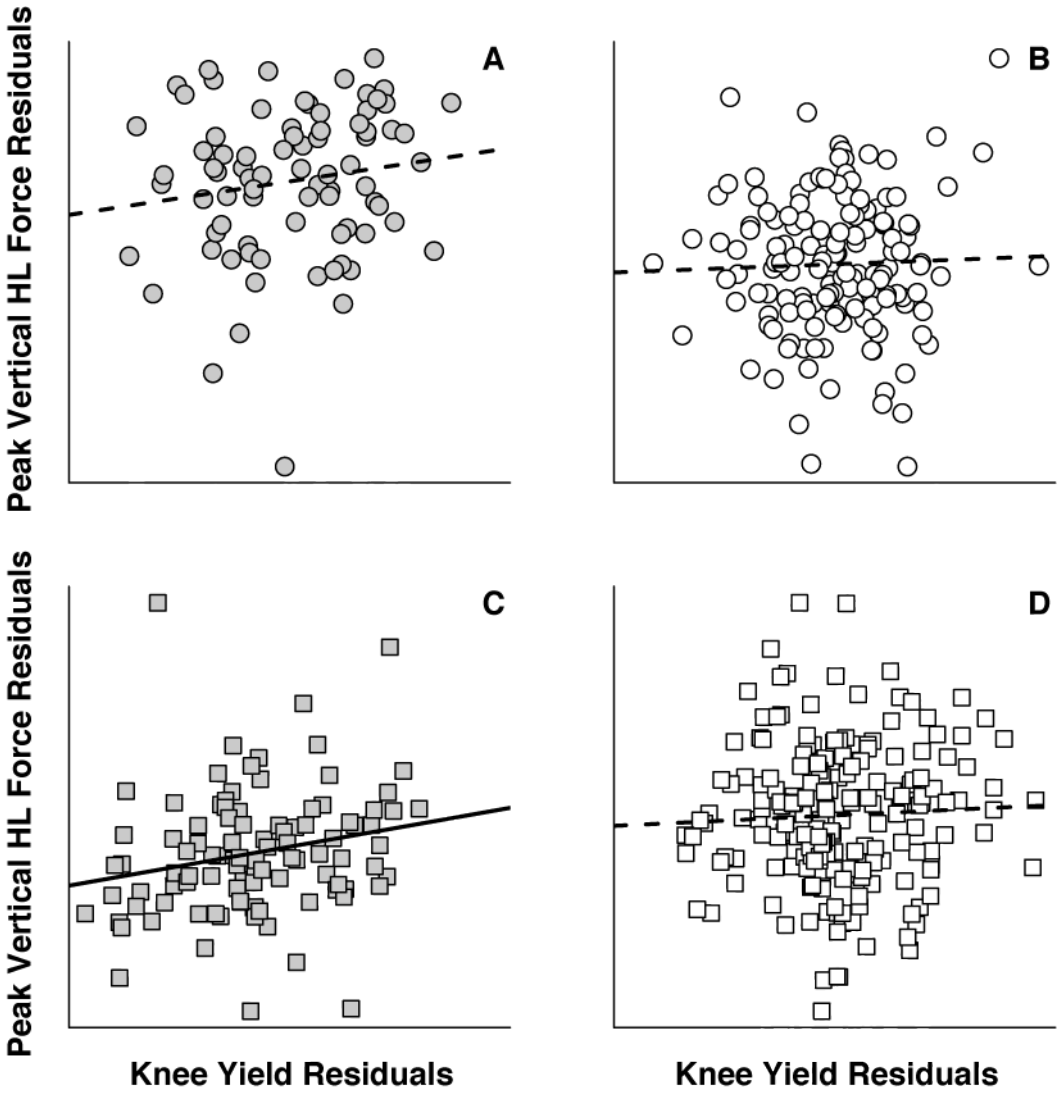

Figure 4.20. Partial regression plots of peak vertical hind limb force against knee yield.
Data are presented for A) symmetrical strides on the ground, B) symmetrical strides on the pole, C) asymmetrical strides on the ground and D) asymmetrical strides on the pole. Symbols and presentation of data follow Figure 4.9.

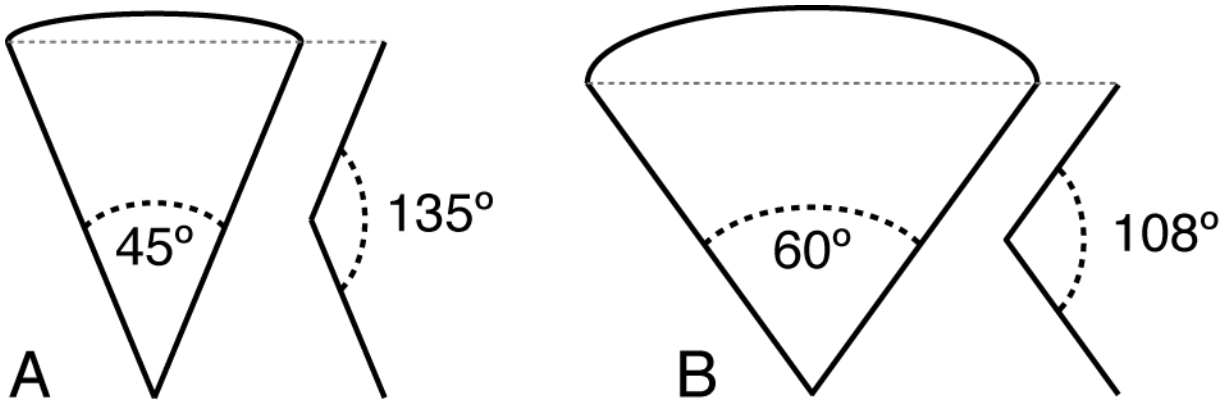

Figure 4.21. Schematic model of the relationship between limb excursion and mid-joint yield.
Two idealized forelimbs are shown: one exhibiting reduced angular excursion (A) and the other more pronounced angular excursion (B). The movement of the limbs is shown throughout stance phase, with the arc at the top representing the trajectory of the shoulder joint if no elbow yield took place. Increasing limb angular excursion requires greater elbow yield to maintain a similar vertical path of the COM. See text for further discussion.

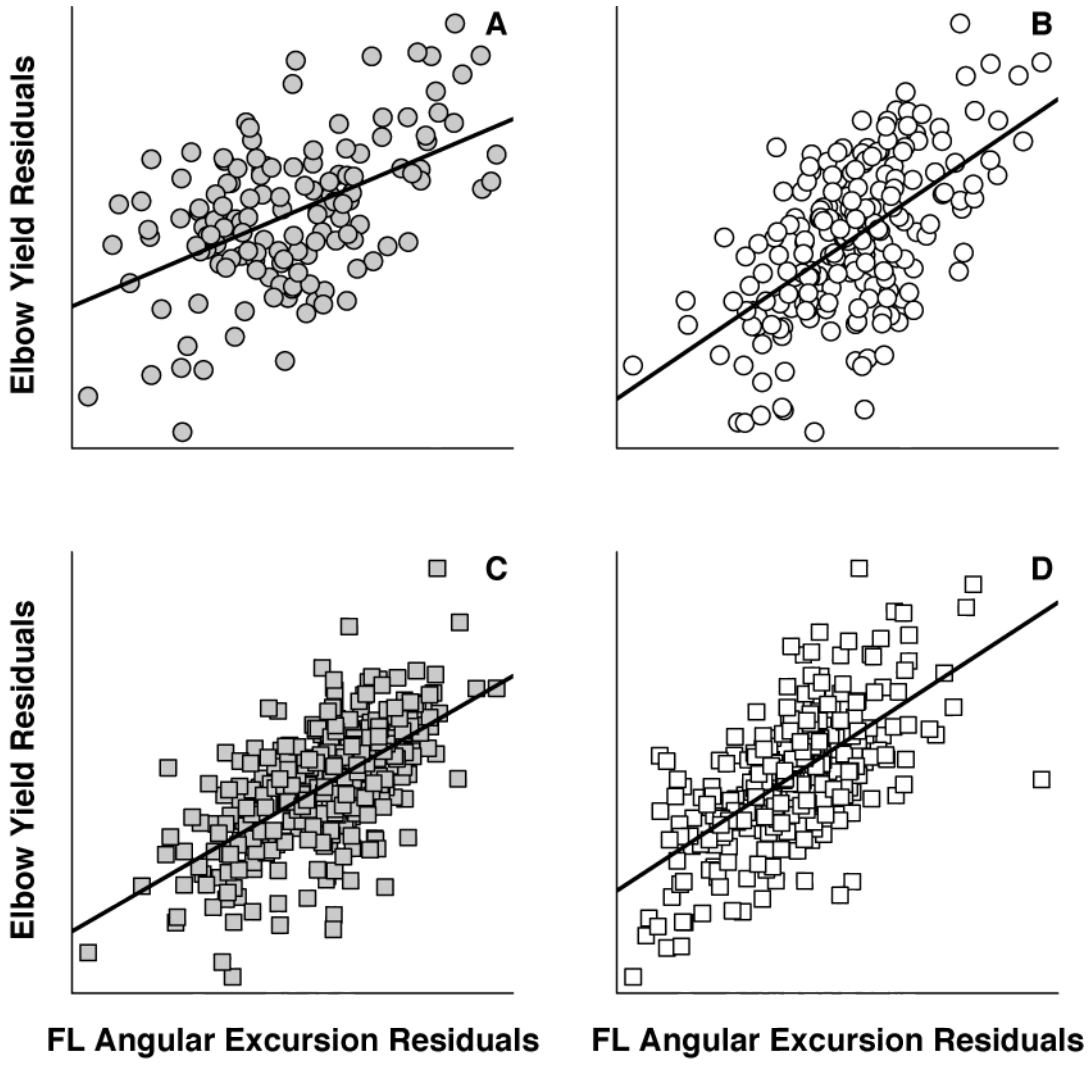

Figure 4.22. Partial regression plots of elbow yield against forelimb angular excursion.
Data are presented for A) symmetrical strides on the ground, B) symmetrical strides on the pole, C) asymmetrical strides on the ground and D) asymmetrical strides on the pole. After controlling for the influence of speed and body size, elbow yield was found to be significantly positively associated with forelimb excursion across gaits and substrates (all $p<0.001$). Symbols and presentation of data follow Figure 4.9.

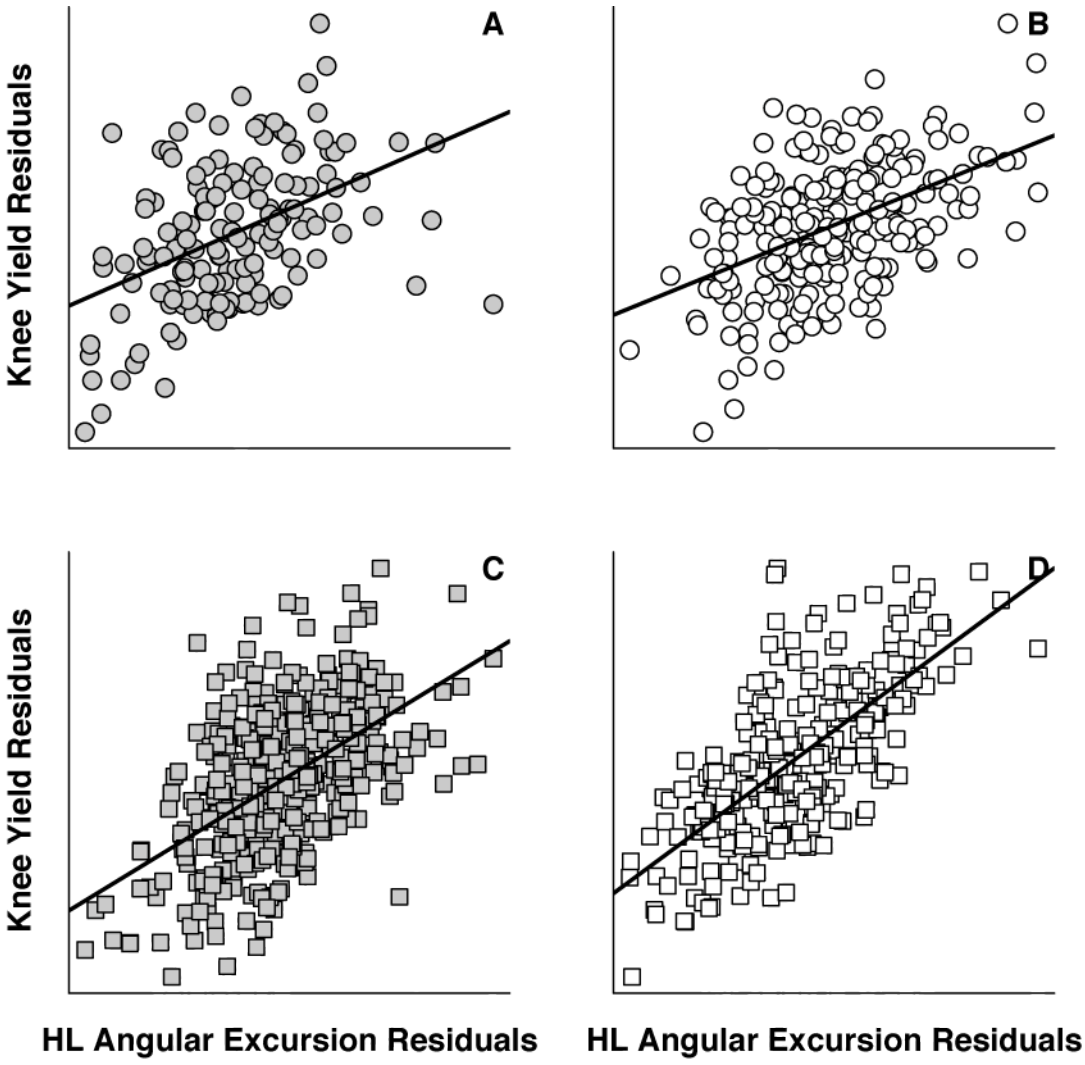

Figure 4.23. Partial regression plots of knee yield against hind limb angular excursion.
Data are presented for A) symmetrical strides on the ground, B) symmetrical strides on the pole, C) asymmetrical strides on the ground and D) asymmetrical strides on the pole. After controlling for the influence of speed and body size, knee yield was found to be significantly positively associated with hind limb excursion across gaits and substrates (all $p<0.001$). Symbols and presentation of data follow Figure 4.9.

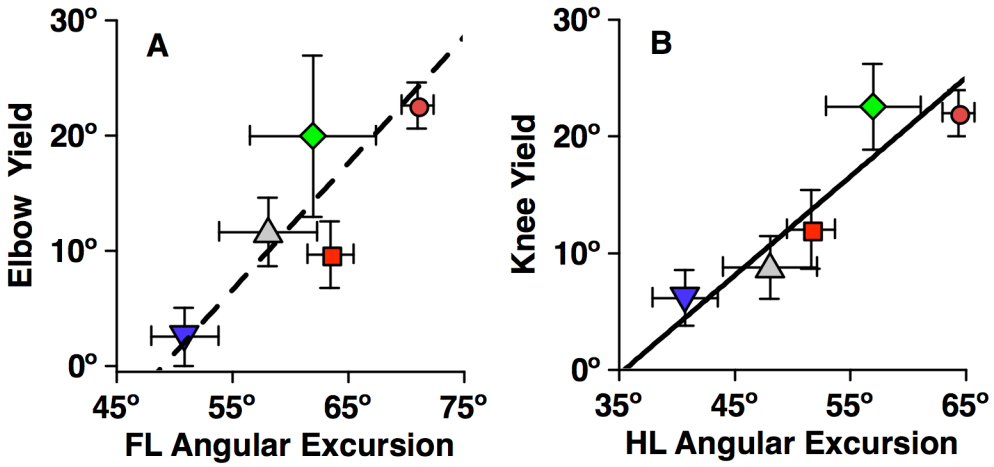

Figure 4.24. Association between limb yield and limb angular excursion across a broad mammalian sample.
Despite the small sample size (N=5 groups) there were distinct positive correlations between mid-joint yield and limb angular excursion across limbs (FL: rho=0.6; *p*(one-tailed)=0.12; HL: rho=0.6; *p*(one-tailed)=0.04). Forelimb angular excursion data from Larson et al. (2000); hind limb angular excursion data from Larson et al. (2001); limb yield data from Larney and Larson (2004). Red circles = primates; green diamonds = marsupials; orange squares = carnivores; gray triangles = rodents; blue inverted triangles = artiodactyls.

Chapter 5: Conclusions

In this dissertation, I used data on ontogenetic changes in body size, limb proportions, body mass distribution and locomotor behavior in growing squirrel monkeys and marmosets as a model system to investigate broader questions of primate and mammalian locomotor ecology and evolution. The three studies presented here illustrate the potential for ontogenetic data to serve as "natural experiments" with which to test hypothetical form-function relationships (German and Meyers, 1989; Hurov, 1991). In the sections below, I review the primary findings from each study and explore some directions for future research.

5.1. Summary

In Chapter 2, "Ontogeny of Limb Joint Mechanics in Squirrel Monkeys (*Saimiri boliviensis*): Implications for Mammalian Limb Growth and Locomotor Development", I used the squirrel monkey data set to examine how changes in limb kinematics and kinetics during growth might mitigate or exacerbate ontogenetic limits on locomotor performance. Relative to whole body mass, newborn primates and other mammals typically have half as much muscle mass as adults (Grand, 1977; Goldspink, 1980; Grand, 1983; Atzeva et al., 2007; Bolter and Zihlman, 2007). Among squirrel monkeys, forelimb muscle mass increases by 50% from neonates to adults and hind limb muscle mass more than doubles (Johnson, 1998). Young animals therefore have relatively less available muscle force than adults, potentially compromising their ability to maintain joint postures during periods of intense limb loading and therefore reducing performance capacity (Carrier, 1996). I found that young squirrel monkeys were able to decrease relative forelimb and hind limb joint moments *via* a combination of changes in limb posture and limb force distribution, thus compensating for potential limits on muscle force at younger ages. My results complement morphometric studies of growing capuchin monkeys (Young, 2005) and other mammals (Carrier, 1983; Peters, 1983) that found that anatomical measures of limb muscle mechanical advantage decline with increasing body size. This study also points to a new functional interpretation of ontogenetic limb scaling in mammals, suggesting that pervasive positive allometry of limb growth (see Tables 2.15 and 2.16) may represent an independent means of reducing substrate reaction force moment arms and moments in immature mammals. Together, this and previous studies suggest that immature mammals may utilize a combination of behavioral and anatomical mechanisms to mitigate ontogenetic limits on locomotor performance (Carrier, 1996). Nonetheless, it is important to note that changes in limb posture, not limb length, explained most of the variation in moment arm length across the ontogenetic squirrel monkey sample, demonstrating the necessity of holistically incorporating morphometric, kinematic and kinetic data into future developmental studies of joint mechanics.

In Chapter 3, "Substrate Determines Asymmetrical Gait Dynamics in Marmosets (*Callithrix jacchus*) and Squirrel Monkeys (*Saimiri boliviensis*)", I used the marmoset and squirrel monkey data sets to investigate the influence of substrate and body size on asymmetrical gait dynamics. Whereas numerous studies have examined how primates modify symmetrical gaits (i.e., walking and running) to increase stability on arboreal

substrates, no study has explicitly focused on how primates might adapt asymmetrical gaits (i.e., galloping and bounding) to ensure arboreal stability. Nevertheless, asymmetrical gaits constitute an important element of most primates' locomotor repertoires, particularly in smaller-bodied taxa (e.g., Vilensky, 1980; Vilensky and Patrick, 1985; Hurov, 1987; Vilensky et al., 1990; Kimura, 1992; Demes et al., 1994; Polk, 2001; Arms et al., 2002; Franz et al., 2005; Schmitt et al., 2006). I found that marmosets and squirrel monkeys displayed numerous kinematic adjustments when using asymmetrical gaits on an elevated pole, including: reducing the vertical excursion of the center of mass, increasing contact durations of both single limbs and forelimb/hind limb pairs, increasing net substrate contact duration across a stride, and using shorter and more frequent strides. Together, these adaptations permitted the monkeys to reduce peak vertical forces when traveling on the pole. Because toppling moments around a branch and branch sway are exacerbated as peak forces increase, reducing peak forces should help to ensure arboreal stability. Marmosets generally showed greater kinematic and kinetic adaptations to pole locomotion than did squirrel monkeys, perhaps as a result of their reduced grasping abilities (Beattie, 1927; Midlo, 1934; Hamrick, 1998) and retreat from the fine-branch foraging environment (Sussman and Kinzey, 1984; Garber, 1992), often understood to be the fundamental adaptive niche for primates (Cartmill, 1972, 1974b; Rasmussen, 1990; Sussman, 1991; Schmitt and Lemelin, 2002). Interestingly, ontogenetic changes in body size had relatively little independent influence on asymmetrical gait dynamics when animals were traveling on the pole, despite biomechanical theory suggesting that potential for arboreal instability is exacerbated as body size increases relative to substrate diameter (Napier, 1967; Cartmill, 1985). It may be that within the ranges of body sizes encompassed in this study (143-346 grams in marmosets and 218-535 grams in squirrel monkeys), the biomechanical challenges posed by a 2.5 cm diameter pole remained fairly constant. Overall, the results of this study demonstrate that primate asymmetrical gait dynamics, often overlooked in previous studies of primate locomotion, merit further investigation.

Finally, in Chapter 4, "Ontogeny of Limb Force Distribution in Squirrel Monkeys (*Saimiri boliviensis*): Implications for Understanding Primate Locomotor Kinetics", I used the ontogenetic squirrel monkey data set as a model system to investigate the biomechanical bases of "hind limb dominance" in limb force distribution among primates. Whereas most mammals generate greater peak vertical forces with their forelimbs, primates typically generate greater peak vertical forces with their hind limbs (Kimura et al., 1979; Reynolds, 1985a, 1985b; Kimura, 1992; Demes et al., 1994; Li et al., 2004; Hanna et al., 2006). A shift from "forelimb dominant" to "hind limb dominant" locomotion has been presented as an adaptive strategy that permitted basal primates to emancipate their forelimbs from a weight-bearing function, thus facilitating foraging and locomotion in the potentially unstable "fine-branch niche" (Cartmill, 1974b, 1974a; Schmitt, 1994, 1999; Cartmill et al., 2002; Schmitt and Lemelin, 2002). I employed morphological, kinematic and kinetic variation in the growing squirrel monkeys to evaluate two previously developed models of mammalian limb force distribution: the Center of Mass (COM) Position model (Gray, 1944; Raichlen et al., 2007) and the Compliant Limb model (Schmitt, 1994, 1998, 1999; Schmitt and Hanna, 2004). The COM Position model predicts that limb force distribution varies as a function of the horizontal distance between the COM vector (i.e., the center of gravity) and the centers of

pressure of the hands and feet. The Compliant Limb model predicts that reductions in peak loading should be associated with increases in substrate contact durations, limb excursions, and limb yield from touchdown to mid-stance. Results provided greater support for the COM Position model. Over the course of squirrel monkey development, relative forelimb peak vertical forces decreased with size whereas relative hind limb peak vertical forces increased with size. Squirrel monkeys thus transitioned from "forelimb dominant" infants to "hind limb dominant" juveniles. Changes in limb force distribution were accompanied by a net caudal translation in the position of the whole-body COM – moving from 40% of horizontal trunk length from the shoulders to the hips at the smallest body sizes to 60% of trunk length at the largest body size. Overall, COM position was able to explain 57% of the variance in forelimb-hind limb force distribution across experiments. Growing monkeys also had their feet closer to the transverse midline of the trunk as body size increased, both on average across a stride and at the moment of peak vertical force, as predicted by the COM Position model. By contrast, limb forces and limb force distribution failed to show any consistent association with measures of gait compliance. In sum, I was able to show that relatively simple parameters, such as whole-body COM position and hand and foot placement, could explain a significant part of the variation in limb force distribution in growing squirrel monkeys, in contrast to previous theories of primate limb force distribution that relied on complex kinematic adjustments (e.g., Reynolds, 1985a; Schmitt, 1994; 1998; 1999).

5.2. Future studies

5.2.1. Expanded dataset of squirrel monkey growth

As detailed in the studies presented above, squirrel monkeys exhibited numerous significant changes in locomotor kinematics and kinetics over development. Some of these kinematic/kinetic changes were clearly tied to somatic growth. For instance, increasing limb length at least partially determined ontogenetic changes in limb joint mechanics (Chapter 2) and the caudal translation of the whole-body COM explained most of the ontogenetic variation in limb force distribution (Chapter 4). In future studies, it would be interesting to explore the interaction between locomotion development and the somatic growth of other morphological domains. For instance, do squirrel monkeys exhibit the same developmental declines of "anatomical mechanical advantage" (i.e., bony muscle lever arm at a joint divided by the length of the limb distal to the joint) documented in other mammalian taxa (Carrier, 1983; Peters, 1983; Young, 2005)? Additionally, although previous studies indicate that whole body muscle mass doubles during squirrel monkey development (e.g., Johnson, 1998), it would be informative to have more detailed data on ontogenetic changes in the relative size and physiological cross-sectional area of individual limb muscles, providing more precise assessments of ontogenetic limits on available muscle force at particular joints and during specific behaviors. Finally, do squirrel monkeys also show the negative allometry of limb bone cross-sectional geometry (i.e., cortical areas and moments of area) that have been documented for other mammalian taxa (e.g., Carrier, 1983; Hartwig-Scherer, 1995; Heinrich et al., 1999; Lammers and German, 2002; Ruff, 2003a; Main and Biewener,

2004, 2007; Young et al., in preparation)? If so, how might such growth-related changes in structural design restrict or facilitate locomotor performance?

5.2.2. Developmental studies of joint mechanics in an expanded mammalian sample

The analyses presented in Chapter 2 represent the first attempt to quantify ontogenetic changes in body size, limb lengths, joint postures and limb kinetics simultaneously in any quadrupedal mammal. As such, it is impossible to say whether the developmental increases in relative joint loading observed among squirrel monkeys are pervasive across mammals or unique to this species. Nevertheless, it appears that most immature mammals are characterized by early deficits in relative muscle mass (Grand, 1977; Goldspink, 1980; Grand, 1983; Atzeva et al., 2007; Bolter and Zihlman, 2007) and increased predation pressure (Werner and Gillam, 1984; Janson and Van Schaik, 1993; Carrier, 1996; Herrel and Gibb, 2006; Bolter and Zihlman, 2007). Given the established variability in limb growth allometry, postural development and ontogenetic patterns of limb loading across mammals (see sections 2.4.1, 2.4.2, 2.4.4 and 4.4), additional developmental studies of joint mechanics would greatly contribute to a general understanding of how morphology and locomotor mechanics interact to cope with ecological demands and facilitate early locomotor efforts. Longitudinal ontogenetic studies of mammals with widely divergent levels of neuromuscular maturity and mobility at birth (i.e., "precocial" versus "altricial" mammals) would be particularly informative (e.g., Schilling, 2005).

5.2.3. Additional studies of callitrichid quadrupedalism

In Chapter 3, I showed that marmosets using asymmetrical gaits on simulated arboreal substrates required significantly greater kinematic "adjustment" to maintain stability than did squirrel monkeys. I interpreted this finding as evidence that marmosets' derived autopodial anatomy and retreat from the fine-branch foraging niche had compromised their ability to travel efficiently on narrow substrates. Given the derived nature of marmoset anatomy (Beattie, 1927; Midlo, 1934; Hamrick, 1998), ecology (Sussman and Kinzey, 1984; Garber, 1992), and locomotor mechanics (Schmitt, 2003a), additional biomechanical studies of the effects of substrate size and orientation on marmoset locomotion could be informative (e.g., Stevens, 2003). Simultaneous study of several callitrichid and cebid genera known to diverge in autopodial anatomy (e.g., Hamrick, 1998; Lemelin and Grafton, 1998) could have great potential for illuminating the functional utility of basal primate locomotor adaptations, such as grasping hands and feet and flattened nails on all digits.

5.2.4. Gait transitions and the scaling of stride frequency and stride length in primates

Most mammals thus far studied exhibit reliable discontinuous transitions in gait use, stride length and stride frequency at set physiological speeds. For example, Heglund et al. (1974) found that speed at the trot-gallop (i.e., symmetrical-asymmetrical) transition closely tracked body mass across an eclectic mammalian sample. Up to the trot-gallop transition, animals increased speed *via* a combination of increasing stride frequency and

increasing stride length. By contrast, past the transition point, stride frequency remained nearly constant and speed was only increased via increases in stride length. Similarly, most mammals exhibit predictable gait transitions when physiological speed is evaluated on the basis of Froude number, transitioning from a walk to a run (i.e., trot) at a Froude number of 0.5 and from symmetrical gaits to asymmetrical gaits at a Froude number between 2 and 3 (Alexander and Jayes, 1983)[5]. In contrast, squirrel monkeys and marmsosets walking on terrestrial and simulated arboreal substrates continued to increase both stride length and stride frequency with speed during asymmetrical gaits (Fig 3.9). Vilensky (1980) found similar results in rhesus macaques (*Macaca mulatta*). Moreover, Froude numbers for symmetrical and asymmetrical gaits widely overlapped across both substrates (Section 4.3.1). It may be that primates, which typically do not use a running trot (Demes et al., 1990; Demes et al., 1994; Preuschoft and Günther, 1994; Schmitt et al., 2006), transition to asymmetrical gaits at lower speeds and stride frequencies, and with less regularity, than other mammals. A broader-based survey of gait transition patterns and associated changes in stride length and frequency across primates is required to elucidate the generality of the patterns observed in this dissertation. Such a survey would be a valuable addition to the mammalian gait literature.

5.2.5. Multiple force platform studies of primate quadrupedalism

Previous studies of primate limb force distribution have primarily relied on measurements of peak vertical forces on a single forelimb or hind limb during a stride (Kimura et al., 1979; Demes et al., 1994; Schmitt and Lemelin, 2002; Schmitt, 2003a; Lemelin and Schmitt, 2004; Schmitt and Hanna, 2004; Schmitt and Lemelin, 2004; Franz et al., 2005; Hanna et al., 2006; Lemelin and Schmitt, 2007), although a few studies have considered limb force distribution within strides (Wallace and Demes, 2007; Chapter 4) or used vertical impulse as a metric (i.e., the area under the force-time curve: Kimura, 1987, 1992, 2000). However, measures of impulse development in each of the four limbs across entire strides are necessary to precisely evaluate the interaction of limb kinematics, COM position and body weight distribution (Bertram et al., 1997). Future studies incorporating three-dimensional tracking of limb kinematics and multiple force platform recording of limb kinetics (i.e., a minimum of four platforms) would be a substantial addition to the literature on primate locomotor kinetics.

For example, simultaneous recording from multiple force platforms would permit direct evaluation of Reynolds' (1985a) hypothesis the primates reduce peak vertical forelimb forces *via* selective activation of hind limb retractor muscles near the moment of hind limb touchdown (see Section 4.1 for a more extended discussion of this hypothesis). Simultaneous changes in forelimb and hind limb peak forces and impulses could be documented for a range of hind limb protraction angles and the corresponding effects on

[5] Alexander and Jayes (1983) calculated Froude number as $u^2(gh)^{-1}$, where u is horizontal speed, g is gravitational acceleration and h is a measure of stature (usually hip height or the cube root of body mass). By contrast, I used $u(gh)^{-2}$ throughout the studies presented above. By this calculation, the walk-trot transition speed would take place at a Froude number of 0.71 and the symmetrical-asymmetrical transition would take place at a Froude number between 1.41 and 1.73.

Vpk ratios could be analyzed. Although there are theoretical reasons to doubt the explanatory power of Reynold's (1985) hypothesis (Gray, 1944; Raichlen et al., 2007; see section 4.1), some kinematic and electromyographic data support the predictions of the model (Kimura et al., 1979; Stern and Susman, 1981; Ishida et al., 1985; Reynolds, 1985b; Larson et al., 2001; Larson and Stern, 2008), suggesting a more thorough kinetic evaluation is warranted.

Multiple force platform studies would also permit more intimate investigation the relationship between limb phase, weight distribution, and COM mechanics during quadrupedal walking. Across a broad multitude of animals, the efficient exchange of forward kinetic and gravitational potential energy *via* pendular mechanics has been shown to be the primary means of reducing the external work required to lift and accelerate the COM during walking (Cavagna et al., 1977; Heglund et al., 1982; Full, 1989; Farley and Ko, 1997; Griffin and Kram, 2000; Reilly and Biknevicius, 2003; Griffin et al., 2004). For a walking biped, pendular mechanics can be easily achieved by vaulting over the stance leg. Only during double limb support, when body weight is being transferred from one limb to the next, do the mechanics become more complicated and energy may be dissipated (Donelan et al., 2002; Ruina et al., 2005). By contrast, quadrupeds are mechanically similar to two bipeds linked by a semi-flexible trunk (e.g., Cartmill et al., 2002). As such, accounting for the sources and limits of mechanical energy exchange in quadrupedal walkers can be more complicated. Fluctuations in potential and kinetic energy at one limb girdle can potentially be offset by fluctuations at the other girdle, reducing the net movement of the COM and limiting energy exchange (Reilly and Biknevicius, 2003). Griffin et al. (2004) recently demonstrated that variation in two parameters, limb phase (i.e., the temporal lag between ipsilateral forelimb-hind limb pairs) and body weight distribution (i.e., the percentage of body weight supported by the forelimbs and the hind limbs), determined vertical COM movements in a sample of walking dogs, showing how control of these parameters could allow quadrupedal mammals to achieve pendular mechanics despite the aforementioned constraints. Nevertheless, Griffin et al. (2004: 3555) note that "a broader comparative survey of animals that naturally vary in limb phase" would be required to more rigorously test their model. Both limb phase and limb force distribution vary widely between and within quadrupedal primates (Vilensky and Gankiewicz, 1989; Vilensky and Moore, 1992; Demes et al., 1994; Stevens, 2003; Schmitt and Hanna, 2004; Hanna et al., 2006; Chapter 4), suggesting that primates may be an ideal group in which to probe the relationship between limb phase, weight distribution and COM mechanics. Multiple force platform recording would facilitate limb-by-limb evaluation of impulse distribution and fluctuations in mechanical energy across a stride, permitting a highly detailed test of the association among these parameters.

Finally, as noted in Section 1.1, most quadrupedal primates differ from most other mammalian quadrupeds in predominantly using diagonal sequence (DS) gaits when walking and running, during which hind limb touchdowns are followed by contralateral forelimb touchdowns. By contrast, most quadrupedal non-primate mammals predominantly use lateral sequence (LS) gaits, during which hind limb touchdowns are followed by ipsilateral forelimb touchdowns (Muybridge, 1887; Hildebrand, 1967; Prost, 1969; Rose, 1973; Rollinson and Martin, 1981; Vilensky and Larson, 1989; Meldrum, 1991; Cartmill et al., 2002; Schmitt and Lemelin, 2002). Although the functional

correlates of gait selection in primates and other mammals remain controversial (Rollinson and Martin, 1981; Vilensky and Larson, 1989; Cartmill et al., 2002; Stevens, 2003; Shapiro and Raichlen, 2005; Cartmill et al., 2007b, 2007a; Shapiro and Raichlen, 2007b; Wallace and Demes, 2007; Young et al., 2007) most researchers agree that DS gaits are foremost an arboreal adaptation. Evidence that non-primate arboreal mammals also use DS gaits bolsters this assertion (White, 1990; McClearn, 1992; Pridmore, 1994; Lemelin et al., 2003; Lemelin and Schmitt, 2007). Some researchers have suggested that DS gaits augment lateral stability, permitting arboreal animals to exert opposing mediolateral forces and torques and counteract tendencies towards disruptive rolling or yawing (Prost, 1969; Crompton et al., 2000). Only multiple force platform recording of simultaneous forelimb and hind limb forces during walking on a variety of substrates can permit thorough evaluation of this hypothesis. Such a study would be a valuable contribution to the literature on the interaction between stability and gait selection in mammals.

Literature Cited

Aiello L, and Dean C (1990) Human Evolutionary Anatomy. San Diego: Academic Press.

Alexander RM (1984) Stride length and speed for adults, children, and fossil hominids. American Journal of Physical Anthropology *63:*23-27.

Alexander RM (2002) Stability and manoeuverability of terrestrial vertebrates. Integrative and Comparative Biology *42:*158-164.

Alexander RM, and Jayes AS (1983) A dynamic similarity hypothesis for the gaits of quadrupedal mammals. Journal of Zoology, London *201:*135-152.

Alexander RM, Jayes AS, Maloiy GMO, and Wathuta EM (1979) Allometry of limb bones of mammals from shrews (*Sorex*) to elephant (*Loxodonta*). Journal of Zoology, London *189:*305-314.

Alexander RM, and Maloiy GMO (1984) Stride lengths and stride frequencies of primates. Journal of Zoology, London *202:*577-582.

Altmann J (1980/2001) Baboon Mothers and Infants. Chicago: University of Chicago Press.

Arms A, Voges D, Fischer MS, and Preuschoft H (2002) Arboreal locomotion in small new-world primates. Zeitschrift fur Morphologie und Anthropologie *83:*243-263.

Atzeva M, Demes B, Kirkbride ML, Burrows AM, and Smith TD (2007) Comparison of hind limb muscle mass in neonate and adult prosimian primates. Journal of Human Evolution *52:*231-242.

Barclay OR (1953) Some aspects of the mechanics of mammalian locomotion. Journal of Experimental Biology *30:*116-120.

Beattie J (1927) The anatomy of the common marmoset. Proceedings of the Zoological Society of London *27:*593-718.

Beck RJ, Andriacchi TP, Kuo KN, Fermier RW, and Galante JO (1981) Changes in the gait patterns of growing children. Journal of Bone and Joint Surgery *63-A:*1452-1457.

Bertram JEA, Lee DV, Case HN, and Todhunter RL (2000) Comparison of the trotting gaits of laborador retrievers and greyhounds. American Journal of Veterinary Research *61:*832-838.

Bertram JEA, Lee DV, Todhunter RL, Foels WS, Williams AJ, and Lust G (1997) Multiple force platform analysis of the canine trot: a new approach to assessing basic characteristics of locomotion. Veterinary and Comparative Orthopaedic Traumatology *10:*160-169.

Bewick GS, Reid B, Jawaid S, Hatcher S, and Shanley L (2004) Postnatal emergence of mature release properties in terminals of rat fast- and slow-twitch muscles. European Journal of Neuroscience *19:*2967-2976.

Biewener AA (1983) Allometry of quadrupedal locomotion: the scaling of duty factor, bone curvature and limb orientation to body size. Journal of Experimental Biology *105:*147-171.

Biewener AA (1989) Scaling body support in mammals: limb posture and muscle mechanics. Science *245:*45-48.

Biewener AA (1990) Biomechanics of mammalian terrestrial locomotion. Science *250:*1097-1103.

Biewener AA (1991) Musculoskeletal design in relation to body size. Journal of Biomechanics *24:*19-29.

Biewener AA (2004) Muscle mechanical advantage of human walking and running: implications for energy cost. Journal of Applied Physiology *97:*2266-2274.

Biewener AA (2005) Biomechanical consequences of scaling. Journal of Experimental Biology *208:*1665-1676.

Biewener AA, and Full RJ (1992) Force platform and kinematic analysis. In AA Biewener (ed.): Biomechanics: Structures and Systems. Oxford: Oxford University Press, pp. 45-73.

Biknevicius AR, Heinrich RE, and Dankoski E (1997) Effects of ontogeny on locomotor kinetics. Journal of Morphology *232:*235.

Biknevicius AR, Mullineaux DR, and Clayton HM (2004) Ground reaction forces and limb function in tölting Icelandic horses. Equine Veterinary Journal *36:*743-747.

Bloch JI, and Boyer DM (2002) Grasping primate origins. Science *298:*1606-1610.

Bloch JI, and Boyer DM (2007) New skeletons of Paleocene-Eocene Plesiadapiformes: a diversity of arboreal positional behaviors in early primates. In MJ Ravosa and M Dagosto (eds.): Primate Origins: Adaptations and Evolution. New York, NY: Springer, pp. 535-581.

Blumberg-Feldman H, and Eilam D (1995) Postnatal development of synchronous stepping in the gerbil (*Gerbillus dasyurus*). Journal of Experimental Biology *198:*363-372.

Boinski S (1987) Birth synchrony in squirrel monkeys (*Saimiri oerstedi*): a strategy to reduce neonatal predation. Behavioral Ecology and Sociobiology *21:*393-400.

Boinski S (1989) The positional behavior and substrate use of squirrel monkeys: ecological implications. Journal of Human Evolution *18:*659-677.

Boinski S (1999) The social organization of squirrel monkeys: implications for ecological models of social evolution. Evolutionary Anthroplogy *8:*101-112.

Boinski S, and Fragaszy DM (1989) The ontogeny of foraging in squirrel monkeys, *Saimiri oerstedi*. Animal Behaviour *37:*415-428.

Boinski S, Kauffman L, Westoll A, Stickler CM, Cropp S, and Ehmke E (2003) Are vigilance, risk from avian predators and group size consequences of habitat structure? A comparison of three species of squirrel monkey (*Saimiri oerstedii*, *S. boliviensis*, and *S. sciureus*). Behaviour *140:*1421-1467.

Boinski S, Sughrue K, Selvaggi L, Quatrone R, Henry M, and Cropp S (2002) An expanded test of the ecological model of primate social evolution: competitive regimes and female bonding in three species of squirrel monkeys (*Saimiri oerstedii, S. boliviensis,* and *S. sciureus*). Behaviour *139:*227-261.

Bolter D, and Zihlman A (2007) Primate growth and development: a functional and evolutionary perspective. In CJ Campbell, A Fuentes, KC MacKinnon, MA Panger and SK Bearder (eds.): Primates in Perspective. New York: Oxford Unversity Press, pp. 408-422.

Box GEP, and Cox DR (1964) An analysis of transformations. Journal of the Royal Statistical Society: Series B (Methodological) *26:*211-243.

Bramblett CA (1967) Pathology in the Darajani baboon. American Journal of Physical Anthropology *26:*331-340.

Brear K, Currey JD, and Pond CM (1990) Ontogenetic changes in the mechanical properties of the femur of the polar bear, *Ursus maritimus*. Journal of Zoology, London *222:*49-58.

Buikstra JE (1975) Healed fractures in *Macaca mulatta*: age, sex and symmetry. Folia Primatologica *23:*140-148.

Bullimore SR, and Donelan JM (2008) Criteria for dynamic similiarity in bouncing gaits. Journal of Theoretical Biology *250:*339-248.

Bundle MW, and Dial KP (2003) Mechanics of wing-assisted incline running (WAIR). Journal of Experimental Biology *206:*4553-4564.

Carrier DR (1983) Postnatal ontogeny of the musculo-skeletal system in the Black-tailed jack rabbit (*Lepus californicus*). Journal of Zoology, London *201:*27-55.

Carrier DR (1995) Ontogeny of jumping performance in the black-tailed jackrabbit (*Lepus californicus*). Zoology: Analysis of Complex Systems *98:*309-313.

Carrier DR (1996) Ontogenetic limits on locomotor performance. Physiological Zoology *69:*467-488.

Carrier DR, Deban S, and Fischbein T (2007) Locomotor function of forelimb protractor and retractor muscles of dogs: evidence of strut-like behavior at the shoulder. Journal of Experimental Biology *211:*150-162.

Carter ML, Pontzer H, Wrangham R, and Peterhans JK (2008) Skeletal pathology in *Pan troglodytes schweinfurthii* in Kibale National Park, Uganda. American Journal of Physical Anthropology *135:*389-403.

Cartmill M (1972) Arboreal adaptations and the origin of the Order Primates. In R Tuttle (ed.): The Functional and Evolutionary Biology of Primates. Chicago: Aldine, pp. 97-122.

Cartmill M (1974a) Pads and claws in arboreal locomotion. In FA Jenkins (ed.): Primate Locomotion. New York, NY: Academic Press, pp. 45-83.

Cartmill M (1974b) Rethinking primate origins. Science *184:*436-443.

Cartmill M (1979) The volar skin of primates: its frictional characteristics and their functional significance. American Journal of Physical Anthropology *50:*497-510.

Cartmill M (1985) Climbing. In M Hildebrand, DM Bramble, KF Liem and DB Wake (eds.): Functional Vertebrate Morphology. Cambridge: Harvard University Press, pp. 73-88.

Cartmill M, Lemelin P, and Schmitt D (2002) Support polygons and symmetrical gaits in mammals. Zoological Journal of the Linnean Society *136:*401-420.

Cartmill M, Lemelin P, and Schmitt D (2007a) Primate gaits and primate origins. In MJ Ravosa and M Dagosto (eds.): Primate Origins: Adaptations and Evolution. New York, NY: Springer.

Cartmill M, Lemelin P, and Schmitt D (2007b) Understanding the apaptive value of diagonal-sequence gaits in primates: a comment on Shapiro and Raichlen, 2005. American Journal of Physical Anthropology *133:*822-825.

Castell R, and Sackett G (1972) Motor behaviors of neonatal rhesus monkeys: measurement techniques and early development. Developmental Psychobiology *6:*191-202.

Cavagna GA (1975) Force platforms as ergometers. Journal of Applied Physiology *39:*174-9.

Cavagna GA, Heglund NC, and Taylor CR (1977) Mechanical work in terrestrial locomotion: two basic mechanisms for minimizing energy expenditure. American Journal of Physiology *233(5):*R243-61.

Cavagna GA, Thys H, and Zamboni A (1976) The sources of external work in level walking and running. The Journal of Physiology *262:*639-657.

Chalmers NR (1980) Developmental relationships among social, manipulatory, postural and locomotor behaviours in olive baboons, *Papio anubis*. Behaviour *74:*22-37.

Chevan A, and Sutherland M (1991) Hierarchical partitioning. The American Statisician *45:*90-96.

Cock AG (1966) Genetical aspects of metrical growth and form in animals. Quarterly Review of Biology *41:*131-190.

Conover WJ, and Iman RI (1981) Rank transformations as a bridge between parametric and nonparametric statistics. The American Statistician *35:*124-133.

Costello MB, and Fragaszy DM (1988) Prehension in *Cebus* and *Saimiri*: I. Grip type and hand preference. American Journal of Primatology *15:*235-245.

Crompton RH (1983) Age differences in locomotion of two subtropical Galaginae. Primates *24:*241-259.

Crompton RH, Li Y, Alexander RM, Wang W, and Günther MM (1996) Segment inertial properties of primates: new techniques for laboratory and field studies of locomotion. American Journal of Physical Anthropology *99:*547-570.

Crompton RH, Li Y, Wang W, Savage R, Payne RC, and Günther MM (2000) Diagonal gait in primates: its role in stability on arboreal substrates. American Journal of Physical Anthropology *(Suppl.) 30:*131-132.

Currey J (1984) The Mechanical Adaptation of Bones. Princeton, NJ: Princeton University Press.

Currey J (2001) Ontogenetic changes in compact bone mineral properties. In SC Cowin (ed.): Bone Mechanics Handbook. Boca Raton, FL: CRC Press, pp. 19.1-19.16.

Dagg AI (1973) Gaits in mammals. Mammal Review *3:*135-154.

Dagosto M (1993) Postcranial anatomy and locomotor behavior in Eocene primates. In DL Gebo (ed.): Postcranial Adaptation in Nonhuman Primates. Dekalb, IL: Northern Illinois University Press, pp. 199-219.

Dagosto M (2007) The postcranial morphotype of Primates. In MJ Ravosa and M Dagosto (eds.): Primate Origins: Adaptations and Evolution. New York, NY: Springer, pp. 489-534.

Day LM, and Jayne BC (2007) Interspecific scaling of the morphology and posture of the limbs during the locomotion of cats (Felidae). Journal of Experimental Biology *210:*642-654.

Demes B, Jungers WL, and Nieschalk U (1990) Size- and speed-related aspects of quadrupedal walking in slender and slow lorises. In FK Jouffroy, MH Stack and C Niemetz (eds.): Gravity, Posture and Locomotion in Primates. Florence: Il Sedicesimo, pp. 175-197.

Demes B, Larson SG, Stern JT, Jr, Jungers WL, Biknevicius AR, and Schmitt D (1994) The kinetics of primate quadrupedalism: "hindlimb drive" reconsidered. Journal of Human Evolution *26:*353-374.

Dial KP (2003) Wing-assisted incline running and the evolution of flight. Science *299:*402-404.

Dial KP, Jackson BE, and Segre P (2008) A fundamental avian wing-stroke provides a new perspective on the evolution of flight. Nature *451:*985-989.

Digby LJ, Ferrari SF, and Saltzman W (2007) Callitrichines: the role of competition in cooperatively breeding species. In CJ Campbell, A Fuentes, KC Mackinnon, MA Panger and SK Bearder (eds.): Primates in Perspective. New York, NY: Oxford University Press, pp. 85-106.

Diop M, Rahmani A, Belli A, Gautheron V, Geyssant A, and Cottalorda J (2005) Influence of speed variation and age on ground reaction forces and stride parameters of children's normal gait. International Journal of Sports Medicine *26:*682-687.

Dolhinow P, and Murphy G (1982) Langur monkey (*Presbytis entellus)* development - the first three months of life. Folia Primatologica *39:*305-331.

Donelan JM, Kram R, and Kuo AD (2002) Mechanical work for step-to-step transitions is a major determinant of the metabolic cost of human walking. Journal of Experimental Biology *205:*3717-3727.

Doran DM (1992) The ontogeny of chimpanzee and pygmy chimpanzee locomotor behavior: a case study of paedomorphism and its behavioral correlates. Journal of Human Evolution *23:*139-157.

Doran DM (1997) Ontogeny of locomotion in mountain gorillas and chimpanzees. Journal of Human Evolution *32:*323-344.

Dunbar DC, and Badam GL (1998) Development of posture and locomotion in free-ranging primates. Neuroscience and Biobehavioral Reviews. *22(4):*541-6.

Eaglen RH, and Boskoff KJ (1978) The birth and early development of a captive sifaka, *Propithecus verreauxi coquereli*. Folia Primatologica *30:*206-19.

Ehrlich A (1974) Infant development in two prosimian species: greater galago and slow loris. Developmental Psychobiology *7:*439-454.

Eilam D (1997) Postnatal development of body architecture and gait in several rodent species. Journal of Experimental Biology *200:*1339-1350.

Elias MF (1977) Relative maturing of cebus and squirrel monkeys at birth and during infancy. Developmental Psychobiology *10:*519-528.

Escobar-Paramo P (1989) The development of the wild black-capped capuchin (*Cebus apella*) at La Macarena, Colombia. Field Studies of New World Monkeys, La Macarena, Colombia *2:*45-56.

Falsetti AB, and Cole TM (1992) Relative growth of the postcranial skeleton in callitrichines. Journal of Human Evolution *23:*79-92.

Falster DS, Warton DI, and Wright IJ (2003) (S)MATR: Standardised major axis tests and routines. Version 1.0. http://www.bio.mq.edu.au/ecology/SMATR.

Farley CT (1991) A mechanical trigger for the trot-gallop transition in horses. Science *253:*306-308.

Farley CT, Glasheen JW, and McMahon TA (1993) Running springs: speed and animal size. Journal of Experimental Biology *185:*71-86.

Farley CT, and Ko TC (1997) Mechanics of locomotion in lizards. Journal of Experimental Biology *200:*2177-2188.

Fedigan LM, Rosenberger AL, Boinski S, Norconk MA, and Garber PA (1996) Critical issues in Cebine evolution and behavior. In MA Norconk, AL Rosenberger and PA Garber (eds.): Adaptive Radiations of Neotropical Primates. New York: Plenum Press, pp. 219-228.

Fischer M (1994) Crouched posture and high fulcrum, a principle in the locomotion of small mammals: the example of the rock hyrax (*Procavia capensis*) (Mammalia: Hyracoidea). Journal of Human Evolution *26:*501-524.

Fischer MS, Schilling N, Schmidt M, Harrhaus D, and Witte H (2002) Basic limb kinematics in small therian mammals. Journal of Experimental Biology *205:*1315-1328.

Fleagle J, Mittermeier RA, and Skopec AL (1981) Differential habitat use by *Cebus apella* and *Saimiri sciureus* in Central Surinam. Primates *22:*361-367.

Fleagle JG (1977) Locomotor behavior and skeletal anatomy of sympatric Malaysian leaf-monkeys (*Presbytis obscura* and *Presbytis melalophos*). Yearbook of Physical Anthropology *20:*440-453.

Fleagle JG (1999) Primate Evolution and Adaptation. San Diego: Academic Press.

Fleagle JG, and Mittermeier RA (1980) Locomotor behavior, body size, and comparative ecology of seven Surinam monkeys. American Journal of Physical Anthropology *52:*301-314.

Fleagle JG, and Samonds K (1975) Physical growth of cebus monkeys (*Cebus albifrons*) during the first year of life. Growth *39:*35-52.

Fontaine R (1990) Positional behavior in Saimiri boliviensis and Ateles geoffroyi. American Journal of Physical Anthropology *82:*485-508.

Fragaszy DM (1990) Early behavioral development in capuchins (*Cebus*). Folia Primatologica *54:*119-128.

Fragaszy DM, Baer J, and Adams-Curtis L (1991) Behavioral development and maternal care in tufted capuchins (*Cebus apella*) and squirrel monkeys (*Saimiri sciureus*) from birth through seven months. Developmental Psychobiology *24:*375-393.

Franz TM, Demes B, and Carlson KJ (2005) Gait mechanics of lemurid primates on terrestrial and arboreal substrates. Journal of Human Evolution *48:*199-217.

Full RJ (1989) Mechanics and energetics of terrestrial locomotion: bipeds to polypeds. In W Wieser and E Gnaiger (eds.): Energy Transformations in Cells and organisms. Stuttgart: Georg Thieme Verlag, pp. 175-182.

Gambaryan PP (1974) How Mammals Run: Anatomical Adaptations. New York, NY: John Wiley & Sons.

Garber PA (1991) A comparative study of positional behavior in three species of tamarin monkey. Primates *32:*219-230.

Garber PA (1992) Vertical clinging, small body size, and the evolution of feeding adaptations in the Callitrichinae. American Journal of Physical Anthropology *88:*469-482.

Gasc JP (1993) Asymmetrical gait of the Saharian rodent *Meriones shawi shawi* (Duvernoy, 1842) (Rodentia, Mammalia): a high-speed cineradiographic analyses. Canadian Journal of Zoology *71:*790-798.

Gebo DL (2004) A shrew-sized origin for primates. Yearbook of Physical Anthropology *47:*40-62.

German RZ, and Meyers LL (1989) The role of time and size in ontogenetic allometry: I. Review. Growth, Development and Aging *53:*101-106.

Goldspink DF (1980) Physiological factors influencing protein turnover and muscle growth in mammals. In DF Goldspink (ed.): Development and Specialization of Skeletal Muscle. Cambridge: Cambridge University Press.

Gomez AM (1992) Primitive and derived patterns of relative growth among species of lorisidae. Journal of Human Evolution *23:*219-233.

Grace JB (2006) Structural Equation Modelling and Natural Systems. Cambridge, UK: Cambridge University Press.

Grand TI (1977) Body weight: its relation to tissue composition, segment distribution, and motor function. II. Development of *Macaca mulatta*. American Journal of Physical Anthropology *47:*241-248.

Grand TI (1983) The anatomy of growth and its relation to locomotor capacity in *Macaca*. In JF Eisenberg and DG Kleiman (eds.): Advances in the Study of Mammalian Behavior. Shippensburg, PA: American Society of Mammalogists, pp. 5-23.

Gray J (1944) Studies in the mechanics of the tetrapod skeleton. Journal of Experimental Biology *20:*88-116.

Gray J (1968) Animal Locomotion. New York: Norton.

Gregory WK (1920) On the structure and relations of *Notharctus*, an American Eocene primate. Memoirs of the American Museum of Natural History *3:*51-243.

Griffin TM, and Kram R (2000) Penguin waddling is not wasteful. Nature *408:*929.

Griffin TM, Main RP, and Farley CT (2004) Biomechanics of quadrupedal walking: how do four-legged animals achieve inverted pendulum-like movements? Journal of Experimental Biology *207:*3545-3558.

Gruss LT (2007) Limb length and locomotor biomechanics in the Genus *Homo*: an experimental study. American Journal of Physical Anthropology *134:*106-116.

Haberman SJ (1978) Analysis of Quantitative Data. London: Academic Press.

Hallemans A, De Clercq D, and Aerts P (2006a) Changes in 3D joint dynamics during the first 5 months after the onset of independent walking: a longitudinal follow-up study. Gait and Posture *24:*270-279.

Hallemans A, De Clercq D, van Dongen S, and Aerts P (2006b) Changes in foot-function parameters during the first 5-months of independent walking: a longitudinal follow-up study. Gait and Posture *23:*142-148.

Hamrick M (2001) Primate origins: evolutionary change in digital ray patterning and segmentation. Journal of Human Evolution *40:*339-351.

Hamrick MW (1998) Functional and adaptive significance of primate pads and claws: evidence from new world anthropoids. American Journal of Physical Anthropology *106:*113-127.

Hanna JB, Polk JD, and Schmitt D (2006) Forelimb and hindlimb forces in walking and galloping primates. American Journal of Physical Anthropology *130:*529-535.

Hartwig WC (1995) Effect of life history on the squirrel monkey (Platyrrhini: *Saimiri*) cranium. American Journal of Physical Anthropology *97:*435-449.

Hartwig-Scherer S (1995) Allometric limb growth and the ontogeny of bone robusticity. American Journal of Physical Anthropology *Suppl. 20:*107-108.

Hartwig-Scherer S, and Martin RD (1992) Allometry and prediction in hominoids: a solution to the problem of intervening variables. American Journal of Physical Anthropology *88:*37-57.

Hedrick T (2007) "DLT Data Viewer 2", Digitizing and DLT in MATLAB. http://www.unc.edu/~thedrick/software1.html.

Heglund NC (1981) A simple design for a force-plate to measure ground reaction forces. Journal of Experimental Biology *93:*333-338.

Heglund NC, Cavagna GA, and Taylor CR (1982) Energetics and mechanics of terrestrial locomotion. III. Energy changes of the centre of mass as a function of speed and body size in birds and mammals. The Journal of Experimental Biology *97:*41-56.

Heglund NC, Taylor CR, and McMahon TA (1974) Scaling stride frequency and gait to animal size: mice to horses. Science *186:*1112-1113.

Heinrich RE, Ruff CB, and Adamczewski JZ (1999) Ontogenetic changes in mineralization and bone geometry in the femur of muskoxen (*Ovibos moschatus*). Journal of Zoology, London *247:*215-223.

Herrel A, and Gibb AC (2006) Ontogeny of performance in vertebrates. Physiological and Biochemical Zoology *79:*1-6.

Hildebrand M (1965) Symmetrical gaits of horses. Science *150:*701-708.

Hildebrand M (1966) Analysis of the symmetrical gaits of tetrapods. Folia Biotheoretica*:*1-22.

Hildebrand M (1967) Symmetrical gaits of primates. American Journal of Physical Anthropology *26:*119-130.

Hildebrand M (1976) Analysis of tetrapod gaits: general considerations and symmetrical gaits. In RM Herman, S Grillner, PSG Stein and DG Stuart (eds.): Neural Control of Locomotion. New York: Plenum Press, pp. 203-236.

Hildebrand M (1977) Analysis of asymmetrical gaits. Journal of Mammalogy *58:*131-156.

Hildebrand M (1980) The adaptive significance of tetrapod gait selection. American Zoologist *20:*255-267.

Hof AL (1996) Scaling gait data to body size. Gait and Posture *4:*222-223.

Howell AB (1944) Speed in Animals. New York: Hafner Publishing Company.

Howland DR, Bregman BS, and Goldberger ME (1995) The development of quadrupedal locomotion in the kitten. Experimental Neurology *135:*93-107.

Huitema BE (1980) The Analysis of Covariance and its Alternatives. New York, NY: John Wiley and Sons.

Hunt KD, Cant JGH, Gebo DL, Rose MD, Walker SE, and Youlatos D (1996) Standardized descriptions of primate locomotor and postural modes. Primates *37:*363-387.

Hurov JR (1982) Diagonal walking in captive infant vervet monkeys. American Journal of Primatology *2:*211-213.

Hurov JR (1987) Terrestrial locomotion and back anatomy in vervets (*Cercopithecus aethiops*) and patas monkeys (*Erythrocebus patas*). American Journal of Primatology *13:*297-311.

Hurov JR (1991) Rethinking primate locomotion: what can we learn from development? Journal of Motor Behavior *23:*211-218.

Hutchinson JR, Famini D, Lair R, and Kram R (2003) Are fast-moving elephants really running? Nature *422:*493-494.

Hutchinson JR, Schwerda D, Famani DJ, Dale RHI, Fischer MS, and Kram R (2006) The locomotor kinematics of Asian and African elephants: changes with speed and size. Journal of Experimental Biology *209:*3812-3827.

Huxley JW (1932) Problems in Relative Growth. London: Cambridge University Press.

Iriarte-Diaz J, Bozinovic F, and Vasquez RA (2006) What explains the trot-gallop transition in small mammals? Journal of Experimental Biology *209:*4061-4066.

Irschick DJ, and Jayne BC (2000) Size matters: Ontogenetic variation in the three-dimensional kinematics of steady-speed locomotion in the lizard *Dipsosaurus dorsalis*. Journal of Experimental Biology *203:*2133-2148.

Irschick DJ, Macrini TE, Koruba S, and Forman J (1998) Ontogenetic differences in morphology, habitat use, behavior, and sprinting capacity in two West Indian *Anolis* lizards. Journal of Herpetology *34:*444-451.

Ishida H, Kumakura H, and Kondo S (1985) Primate bipedalism and quadrupedalism: comparative electromyography. In S Kondo, H Ishida, T Kimura, M Okada, N Yamazaki and JH Prost (eds.): Primate Morphophysiology, Locomotor Analyses and Human Bipedalism. Tokyo: University of Tokyo Press, pp. 59-79.

Jack KM (2007) The Cebines: toward an explanation of variable social structure. In CJ Campbell, A Fuentes, KC MacKinnon, MA Panger and SK Bearder (eds.): Primates in Perspective. New York, NY: Oxford University Press, pp. 107-123.

Janson CH, and Boinski S (1992) Morphological and behavioral adaptations for foraging in generalist primates: the case of cebines. American Journal of Physical Anthropology *88:*483-498.

Janson CH, and Van Schaik CP (1993) Ecological risk aversion in juvenile primates: slow and steady wins the race. In ME Pereira and LA Fairbanks (eds.): Juveniles

primates: life history, development, and behavior. New York: Oxford University Press, pp. 57-74.

Jenkins FA (1971) Limb posture and locomotion in Virginia opossum (*Didelphis marsupialis*) and in other non-cursorial mammals. Journal of Zoology, London *165:*303-315.

Jenkins FA (1974) Tree shrew locomotion and the origins of primate arborealism. In FA Jenkins (ed.): Primate Locomotion. New York and London: Academic Press, pp. 85-115.

Johnson VS (1998) A comparative study of the skeletal and muscular development of the squirrel monkey and how it relates to the locomotor patterns between the infant and the adult (*Saimiri boliviensis*). M. Sc. Thesis, University of Arizona, Arizona State University.

Jouffroy FK, and Medina MF (1996) Developmental changes in the fibre composition of elbow, knee, and ankle extensor muscles in cercopithecid monkeys. Folia Primatologica *66:*55-67.

Jouffroy FK, and Medina MF (2004) Comparative fiber-type composition and size in the antigravity muscles of primate limbs. In FC Anapol, RZ German and NG Jablonski (eds.): Shaping Primate Evolution: Form, Function, and Behavior. Cambridge: Cambridge University Press, pp. 135-161.

Julienlaferriere D, and Atramentowicz M (1990) Feeding and reproduction of three Didelphid marsupials in two neotropical forests (French-Guiana). Biotropica *22:*404-415.

Jungers WL (1984) Aspects of size and scaling in primate biology with special reference to the locomotor skeleton. Yearbook of Physical Anthropology *27:*73-97.

Jungers WL (1985) Body size and scaling of limb proportions in primates. In WL Jungers (ed.): Size and Scaling in Primate Biology. New York, NY: Plenum Press, pp. 345-381.

Jungers WL, and Cole MS (1992) Relative growth and shape of the locomotor skeleton in lesser apes. Journal of Human Evolution *23:*93-105.

Jungers WL, and Fleagle JG (1980) Postnatal growth allometry of the extremities in *Cebus albifrons* and *Cebus apella*: a longitudinal and comparative study. American Journal of Physical Anthropology *53:*471-478.

Jurmain R (1997) Skeletal evidence of trauma in African apes, with special reference to the Gombe chimpanzees. Primates *38:*1-14.

Kaack B, Walker L, and Brizzee KR (1979) The growth and development of the squirrel monkey (*Saimiri sciureus*). Growth *43:*116-135.

Kimura T (1987) Development of chimpanzee locomotion on level surfaces. Human Evolution *2:*107-119.

Kimura T (1992) Hindlimb dominance during primate high-speed locomotion. Primates *33:*465-476.

Kimura T (2000) Development of quadrupedal locomotion on level surfaces in Japanese macaques. Folia Primatologica *71:*323-333.

Kimura T, Okada M, and Ishida H (1979) Kinesiological characteristics of primate walking: its significance in human walking. In ME Morbeck, H Preuschoft and N Gomberg (eds.): Environment, Behavior and Morphology: Dynamic Interactions in Primates. New York: G. Fischer.

Koff D (1995) Joint kinematics: camera-based systems. In RL Craik and CA Oatis (eds.): Gait Analysis: Theory and Applications. St. Louis: Mosby-Year Book, pp. 183-204.

Lammers AR, and Biknevicius AR (2004) The biodynamics of arboreal loocmotion: the effects of substrate diameter on locomotor kinetics in the gray short-tailed opossum (*Monodelphis domestica*). Journal of Experimental Biology *207:*4325-4336.

Lammers AR, and German RZ (2002) Ontogenetic allometry in the locomotor skeleton of specialized half-bounding mammals. Journal of Zoology, London *258:*485-495.

Lande R (1977) On comparing coefficients of variation. Systematic Zoology *26:*214-217.

Larney E, and Larson SG (2004) Compliant walking in primates: elbow and knee yield in primates compared to other mammals. American Journal of Physical Anthropology *125:*42-50.

Larson SG (1993) Functional morphology of the shoulder in primates. In DL Gebo (ed.): Postcranial Adaptation in Nonhuman Primates. Dekalb: Northern Illinois University Press, pp. 45-69.

Larson SG (1998) Unique aspects of quadrupedal locomotion in nonhuman primates. In E Strasser, J Fleagle, A Rosenberger and H McHenry (eds.): Primate Locomotion. New York: Plenum Press, pp. 157-173.

Larson SG (2007) Morphological correlates of forelimb protraction in quadrupedal primates. In MJ Ravosa and M Dagosto (eds.): Primate Origins: Adaptations and Evolution. New York, NY: Springer.

Larson SG, Schmitt D, Lemelin P, and Hamrick M (2000) Uniqueness of primate forelimb posture during quadrupedal locomotion. American Journal of Physical Anthropology *112:*87-101.

Larson SG, Schmitt D, Lemelin P, and Hamrick M (2001) Limb excursion during quadrupedal walking: how do primates compare to other mammals? Journal of Zoology, London *255:*353-365.

Larson SG, and Stern JT (2006) Maintenance of above-branch balance during primate arboreal quadrupedalism: coordinated use of forearm rotators and tail motion. American Journal of Physical Anthropology *129:*71-81.

Larson SG, and Stern JT (2008) The role of primate hip extensors in diminishing forelimb forces during quadrupedalism. American Journal of Physical Anthropology *135:*137-138.

Lawler RR (2006) Sifaka positional behavior: ontogenetic and quantitative genetic approaches. American Journal of Physical Anthropology *131:*261-271.

Lee DV, Stakebake EF, Walter RM, and Carrier DR (2004) Effects of mass distribution on the mechanics of level trotting in dogs. Journal of Experimental Biology *207:*1715-1728.

Lemelin P (1999) Morphological correlates of substrate use in didelphid marsupials: implications for primate origins. Journal of Zoology, London *247:*165-175.

Lemelin P, and Grafton BW (1998) Grasping performance in *Saguinas midas* and the evolution of hand prehensility in primates. In E Strasser, J Fleagle, A Rosenberger and H McHenry (eds.): Primate Locomotion: Recent Advances. New York, NY: Plenum Press, pp. 131-144.

Lemelin P, and Schmitt D (2004) Seasonal variation in body mass and locomotor kinetics of the fat-tailed dwarf lemur (*Cheirogaleus medius*). Journal of Morphology *260:*65-71.

Lemelin P, and Schmitt D (2007) Origins of grasping and locomotor adaptations in primates: comparative and experimental approaches using an opossum model. In MJ Ravosa and M Dagosto (eds.): Primate Origins: Adaptations and Evolution. New York, NY: Springer.

Lemelin P, Schmitt D, and Cartmill M (2003) Footfall patterns and interlimb coordination in opossums (Family Didelphidae): evidence for the evolution of diagonal sequence gaits in primates. Journal of Zoology, London *260:*423-429.

Lentle RG, Kruger MC, Mellor DJ, Birtles M, and Moughan PJ (2006) Limb development in pouch young of the brushtail possum (*Trichosurus vulpecula*) and tammar wallaby *(Macropus eugenii*). Journal of Zoology *270:*122-131.

Levitch LC (1987) Ontogenetic allometry of the postcranial skeleton in platyrrhines, with special emphasis on its relationship to the evolution of small body size in the callitrichidae. PhD Dissertation, University of Washington, Seattle, WA.

Li CC (1975) Path Analysis - a Primer. Pacific Grove, CA: The Boxwood Press.

Li Y, Crompton RH, Wang W, Savage R, and Günther MM (2004) Hind limb drive, hind limb steering? Functional differences between fore and hind limbs in chimpanzee quadrupedalism. In FC Anapol, RZ German and NG Jablonski (eds.): Shaping Primate Evolution. Cambridge: Cambridge University Press, pp. 258-277.

Liu MF, He P, Aherne FX, and Berg RT (1999) Postnatal limb bone growth in relation to live weight in pigs from birth to 84 days of age. Journal of Animal Science *77:*1693-1701.

Lovell NC (1990) Patterns of Illness and Injury in Great Apes: a Skeletal Analysis. Washington, DC: Smithsonian Institution Press.

Lovell NC (1991) An evolutionary framework for assessing illness and injury in nonhuman primates. Yearbook of Physical Anthropology *34:*117-155.

Mack D (1979) Growth and development of infant red howling monkeys (*Alouatta seniculus*) in a free-ranging population. In JF Eisenberg (ed.): Vertebrate Ecology in the Northern Neotropics. Washington, D.C.: Smithsonian Institution Press, pp. 127-136.

MacNally R (2002) Multiple regression and inference in ecology and conservation biology: further comments on identifying important predictor variables. Biodiversity and Conservation *11:*1397-1401.

MacNally R, and Walsh CJ (2004) Hierarchical partitioning public-domain software. Biodiversity and Conservation *13:*659-660.

Main RP, and Biewener AA (2004) Ontogenetic patterns of limb loading, *in vivo* bone strains and growth in the goat radius. Journal of Experimental Biology *207:*2577-2588.

Main RP, and Biewener AA (2007) Skeletal strain patterns and growth in the emu hindlimb during ontogeny. Journal of Experimental Biology *210:*2676-2690.

Martin RD (1990) Primate Origins and Evolution: a Phylogenetic Reconstruction. Princeton: Princeton University Press.

McClearn D (1992) Locomotion, posture, and feeding behavior of kinkajous, coatis, and raccoons. Journal of Mammalogy *73:*245-261.

McGraw WS (1996) Cercopithecoid locomotion, support use, and support availablility in the Tai Forest, Ivory Coas. American Journal of Physical Anthropology *100:*507-522.

McMahon TA (1985) The role of compliance in mammalian running. Journal of Experimental Biology *115:*263-282.

McMahon TA, Valiant G, and Frederick EC (1987) Groucho running. Journal of Applied Psychology *62:*2326-2337.

Meldrum DJ (1991) Kinematics of the Cercopithecine foot on arboreal and terrestrial substrates with implications for the interpretation of hominid terrestrial adaptations. American Journal of Physical Anthropology *84:*273-289.

Midlo C (1934) Form of hand and foot in primates. American Journal of Physical Anthropology *19:*337-389.

Missler M, Wolff JR, Rothe H, Heger W, Merker H-J, Treiber A, Scheid R, and Crook GA (1992) Developmental biology of the common marmoset: proposal for a "postnatal staging". Journal of Medical Primatology *21:*285-298.

Mitchell CL (1990) The ecological basis for female social dominance: a behavioral study of the squirrel monkey (*Saimiri sciureus*) in the wild. PhD Dissertation, Princeton University, Princeton, NJ.

Moermond T (1979) Habitat community structure of *Anolis* lizards. Ecology *60:*152-164.

Moisio KC, Sumner DR, Shott S, and Hurwitz DE (2003) Normalization of joint moments during gait: a comparison of two techniques. Journal of Biomechanics *36:*599-603.

Morbeck ME (1976) Leaping, bounding and bipedalism in *Colobus guereza*: a spectrum of positional behaviors. Yearbook of Physical Anthropology *20:*408-420.

Morland HS (1990) Parental behavior and infant development in ruffed lemurs (*Varecia variegata*) in a northeast Madagascar rain forest. American Journal of Primatology *20:*253-265.

Mosimann JE, and James FC (1979) New statistical methods for allometry with application to Florida red-winged blackbirds. Evolution *33:*444-459.

Muir GD, Gosline JM, and Steeves JD (1996) Ontogeny of bipedal locomotion: Walking and running in the chick. Journal of Physiology-London *493:*589-601.

Muybridge E (1887) Animal Locomotion. New York, NY: Dover.

Nakano Y (1996) Footfall patterns in the early development of the quadrupedal walking of Japanese macaques. Folia Primatologica *66:*113-125.

Napier JR (1967) Evolutionary aspects of primate locomotion. American Journal of Physical Anthropology *27:*333-342.

Napier JR, and Napier PH (1985) The Natural History of the Primates. Cambridge, MA: MIT Press.

Negayama K, Kondo K, and Itoigawa N (1983) Development of locomotor behavior in infant Japanese macaques (*Macaca fuscata*). Annales de Sciences Naturelles: Zoologie *5:*169-180.

Ozkaya N, and Nordin M (1999) Fundamentals of Biomechanics: Equilibrium, Motion and Deformation. New York: Springer.

Pennycuick CJ (1975) On the running of the gnu (*Connochaetes taurinus*) and other animals. Journal of Experimental Biology *63:*775-799.

Perry AK, Blickhan R, Biewener AA, Heglund NC, and Taylor CR (1988) Preferred speeds in terrestrial vertebrates: are they equivalent? Journal of Experimental Biology *137:*207-219.

Peters SE (1983) Postnatal development of gait behavior and functional allometry in the domestic cat. Journal of Zoology, London *199:*461-486.

Pitman ETG (1939) A note on normal correlation. Biometrika *31:*9-12.

Plagenhoef S (1979) Dynamics of human and animal motion. In ME Morbeck, H Preuschoft and N Gomberg (eds.): Environment, Behavior, and Morphology: Dynamic Interactions in Primates. New York: Gustav Fisher, pp. 95-118.

Polk JD (2001) The Influence of Body Size and Proportions on Primate Quadrupedal Locomotion. Ph.D. Dissertation, Stony Brook University, State University of New York at Stony Brook.

Polk JD (2002) Adaptive and phylogenetic influences on musculoskeletal design in cercopithecine primates. Journal of Experimental Biology *205:*3399-3412.

Polk JD (2004) Influences on limb proportions and body size on locomotor kinematics in terrestrial primates and fossil hominins. Journal of Human Evolution *47:*237-252.

Polk JD, Demes B, Jungers WL, Biknevicius AR, Heinrich RE, and Runestad JA (2000) A comparison of primate, carnivoran and rodent limb bone cross-sectional properties: are primates really unique? Journal of Human Evolution *39:*297-325.

Polk JD, Psutka SP, and Demes B (2005) Sampling frequencies and measurement error for linear and temporal gait parameters in primate locomotion. Journal of Human Evolution *49:*665-679.

Pontzer H (2005) A new model predicting locomotor cost from limb length via force production. Journal of Experimental Biology *208:*1513-1524.

Preuschoft H, and Günther MM (1994) Biomechanics and body shape in primates compared with horses. Zeitschrift fur Morphologie und Anthropologie *80:*149-165.

Preuschoft H, Witte H, Christian A, and Fischer M (1996) Size influences on primate locomotion and body shape, with special emphasis on the locomotion of 'small mammals'. Folia Primatologica *66:*93-112.

Preuschoft H, Witte H, Christian A, and Recknagel S (1992) Körpergestalt und Locomotion bei grossen Säugetieren. Verhandlungen der Deutschen Zoologischen Gesellschaft *87:*147-163.

Pridmore PA (1994) Locomotion in *Dromiciops australis* (Marsupialia: Microbiotheriidae). Australian Journal of Zoology *42:*679-699.

Prost JH (1969) A replication study on monkey gaits. American Journal of Physical Anthropology *30:*203-208.

Prost JH, and Sussman RW (1969) Monkey locomotion on inclined surfaces. American Journal of Physical Anthropology *31:*53-58.

Quinn GP, and Keough MJ (2002) Experimental Design and Data Analysis for Biologists. Cambridge, UK: Cambridge University Press.

Radhakrishna S, and Singh M (2004) Infant development in the slender loris (*Loris lydekkerianus lydekkerianus*). Current Science *86:*1121-1127.

Raichlen DA (2004a) Convergence of forelimb and hindlimb Natural Pendular Period in baboons (*Papio cynocephalus*) and its implication for the evolution of primate quadrupedalism. Journal of Human Evolution *46:*719-738.

Raichlen DA (2004b) The Relationship between Limb Shape and Locomotor Mechanics and Energetics in Infant Baboons (*Papio cynocephalus*). PhD Dissertation, University of Texas at Austin, Austin, TX.

Raichlen DA (2005a) Effects of limb mass distribution on the ontogeny of quadrupedalism in infant baboons (*Papio cynocephalus*) and implications for the evolution of primate quadrupedalism. Journal of Human Evolution *49:*415-431.

Raichlen DA (2005b) Ontogeny of limb mass distribution in infant baboons (*Papio cynocephalus*). Journal of Human Evolution *49:*452-467.

Raichlen DA (2006) Effects of limb mass distribution on mechanical power outputs during quadrupedalism. Journal of Experimental Biology *209:*633-644.

Raichlen DA, Shapiro LJ, Pontzer H, and Sockol MD (2007) The evolution of mammalian locomotor biomechanics: adaptations or spandrels? Oral presentation at the International Conference of Vertebrate Morphology, July 2007.

Rasband WS (1997-2007) ImageJ. Bethesda. Maryland, USA: U.S. National Institutes of Health: http://rsb.info.nih.gov/ij/.

Rasmussen DT (1990) Primate origins: lessons from a neotropical marsupial. American Journal of Primatology *22:*263-277.

Ravosa MJ, Meyers DM, and Glander KE (1993) Relative growth of the limbs and trunk in sifakas - heterochronic, ecological, and functional considerations. American Journal of Physical Anthropology *92:*499-520.

Reilly SM, and Biknevicius AR (2003) Integrating kinetic and kinematic approaches to the analysis of terrestrial locomotion. In VL Bels, J-P Gasc and A Casinos (eds.): Vertebrate Biomechanics and Evolution. Oxford: BIOS Scientific Publishers Ltd.

Reilly SM, McElroy EJ, and Biknevicius AR (2007) Posture, gait and the ecological relevance of locomotor costs and energy-saving mechanisms in tetrapods. Zoology *104:*271-289.

Renous S, Herbin M, and Gasc JP (2004) Contribution to the analysis of gaits: practical elements to complement the Hildebrand method. Comptes Rendus Biologies *327:*99-103.

Reynolds HM (1974) Measurement of the Inertial Properties of the Segmented Savannah Baboon, Southern Methodist University, Southern Methodist University.

Reynolds TR (1985a) Mechanics of increased support of weight by the hindlimbs in primates. American Journal of Physical Anthropology *67:*335-349.

Reynolds TR (1985b) Stresses on the limbs of quadrupedal primates. American Journal of Physical Anthropology *67:*351-362.

Reynolds TR (1987) Stride length and its determinants in humans, early hominids, primates, and mammals. American Journal of Physical Anthropology *72:*101-115.

Ricker WE (1984) Computation and uses of central trend lines. Canadian Journal of Zoology *62:*1897-1905.

Riskin DK, Bertram JEA, and Hermanson JW (2005) Testing the hindlimb-strength hypothesis: non-aerial locomotion by Chiroptera is not constrained by the dimensions of the femur or tibia. Journal of Experimental Biology *208:*1309-1319.

Rollinson J, and Martin RD (1981) Comparative aspects of primate locomotion, with special reference to arboreal cercopithecines. Symposia of the Zoological Society of London *48:*377-427.

Rose MD (1973) Quadrupedalism in primates. Primates *14:*337-357.

Rose MD (1977) Positional behavior of olive baboons (*Papio anubis*) and its relationship to maintenance and social activities. Primates *18:*59-116.

Rosenberger A, and Stafford BJ (1994) Locomotion in captive *Leontopithecus* and *Callimico*: a multimedia study. American Journal of Physical Anthropology *94:*379-394.

Ross C (1991) Life history patterns of new world primates. International Journal of Primatology *12:*481-502.

Ross CF, and Reed DA (2007) Modulation of mastication to variation in food material properties in *Cebus capucinus*. American Journal of Physical Anthropology *Supp 44:*203.

Ruff CB (2003a) Growth in bone strength, body size, and muscle size in a juvenile longitudinal sample. Bone *33:*317-329.

Ruff CB (2003b) Ontogenetic adaptation to bipedalism: age changes in femoral to humeral length and strength proportions in humans, with a comparison to baboons. Journal of Human Evolution *45:*317-349.

Ruina A, Bertram JEA, and Srinivasan M (2005) A collisional model of the energetic cost of support work in walking and galloping, pseudo-elastic leg behavior in running and the walk-to-run transition. Journal of Theoretical Biology *237:*170-192.

Schaefer MS, and Nash LT (2007) Limb growth in captive *Galago senegalensis*: getting in shape to be an adult. American Journal of Primatology *69:*103-111.

Schermelleh-Engel K, Moosbrugger H, and Muller H (2003) Evaluating the fit of structural equation models: tests of significance and descriptive goodness of fit measures. Methods of Psychological Research - Online *8:*23-74.

Schilling N (2005) Ontogenetic development of locomotion in small mammals - a kinematic study. Journal of Experimental Biology *208:*4013-4034.

Schilling N, and Hackert R (2006) Sagittal spine movements of small therian mammals during asymmetrical gaits. Journal of Experimental Biology *209:*3925-3939.

Schilling N, and Petrovitch A (2006) Postnatal allometry of the skeleton in *Tupaia glis* (Scandentia: Tupaiidae) and *Galea musteloides* (Rodentia: Caviidae) - a test of the three-segment limb hypothesis. Zoology *109:*148-162.

Schmidt M (2005) Quadrupedal locomotion in squirrel monkeys (Cebidae: *Saimiri sciureus*): a cineradiographic study of limb kinematics and related substrate reaction forces. American Journal of Physical Anthropology *128:*359-370.

Schmidt M, and Fischer MS (2000) Cineradiographic study of forelimb movements during quadrupedal walking in the brown lemur (*Eulemur fulvus*, Primates: Lemuridae). American Journal of Physical Anthropology *111*.

Schmidt-Nielsen K (1975) Scaling in biology: the consequences of size. Journal of Experimental Zoology *194:*287-308.

Schmitt D (1994) Forelimb mechanics as a function of substrate type during quadrupedalism in two anthropoid primates. Journal of Human Evolution *26*.

Schmitt D (1995) A Kinematic and Kinetic Analysis of Forelimb Use during Arboreal and Terrestrial Quadrupedalism in Old World Monkeys. Ph.D. Dissertation, Stony Brook University, State University of New York at Stony Brook.

Schmitt D (1998) Forelimb mechanics during arboreal and terrestrial quadrupedalism in Old World monkeys. In E Strasser, J Fleagle, A Rosenberger and H McHenry (eds.): Primate Locomotion: Recent Advances. New York, NY: Plenum Press, pp. 175-200.

Schmitt D (1999) Compliant walking in primates. Journal of Zoology, London *248:*149-160.

Schmitt D (2003a) Evolutionary implications of the unusual walking mechanics of the common marmoset (*C. jacchus*). American Journal of Physical Anthropology *122:*28-37.

Schmitt D (2003b) Insights into the evolution of human bipedalism from experimental studies of humans and other primates. Journal of Experimental Biology *206:*1437-1448.

Schmitt D (2003c) Substrate size and primate forelimb mechanics: implications for understanding the evolution of primate locomotion. International Journal of Primatology *24:*1023-1036.

Schmitt D, Cartmill M, Griffin T, M., Hanna JB, and Lemelin P (2006) Adaptive value of ambling gaits in primates and other mammals. Journal of Experimental Biology *209:*2042-2049.

Schmitt D, and Hanna JB (2004) Substrate alters forelimb to hindlimb peak force ratios in primates. Journal of Human Evolution *46:*239-254.

Schmitt D, and Lemelin P (2002) Origins of primate locomotion: gait mechanics of the woolly opossum. American Journal of Physical Anthropology *118:*231-238.

Schmitt D, and Lemelin P (2004) Locomotor mechanics of the slender loris. Journal of Human Evolution *47:*85-94.

Schmitt D, Pai AK, and Bishop KL (2007) Center of mass movements in primates. American Journal of Physical Anthropology *S44:*209.

Schmitt D, Pai AM, O'Neill MC, and Bishop KL (2008) Center of mass movements in arboreal and terrestrial prosimians. American Journal of Physical Anthropology *S46:*187-188.

Schoener TW, and Schoener A (1971a) Structural habitats of West Indian *Anolis* lizards I. Lowland Jamaica. Breviora *368:*1-53.

Schoener TW, and Schoener A (1971b) Structural habitats of West Indian *Anolis* lizards II. Puerto Rican uplands. Breviora *375:*1-39.

Schradin C, and Anzenberger G (2001) Costs of infant carrying in common marmosets, Callithrix jacchus: an experimental analysis. Animal Behaviour *62:*289-295.

Schultz AH (1944) Age changes and variability in gibbons. A morphological study on a populations sample of a man-like ape. American Journal of Physical Anthropology *2:*1-129.

Schultz AH (1956) Postembryonic age changes. Primatologia *1:*887-964.

Schusterman RJ, and Sjoberg A (1968) Early behavior patterns of squirrel monkeys (*Saimiri sciureus*). In CA Carpenter (ed.): Proceedings of the Second International Congress of Primatology. Volume 1: Behavior. New York: Karger, pp. 194-203.

Shapiro LJ, and Raichlen DA (2005) Lateral sequence walking in infant *Papio cynocephalus*: implications for the evolution of diagonal sequence walking in primates. American Journal of Physical Anthropology *126:*205-213.

Shapiro LJ, and Raichlen DA (2006) Limb proportions and the ontogeny of quadrupedal walking in infant baboons (*Papio cynocephalus*). Journal of Zoology *269:*191-203.

Shapiro LJ, and Raichlen DA (2007a) Center of mass position, quadrupedalism, and stability: where do primates fall? American Journal of Physical Anthropology *44:*215.

Shapiro LJ, and Raichlen DA (2007b) A response to Cartmill et al.: primate gaits and arboreal stability. American Journal of Physical Anthropology *133:*825-827.

Shapiro LJ, Zeininger AD, and VandeBerg JL (2008) The influence of body size and substrate size on quadrupedalism in *Monodelphis domestica*. American Journal of Physical Anthropology *135 (Suppl. 46):*191.

Shipley B (2000) Cause and Correlation in Biology. Cambridge, UK: Cambridge University Press.

Silcox MT (2007) Primate taxonomy, Plesiadapiforms, and approaches to primate origins. In MJ Ravosa and M Dagosto (eds.): Primate Origins: Adaptations and Evolution. New York, NY: Springer, pp. 143-178.

Smith RJ, and Jungers WL (1997) Body mass in comparative primatology. Journal of Human Evolution *32:*523-559.

Sokal RR, and Rohlf FJ (1995) Biometry. New York: W.H. Freeman.

Soligo C, and Martin RD (2006) Adaptive origins of primates revisted. Journal of Human Evolution *50:*414-430.

Stafford BJ, Rosenberger AL, Baker AJ, Beck BB, Dietz JM, and Kleiman DG (1996) Locomotion of golden lion tamarins (*Leontopithecus rosalia*): the effects of

foraging adaptations and substrate characteristics on locomotor behavior. In MA Norconk, AL Rosenberger and PA Garber (eds.): Adaptive Radiations of Neotropical Primates. New York: Plenum Press.

Stern JT (1975) Before bipedality. Yearbook of Physical Anthropology *19:*59-68.

Stern JT, Jr, and Susman RL (1981) Electromyography of the gluteal muscles in *Hylobates*, *Pongo*, and *Pan*: implications for the evolution of hominid bipedality. American Journal of Physical Anthropology *55:*153-166.

Stevens NJ (2003) The Influence of Substrate Size, Orientation and Compliance upon Prosimian Arboreal Quadrupedalism, Stony Brook University, State University of New York at Stony Brook.

Stevens NJ (2007) The effect of branch diameter on primate gait sequence pattern. American Journal of Primatology *70:*1-7.

Stevens NJ, Schmitt DO, Cole TM, III, and Chan L-K (2006) Technical note: out-of-plane angular correction based on a trigonometric function for use in two-dimensional kinematic studies. American Journal of Physical Anthropology *129:*399-402.

Sugardjito J, and van Hooff JARAM (1986) Age-sex class differences in the positional behavior of the Sumatran Orangutan (*Pongo pygmaeus abelii*) in the Gunung Leuser National Park, Indonesia. Folia Primatologica *47:*14-25.

Sukhanov VB (1974) General System of Symmetrical Locomotion of Terrestrial Vertebrates and Some Features of Movement of Lower Tetrapods. New Delhi: Amerind Publishing Co. Pvt. Ltd.

Sussman RW (1991) Primate origins and the evolution of angiosperms. American Journal of Primatology *23:*209-223.

Sussman RW, and Kinzey WG (1984) The ecological role of the Callitrichidae: a review. American Journal of Physical Anthropology *64:*419-449.

Taylor ME (1970) Locomotion in some East African viverrids. Journal of Mammalogy *51:*42-51.

Terborgh J (1983) Five New World Primates: a Study in Comparative Ecology. Princeton, NJ: Princeton University Press.

Thurm D, Samonds KW, and Fleagle JG (1975) An atlas of the skeletal maturation of the cebus monkey: the first year. Boston: Harvard School of Public Health.

Tomanek RJ (1975) A histochemical study of postnatal differentiation of skeletal muscle with reference to functional overload. Developmental Biology *42:*305-314.

Tomita M (1967) A study on the movement pattern of four limbs in walking. Journal of the Anthropological Society of Nippon *75:*120-146.

Torzilli PA, Takebe K, Burnstein AH, and Heiple KG (1981) Structural properties of immature canine bone. ASME Journal of Biomechanical Engineering *104:*12-20.

Trillmich F, Bieneck M, Geissler E, and Bischof HJ (2003) Ontogeny of running performance in the wild guinea pig (*Cavia aperea*). Mammalian Biology *68:*214-223.

Turner TR, Anapol F, and Jolly CJ (1997) Growth, development, and sexual dimorphism in vervet monkeys (*Cercopithecus aethiops*) at four sites in Kenya. American Journal of Physical Anthropology *103:*19-35.

Turnquist JE, and Wells JP (1994) Ontogeny of locomotion in rhesus macaques (*Macaca mulatta*): I. Early postnatal ontogeny of the musculoskeletal system. Journal of Human Evolution *26:*487-499.

Vilensky JA (1980) Trot-gallop transition in a macaque. American Journal of Physical Anthropology *53:*347-348.

Vilensky JA (1994) Squirrel monkey locomotion on an inclined treadmill: implications for the evolution of gaits. Journal of Human Evolution *26:*375-386.

Vilensky JA, and Gankiewicz E (1986) Effects of size on vervet (*Cercopithecus aethiops*) gait parameters: a preliminary analysis. Folia Primatologica *46:*104-117.

Vilensky JA, and Gankiewicz E (1989) Early development of locomotor behavior in vervet monkeys. American Journal of Primatology *17:*11-25.

Vilensky JA, and Larson SG (1989) Primate locomotion: utilization and control of symmetrical gaits. Annual Review of Anthropology *18:*17-35.

Vilensky JA, Libii JN, and Moore AM (1991) Trot-gallop gait transitions in quadrupeds. Physiology and Behavior *50:*835-842.

Vilensky JA, and Moore AM (1992) Utilization of lateral- and diagonal-sequence gaits at identical speeds by individual vervet monkeys. In S Matano, RH Tuttle, H Ishida and M Goodman (eds.): Topics in Primatology, Volume 3: Evolutionary Biology, Reproductive Endocrinology and Virology. Tokyo: University of Tokyo Press, pp. 129-137.

Vilensky JA, Moore-Kuhns M, and Moore AM (1990) Angular displacement patterns of leading and trailing limb joints during galloping in monkeys. American Journal of Primatology *22:*227-239.

Vilensky JA, and Patrick MC (1985) Gait characteristics of two squirrel monkeys, with emphasis on relationships with speed and neural control. American Journal of Physical Anthropology *68:*429-444.

Vilensky JA, Wilson P, Gankiewicz E, and Townsend DW (1989) An analysis of air-stepping in normal infant vervet monkeys. Journal of Motor Behavior *21:*429-456.

von Mering F, and Fischer MS (1999) Fibre type regionalization of forelimb muscles in two mammalian species, *Galea musteloides* (Rodentia, Caviidae) and *Tupaia belangeri* (Scandentia, Tupaiidae), with comments on postnatal myogenesis. Zoomorphology *119:*117-126.

Wallace IJ, and Demes B (2007) Symmetrical gaits of *Cebus apella*: implications for the functional significance of diagonal sequence gait in primates. Journal of Human Evolution *DOI:10.1006/j.jhevol.2007.10.008*.

Walter RM, and Carrier DR (2007) Ground forces applied by galloping dogs. Journal of Experimental Biology *230:*208-216.

Wells JP, and DeMenthon DF (1987) Measurement of body segment mass, center of gravity, and determination of moments of inertia by double pendulum in *Lemur fulvus*. American Journal of Primatology *12:*299-308.

Wells RP (1981) The projection of the ground reaction force as a predictor of internal joint moments. Bulletin of Prosthetics Research *18:*15-19.

Werner EE, and Gillam JF (1984) The ontogenetic niche and species interactions in size-structured populations. Annual Review of Ecology and Systematics *15:*393-425.

Westerga J, and Gramsbergen A (1990) The development of locomotion in the rat. Developmental Brain Research *57:*163-174.

White TD (1990) Gait selection In the brush-tail possum (*Trichosurus vulpecula*), the northern quoll (*Dasyurus hallucatus*), and the virginia opossum (*Didelphis virginiana*). Journal of Mammalogy *71:*79-84.

Whitehead PF, and Larson SG (1994) Shoulder motion during quadrupedal walking in *Cercopithecus aethiops:* integration of cineradiographic and electromyographic data. Journal of Human Evolution *26:*525-544.

Williams L (2004) Assessment of temperament in nursery and dam reared squirrel monkeys. Folia Primatologica *75 (Supplement 1):*426.

Winter DA (2005) Biomechanics and Motor Control of Human Movement. Hoboken, NJ: John Wiley & Sones, Inc.

Witte H, Biltzinger J, Hackert R, Schilling N, Schmidt M, Reich C, and Fischer MS (2002) Torque patterns of the limbs of small therian mammals during locomotion on flat ground. Journal of Experimental Biology *205:*1339-1353.

Workman C, and Covert HH (2005) Learning the ropes: the ontogeny of locomotion in the red-shanked douc (*Pygathrix nemaeus*), Delacour's (*Trachypithecus delacouri*), and Hatinh langurs (*Trachypithecus hatinhensis*) I. Positional behaviors. American Journal of Physical Anthropology *128:*371-380.

Wright KA (2003) Differences in patterns of locomotor behavior and habitat use in adult and juvenile *Cebus apella* and *Cebus olivaceus*. American Journal of Physical Anthropology *Supplement 36:*228.

Youlatos D (1999) Comparative locomotion of six sympatric primates in Ecuador. Annales des Sciences Naturelles: Zoologie et Biologie Animale *20:*161-168.

Young JW (2005) Ontogeny of muscle mechanical advantage in capuchin monkeys (*Cebus albifrons* and *Cebus apella*). Journal of Zoology, London *267:*351-362.

Young JW, and Fernández D (2006) Ontogeny of limb bone geometry and bone strength in an arboreal primate (*Cebus albifrons*). Integrative and Comparative Biology *45:*1101.

Young JW, Fernández D, and Fleagle JG (in preparation) Ontogeny of limb bone geometry in capuchin monkeys (*Cebus albifrons* and *Cebus apella*).

Young JW, Patel BA, and Stevens NJ (2007) Body mass distribution and gait mechanics in fat-tailed dwarf lemurs (*Cheirogaleus medius*) and patas monkeys (*Erythrocebus patas*). Journal of Human Evolution *53:*26-40.

Zeininger AD (2007) Ontogeny of Digitigrade Hand and Foot Postures in Infant Babbons (*Papio cynocephalus*). M.A. Thesis, University of Texas at Austin, Austin, TX.